NASA Contractor Report 4235

Study of High-Speed Civil Transports

Douglas Aircraft Company
New Commercial Programs

CONTRACT NAS1-18378
DECEMBER 1989

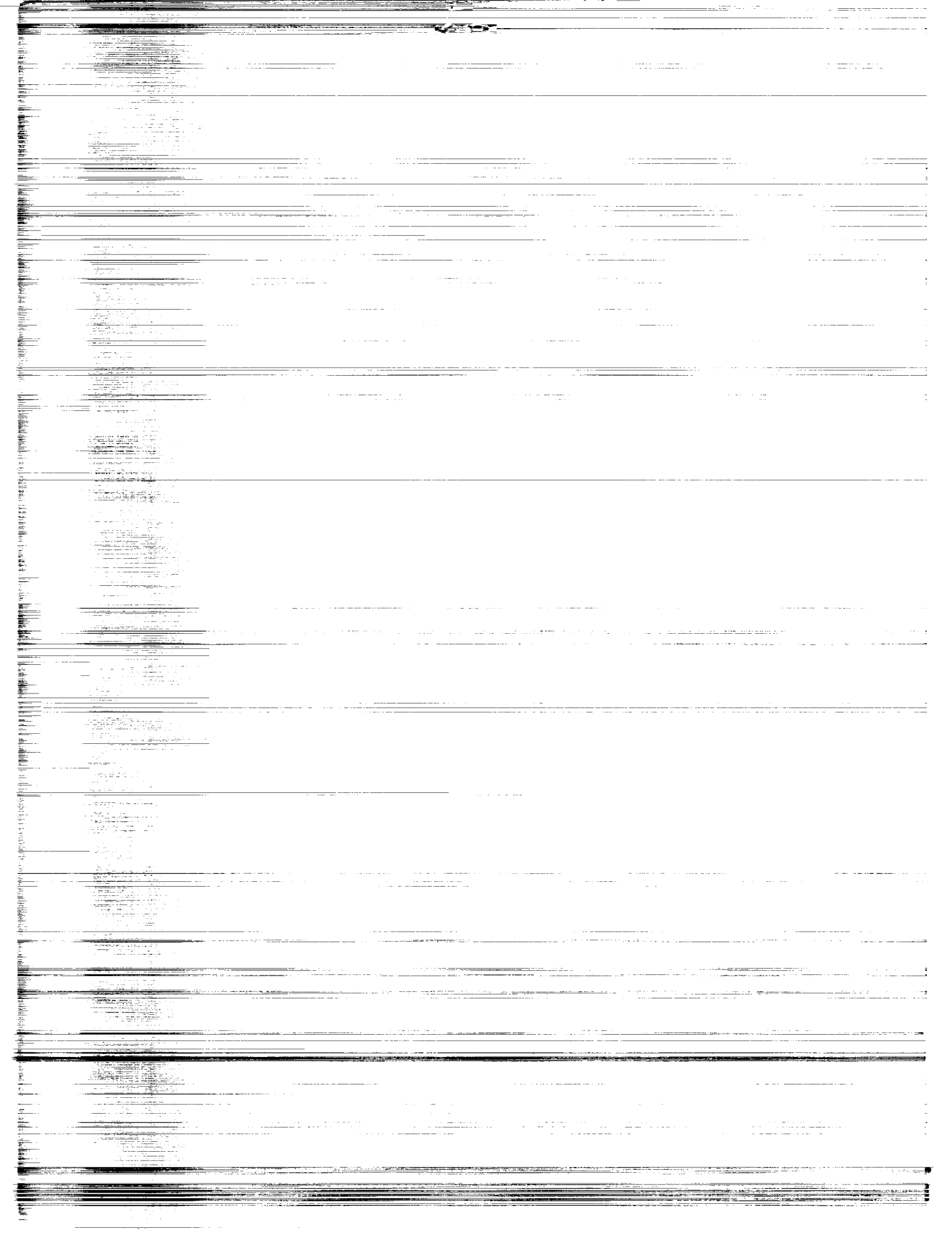

NASA Contractor Report 4235

Study of High-Speed Civil Transports

Douglas Aircraft Company
New Commercial Programs
Long Beach, California

Prepared for
Langley Research Center
under Contract NAS1-18378

National Aeronautics and
Space Administration
Office of Management
Scientific and Technical
Information Division

1989

FIGURES

TABLES

GLOSSARY

A	area
A_J	nozzle exit area
ADP	Advanced Ducted Prop (P&W geared subsonic very high bypass ratio turbofan)
ADS	Automated Dependent Surveillance
AERA	Automatic En Route ATC
Al	Aluminum
Al MMC	Aluminum Metal Matrix Composite
Alt	Altitude
AMI	Advanced Manned Interceptor
AST	Advanced Supersonic Transport
ATA	Air Transport Association
ATR	Air Turboramjet
BTU	British Thermal Units
C	Compressor or Centigrade
C_{f_g}	Nozzle Gross Thrust Coefficient
C_L	coefficient of lift
Cv	nozzle velocity coefficient
$\bar{c}_w$	mean aerodynamic chord wing trapezoidal area
CASE	Computer-Aided Sizing and Evaluation System
CCTV	Closed Circuit Television
CFD	Computational Fluid Dynamics
CFR	Code of Federal Regulations
COP	coefficient of performance
dB	decibel (reference pressure re. 20 μPa)
dB(A)	unit of A-weighted noise level
D/B	duct burner
DEG	degrees
E	Expander or Modulus of Elasticity, psi
ECS	Environmental Control System
EINOx	NOx Emissions Index (lb NOx per 1,000 lb fuel burned)
EPA	Environmental Protection Agency
EPNdB	Unit of Effective Perceived Noise Level
EPNL	Effective Perceived Noise Level
F	Fan or Fahrenheit
F_N	thrust per engine
F_{su}	Ultimate Shear Strength, psi
F_{tu}	Ultimate Tensile Strength, psi
$F_{(x)}$	Whitham F function
FAA	Federal Aviation Administration
FAD	Fuel Advisory Departures
FEM	Finite Element Model
FDL	Flight Dynamics Laboratory
FOBOOM	Sonic Boom Analysis, Wyle Laboratories
fps	feet per second
FRP	fuselage reference plane
ft	feet
ft^2	square foot
ft^3	cubic foot

GE	General Electric Aircraft Engines
GNP	Gross National Product
GPS	Global Positioning System
GW	Gross Weight
h	convective heat transfer coefficient, (BTU/hr-ft^2-°F)
HABP	Arbitrary Body Program
HSCT	High Speed Civil Transport
HSPA	High Speed Propulsion Assessment
i_H	Horizontal Tail Incidence
I_{SP}	Specific Impulse (secs)
IATA	International Air Transport Association
ICAO	International Civic Aviation Organization
IGV	Inlet Guide Vane
IHPTET	Integrated High Performance Turbine Engine Technology
IN.	inches
IOC	Initial Operational Capability
IVP	Inverted Velocity Profile
L_{Cdn}	Day-Night Average C-Weighted Sound Exposure Level
L_{ce}	C-Weighted Sound Exposure Level in decibels
lb	pounds
LFC	Laminar Flow Control
LNG	liquid methane
M	flow rate or Mach number
MAD	Materials Availability Date
MAPES	Mass Properties Estimation System
max p	maxium overpressure
MDBOOM	Sonic Boom Analysis, Douglas Aircraft
MEW	Manufacturer Empty Weight
MMLI	modularized multilayer insulation
N_E	number of engines
NASP	National AeroSpace Plane
NBP	Normal Boiling Point
NMI	nautical miles
NOx	Oxides of Nitrogen (all species)
OASPL	Overall Sound Pressure Level
OEW	Operator's Empty Weight
P	pressure or perceived level (Mark VII)
PC	Power Code or Polymetric Composite
PL	payload
PS	Power Setting (P&W)
P&W	Pratt & Whitney
PEEK	poly ether-ether keytone
PLdB	Steven Mark VII Perceived Level of Loudness in decibels
psf	lb/ft^2
Psia	pounds per square inch, absolute
q	heat flow, BTU/hr-ft^2
Q_A	heat flow by aerodynamic heating (BTU/hr)
Q_R	heat flow by radiation (BTU/hr)
R	Rankine
R&D	Research and Development

Re/l	Unit Reynolds Number per foot
ROMS	Revolutionary Opportunities for Materials and Structures
RSR	rapidly solidification rate
S_W	wing area
S_X	stress in x-direction, psi
SCAR	Supersonic Cruise Aircraft Research
SCR	Supersonic Cruise Research
SEEB	Sonic Boom Analysis, NASA – LRC
SERN	Single Expansion Ramp Nozzle
SFC	Specific Fuel Consumption
SLS	Sea Level Static
Sq. In.	square inches
T	temperature or turbine
t	average thickness, inch
T_f	fuel temperature
T_J	nozzle exit total temperature
T_R	recovery temperature
T_W	wall outer surface temperature
T/W	(Engine) Thrust/Weight Ratio
TAD	Technology Availability Date
Ti	Titanium
Ti MMC	Titanium Metal Matrix Composite
TOFL	takeoff field length
TOGW	takeoff gross weight
TOSLS	takeoff sea-level static
TP	Triple Point
TPS	Thermal Protection System
TSJF	Thermally Stable Jet Fuel
UPC	Unique Propulsion Concepts
V_{app}	approach speed
V_H	tail volume
V_J	nozzle bulk average exit velocity
VABI	Variable Area Bypass Injector (GE concept)
VCE	Variable Cycle Engine (GE mixed flow turbofan)
VCHJ	Variable Cycle Hypersonic Jet
VHBR	very high bypass ratio
VSCE	Variable Stream Control Engine
W_a	engine airflow
W_{corr}	corrected airflow (lb/sec)
W_f	fuel flow per engine
W_t	weight
X	downstream distance from nose or leading edge
$X_{suction}$	chordwise extent of boundary layer suction
X_{TR}	chordwise location of boundary layer suction
σ	Stefan-Boltzmann Constant (0.1714×10^{-8} BTU/hr-ft^2-°R^4)
ε	emissivity or heat exchanger effectiveness
ΔX_I	insulation thickness, inch
2D-CD	Two-Dimensional, Convergent Divergent
α_F	aircraft angle of attack
δ_e	elevator deflection angle

δ_f	wing trailing-edge flap angle
$\delta_{f,\ L.E.}$	wing leading-edge flap angle
$\Delta Re_{X_{TR}}$	Laminar Run Reynolds Number Increment
$>$	greater than
τ	turbulence spread angle
τ	slenderness coefficient = volume/(wing area)$^{3/2}$
ρ	density, lb/in.^{3}
μPa	micro pascals
Δp	overpressure

FOREWORD

The High-Speed Civil Transport study integrated results of technical and economic analysis of various aircraft to determine their commercial potential and corresponding technology requirements. This extended beyond previous primarily technology-oriented activities such as the Advanced Supersonic Transport (AST) and Supersonic Cruise Research (SCR), as well as included consideration of ongoing technology developments of the National AeroSpace Plane (NASP) program. Appropriate technologies were assessed in terms of the commercial value of high-speed civil transport (HSCT) aircraft.

Work was accomplished by Douglas Aircraft Company in Long Beach, California. This work commenced in October 1986 at the direction of the NASA Langley Research Center, Hampton, Virginia, and was jointly funded under Contract NAS1-18378.

The NASA Contracting Officer's Technical Representative was Mr. Robert W. Koenig during the initial phases and Mr. Charles E. K. Morris, Jr., during the final phases; the Douglas program manager was Mr. Donald A. Graf. Principal investigators were Mr. H. Robert Welge, aerodynamics, acoustics, and assistant program manager; Mr. Gordon L. Hamilton, propulsion, fuels, emissions, and thermal; Mr. M. A. "Pete" Price, structures and materials; Mr. Bruce W. Kimoto, systems and weights; Mr. Richard T. Cathers, configuration integration; Mr. John W. Stroup, market research; Mr. Marc L. Schoen, airports; and Mr. Maurice Platt, manufacturing and development costing. McDonnell Aircraft Company technical staff provided consultation relating to NASP technologies.

Other Douglas HSCT team members are:

Administration	E. C. Anderson
Aerodynamics and Acoustics	G. A. Intemann, J. A. Harbauer, Dr. D. L. Antani, R. A. Sohn, A. Mooiweer, A. K. Anderson, G. S. Page, Dr. A. G. Powell, A. K. Mortlock
Business Operations	M. L. Shell
Configuration	R. E. Lindenmuth
Economics and Market Research	M. J. Berger
Human Factors	Dr. A. N. DeGaston
Laminar Flow	W. E. Pearce, N. M. Jerstad
Product Support	R.E. Swartzbacker
Propulsion	F. R. Mastroly, J. A. Meyer, Dr. Y. Oida, C. R. Ross
Structures and Materials	Dr. E. G. Chow, D. E. Kerans, C. Y. Kam
Weights	G. J. Espil

This Page
Intentionally Left Blank

SUMMARY

The Douglas Aircraft Company has conducted a study of the potential of high-speed commercial transports. This has encompassed market studies, cruise Mach assessment, technology needs, environmental considerations, and the U.S. economy. This study included an initial screening from Mach 2 to Mach 25, followed by focus on the Mach 2 to Mach 5 region, and finally, comparison of Mach 3.2 and Mach 5.0. This later effort highlighted different fuels, with Mach 3.2 representing the upper end of kerosene-fuel feasibility and Mach 5.0 representing liquid methane potential. An important aspect of this study involved assessment of the technologies of the National AeroSpace Plane (NASP) program. Overall objectives of this two-year study were to provide direction for NASA's high-speed transport research and technology efforts in line with the goal of U.S. aeronautical leadership.

Market

1. Market projections for the 2000 to 2025 time period indicate sufficient passenger traffic for ranges beyond 2,000 nautical miles to support a fleet of economically viable and environmentally compatible high-speed commercial transports. Fleet needs could total 1,500 or more 300-seat aircraft by 2025.
2. The Pacific Rim area will become the major traffic region after the year 2000, leading to the establishment of design range objectives of 6,500 nautical miles.
3. Ticket prices above competitive subsonic commercial service provide considerable leverage for economic viability. Market elasticity is much greater for coach passengers compared to first class for high-speed transports. Market capture of coach passengers erodes sharply with ticket prices as small as 10 percent to 20 percent above subsonic fare level.
4. Economic viability places emphasis on environmentally acceptable supersonic flight over land. The constraint of no supersonic flight over land reduces potential aircraft productivity (i.e., seat miles per year) by 10 to 20 percent for the Mach 3.2 concept.

Cruise Speed

1. Aircraft productivity increases with cruise speed up to about Mach 5 to Mach 6 for market applications ranging from 2,000 to 6,500 nautical miles. Above this point, the relative significance of cruise speed diminishes and productivity is virtually constant.
2. Design mission gross weights increase with cruise Mach number and, correspondingly, advanced technology requirements and costs are greater.
3. Cruise speeds of Mach 5 and Mach 6 using cryogenic fuels (LNG) do not result in competitive opportunities before the 2010 time frame. Liquid methane's energy content falls short of Mach 5 requirements, and liquid hydrogen aircraft (Mach 6) are not competitive due to the high fuel cost.
4. Economic studies of the Mach 3.2 concept suggest viability could be achieved through modest fare premiums and successful research in providing significant gross weight reductions and propulsive efficiency improvements.

Technology Needs

1. Current technology is not adequate to produce an economically viable high-speed transport.
2. Technology needs can be defined to allow development of an economically attractive Mach 3.2, next-generation-after Concorde, high-speed transport.

Environmental Considerations

1. Advanced engine technology has been identified that offers the potential for reductions in nitrous oxides to very low levels. The determination of specific engine emission requirements must await the results of studies involving models of the earth's atmosphere and engine-emission projections for worldwide HSCT fleet applications.
2. FAR 36 Stage 3 airport noise requirements for a design range of 6,500 nautical miles cannot be met with technology projections of this study. Oversizing engines to reduce the noise is not economically attractive; further innovative suppressor research is required.
3. Concepts considered in this study are estimated to be capable of significant performance objectives – 300 passenger/6,500 nautical miles – with slightly lower sonic boom characteristics than Concorde (100 passengers/3,200 nautical miles). Sonic boom acceptability criteria plus further refinement of HSCT concepts through configuration shaping and operational constraints is necessary to determine conditions of environmental compliance.

Economy

1. From the standpoint of the U.S. economy, a 1,000-unit HSCT program would create an estimated 200,000 jobs over the life of the program. This translates into a projected $500 billion GNP increase and represents improvement in the balance of trade of approximately $100 billion.

Recommendations

1. Research must focus on resolving environmental issues; criteria acceptability must be achieved on a international basis in concert with the research before production development begins.
2. Research and technology development should focus on concepts using a kerosene-type fuel targeting on initial aircraft deliveries in the 2000 to 2010 time frame.
3. NASP technology and learning will have measurable value; however, a commercially oriented high-speed technologies development program is vital to any ongoing efforts by the U.S. industry to maintain aviation technology leadership.

1.0 INTRODUCTION

1.1 Background

Commercial aviation has grown steadily from the days of multistop/multimode transportation to become a mature, highly competitive service to both the business community and the vacation/pleasure traveler. Commercial aviation has become a vital element of the U.S. economy by providing employment on the local level and making significant contributions to the national balance of trade on a worldwide basis.

Jets in the 1950s and jumbo-sized aircraft in the 1970s have increased productivity and contributed to holding passenger ticket prices below inflationary trends. Efforts to continue productivity advancements through supersonic transports, however, have been unsuccessful – the U.S. SST was cancelled in 1971 and the British/French Concorde program saw only 18 aircraft manufactured, resulting in very limited service between the U.S. and Europe. Concorde has been successful in demonstrating safe and reliable schedule service and is expected to operate through the turn of the century.

Worldwide passenger traffic will triple by the year 2000, according to market projections that foresee particular demand in a growing Pacific region noted for long route segments and flight times – very appropriate for high-speed transport aircraft.

Following cancellation of the U.S. SST, NASA has continued supersonic technology development activities with the SCAR program and follow-on work in materials, computational fluid dynamics, and propulsion technology. In 1985, the White House Office of Science and Technology policy report on aeronautical research resulted in establishment of an Aeronautical Policy Review Committee, which developed aeronautical research and development goals in subsonics, supersonics, and transatmospherics for continued U.S. leadership in aeronautics.

In late 1986, NASA commissioned a two-year High-Speed Civil Transport (HSCT) study to determine the best opportunities for a viable supersonic transport. The Douglas Aircraft Company conducted a two-year study under NASA contract NAS1-19378. This systems-type study began with a broad scope and then focused on the crucial issues for the best HSCT concepts. Initially, the study considered cruise speeds ranging from Mach 2 to 25 and an associated range of aerodynamic concepts, propulsion systems and fuels, materials, and structures. The study was organized into three phases, as shown in Figure 1-1. Major ele-

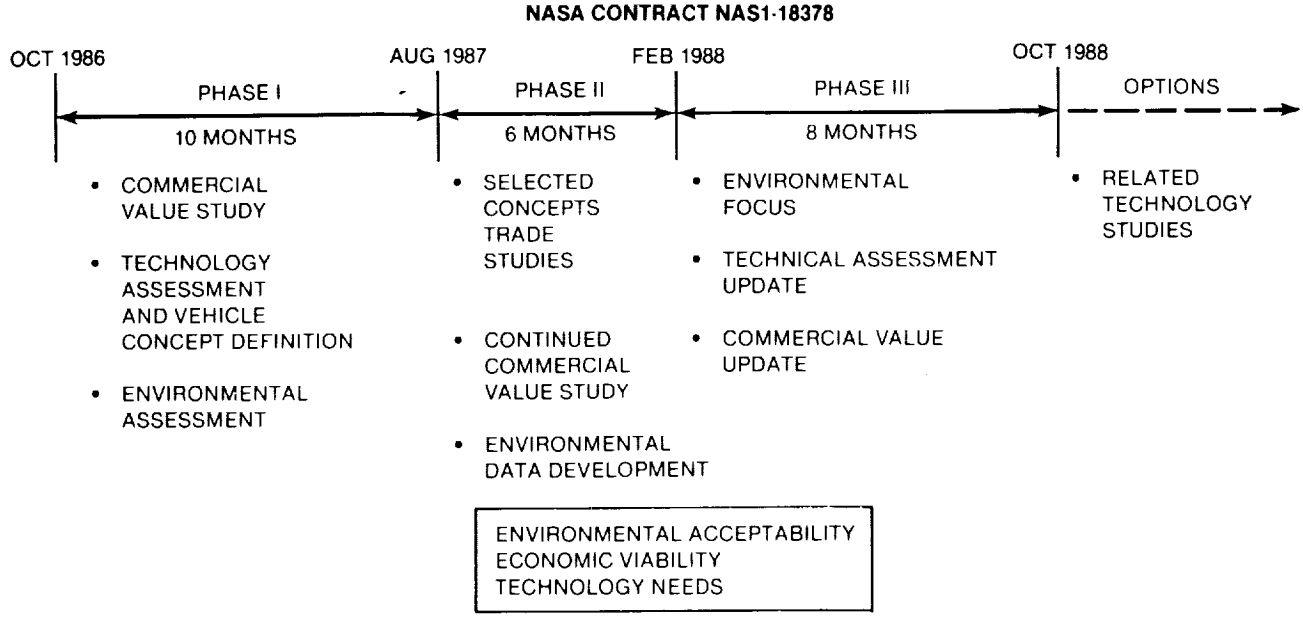

FIGURE 1-1. HIGH-SPEED CIVIL TRANSPORT STUDY

ments included (1) evaluations of HSCT operating and production costs, and comparisons of vehicle cost and worth, (2) vehicle technology assessment based on all the traditional disciplines and their integration into vehicle concepts, and (3) definition and assessment of the more promising concepts in more detail. In addition, special factors such as airport infrastructure, fuel technology, and the environmental concerns for sonic boom, community noise, and emissions were included.

Engine data were obtained through subcontracts to Aerojet TechSystems, General Electric Aircraft Engines, and Pratt & Whitney. In addition, subcontracts also have produced expertise in such areas as air traffic control, cryogenic fuels technology, airport facilities development, exergy analysis, sonic boom technology, and market-related issues (such as schedule synthesis and passenger value-of-time). Airline viewpoints have been incorporated from both U.S. and overseas airlines on an ad hoc basis.

1.2 Study Approach

The overall study began with an initial screening to compare technologies through definition of concepts from Mach 2 to Mach 25. Phase I assessments were based on vehicle concepts designed to carry 300 passengers a distance of 6,500 nautical miles as determined from the Phase I commercial value analysis. An advanced subsonic transport of like-year technology and identical payload-range characteristics was defined in Phase I for purposes of economic comparison with HSCT concepts. At the conclusion of Phase I, concepts utilizing hydrogen fuel with design Mach numbers above 6 were eliminated from further study because of their relative low economic performance.

Phase II focused on Mach 2.2., Mach 3.2, and Mach 5.0 with specific technology applications incorporating engine performance data tailored to the HSCT mission profile characteristics. Phase II was conducted without environmental restrictions for supersonic cruise over land, community noise, or accountability for engine emissions/atmospheric interactions; this established baselines for follow-on evaluations. The methods and data base to address the environmental restrictions were being developed at this stage of the study. Concepts with cruise speeds of Mach 3.2 and Mach 5.0 were selected for more detailed study in Phase III. The Mach 3.2 concept utilizes thermally stable jet fuel (TSJF) and the Mach 5.0 requires liquid methane (LNG).

The focus of Phase III was environmental acceptability. Since future NASA research may be directed based on the results of this work, it was considered imperative to assess Mach 3.2 and Mach 5.0. Specific analysis included sonic boom characteristics reflecting significantly different speeds and cruise altitude; work was accomplished on engine emissions and resulting atmospheric interaction due to the broadly differing fuels and their combustion characteristics. Community noise analysis covered a broad range of engine jet velocities. Updated engine performance data were utilized in Phase III for baseline engines selected earlier. Phase III included integration of NASP technologies, particularly in materials and structures, to access contributions that this ongoing program might provide to civil aviation.

Commercial value studies provided integrated technology assessments and thereby a means of focus. Market research provided both the 300-passenger payload objective and the 6,500-nautical-mile-range objective. Passenger fare levels were consistant with current experience, and fare premiums were considered parametrically. Commercial value analysis included estimates of aircraft operating costs, as well as aircraft worth as would be used by the airlines in judging acquisition alternatives. Throughout this study, informal individual meetings with major U.S. and overseas airlines have provided the needed user response to the assumptions, findings, and conclusions of this effort. Airport fuel-related facilities for unconventional fuels (e.g., beyond the current Jet A commercial standard) have been estimated by qualified experts in airport planning, design, and development. Fuel-related costs for the facilities and the unique operating requirements have been estimated.

This approach produced a HSCT worth which, when compared to the estimated selling price based on manufacturing and development costs, provides insight as to economic viability. HSCT routing itineraries provided engine emissions data for NASA's atmospheric interaction studies.

1.3 Assumptions

The following assumptions evolved throughout the course of Phases I, II, and III of this study.

Mission/Design Requirements:

- Payload: 300 passengers; 3 classes, 10-percent first/30-percent business/60-percent coach
- Range: 6,500 nautical miles with 300 passengers and baggage
- Cargo: 5,000 pounds, 500 cubic feet
- Configuration size limitation: maximum takeoff gross weight equal to or less than 1,000,000 pounds; pavement loading equal to or less than MD-11 or 747
- Fuel reserve: 5 percent block fuel, 200 nautical mile subsonic diversion to alternate airport, and 30 minutes hold at 2,000 feet altitude
- Minimum/maximum balanced field length: 11,000 feet (maximum), standard day, sea level, 35-foot obstacle
- Landing performance: 11,000 feet (maximum) includes braking, air run from 35 feet and wet runway conditions.
- Approach: 140 knots or less at end-of-mission weight
- Limiting floor angle at cruise or on ground: cruise 3 degrees; ground, 2 degrees (for cargo hold)
- Thrust margins: power throttled to cabin rate of climb equal to or less than 300 feet per minute (sea level), with an 8,000-foot cabin pressure at cruise
- Acceleration: passengers subjected to no more than 0.2 to 0.3 g's maximum
- Cabin environments: consistent with current standards

Vehicle Analyses:

Airframe

- Service life: 25 years
- Number landing/takeoff cycles: Mach 3.2 – 24,000; Mach 5.0 – 30,000
- Maximum q: Mach 3.2 – 1370 pounds per square foot; Mach 5.0 – 1,420 pounds per square foot
- Load factors: + 2.5, 1.0 (V-N diagram); 66 feet per second gust criteria. Design load safety factors: 1.5 with calculated temperatures

Propulsion

- Analysis for inlet efficiency: MIL-STD with method of characteristics and boundary layer bleed analysis including local Mach effects
- Analyses for exhaust: engine manufactures' data with method of characteristics analysis and additional viscous losses
- Methane: 99.99-percent purity, boiloff collected and recycled, 1 percent lost in boiloff from aircraft
- Fuel utility as onboard heat sink: absorb thermal loads over flight profile, also used for Mach 5.0 active cooling

Aerodynamics

- Vehicle stability: Mach 3.2 – 10 percent negative rigid static margin; Mach 5.0 – 9 percent negative rigid static margin

Technology Status

- Readiness date: Mach 3.2 – 2000/2010; Mach 5.0 – 2010/2020

Commercial Value Analyses:

Market

- Economic scenario for future: regional forecast under three economic scenarios. (1) extrapolation with current growth rates, (2) maturation of high growth markets, and (3) maturation and growth paralleling rates of growth in general economy
- Market definition: ranges greater than 2,000 miles; top international city pairs for 10 IATA regions
- Stimulation of market due to speed/time-savings: 10 percent of dollar value of time savings (net of fare premium) is converted into additional trips
- Market split for HSCT, business-to-personal ratio: 50/50; market share determined by values of time, fare premiums, and time savings
- Value of time: first class, $90 per hour; business, $30 per hour; full coach, $22.50 per hour; and discount coach $5 per hour

Operations, Schedules, and Routes

- Supersonic great circle over land route baseline; supersonic cruise over land with comparison to subsonic cruise over land for environmental compatibility
- Airline representation: global airline with 309 city pairs for economic analysis; specific airline practices considered for scheduling and utilization
- Airport representation: specific airports considered for routings with current curfew limitations; one airport per IATA region representation for emissions analysis
- Turn/through time: 2 hours standard; 1 hour goal

Finance and Revenue

- Cost elements: standard ATA definition of direct and indirect operating costs. Direct operating cost – fuel, crew, maintenance, ownership; indirect – passenger service and reservations, aircraft handling and service, landing fees, food, general and administrative
- Standard dollars: 1987
- "Should cost": aircraft worth based on the airline target rate of return
- "Will cost": aircraft flyaway price based on the manufacturer's cost including target rate of return
- Fuel costs: reference prices, Jet A – $0.60/EGJA delivered to aircraft, TSJF (thermally stable jet fuel) for Mach 3.2 – $0.75/EGJA delivered to airport, LNG for Mach 5.0 – $0.33/EGJA natural gas pipeline feedstock delivered to airport plus airport fuel facility costs
- Production runs: 1,500-unit target
- Fare constraints: zero premium level based on current subsonic published "Y" class fare
- Parameters for ROI definition: direct and indirect operating costs, passenger revenue, economic life, and tax law – 10-percent ROI level required

Environment:

Sonic Boom

- Initial design/operational constraint in cruise: design, no constraints except for overall length; operational, cruise speed and flight track diversions

- Initial human response model/criteria: Stevens Mark VII loudness/P = 90PI dB; C-Weighted Sound Exposure Level/CSEL = 102dB

Community Noise

- Rules: current FAR 36 Stage 3

Atmospheric Chemistry

- Modeling of fleet, market, and routes: model based on representative city pair for each of 10 IATA regions with traffic and fleet size consistent with airline servicing 309 city pairs

1.4 Concept Screening

Phase I Results. The Phase I effort consisted of a broad screening analysis of the Mach 2 to 25 range. Figure 1-2 presents a matrix of specific vehicles considered with their associated fuels. An advanced subsonic transport incorporating technologies expected in the year 2000 and using conventional Jet A fuel (commercial standard) was defined to provide an economics baseline. Mach 2.2 and Mach 4 vehicles used a kerosene-type fuel with higher thermal capability necessary for the projected thermal environment. The candidate fuels are compared on Figure 1-3 in terms of their relative energy per unit volume and projected Mach range. Endothermic fuels were eliminated very early in Phase I because of price and availability. Liquid methane offers a 16-percent higher energy per pound; however, liquid methane has an energy density

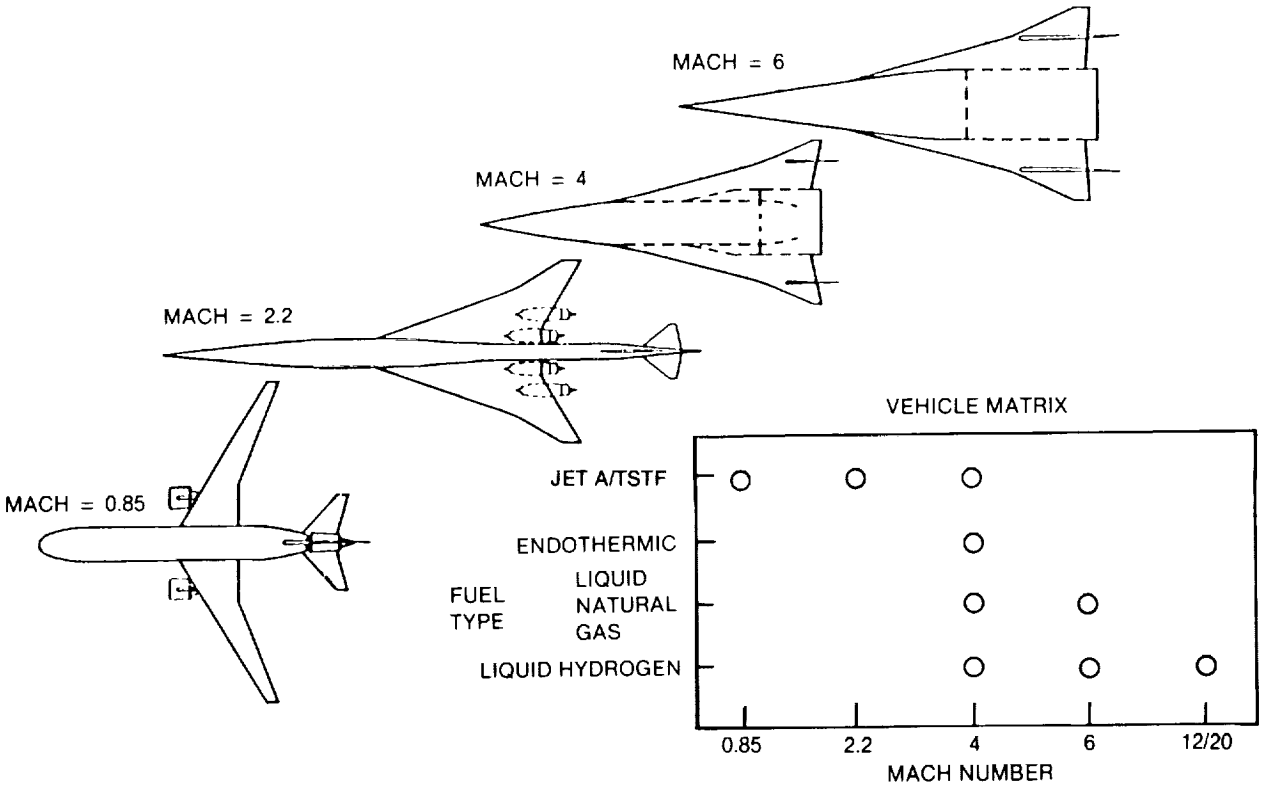

FIGURE 1-2. HSCT STUDY CONCEPTS — PHASE I

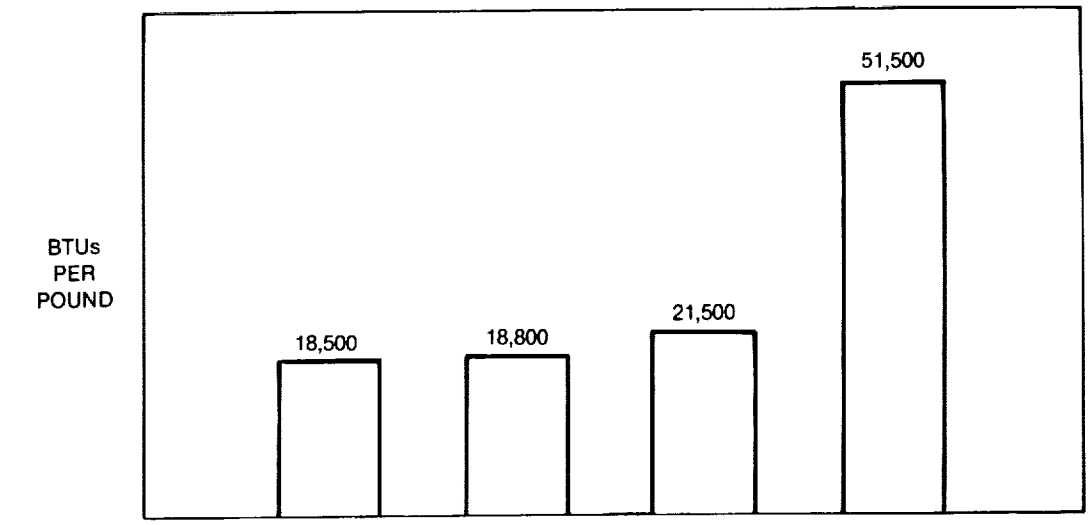

FIGURE 1-3. CANDIDATE FUELS

only 60 percent of that of kerosene-type fuels. Liquid hydrogen (LH_2) also offers an increase of energy (180 percent) at a still further reduced energy density (25 percent).

Phase I market research studies initially encompassed all international air traffic (18 IATA regions, Figure 1-4). The ten regions considered as best potential were then studied in more detail. Of these, four (Figure 1-5) comprise between 85 percent to 90 percent of the total international traffic. The North Atlantic and North and Mid-Pacific are the major traffic regions. In 1986, the North Atlantic recorded more than twice the revenue passenger miles compared to the North and Mid-Pacific. By the year 2000, equal traffic is expected in these two major sectors. Overall, traffic is predicted to total 446.1 billion available seat miles (ASM), with 53 percent being overseas markets. These projections are based on individual country economics, trade characteristics, and priorities.

Passenger traffic was projected to the year 2025 to estimate total HSCT needs and resulting production scaling. Three scenarios were considered with a growth to 2,386.6 billion seat-miles considered most likely (Figure 1-6). This represents five times the traffic projected for the year 2000. It should be emphasized that these data do not represent exhaustive market research for HSCT opportunities, but is a representation of market application for productivity and utilization analysis and first order market assessment. Based on this market analysis and previous Douglas supersonic aircraft studies, a vehicle size of approximately 300 seats is necessary for competitive economics; therefore, all vehicles were sized accordingly.

Range requirements based on the foregoing will be mandated by the key Pacific markets (Figure 1-7). Ranges vary from slightly less than 4,000 statute miles for the Honolulu to Tokyo market, to approximately 5,500 statute miles for the Los Angeles to Tokyo market, to nearly 7,000 statute miles for the New York to Tokyo market. Los Angeles to Sydney, with 7,500 statute miles represents the upper nonstop range requirement. This range capability captures 80 percent of all long-range, nonstop traffic, and was adopted as a Phase I design requirement.

In addition to the 7,500 statute mile design range (6,500 nautical miles), other design objectives were established based on the assumption that for an HSCT to be viable, it must be operable from current airports. This included a maximum takeoff field length of 11,000 feet and maximum takeoff gross weight of

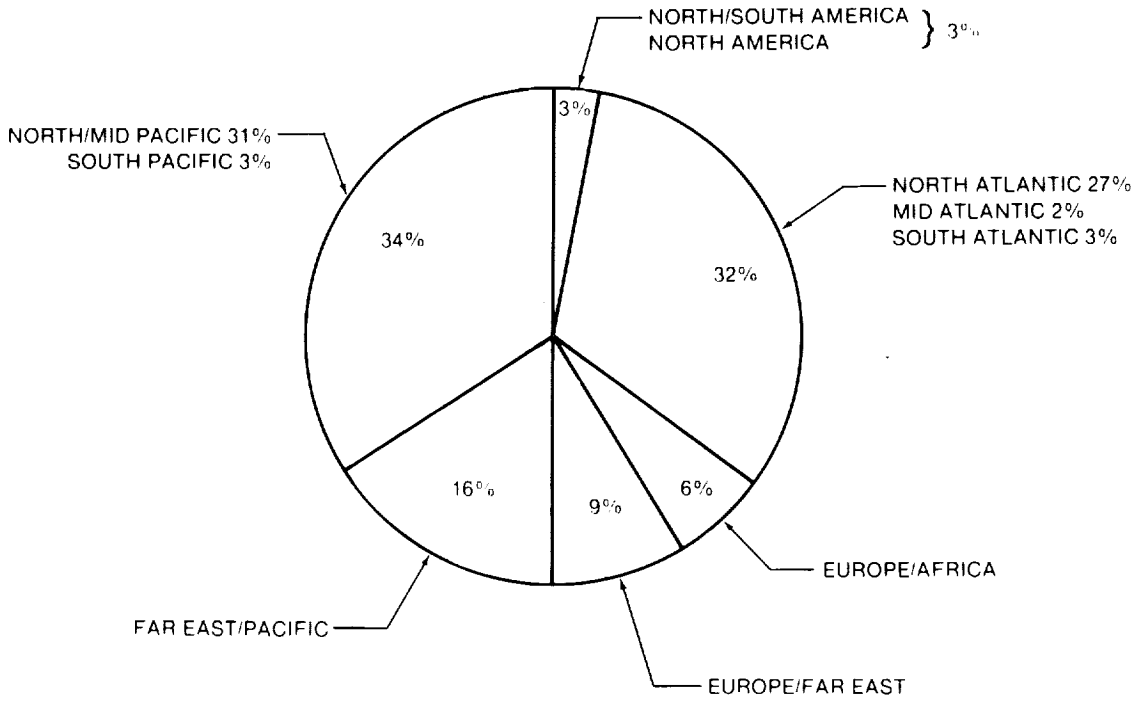

FIGURE 1-4. HSCT APPLICATIONS

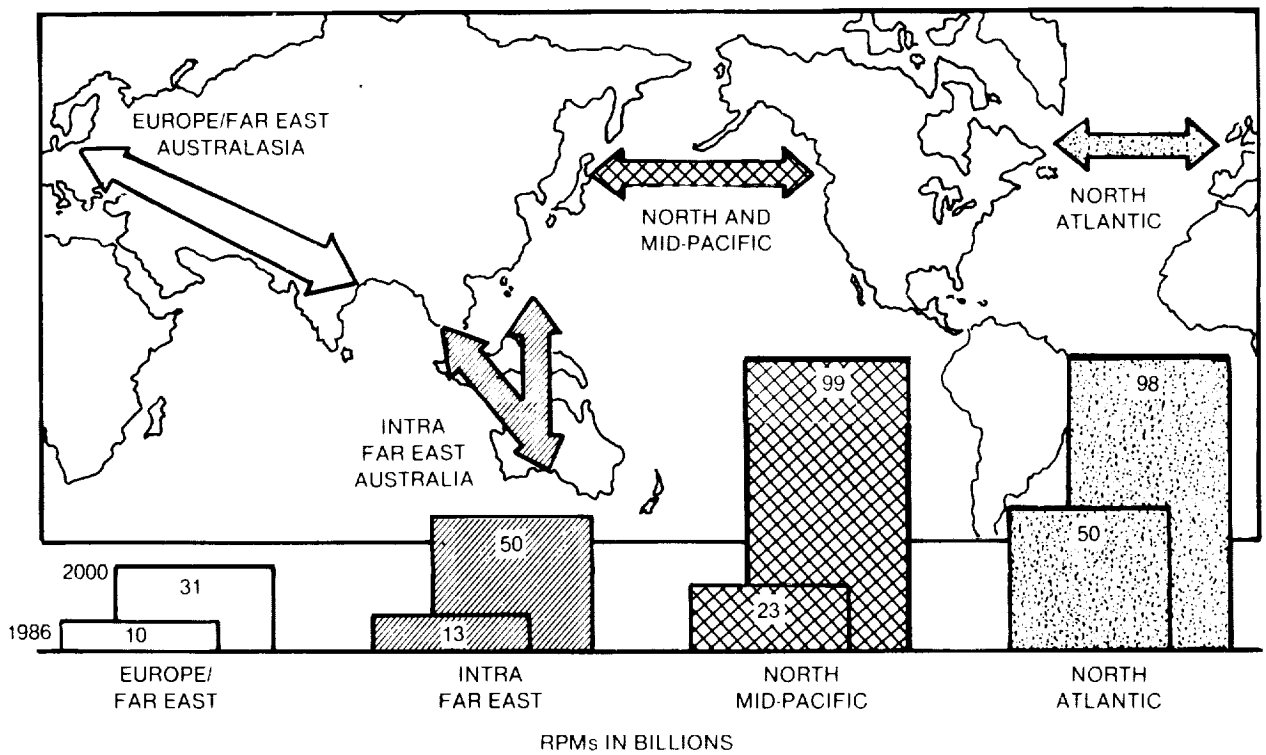

FIGURE 1-5. INTERNATIONAL PASSENGER TRAFFIC — MAJOR REGIONS — 85-90 PERCENT OF TOTAL

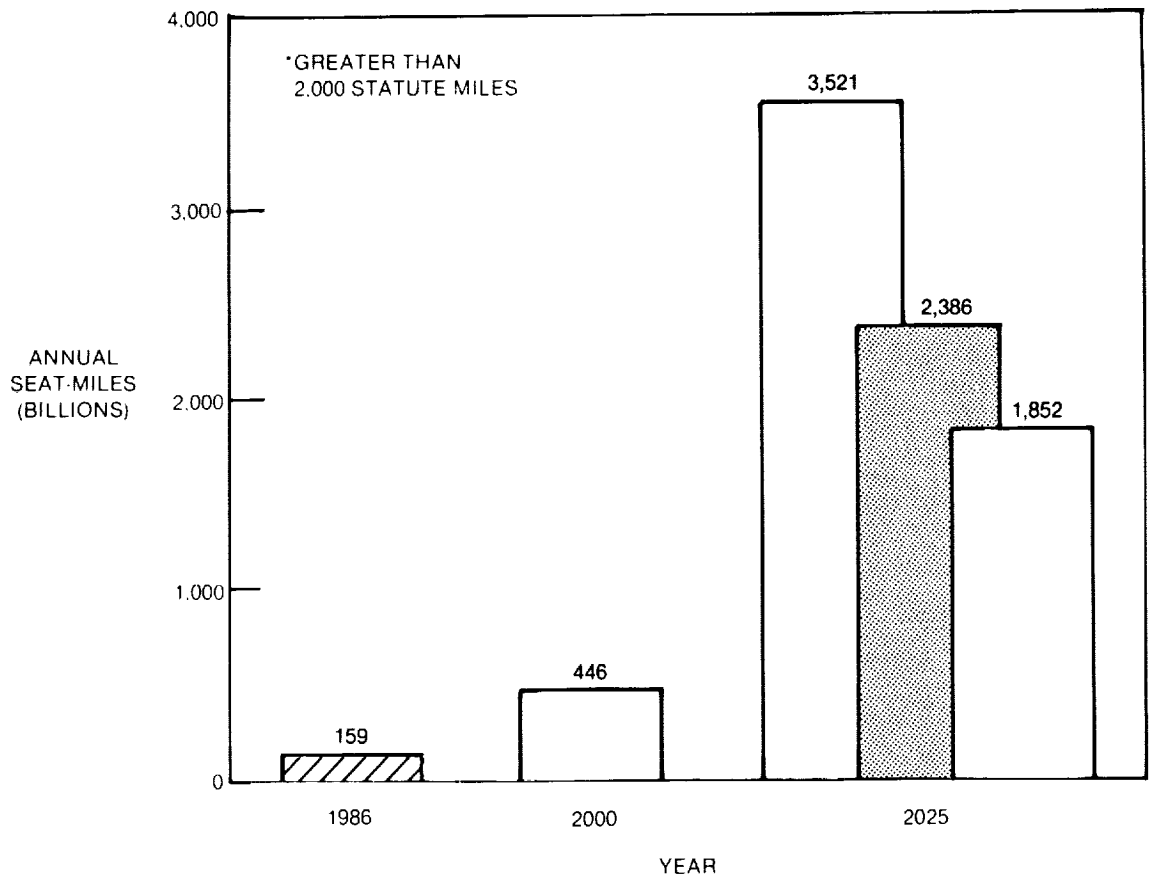

FIGURE 1-6. PASSENGER TRAFFIC FORECAST

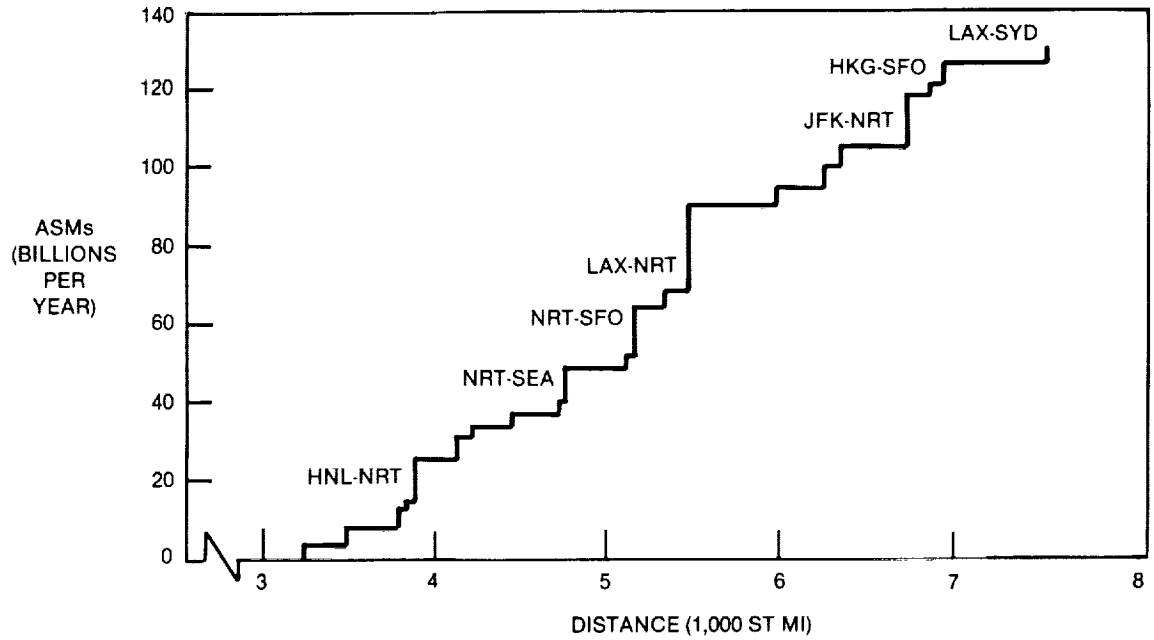

FIGURE 1-7. TOP PACIFIC MARKETS FOR YEAR 2000 CONSTITUTING 80 PERCENT OF TRANS-PACIFIC ASMs

1,000,000 pounds such that airport capabilities would not be exceeded. Approach speeds of 140 knots would maintain compatibility with ATC approach and 1/10 g. acceleration during climb would assure passenger comfort. Environmental acceptability was a requirement and will be the subject of further study.

In Phase I, engine performance was based to a significant extent on data generated for noncommercial requirements such as the HSPA (high-speed propulsion assessment) program. Figure 1-8 compares the resulting HSCT-oriented propulsion data with a potential upper level overall cruise propulsive efficiency. This was evolved from studies of engine component performance and represents a variety of engines and fuel types. In all cases, the potential propulsive efficiency is well above that of the Concorde (38 percent at Mach 2.0).

From a marketing standpoint the HSCT is expected to provide benefits in all areas of operation – passengers as well as cargo (Table 1-1) – with its value measured through aircraft productivity in terms of seat miles per year for passenger applications. In Phase I, the market research highlighted 309 international city pairs as candidates for HSCT service. A global concept airline routing system was developed to allow determination of aircraft use in terms of (1) HSCT speed potential, (2) real-world constraints including airport curfews (current regulations), and (3) passenger preferred times of day for travel. From this, aircraft productivity (seat-miles-per-year) was determined as a function of cruise Mach number (Figure 1-9) based on a two-hour aircraft turnaround. This is consistent with current airline scheduling for large transport aircraft.

Data showed the expected increase in productivity as cruise speed increased. In the Mach 4 to 5 range, productivity gains begin to diminish; above Mach 6, very little additional productivity is achievable. This trend reflects the increased distances required for climb and descent with increased Mach number and reduced contribution of cruise Mach distance to overall productivity. Thus, Mach 5 to Mach 6 represents the commercial upper limit within the current air transportation system of nonstop, point-to-point service.

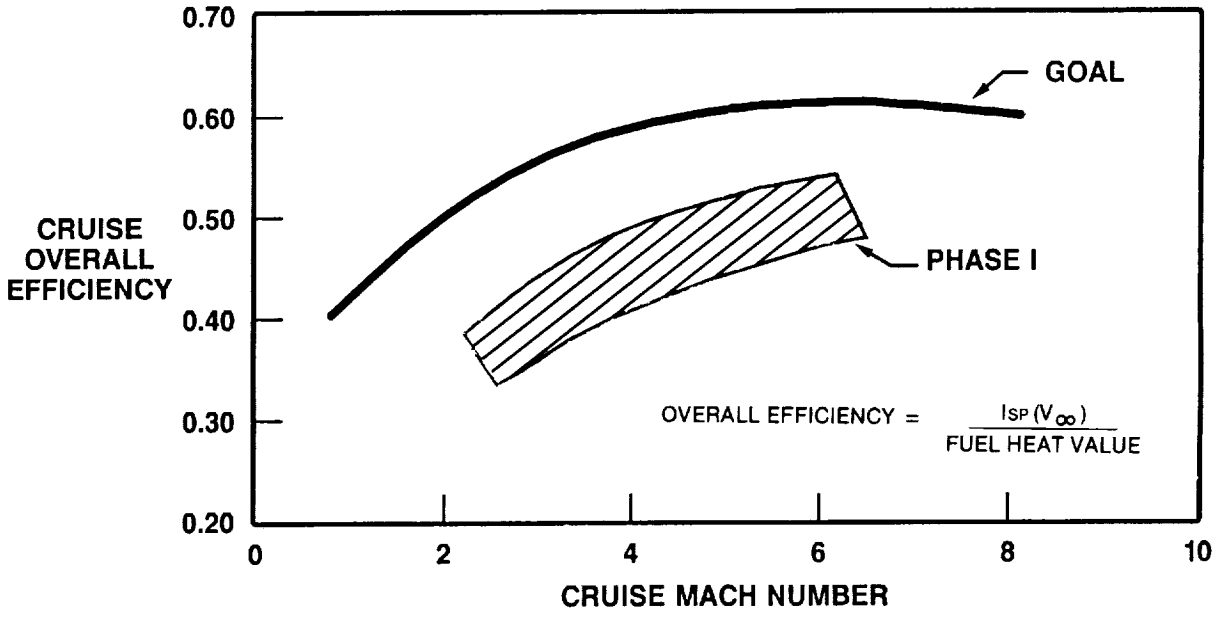

FIGURE 1-8. PROPULSION TECHNOLOGY, PHASE I

TABLE 1-1
HIGH-SPEED, COMMERCIAL TRANSPORTATION BENEFITS

FOR PASSENGERS, REDUCED TRAVEL TIME RESULTS IN
- REDUCED JET LAG
- LESS PHYSICAL HARDSHIPS, ENHANCED COMFORT

FOR BUSINESS TRAVELERS
- "SAME DAY" BUSINESS
- REDUCED "EN ROUTE" COSTS

FOR BUSINESS
- EXPRESS WORLDWIDE MAIL/PACKAGE SERVICE
- SHORTENED INVENTORY PIPELINES

FOR AIRLINES
- INCREASED PRODUCTIVITY/REVENUE AND PROFIT
- REDUCED TIME-RELATED COSTS
- MARKET STIMULATION

FOR THE U.S.
- GNP CONTRIBUTION
- EXPORT/FAVORABLE TRADE
- U.S. LEADERSHIP

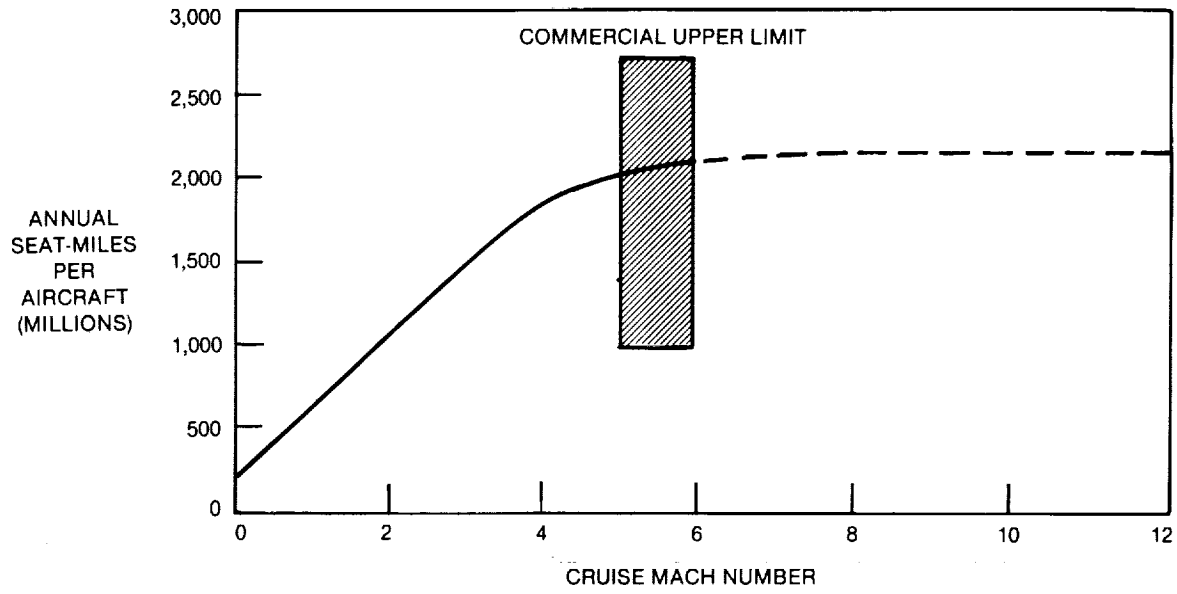

FIGURE 1-9. AIRCRAFT PRODUCTIVITY — 300 SEATS

Airline economics studies included both direct operating costs (DOC) and indirect operating costs (IOC) for each HSCT concept as well as revenue accountability based on the different classes of travel (i.e., first, business, coach) and current ticket pricing. Combining the technical performance and economic estimates into a single figure of merit was achieved through determination of aircraft worth. This is an important measure to airlines and includes a 10-percent return on investment to the airline operator. Aircraft worth is based on year-2000 traffic for a global system of 309 city pairs of 2,000 statute miles or greater distance and aircraft productivity.

Phase I results are summarized in Figure 1-10, which includes the estimated aircraft worth for each concept considered in Phase I together with the estimated flyaway (i.e., manufactures' cost plus profit) price for each aircraft. Differences between worth and price are shown, with only the methane-fueled Mach 4 and Mach 6 concepts showing positive results. The hydrogen-fueled concepts fell short in aircraft worth because of high LH_2 fuel cost. Both the kerosene-fueled Mach 2.2 and Mach 4 concepts fell short due to estimated flyaway prices. Based on these comparisons, the hydrogen fuel HSCTs were dropped from further consideration.

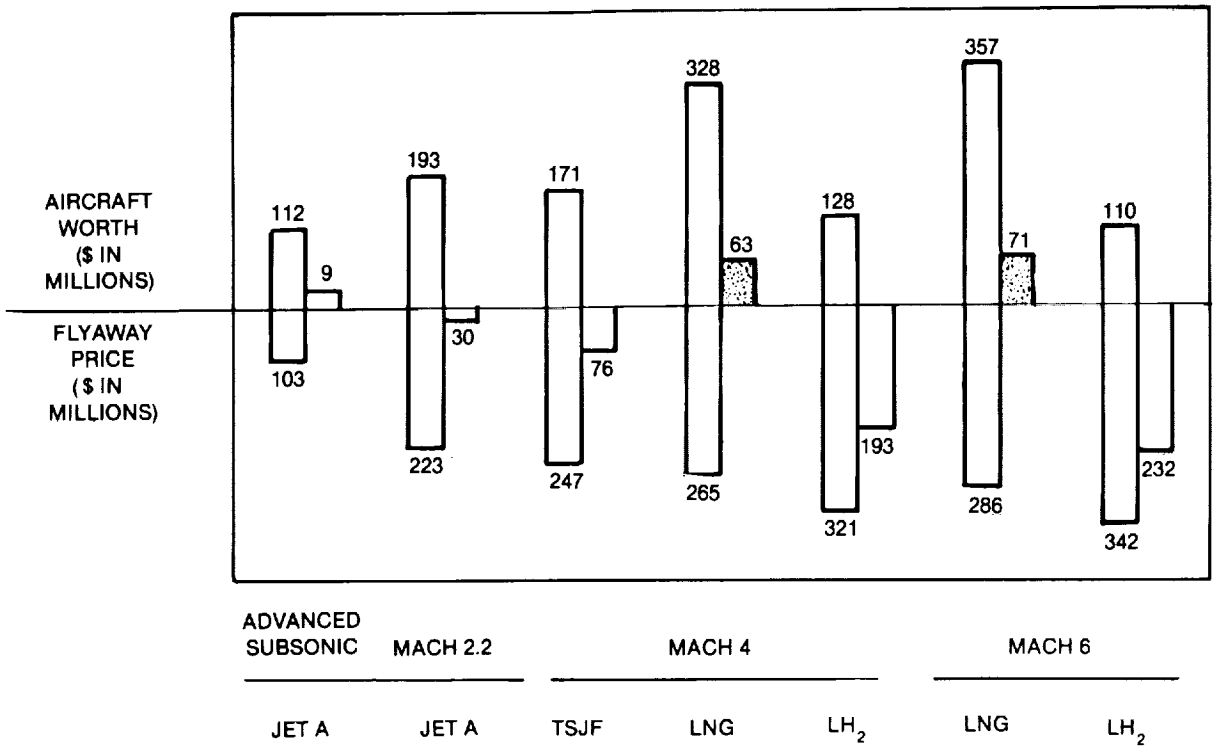

FIGURE 1-10. PHASE I ECONOMIC COMPARISON — 300 SEATS/1987 DOLLARS

The Phase I approach was based on goal oriented takeoff gross weight of 700,000 pounds. Parallel studies in Phase I quantified the technological improvements necessary to achieve this goal weight as a function of cruise Mach number (Figure 1-11). These noted improvements were initially assumed evenly distributed or charged to each discipline: aerodynamics, propulsion, and structures. As expected, requirements for technological improvements increased with advancing Mach numbers.

Based on the foregoing analysis, the following Mach numbers were selected for study during Phase II (Figure 1-12). The rationale for their selection is given below:

- Mach 2.2
  - Revelance to previous AST studies
  - Jet A fuel
  - Lightest TOGW
  - Least aggressive technology requirements
- Mach 3.2
  - Higher productivity
  - Upper limit of kerosene-based fuel
  - Application of more aggressive technologies
- Mach 5.0
  - Highest productivity
  - Application of methane fuel
  - Aggressive technology application
  - Application of NASP technologies

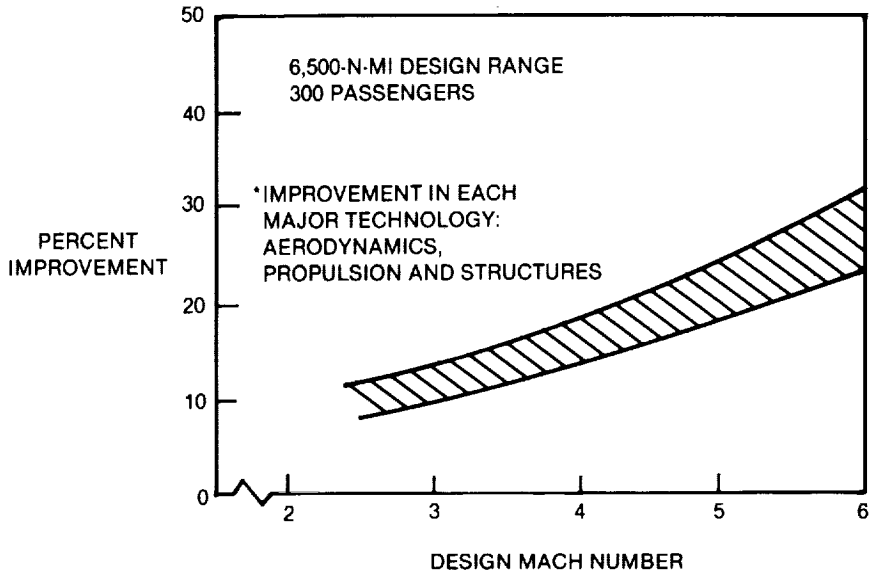

FIGURE 1-11. TECHNOLOGICAL REQUIREMENTS

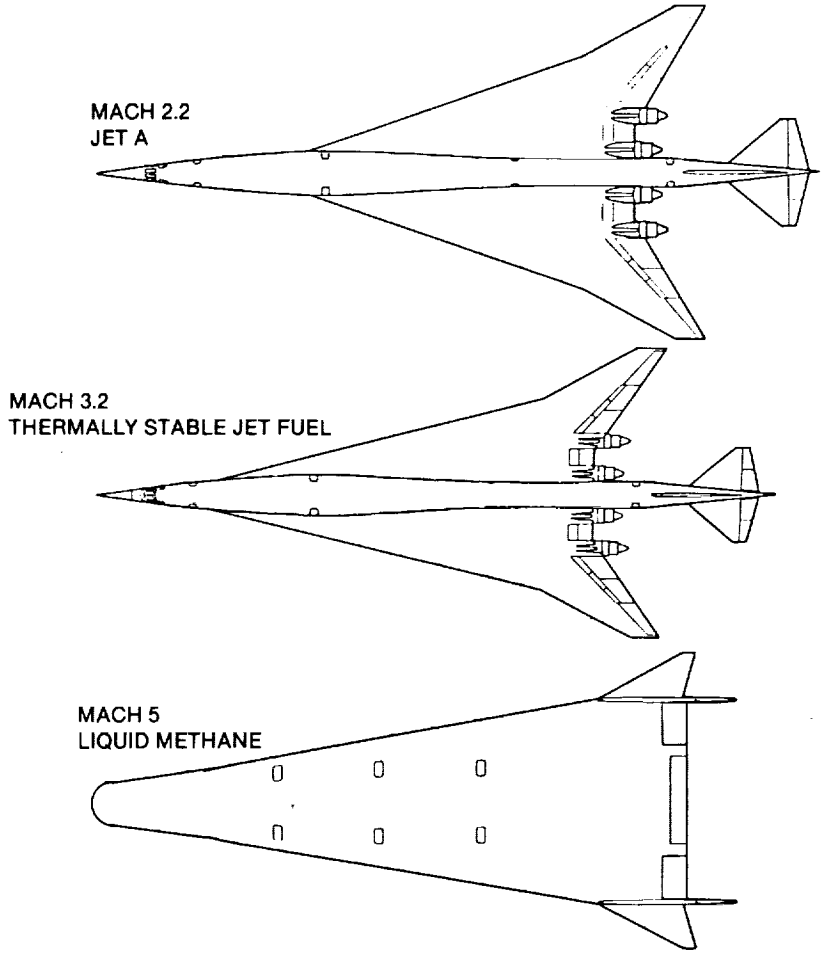

FIGURE 1-12. REPRESENTATIVE HSCT CONCEPTS

Phase II Results. Phase II consisted of technology application and integration of the three selected concepts; tailored HSCT engine data were incorporated, and all evaluations were conducted assuming supersonic cruise missions over land. This basic assumption represented the best that could be achieved from the operations and economics point-of-view and provided a reference point for Phase III assessments. Adequate sonic boom computational techniques for Mach 5 applications were being developed and not available for Phase II.

Payload and range requirements established in Phase I were maintained for Phase II; 300 passengers and 6,500 nautical miles range. Phase II engine performance requirements were tailored to HSCT requirements and included climb, cruise at altitude to achieve good aerodynamic performance, descent according to commercial standards, and allowance for subsonic flight diversion to alternate airports. Propulsive efficiency levels were improved over Phase I; however, they fell short of the previously defined upper potential level (Figure 1-13). Technology integration and performance assessment resulted in bettering the Phase I gross weight goal of 700,000 pounds for the Mach 2.2 and Mach 3.2 concepts. The Mach 5.0 concept was sized to nearly a million pounds (Figure 1-14).

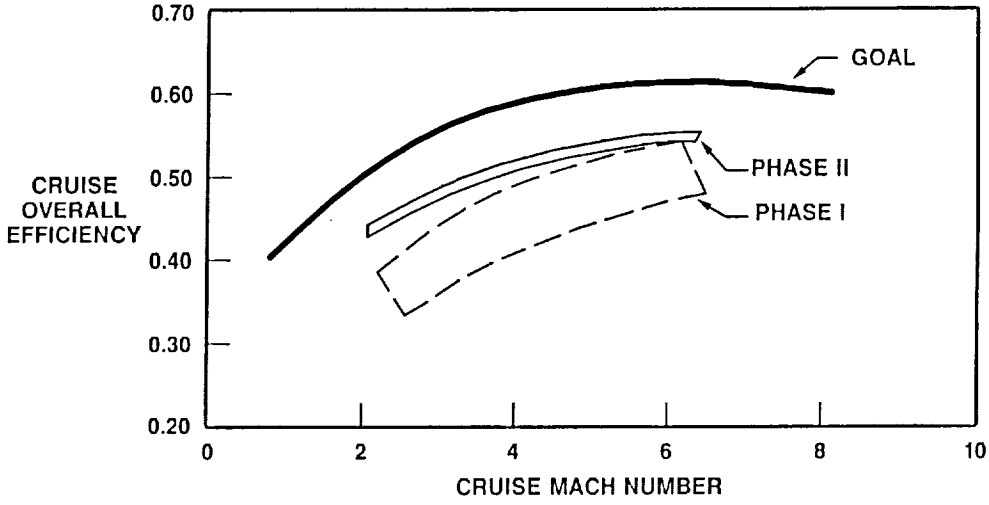

FIGURE 1-13. PROPULSION TECHNOLOGY — PHASE II

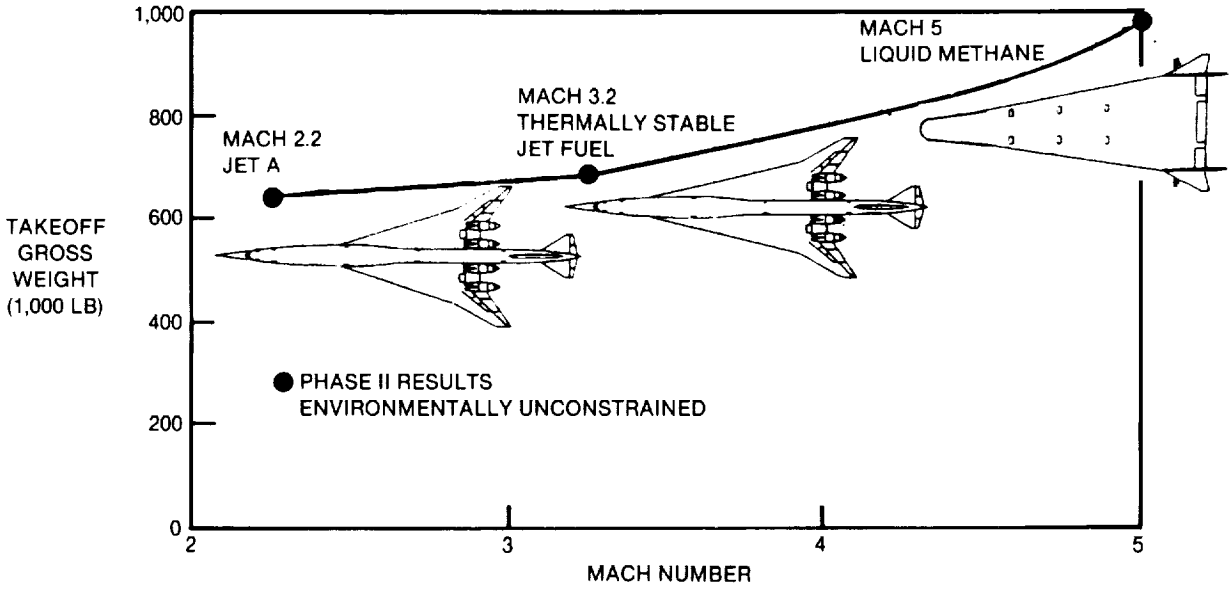

FIGURE 1-14. PHASE II MACH NUMBER — GROSS WEIGHT 300 SEATS/6,500 NAUTICAL MILES

Sonic boom analysis based on available methods indicated no significant variation between the concepts (Figure 1-15). The projected sound levels mirrored the Concorde sonic boom level but at a design weight representing three times the passenger payload and over twice the design range.

All concepts were estimated to be in the $200-million-aircraft-worth range for a two-hour turnaround standard (Figure 1-16). These estimates were based on fuel prices derived from a NASA-Lewis-led U.S.

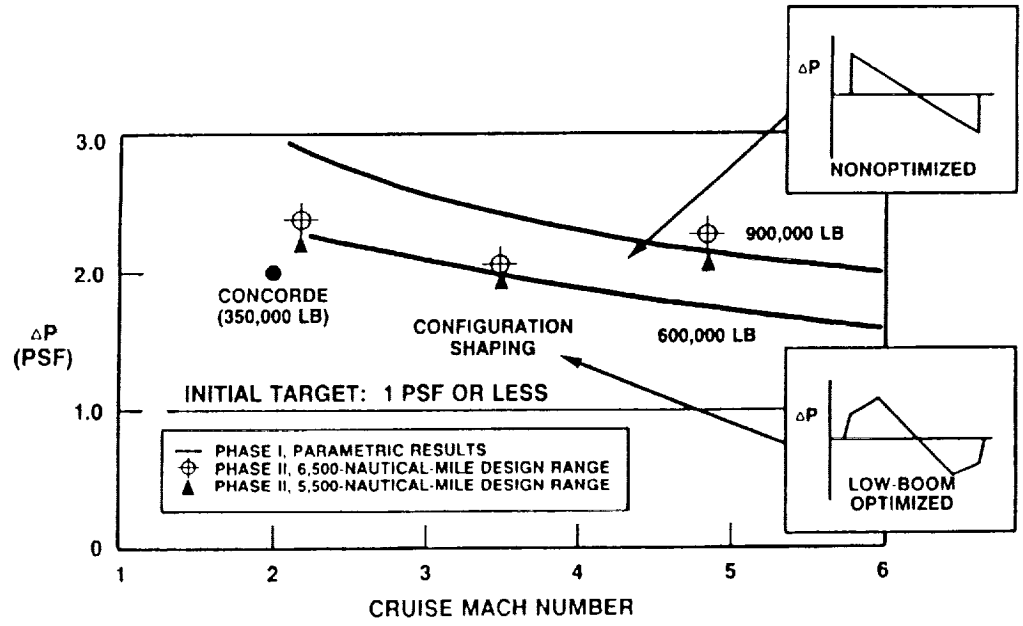

FIGURE 1-15. PHASE II SONIC BOOM GROUND LEVEL OVERPRESSURE

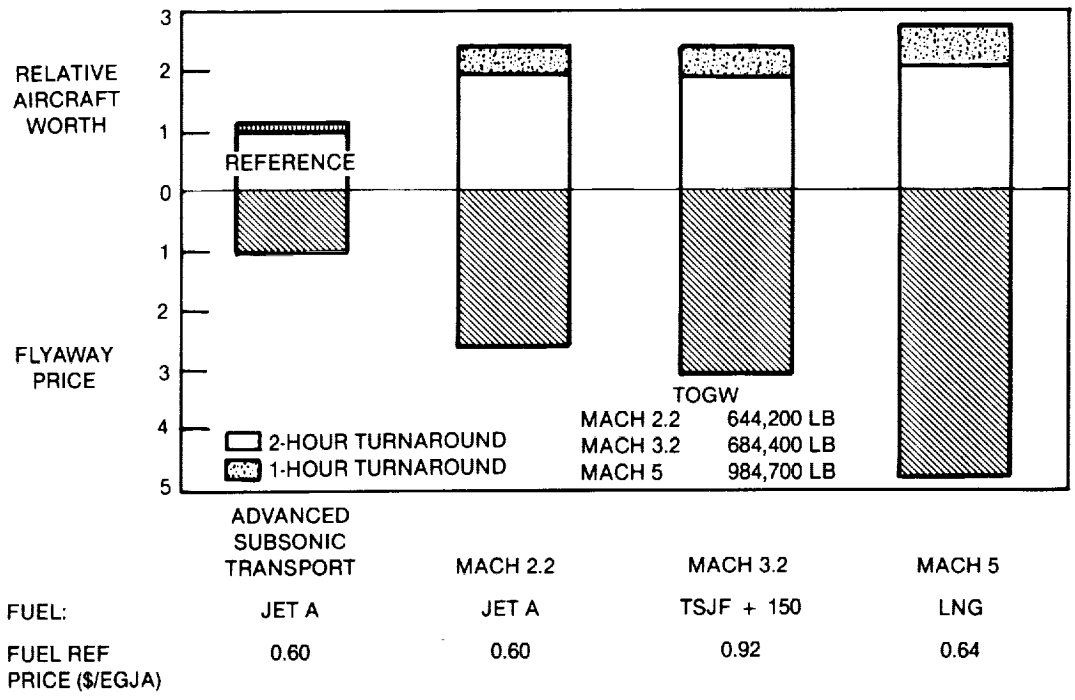

FIGURE 1-16. PHASE II ECONOMIC COMPARISON — 300 SEATS/ZERO FARE PREMIUM

industry-wide fuels workshop. Also included were incremental fuel related costs representing special fuel facilities investments and related operating costs. Flyaway prices varied from $268 million for Mach 2.2 concept, to $316 million for Mach 3.2 concept, to $495 million for Mach 5.0 concept.

The Mach 3.2 and Mach 5.0 concepts were selected for continued refinement and evaluation in Phase III with focus on environmental compatibility since these concepts offered different configurations, cruise altitudes, and fuel types potentially leading to relative advantages in terms of environmental characteristics. The Mach 3.2 concept was selected as the upper-speed limit for kerosene-based fuels. In addition, Phase III would provide the opportunity for an integrated assessment of the NASP technologies (particularly in materials and structures) that was not possible in earlier phases because of the manner of the technology integration (e.g., statistical weight estimation versus component sizing based on loads and temperature predictions).

This Page
Intentionally Left Blank

2.0 TECHNOLOGY INTEGRATION

2.1 Concept Development

The development of the High-Speed Civil Transport benefitted from previous and ongoing related work. This includes the supersonic transport work of the 1960s; the advanced supersonic work (AST) activity of the 1970s including follow-on research by NASA, the Concorde, and the National AeroSpace Plane (NASP).

Through Phases I, II, and III, an advanced subsonic transport (which incorporates projected technology improvements for the year 2000) has been used for economic comparisons. The vehicle features an advanced high-aspect-ratio wing, aft empennage, constant cross-section cabin, advanced systems, and very-high-bypass ducted fan engines burning conventional Jet A fuel. The configuration designation is D0.85-2, as shown in Figure 2-1.

Phase I and II highlighed the importance of technology/commercial value. Phase III technical and market research activity centered on key factors regarding environmental acceptability and commercial value assessment of two differing HSCT candidates: one that cruised at Mach 3.2 and the other that cruised at Mach 5.0. The former used thermally stable jet fuel (TSJF) due to elevated temperatures in cruise; the latter used liquid methane (LNG) fuel.

The HSCT concept development process was based on the establishment of baseline configurations through progressive refinements of earlier studies. The development process incorporated departures from the baseline configurations as required for environmental acceptance. Technical areas with potential for baseline improvements have been identified for future studies.

HSCT prime design objectives are: (1) accommodation of 300 passengers and (2) a design range of 6,500 nautical miles (7,500 statute miles). In addition to passenger baggage, 500 cubic feet of volume is provided for 5,000 pounds of cargo.

In the definition process of a commercially efficient supersonic transport, emphasis has been placed on the following design areas:

- External vehicle shaping – aerodynamic integration with the propulsion system
- Airframe structure – wide range of external and internal temperatures and pressures
- Fuel tank distribution – center of gravity
- Passenger cabin – safety at cruise altitudes, FAA emergency evacuation requirements, and contemporary comfort-level standards
- Landing gear system – acceptable flotation on current international airports
- Safety, reliability, and maintainability – commercial passenger transportation requirements
- Major components and systems – production and assembly

As a U.S. civil aircraft, the HSCT will be certified and operated per FAA code of Federal Regulations (CFR) Title 14, Chapter I. As a transport category airplane, the design and certification will conform to Subchapter C, Part 25, and be operated under Subchapter F, Part 91, and Subchapter G, Part 121.

Mach 3.2. The Phase III baseline configuration D3.2-3A (Figure 2-2) features a double-sweep arrow planform wing, conical-taper single-lobe fuselage, aft vertical and horizontal empennage, four Pratt & Whitney (P&W) duct-burning turbofan engines, TSJF, and a tricycle landing gear. The fuselage was designed to accommodate a nominal seating arrangement of three classes: 10-, 30-, and 60-percent for first, business, and coach classes, respectively. The concept developed was unaffected by constraints for sonic boom optimization. Supersonic drag considerations necessitate use of a varying cabin cross-section. The fuselage incorporates single-lobe shaped cross sections with the width varying according to longitudinal location. The maximum section is determined by a twin aisle with seven-across coach seats – the minimum section is determined by a single aisle, five-across seating arrangement. The maximum section will accommodate six-across first/business-class seats, and the minimum section will hold four-across business-class seats. All seat sizes are consistent with those used on MD-80 and MD-11 aircraft (Figure 2-3).

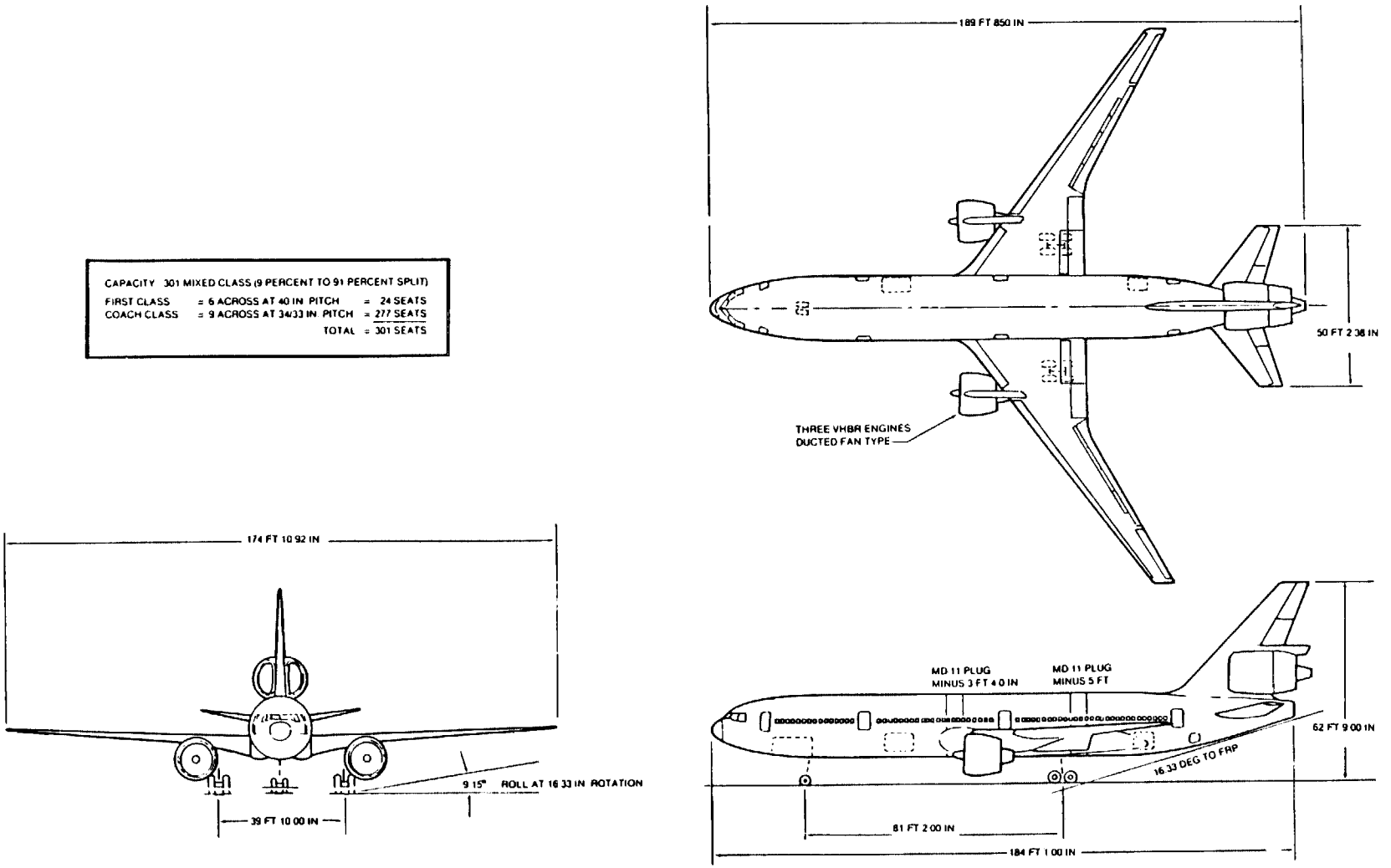

FIGURE 2-1. GENERAL ARRANGEMENT — D0.85-1 CONCEPT

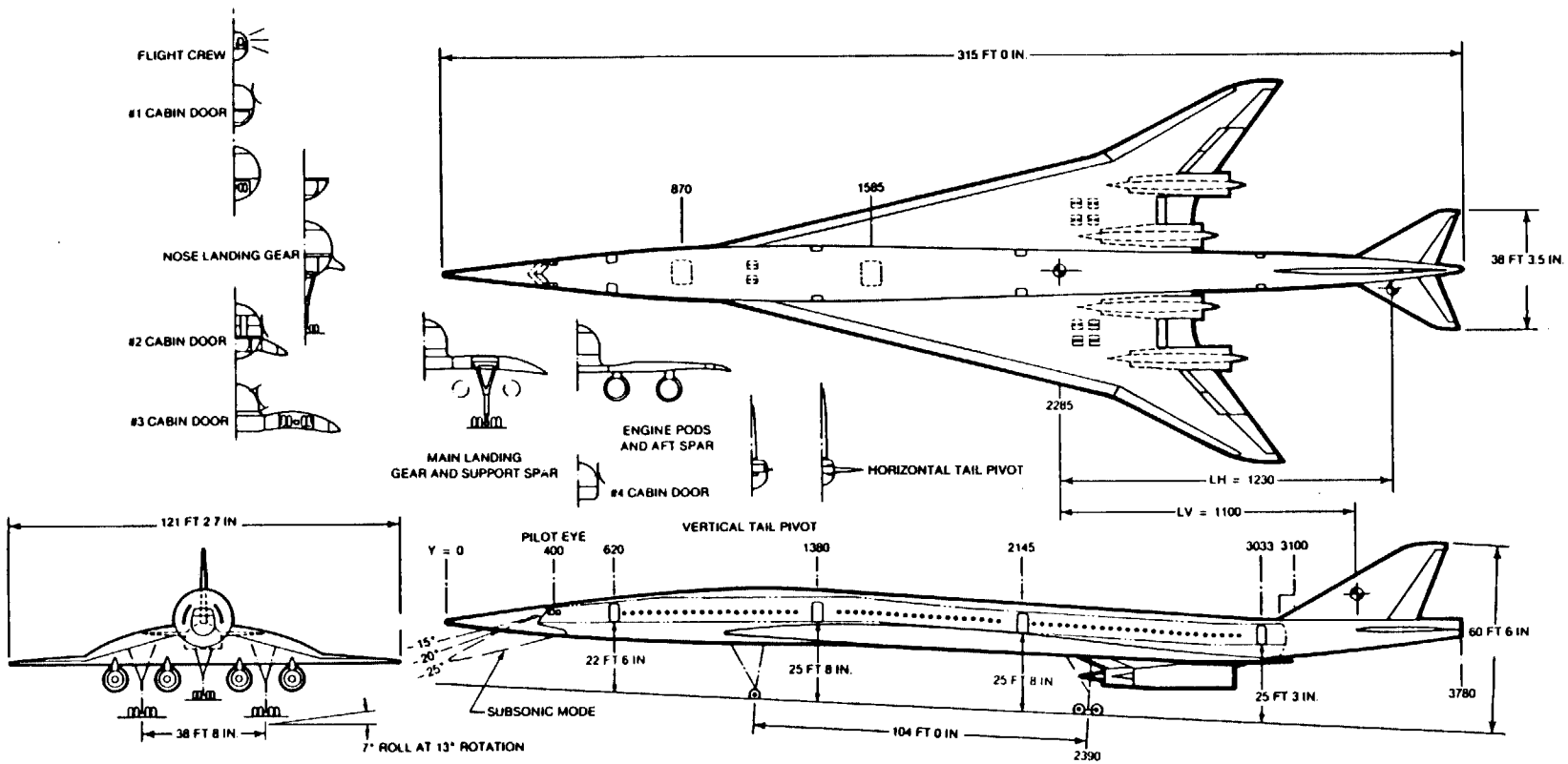

PAYLOAD			
FIRST CLASS	= 10 PERCENT	= 4 ACROSS AT 42 IN. PITCH	= 30 SEATS
BUSINESS CLASS	= 30 PERCENT	= 4-6 ACROSS AT 38 IN. PITCH	= 90 SEATS
COACH CLASS	= 60 PERCENT	= 4-5 ACROSS AT 32 IN. PITCH	= 180 SEATS
TOTAL	= 100 PERCENT		= 300 SEATS

FIGURE 2-2. GENERAL ARRANGEMENT — D3.2-3A CONCEPT

The baseline interior arrangement (Figure 2-4) provides contemporary service for 300 passengers based on a maximum flight duration of five hours. Each class (first, business, and coach) has its own galley, lavatories, coatrooms, and cabin attendant stations. Four cabin doors per side are evenly distributed for rapid evacuation. Adjacent attendant seats are provided. Slide packs are located on each door and deployed over the wing. Cabin windows are incorporated. Five optional interior arrangements have been defined reflecting two- and one-class seating options. Capacities varies from 239 seats in an all-business configuration to 392 seats in an all-coach class configuration (Figure 2-5).

The production breakdown for the baseline configuration (Figure 2-6) was utilized in estimating development and production cost. Modules are dimensionally sized at a structural splice break.

A major environmental issue lies in the affect on the ground of the sonic boom resulting from supersonic cruise flight. Two design concepts were developed: one for supersonic cruise over land and the other for subsonic cruise over land. A derivative of the baseline configuration was developed to increase performance efficiency during subsonic flight over land. This concept, configuration D3.2-4B, incorporates a wing planform modified to increase the span and reduce the leading edge sweep of the outer wing panels (Figure 2-7). In both situations, it is assumed that all overwater flights are supersonic.

The D3.2-3A baseline incorporates a cabin structure with conventional safelife characteristics. Concern about rapid decompression at high-cruise altitudes has led to another avenue of study – the fail-safe concept. The fail-safe airframe is one where the pressure cabin is independent of the primary airframe. Thus, a primary panel failure would not affect the pressure cabin integrity (Figure 2-8).

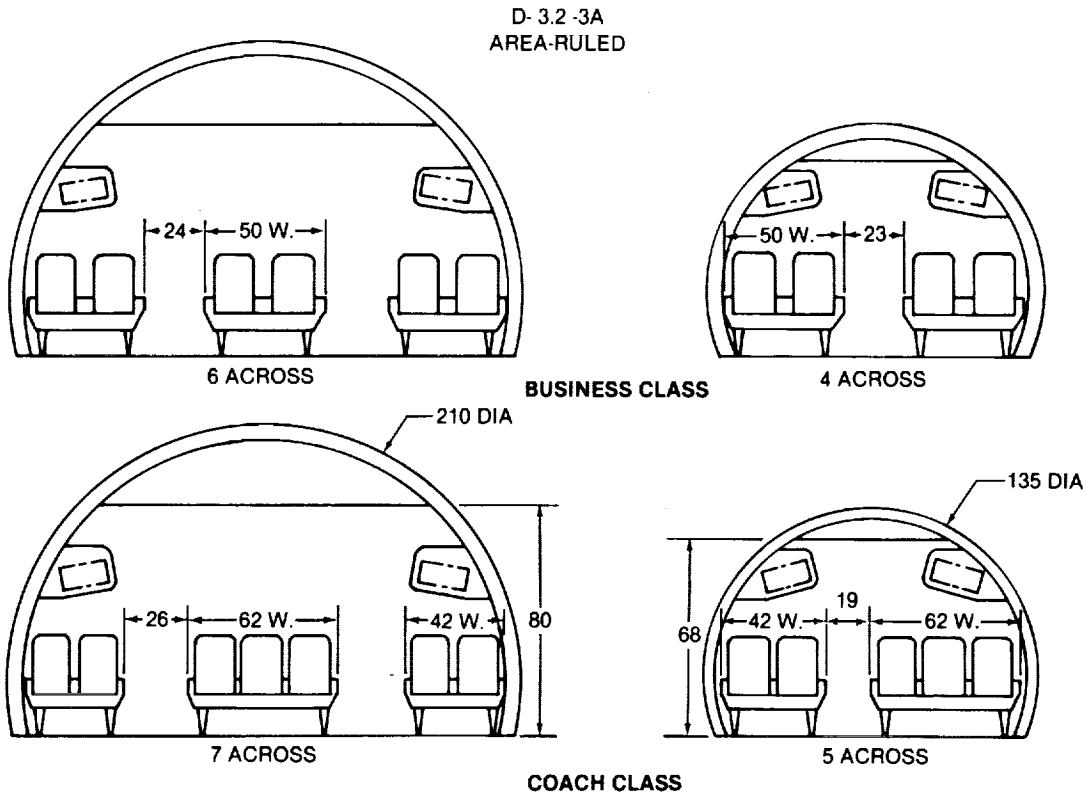

FIGURE 2-3. CABIN SECTIONS

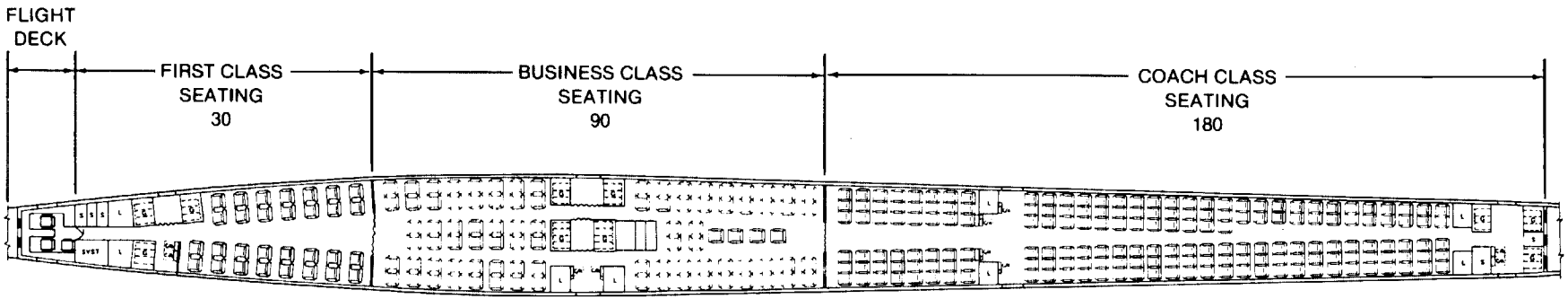

GALLEY CART = 32
LAVATORY = 10
COAT ROOM = 150 IN.
ATTENDANT = 10

FIGURE 2-4. D3.2-3A CONCEPT BASELINE INTERIOR

SEATING, CLASS SPLIT, PERCENT			TOTAL SEATING
FIRST	BUSINESS	COACH	
0	100	0	239
0	66	34	306
0	50	50	291
0	40	60	278
0	0	100	392

FIGURE 2-5. PAYLOAD COMPARTMENT

Mach 5.0. The D5.0-15A baseline configuration (Figure 2-9) features a highly swept delta planform with a buried internal passenger cabin. The upper surface is dictated by the internal cabin section and faired in straight line elements to the tip chord. Twin vertical tails are located outboard of and adjacent to the horizontal tip pitch/roll control surfaces. The single propulsion pod contains four GE vari-cycle hyper jet engines (VCHJ). The propulsion system is highly integrated with the forebody and inlet and with nozzle in the aft body. The landing gear has twin nose struts with dual wheels, and the main gear has two struts with 12 wheels each. Liquid methane fuel tanks are multilobe-type arranged longitudinally and symmetrically around the center of gravity and are outboard of the pressurized cabin. The primary structure, cabin, and fuel tanks are structurally independent. The airframe utilizes the fail-safe concept with the pressure cabin independently suspended from longitudinal trusses.

The cabin cross section is a double-lobe type providing for twin aisles and eight-across coach seats, thereby minimizing frontal area and volume. The minimum 18-inch aisle width and 85-inch aisle height accommodates passenger space requirement within at least the 95 percentile. Seat widths are similar to MD-80/MD-11 size (i.e., 42-inch double-seat assembly for coach class). Overhead stowage bins are capable of two cubic feet per passenger. Lower cargo bays are sized for multi-shelf containers. Centerline structure is kept open by using individual stanchions.

The baseline interior arrangement has three-class split consisting of 10-percent first class, 30-percent business class, and 60-percent coach class. Each class section has its own lavatories, galley, coatroom, and cabin attendants. Three type A cabin doors per side lead to vertical entry/exit chutes. Cabin attendants seats are adjacent to each door. No cabin windows are provided. Galley service is provided using carts for flight of three hours duration.

To provide realistic weight and production cost evaluations, a baseline configuration production breakdown was defined, as shown in Figure 2-10. Each module has been dimensionally sized at a structural splice break. These elements are useful in establishing a basis for cost-sharing in the development/production phase of the program.

A major environmental issue is in the effect of sonic boom resulting from supersonic flight. Two basic operational approaches have been investigated: supersonic cruise flight over both land and water, and subsonic cruise flight over land and supersonic cruise flight over water.

2.2 Aerodynamics

The following sections describe the aerodynamic analysis performed on the concepts considered in Phase III: the Mach 0.85 concept, the two Mach 3.2 concepts (D3.2-3A and D3.2-4B), and the Mach 5.0 concept (D5.0-15A). Several operational approaches were considered: the D3.2-3A was evaluated for both

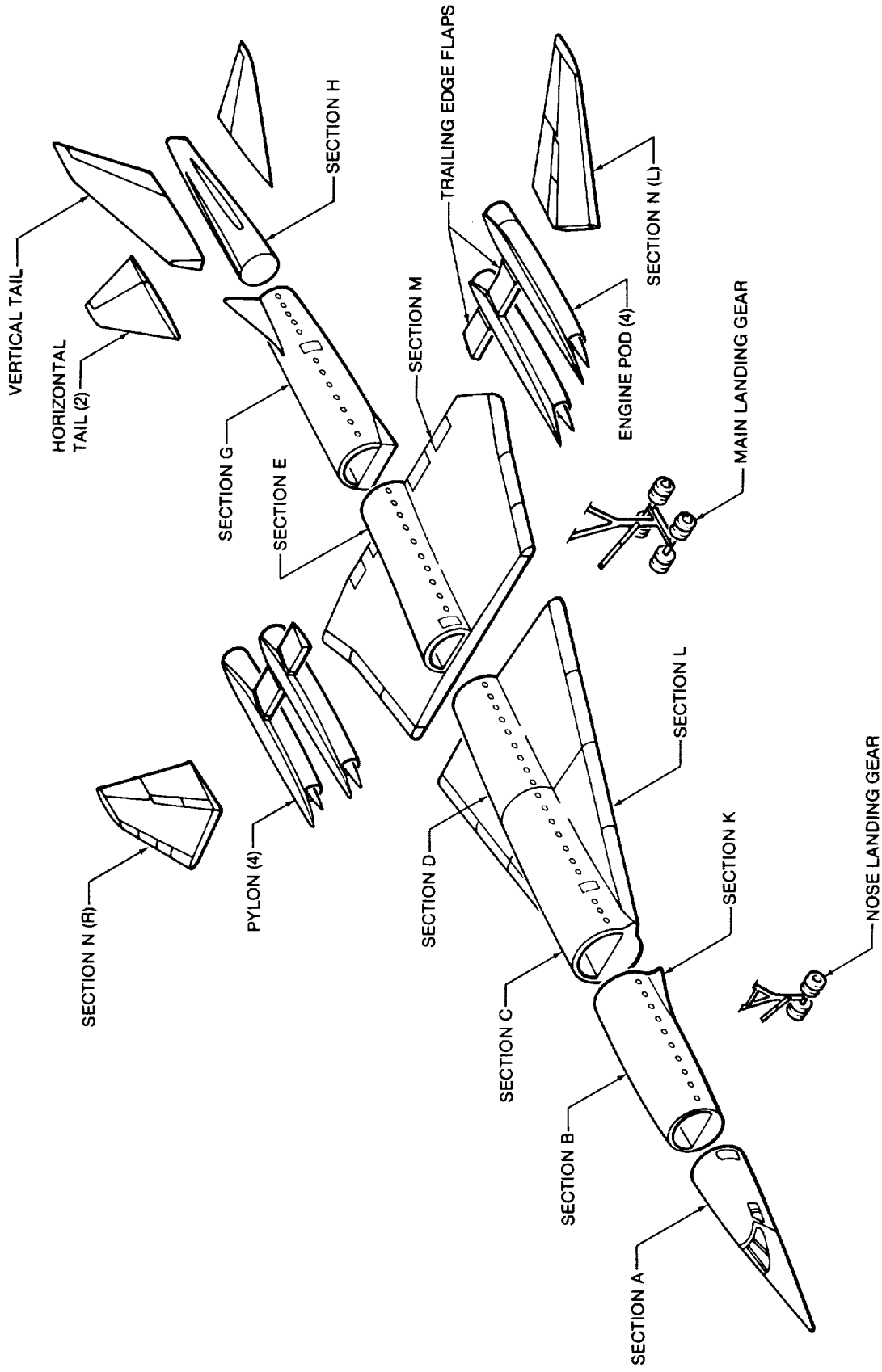

FIGURE 2-6. D3.2-3A CONCEPT PRODUCTION BREAKDOWN

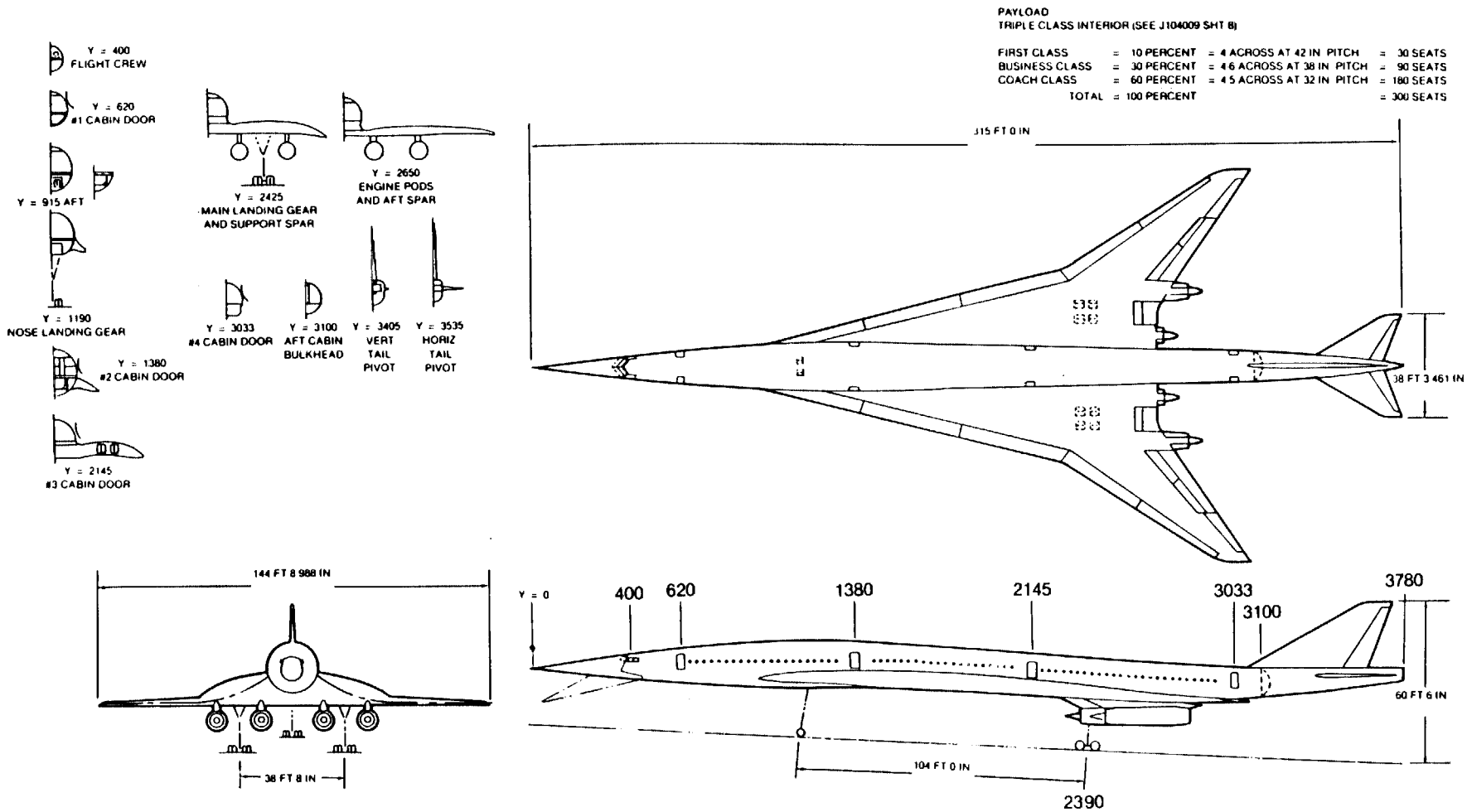

FIGURE 2-7. GENERAL ARRANGEMENT — D3.2-4B CONCEPT

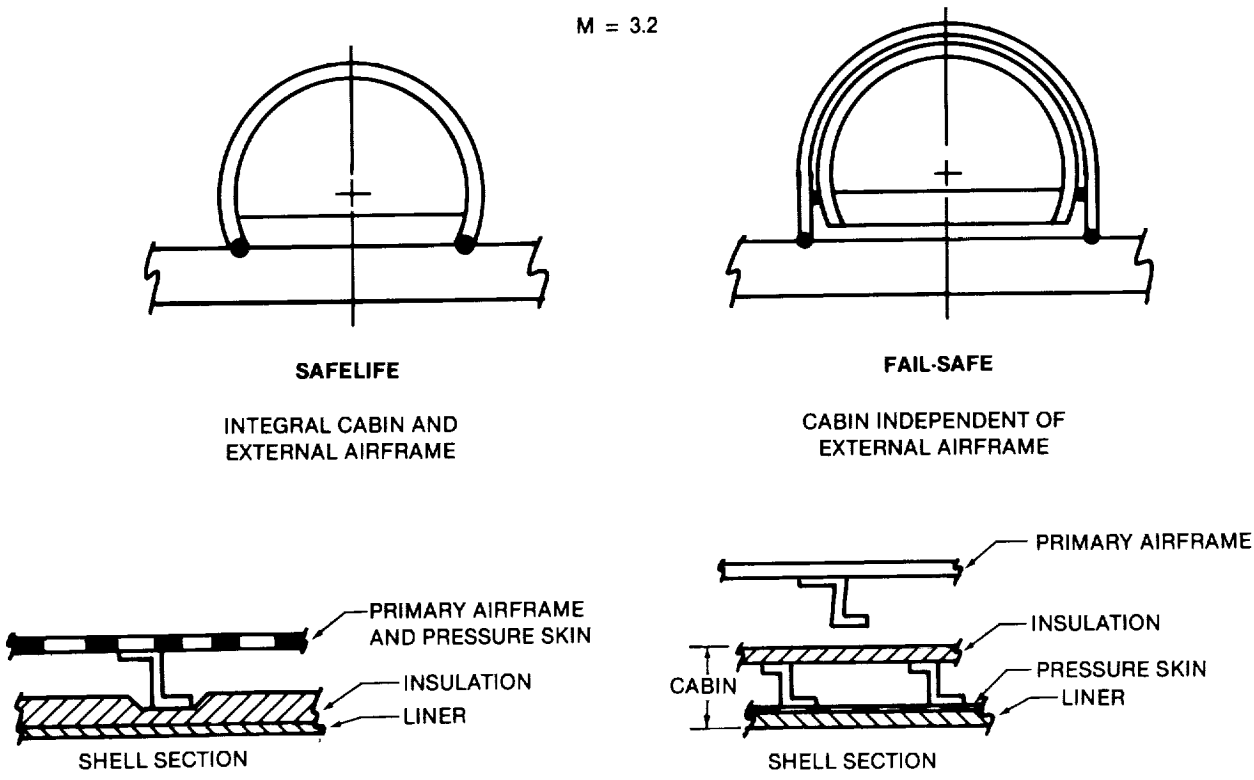

FIGURE 2-8. CABIN STRUCTURE PHILOSOPHY

supersonic and subsonic cruise, the D3.2-4B was evaluated for a subsonic cruise over land, and the D5.0-15A was evaluated for both supersonic and subsonic cruise over land. This section addresses the primary design features, thrust-drag bookkeeping methods, skin-friction analysis, and the low-speed, transonic, and high-speed aerodynamics analyses. Table 2-1 summarizes the aerodynamic characteristics of all three HSCT concepts.

Mach 0.85. The final Mach 0.85 concept (Figure 2-1) was based on Douglas Aircraft Company's development work for the MD-11. It employs a shortened MD-11 fuselage for consistency with a 300-passenger, two-class interior and an all new advanced supercritical high aspect ratio wing. This concept had a reference trapezoidal wing area of 2,680 square feet, and an adjusted wing area of 3,143 square feet. The trapezoidal aspect ratio was 11.41, the adjusted aspect ratio was 9.73, and the trapezoidal taper ratio was 0.242. The quarter-chord sweep was 35.75 degrees and the span was 174.92 feet. The high-lift system consisted of single-segment fowler-motion flaps. Riblets were applied to the wing lower surface, the tail, the fuselage, and nacelles. A hybrid laminar flow control system was included. Suction was applied up to the wing front spar on the upper wing surface only. The trimmed lift-to-drag ratio for the concept was 21.5, including a 9-percent benefit for laminar flow control.

Mach 3.2. Douglas Aircraft Company's final Phase III, Mach 3.2 concept, D3.2-3A (Figure 2-2), was based on the design work conducted for the 1979 AST (Advanced Supersonic Transport), developed under joint NASA/McDonnell Douglas funding. The basic arrow-wing AST planform was modified with increased leading- and trailing-edge sweep to improve supersonic performance at Mach 3.2 cruise. The final Phase III wing design had a planform reference area of 9,500 square feet, an aspect ratio of 1.547, an inboard leading edge sweep of 76 degrees, a sweep break at 65-percent span, and an outer panel leading edge sweep of 62 degrees.

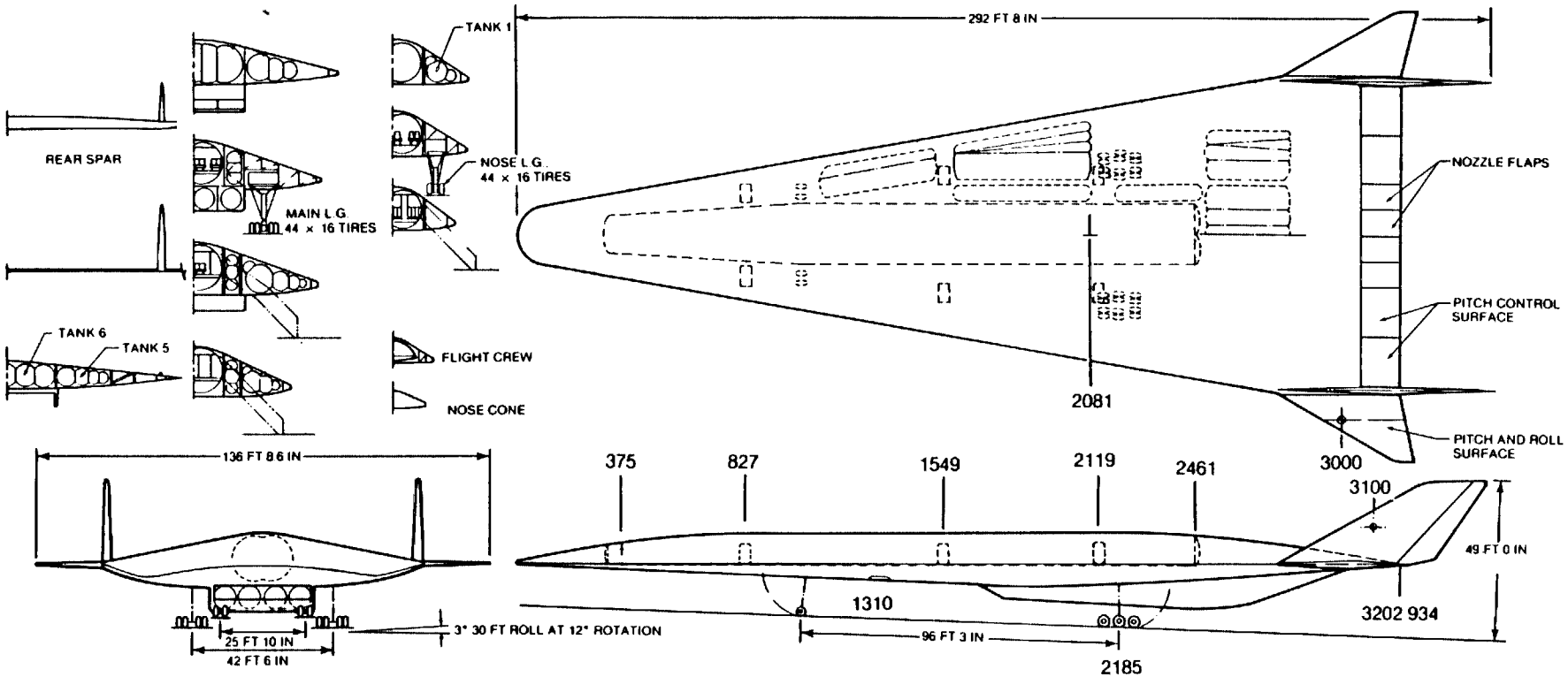

PHASE II BASELINE

PAYLOAD
3-CLASS INTERIOR

FIRST CLASS	= 4 ACROSS AT 42 IN PITCH	=	30 SEATS
BUSINESS CLASS	= 6 ACROSS AT 38 IN PITCH	=	90 SEATS
COACH CLASS	= 8 ACROSS AT 32 IN PITCH	=	180 SEATS
	TOTAL	=	300 SEATS

FIGURE 2-9. GENERAL ARRANGEMENT — D5.0-15A CONCEPT

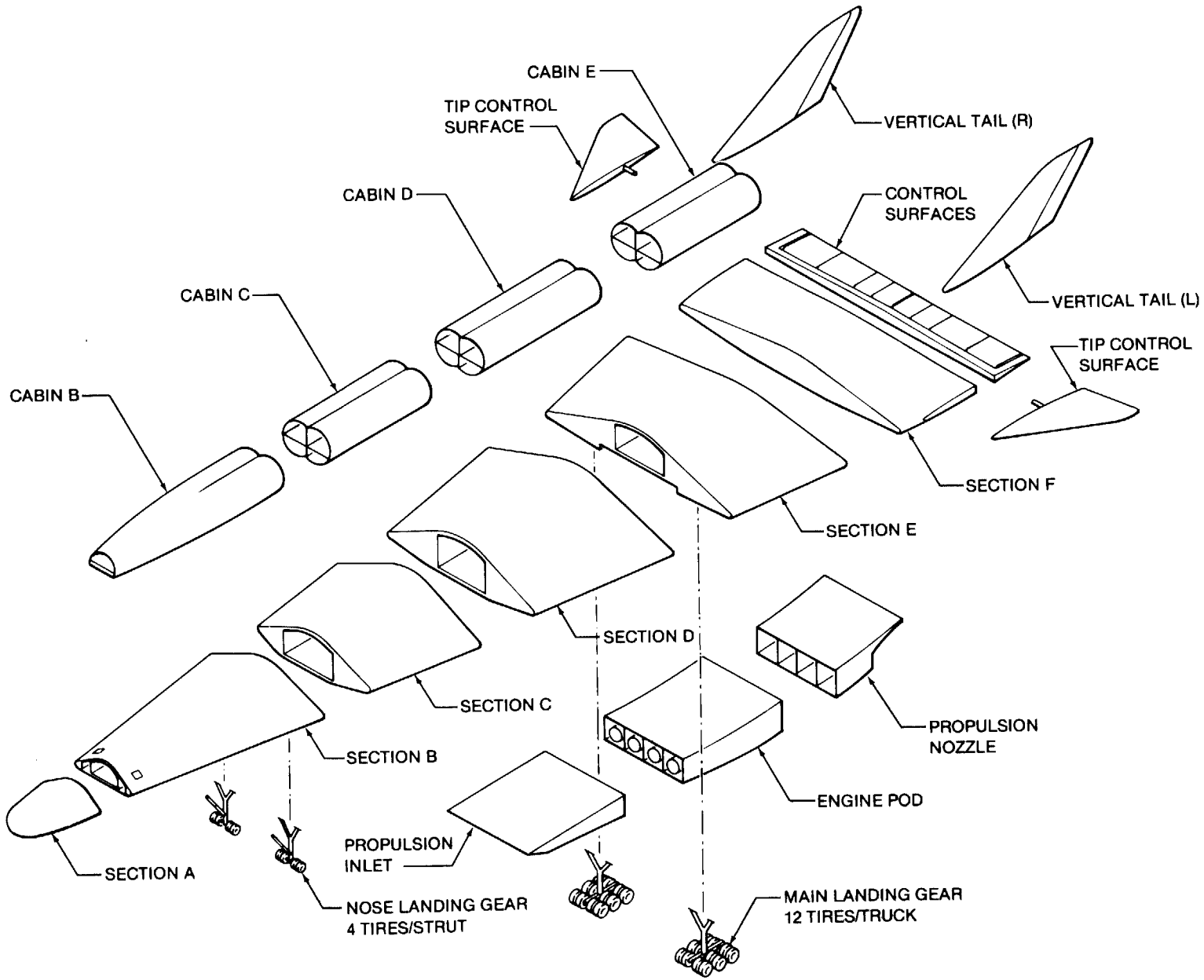

FIGURE 2-10. D5.0-15A CONCEPT PRODUCTION BREAKDOWN

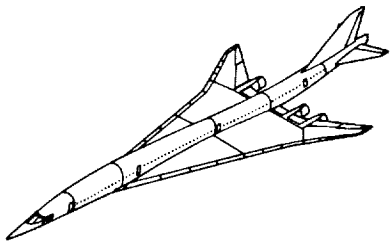

D3.2-3A

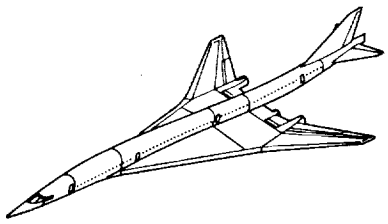

D3.2-4B

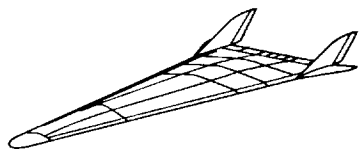

D5.0-15A

TABLE 2-1
AERODYNAMIC CONFIGURATION SUMMARY

CONFIGURATION	D-3.2-3A	D-3.2-4B	D-5.0-15A
REFERENCE AREA	9,500	9,500	17,000
ASPECT RATIO	1.547	2.206	1.0995
LEADING EDGE SWEEP	76°/62°	76°/57°	80°/60°
SPAN BREAK (%)	0.65	0.49	0.65
HIGH LIFT DEVICES	LEADING EDGE FLAPS TRAILING EDGE PLAIN FLAPS	LEADING EDGE FLAPS TRAILING EDGE PLAIN FLAPS	TRAILING EDGE PLAIN FLAPS

The wing camber was optimized for a maximum wing-body trimmed lift-to-drag ratio at cruise for C_L = 0.091. The wing thickness distribution was based on previous AST studies.The wing airfoil is a modified NACA 64 series airfoil inboard of the planform break and a biconvex section outboard of the planform break. The fuselage area distribution and camber were optimized to result in a minimum wave drag due to volume at Mach 3.2 cruise conditions. The resulting Mach 3.2 area distribution is shown in Figure 2-11. The engine nozzles were set 8 degrees down from the zero-lift angle to minimize the trim drag penalty.

The high-lift system consisted of plain, trailing-edge flaps and full-span, simple-drooped leading-edge flaps, which were developed and tested during the AST studies (Figure 2-12). The nacelles were staggered for minimizing wave drag. Laminar flow control was included in the D3.2-3A baseline concept and aerodynamic analysis. Inboard of the wing planform break, the laminar flow control suction region was limited by the fuel tank boundaries. Outboard of the planform break, suction was applied up to the flap hinge line. Suction regions are illustrated in Figure 2-13.

Control surfaces required for D3.2-3A are illustrated in Figure 2-14 (Reference 2-1). Longitudinal control and trim capability were provided by a totally movable horizontal surface with a geared elevator. Four separate elevator panels were used to provide redundancy. Ailerons and multiple spoiler panels provided lateral control. Directional control was provided by a rudder, divided into three segments for redundancy.

Stability and control augmentation was required on all axes. On the longitudinal axis, negative stability margins as high as 10 percent were allowed. To prevent exceeding these margins, a fuel management system was required. In addition, pitch-up compensation (Figure 2-15) was required at low speeds and high angles of attack. This system monitored the angles of attack and supplied the necessary longitudinal control

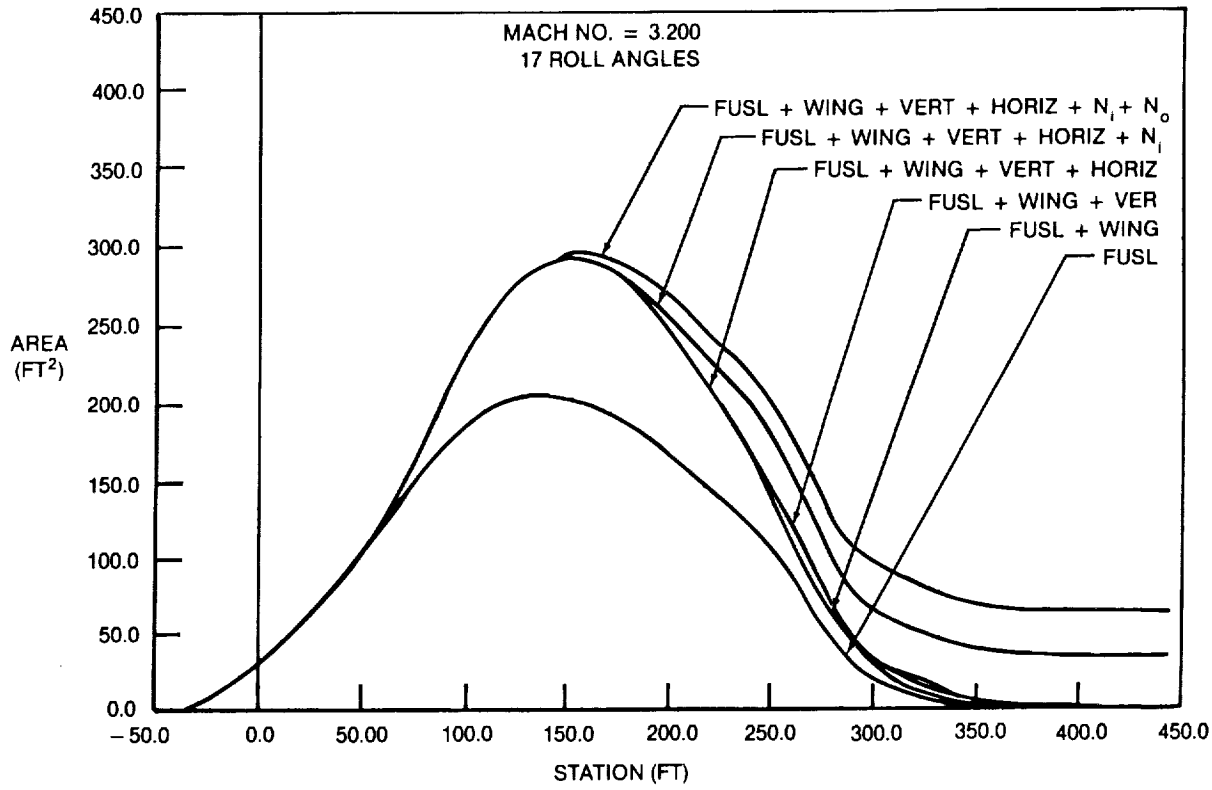

FIGURE 2-11. D3.2-3A AREA DISTRIBUTION AT MACH 3.2

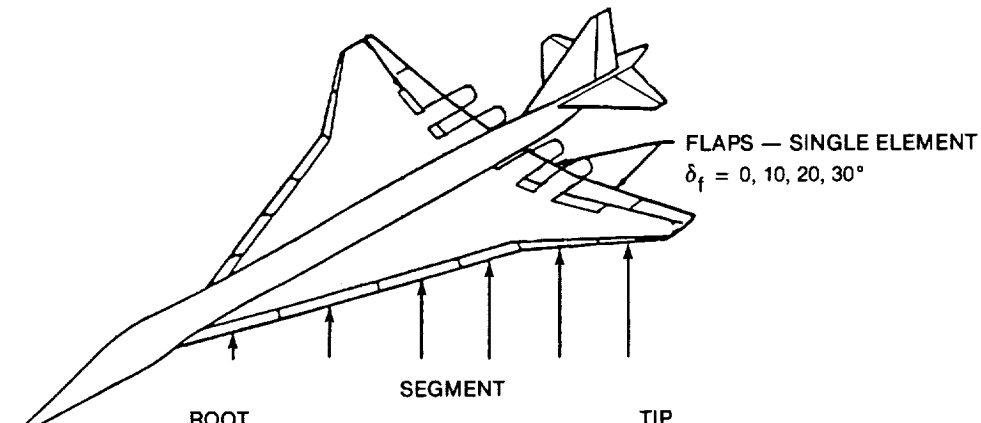

SCHEDULE	1	2	3	4	5	6
CLEAN	0	0	0	0	0	0
R	13	34	35	35	19	29

LEADING EDGE FLAP DEFLECTION SCHEDULES

FIGURE 2-12. HIGH LIFT SYSTEM FOR D3.2-3A AND D3.2-4B CONCEPTS

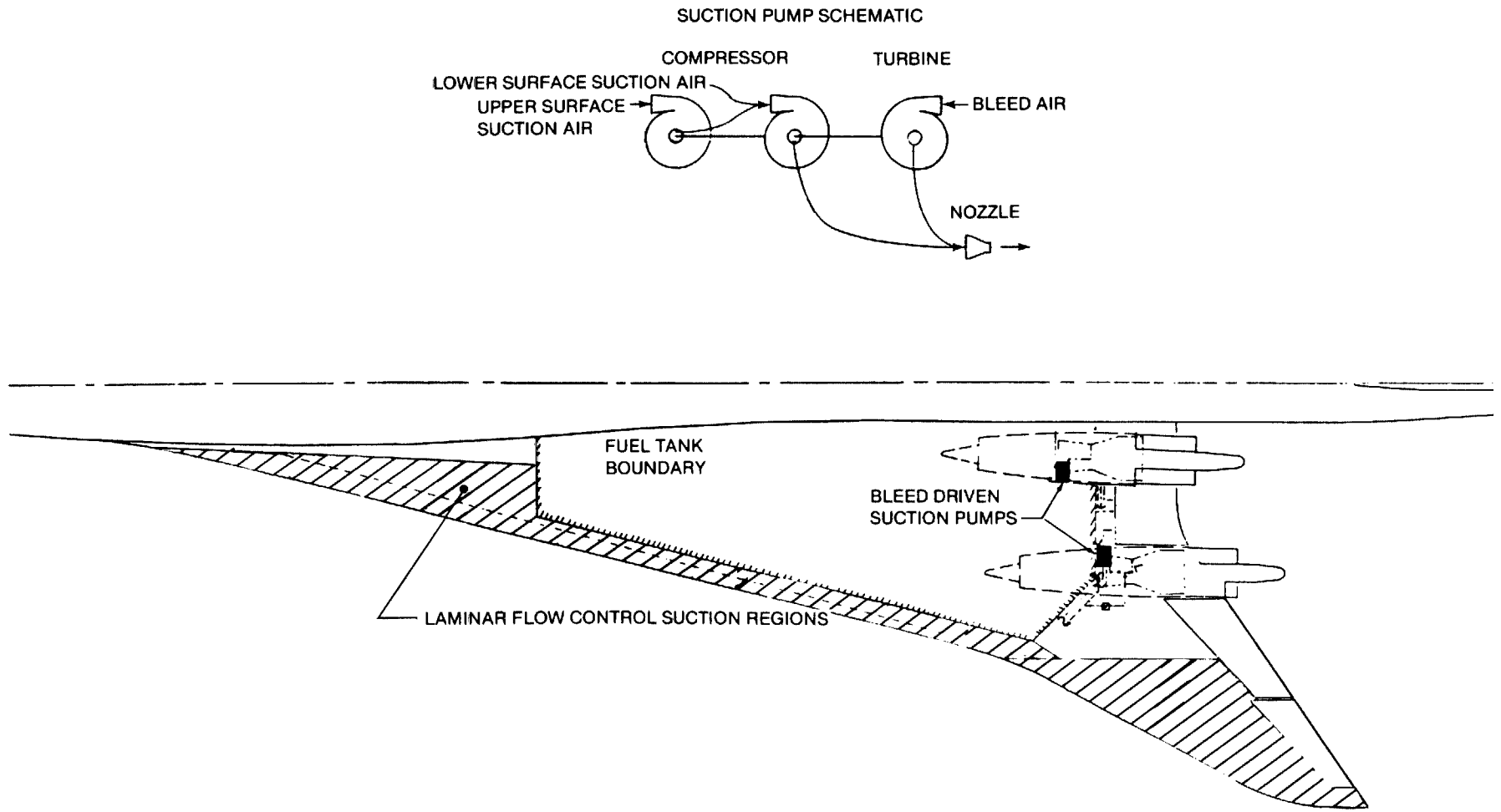

FIGURE 2-13. LAMINAR FLOW CONTROL SUCTION REGION — D3.2-3A CONCEPT

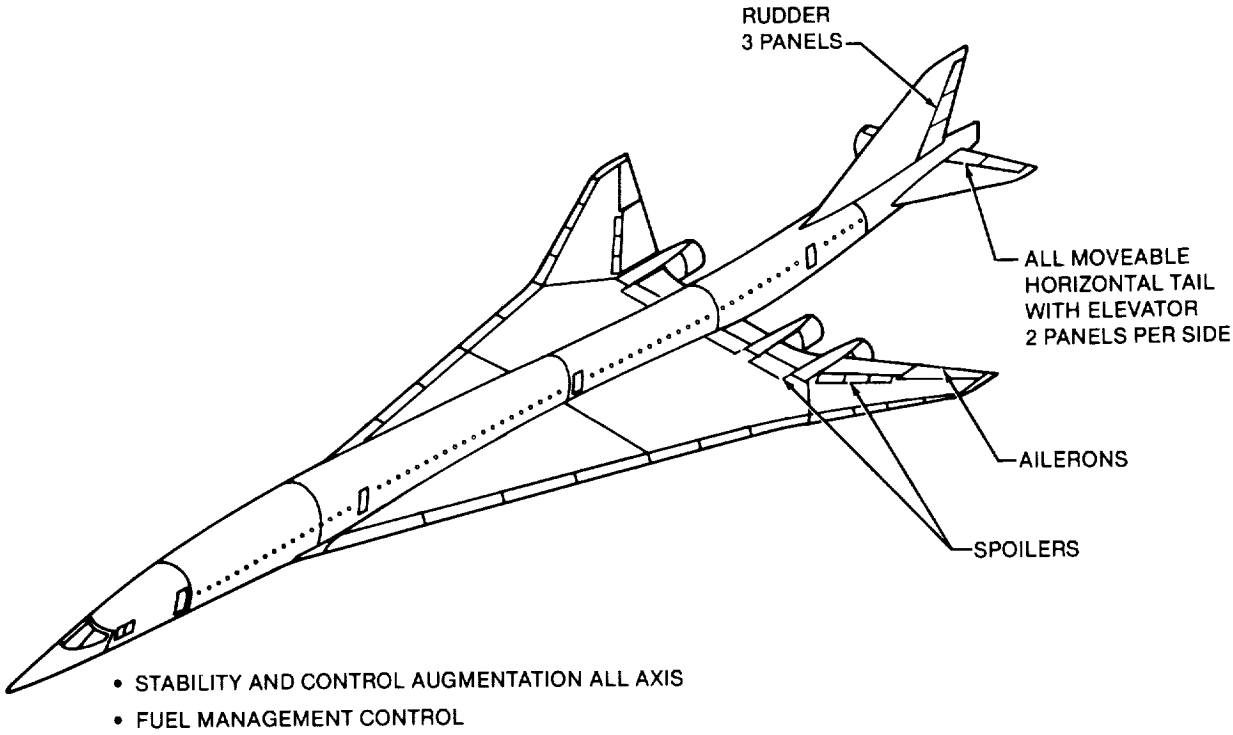

FIGURE 2-14. D3.2-3A CONCEPT CONTROL SYSTEM DESIGN FEATURES

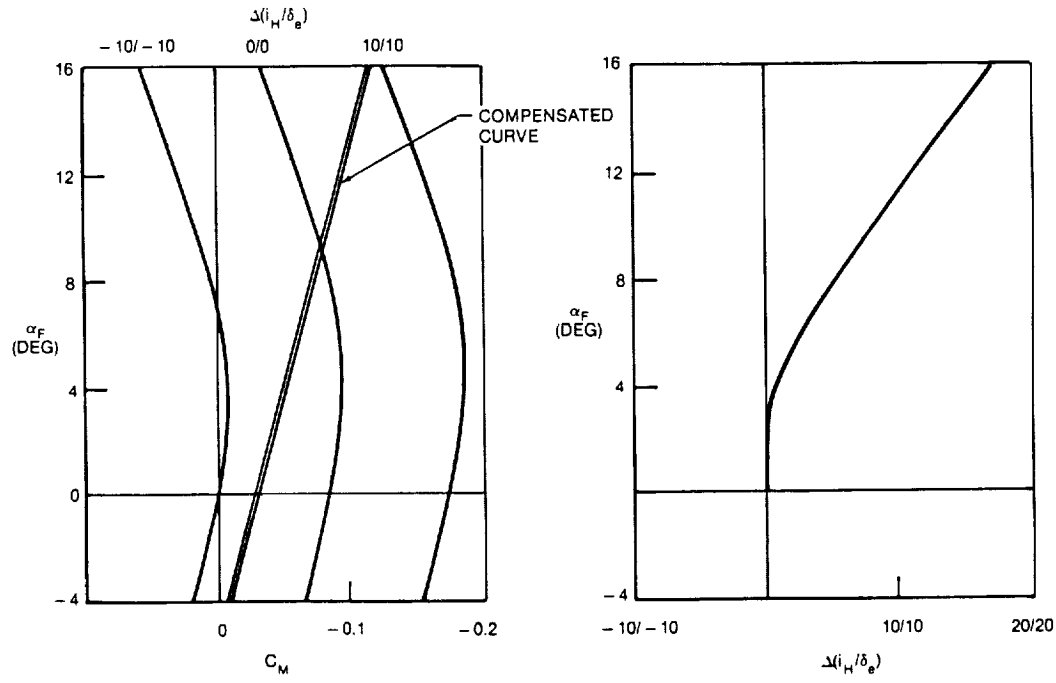

FIGURE 2-15. D3.2-3A CONCEPT LOW-SPEED PITCH-UP COMPENSATION

deflections required to remove any pitch-up tendency. Lateral/directional augmentation was required for dutch roll damping as well as compensation for yawing caused by inlet or engine malfunction.

The division of the airframe and propulsion system forces for the Mach 3.2 concept was as follows: The pitching moments caused by inlet ram drag and nozzle gross thrust were included in the trim drag analysis; the inlet and nozzle losses, along with the nacelle skin-friction drags, were included with the engine performance. To obtain the correct evaluation of fuel flows the mission analysis program used lift versus thrust required rather than lift versus drag.

Skin friction analysis for D3.2-3A, including the effect of LFC, is based on Reynolds number and flat plate skin-friction drag coefficients across the entire Mach range. Figure 2-16 shows the assumed turbulence spread angle from the fuselage as a function of Mach number. Figure 2-17 defines the extent of the laminar

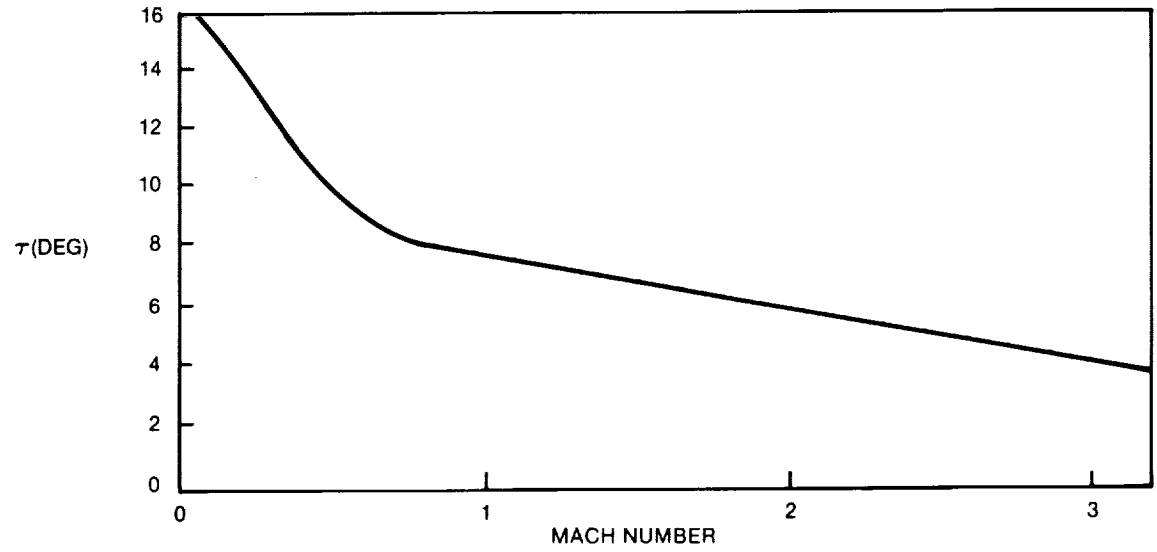

FIGURE 2-16. TURBULENCE SPREAD ANGLE

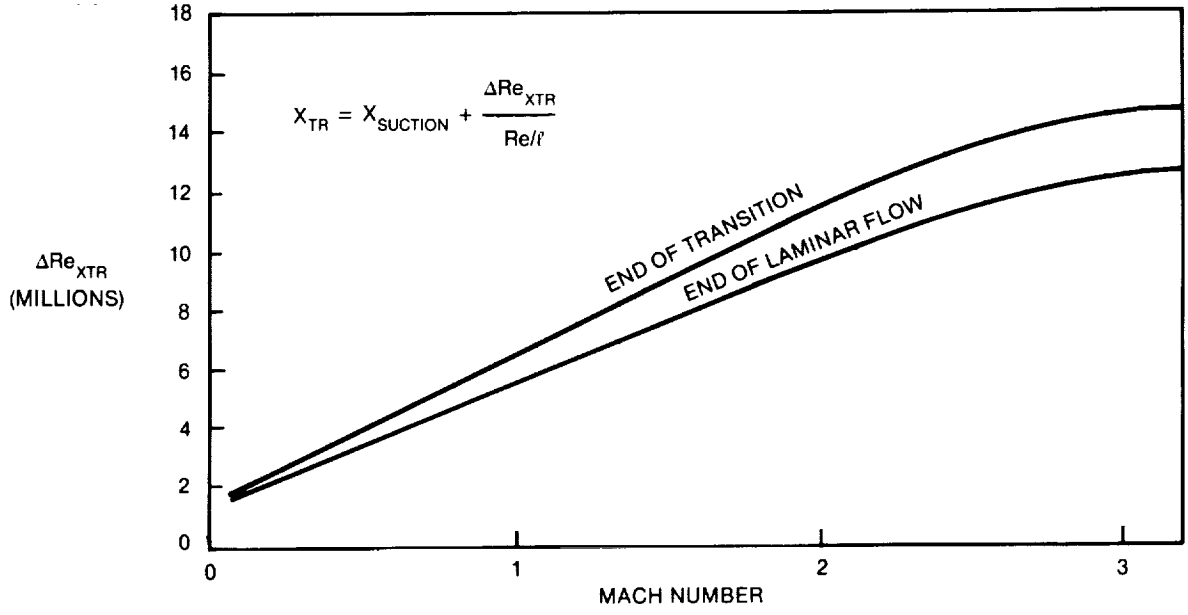

FIGURE 2-17. TRANSITION REYNOLDS NUMBER INCREMENT (FLAT ROOFTOP)

run past the end of the suction region and the start of fully turbulent flow after the transition region, as a function of Mach number. The laminar-flow transition pattern for D3.2-3A is shown in Figure 2-18. Subsonically, the flow on both the upper and lower surfaces was laminar inboard of the wing leading-edge sweep break. Subsonically, the flow on the outboard panel on the lower surface was maintained laminar, but the flow on the upper surface was turbulent. Supersonically, the flow on both the inboard and outboard panels was maintained laminar for both the upper and lower surfaces.

Low-speed aerodynamic data are based on the results of the previous AST wind tunnel tests (Reference 2-1). The test data were adjusted to account for the change in skin friction and aspect ratio. Figure 2-12 shows the two configurations considered: (1) clean leading edge, and (2) leading-edge flap deflection schedule R. Landing gear drag used for D3.2-3A takeoff performance analysis was based on DC-10 data.

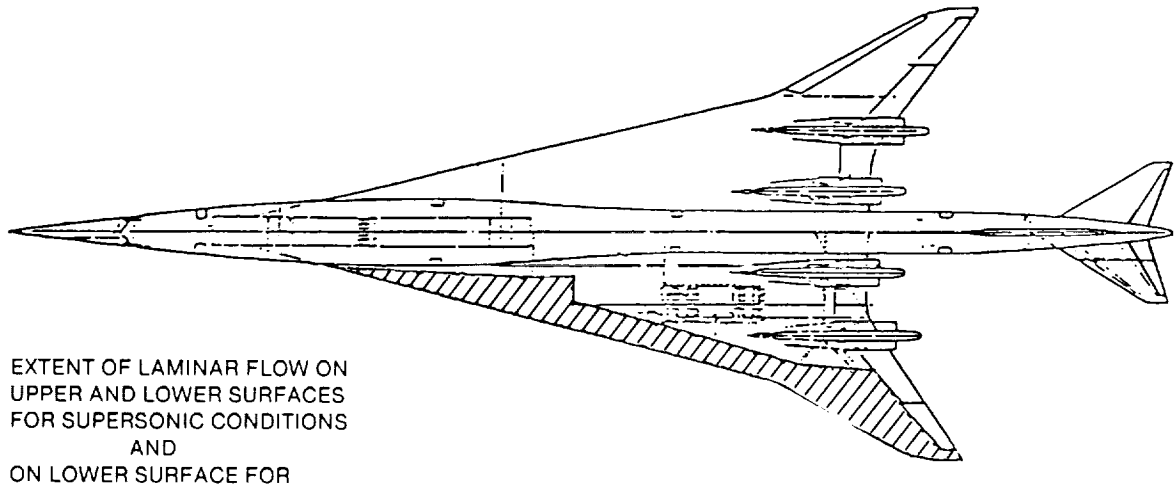

EXTENT OF LAMINAR FLOW ON
UPPER AND LOWER SURFACES
FOR SUPERSONIC CONDITIONS
AND
ON LOWER SURFACE FOR
SUBSONIC CONDITIONS

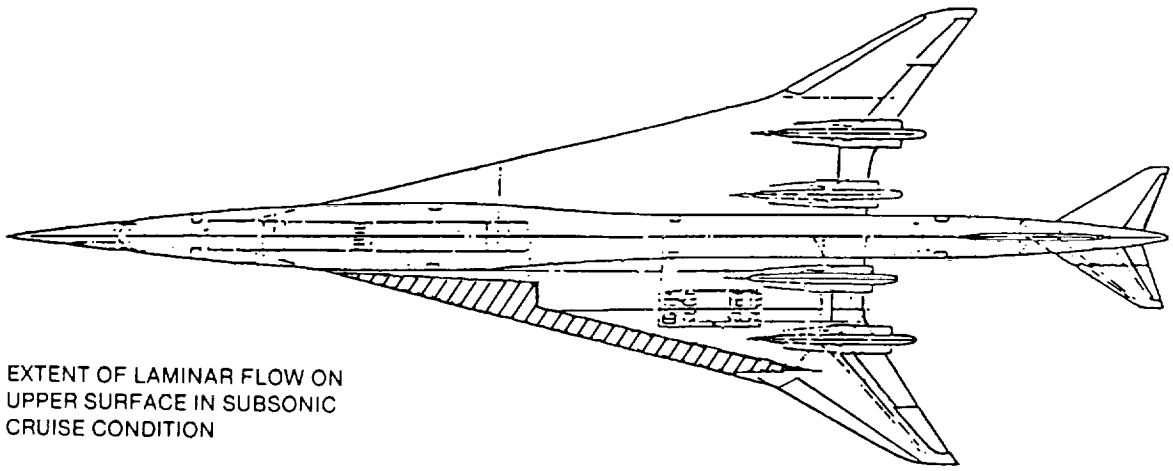

EXTENT OF LAMINAR FLOW ON
UPPER SURFACE IN SUBSONIC
CRUISE CONDITION

FIGURE 2-18. EXTENT OF LAMINAR FLOW FOR D3.2-3A CONCEPT

Transonic aerodynamics characteristics for D3.2-3A were obtained by scaling the AST data for aspect ratio and adjusting for skin friction. The untrimmed aerodynamic data were then corrected to trimmed values using a nonplanar trim program that includes engine thrust effects.

The supersonic lift-dependent drag was calculated by the Woodward (linear theory) program (Reference 2-2). Wave drag due to volume was evaluated using the wave drag capability of the Hypersonic Arbitrary Body Program (HABP), (Reference 2-3). High-speed drag is broken down into: a skin-friction component, the wave drag due to volume, an induced-drag term including the wave drag due to lift, and trim drag.

The trimmed low-speed lift-to-drag curves for the clean leading edge and leading-edge schedule R are shown in Figures 2-19 and 2-20, respectively. The maximum trimmed cruise lift-to-drag ratio of D3.2-3A is shown in Figure 2-21 for the subsonic and supersonic flight profiles over land. The difference in the subsonic lift-to-drag ratios was due only to the dissimilar skin friction drags. The lower viscous drag at any particular subsonic Mach number for the supersonic flight profiles over land was caused by a higher Reynolds number (i.e., lower altitude) than the subsonic flight profile over land. Supersonically, the implied flight trajectories were assumed to be identical, and the climb schedule altitude mismatch around Mach 1.0 was neglected. Figure 2-22 shows the drag breakdown at the cruising Mach number of 3.2, including the induced and viscous drags, the LFC benefit, and the wave drag due to volume. All other terms (camber, interference, and trim drags) were included in the miscellaneous drag term. Thrust effects attributable to vectoring the nozzles 8 degrees were included in the performance analysis inputs.

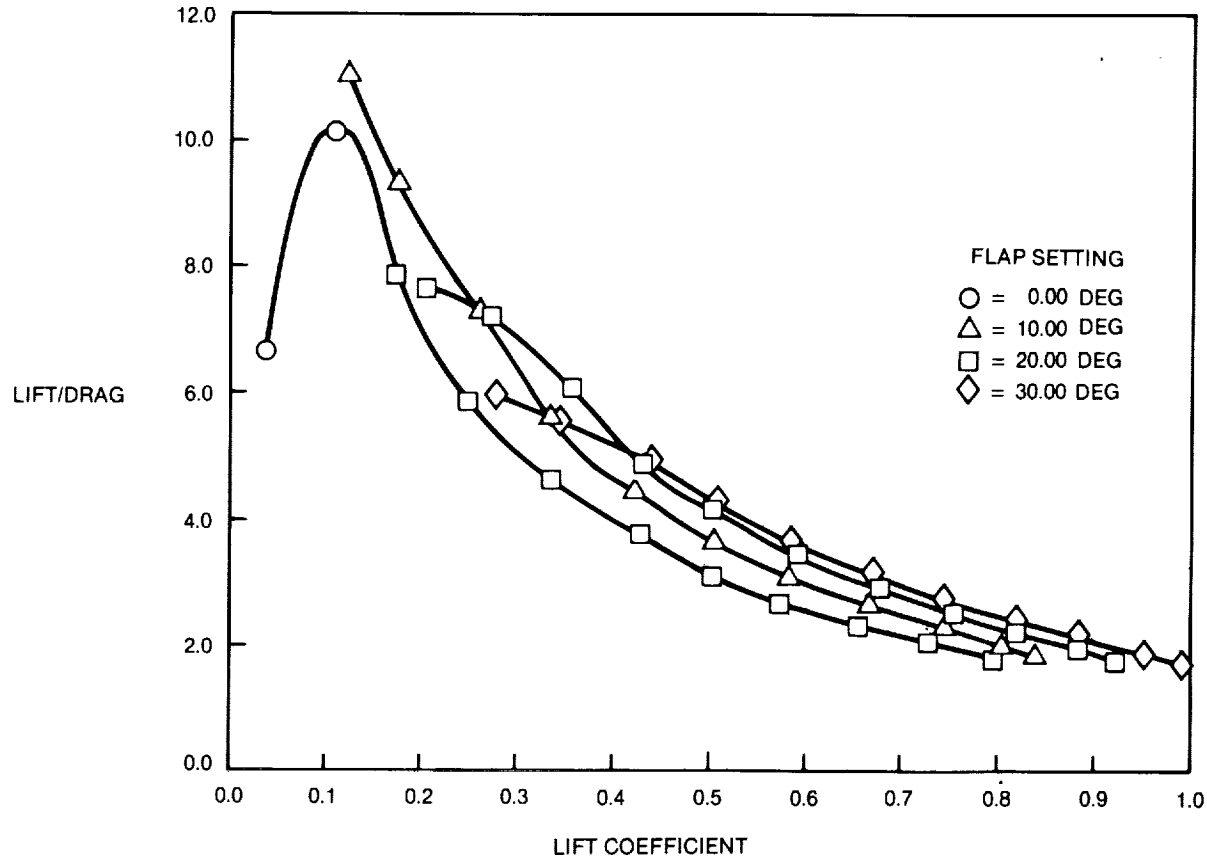

FIGURE 2-19. TRIMMED LOW-SPEED LIFT/DRAG — D3.2-3A CONCEPT CLEAN LEADING EDGE

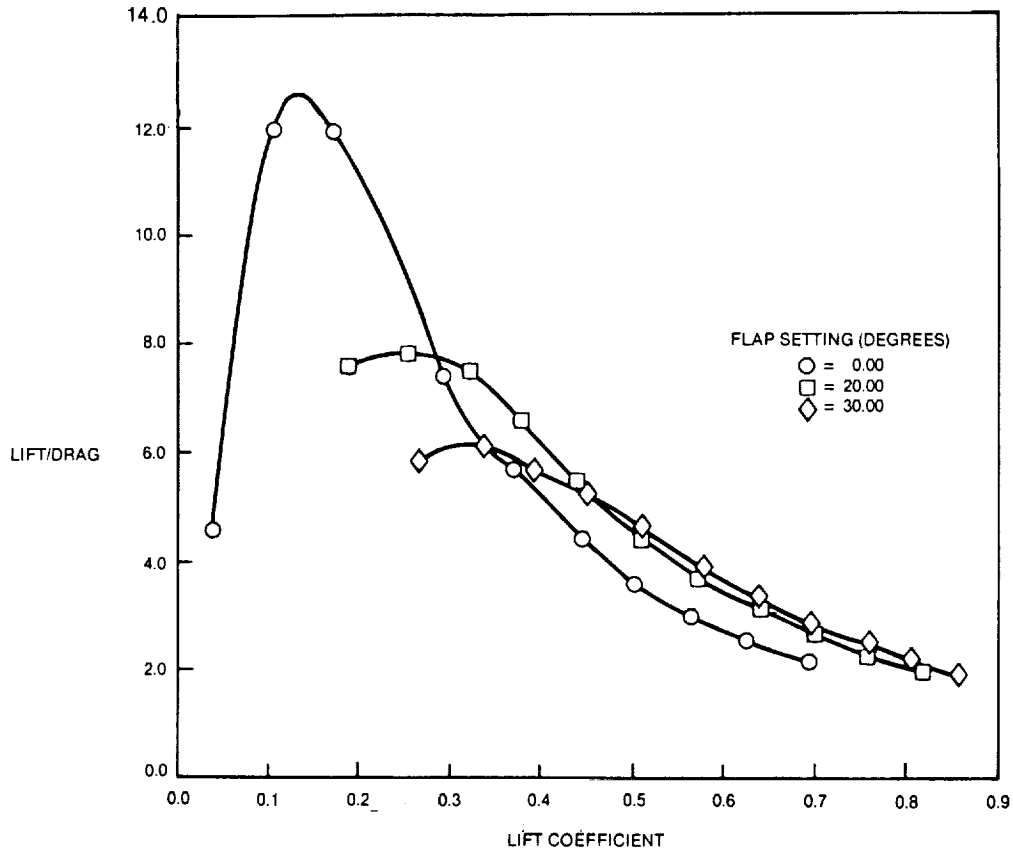

FIGURE 2-20. TRIMMED LOW-SPEED LIFT/DRAG — D3.2-3A CONCEPT LEADING EDGE SCHEDULE R

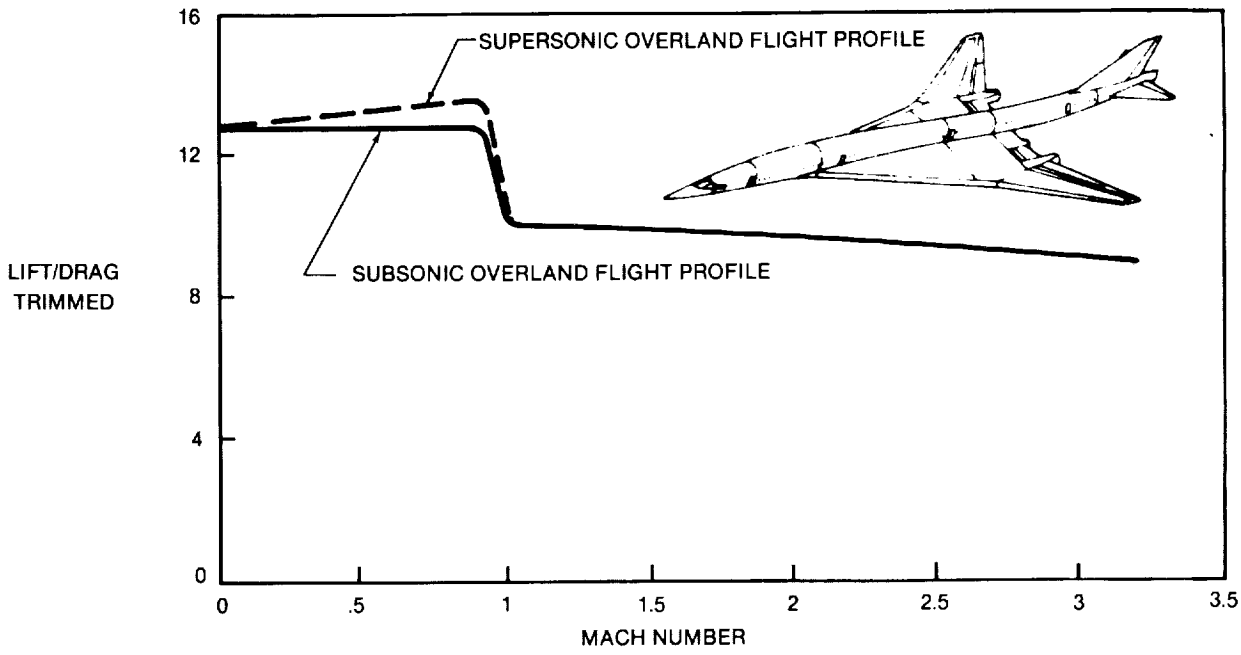

FIGURE 2-21. LIFT/DRAG VERSUS MACH NUMBER — D3.2-3A CONCEPT

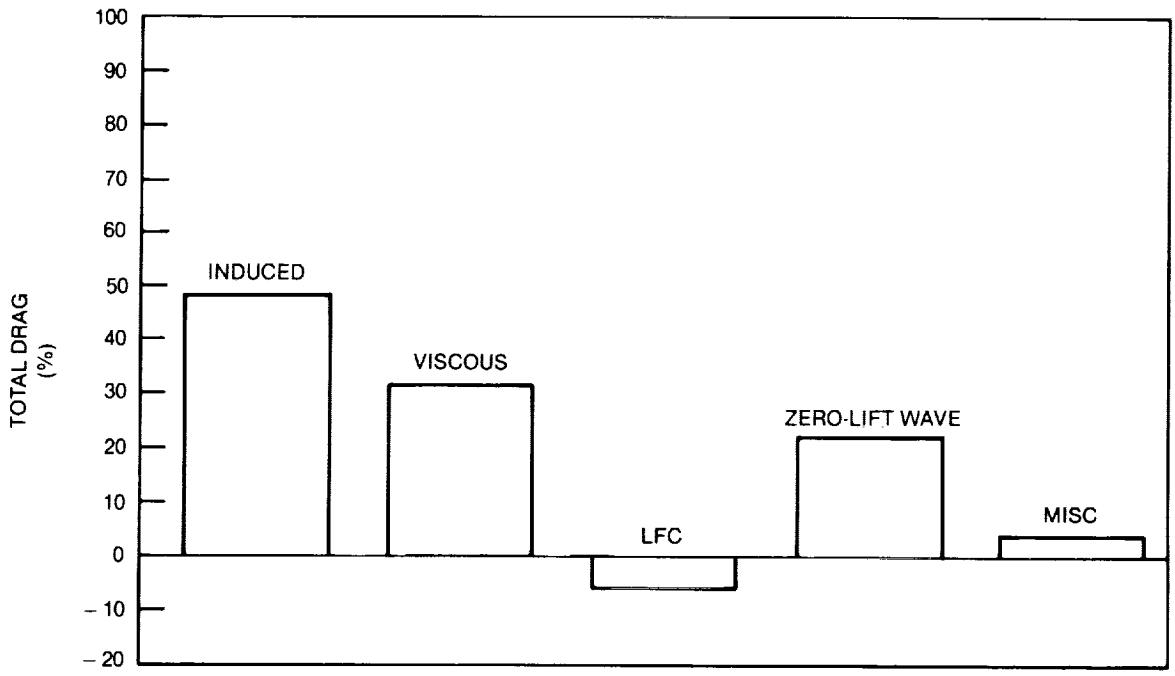

FIGURE 2-22. DRAG BREAKDOWN — D3.2-3A CONCEPT

Center-of-gravity limits for D3.2-3A are illustrated in Figures 2-23 and 2-24. Nosewheel liftoff with trim set for initial climb-out is the critical forward limit. Several aft limits are shown. The most critical was the nosewheel steering limit when full thrust was applied. The stability limit at the 10-percent negative margin is partially illustrated in Figure 2-23 and shown for the entire Mach range in Figure 2-24. Note that these are all rigid aircraft limits. It was anticipated that aeroelastic effects could cause the stability limits to become critical at the Mach number extremes.

To evaluate the impact of subsonic flight over land (in the event that supersonic flight over land is not possible) an alternate aircraft was configured with improved subsonic aerodynamic efficiency. The higher aspect ratio D3.2-4B evolved from the D3.2-3A design. The wing maintained the same 9,500 square feet planform reference area as D3.2-3A, but had an increased aspect ratio of 2.206 for a better low-speed performance. The leading-edge sweep inboard of the planform break was maintained at 76 degrees, but the planform break was moved inboard to 49-percent semi-span. Outboard of the planform break, the leading edge sweep was decreased to 57 degrees.

The final D3.2-4B design incorporated the same procedure as D3.2-3A for optimizing wing camber and thickness distribution. The final D3.2-3A fuselage was adjusted for application to the D3.2-4B concept. The engine nozzles were vectored 8 degrees down, based on a nonplanar trim with thrust analysis. The D3.2-4B used the same high-lift system as D3.2-3A, with full-span, simple drooped leading-edge flaps and plain trailing-edge flaps. Laminar flow control also was included in D3.2-4B. Figure 2-25 shows the D3.2-4B suction regions. Control surfaces and augmentation systems of D3.2-4B were similar to those of D3.2-3A.

The thrust-drag bookkeeping methods used on D3.2-4B were identical to those of D3.2-3A. To obtain the correct evaluation of fuel flows, lift versus thrust-required values were used rather than lift versus drag.

Aerodynamic evaluations of D3.2-4B included laminar flow control. The assumptions upon which the laminar flow estimates were made were consistent with those used in the D3.2-3A evaluation. The turbulence spread angle from the side of body, and the laminar run past the end of suction, is the same as that used in the D3.2-3A analysis (Figures 2-16 and 2-17). Skin friction analysis for D3.2-4B was based on flat plate boundary layer analysis as a function of Reynolds number and transition location, across the entire flight Mach number range. The extent of laminar flow for D3.2-4B is shown in Figure 2-26.

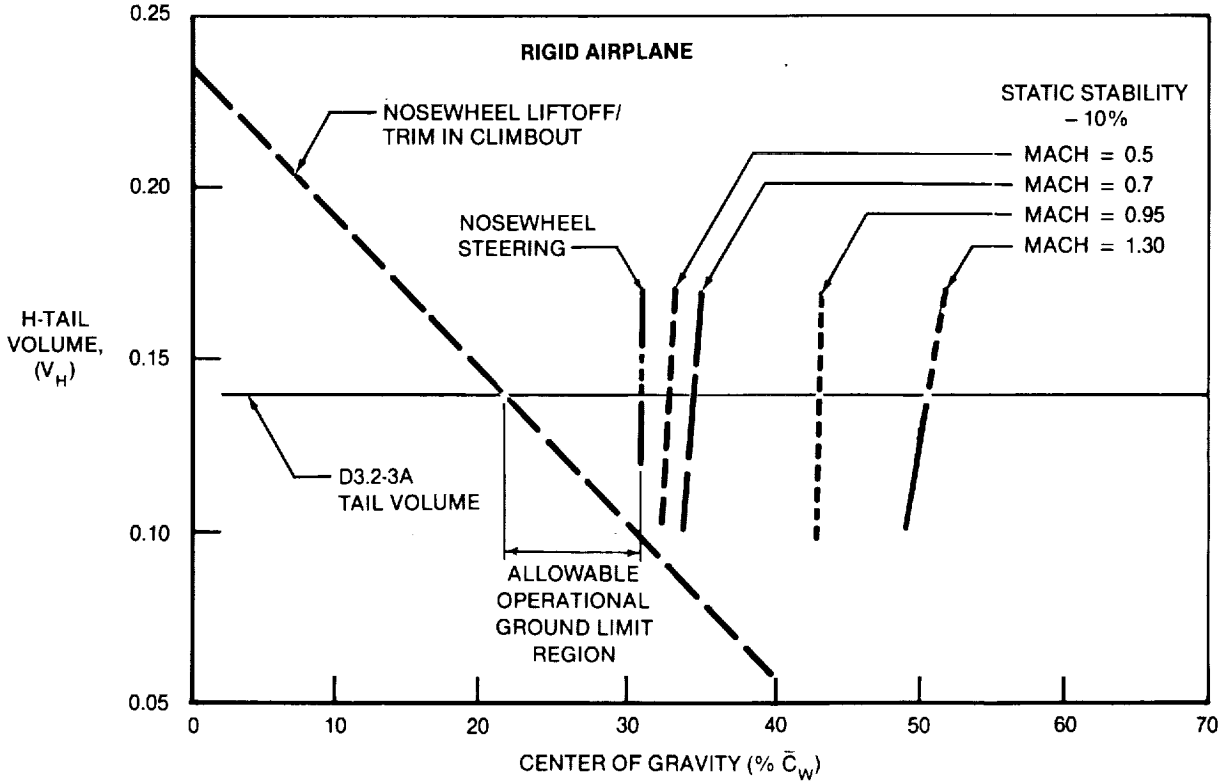

FIGURE 2-23. D3.2-3A CONCEPT ESTIMATED CENTER-OF-GRAVITY LIMITS

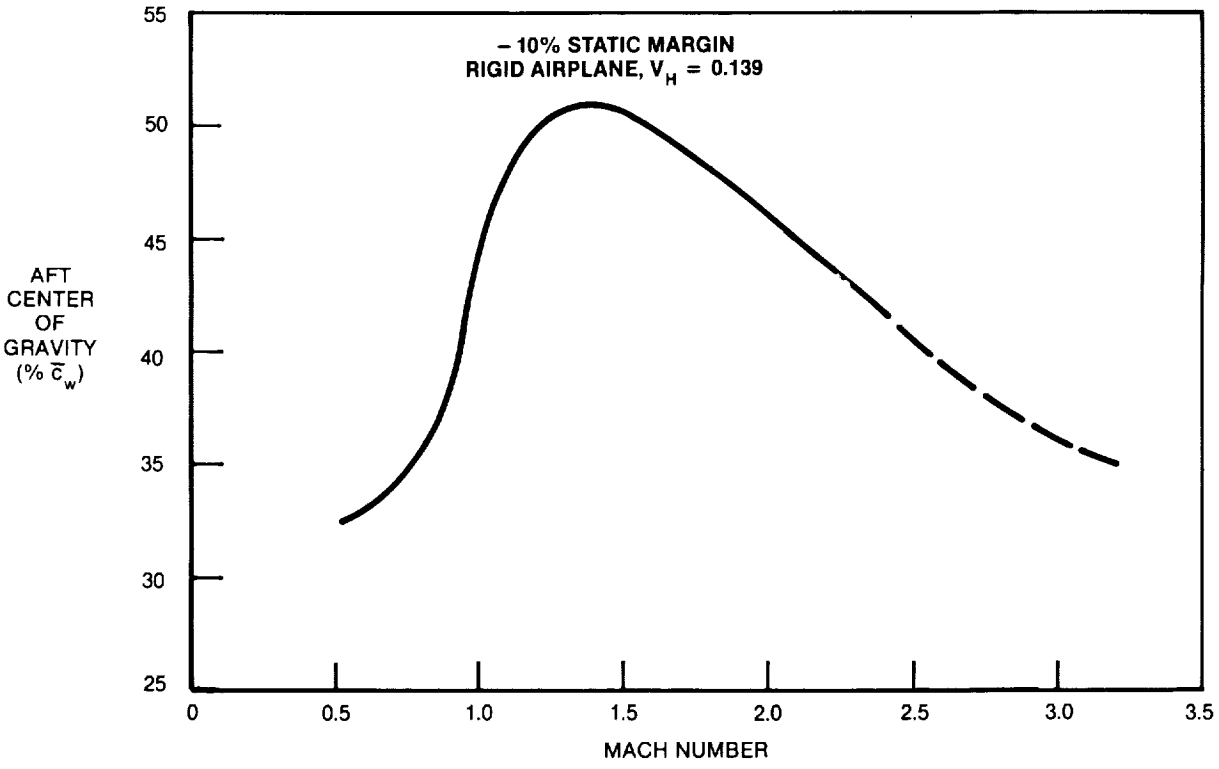

FIGURE 2-24. D3.2-3A CONCEPT ESTIMATED AFT CENTER-OF-GRAVITY LIMITS

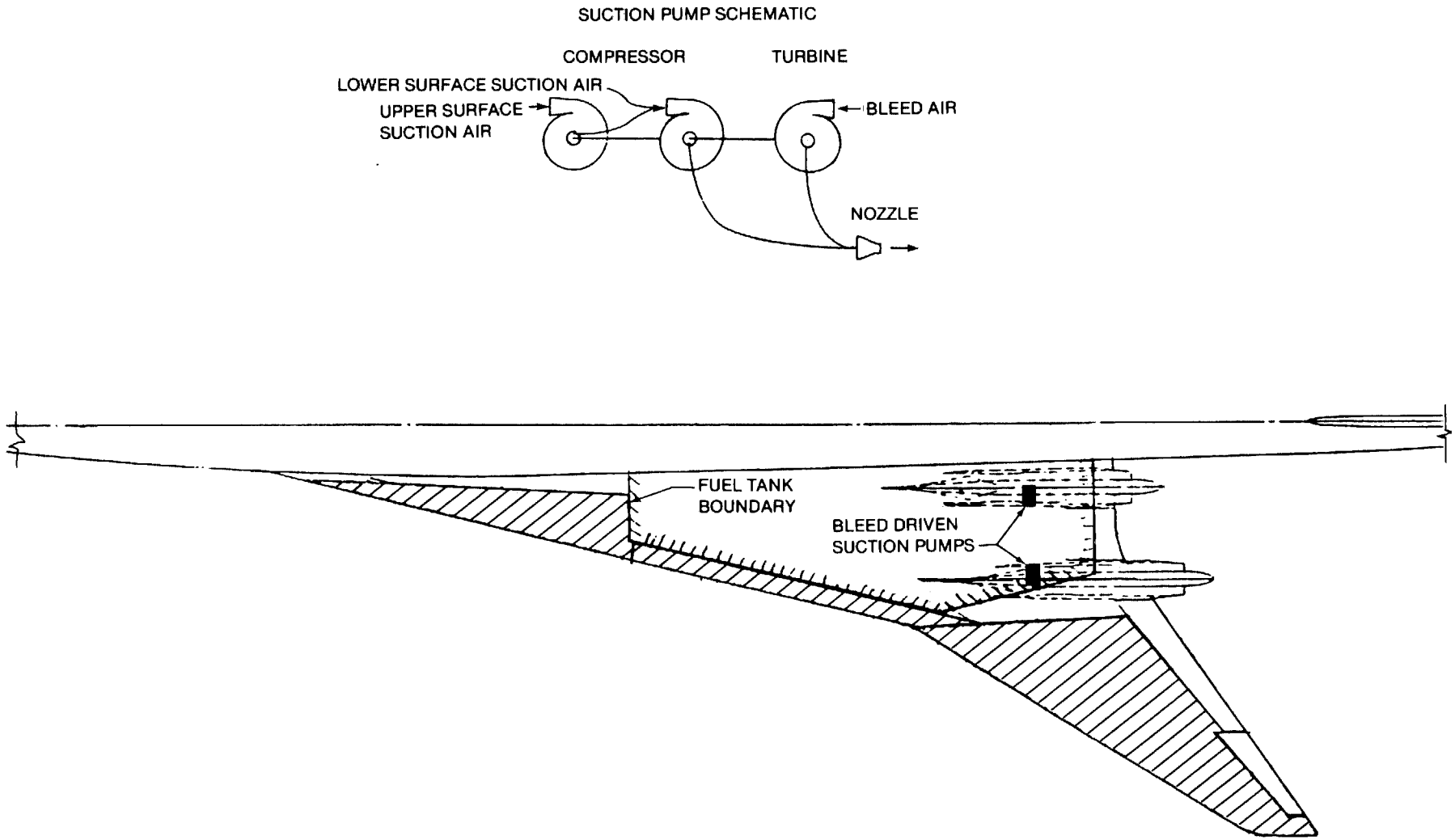

FIGURE 2-25. LAMINAR FLOW CONTROL SUCTION REGION FOR D3.2-4B CONCEPT

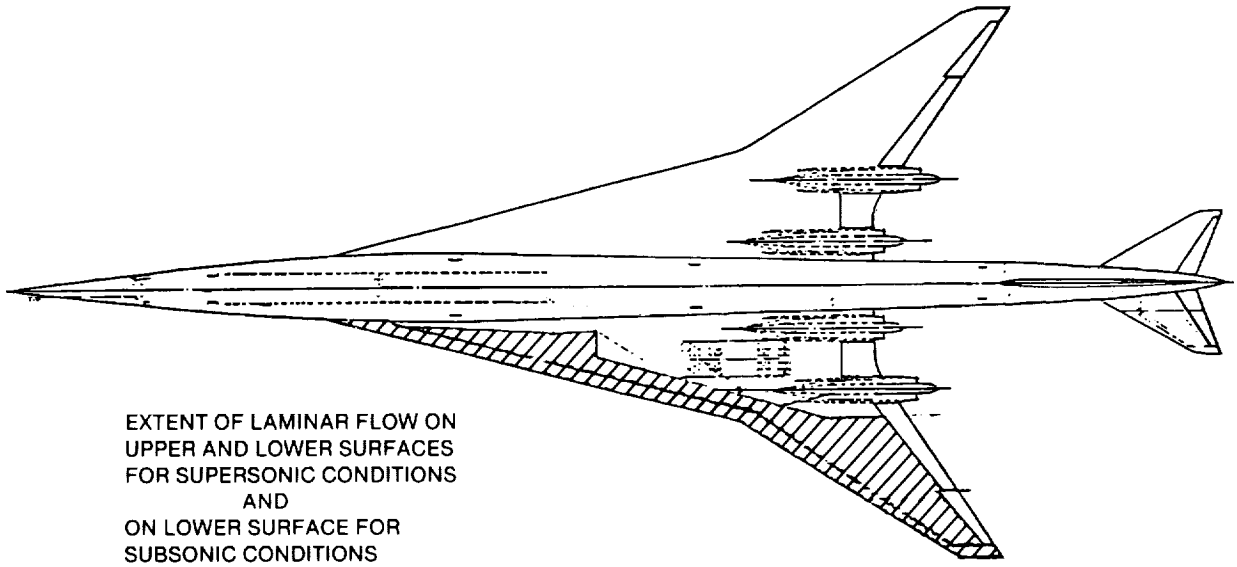

EXTENT OF LAMINAR FLOW ON
UPPER AND LOWER SURFACES
FOR SUPERSONIC CONDITIONS
AND
ON LOWER SURFACE FOR
SUBSONIC CONDITIONS

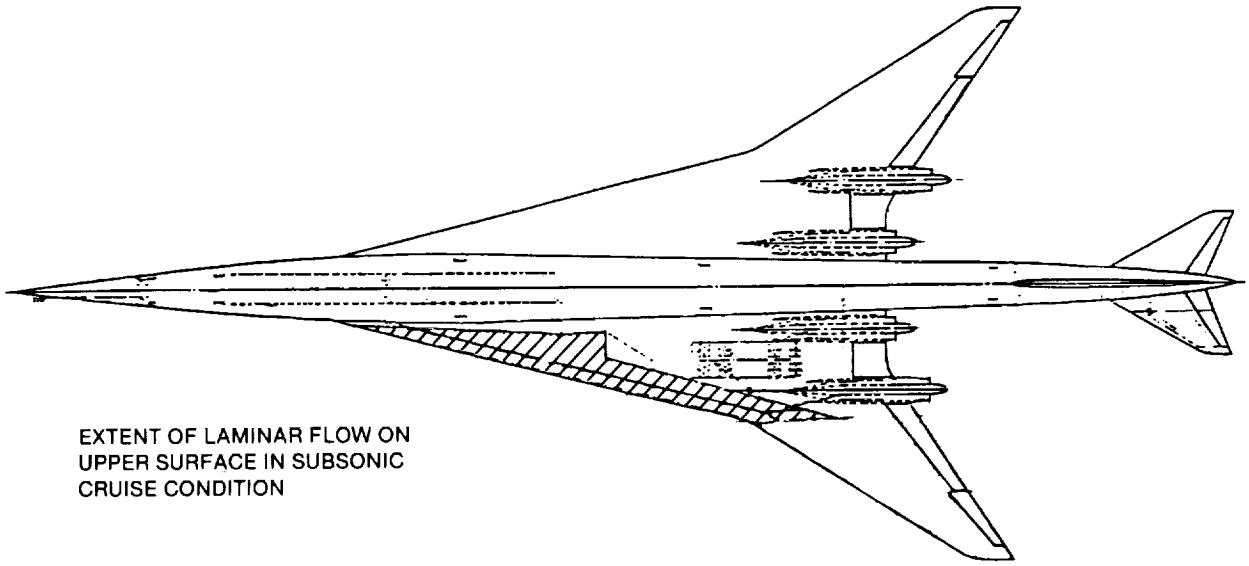

EXTENT OF LAMINAR FLOW ON
UPPER SURFACE IN SUBSONIC
CRUISE CONDITION

FIGURE 2-26. EXTENT OF LAMINAR FLOW FOR D3.2-4B CONCEPT

Low-speed aerodynamic characteristics were obtained by adjusting the viscous drag term in the D3.2-3A low-speed drag polar and scaling the lift curve and drag polar for the increased aspect ratio of D3.2-4B. The high-lift system of the D3.2-4B, like the D3.2-3A, incorporated full-span drooped leading-edge flaps and plain trailing-edge flaps (Figure 2-12). Takeoff performance for D3.2-4B included a landing gear drag term identical to that of D3.2-3A.

Transonic aerodynamic parameters were obtained by scaling the aerodynamic parameters of D3.2-3A for aspect ratio and adjusting the skin friction drag.

Supersonic drag due to lift characteristics of the D3.2-4B wing planform were obtained using the Woodward analysis. The D3.2-4B wing was analyzed as an isolated wing, and adjusted to represent the integrated wing-body based on results from the D3.2-3A development. Drag estimates for integration of the D3.2-4B planform to the fuselage were made based on an in-house, alternate wing planform study database. An additional three counts of drag which were not included in the Woodward gross-wing analysis were added to approximate the body lift loss of the wing-body. The D3.2-3A wave drag value was increased by five counts to approximate the wave drag increment of the new wing.

The analysis performed on D3.2-3A did not identify any initial problems with the stability and control system. As a result, analysis of the D3.2-4B assumed performance characteristics similar to D3.2-3A, and an additional detailed stability and control analysis was not performed. The final trimmed low-speed lift-to-drag curves, with leading-edge flaps extended in accordance with schedule R, are given in Figure 2-27. Inputs for the performance analysis included the thrust effects caused by vectoring the nozzles eight degrees

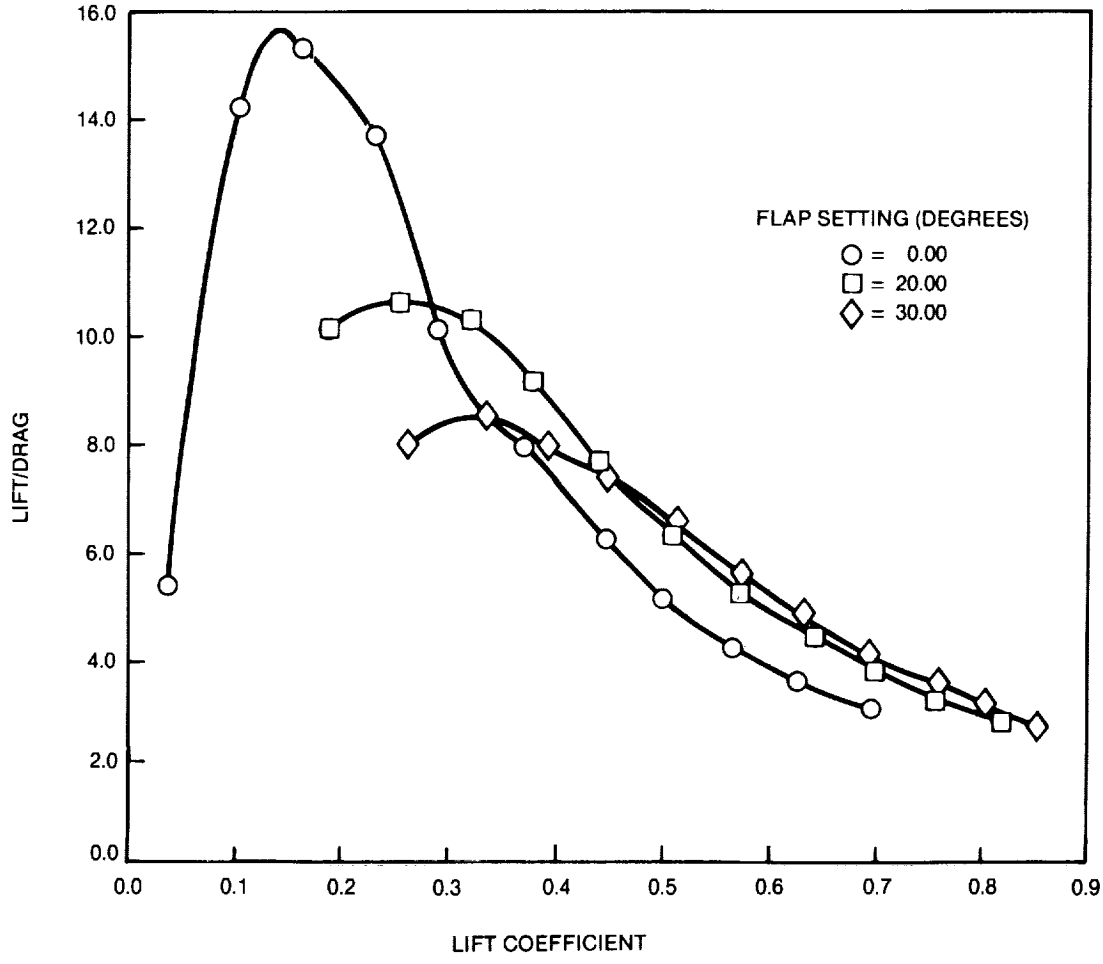

FIGURE 2-27. TRIMMED LOW-SPEED LIFT/DRAG — D3.2-4B CONCEPT LEADING EDGE SCHEDULE R

down. The maximum cruise lift-to-drag ratio of D3.2-4B compared with D3.2-3A is shown in Figure 2-28 for the entire Mach range. The drag breakdown at cruise is shown in Figure 2-29.

Mach 5.0. D5.0-15A was derived from the fully blended concepts developed during Phases I and II. The initial Phase I concepts, based on previous NASA and industry studies (References 2-4 and 2-5), were

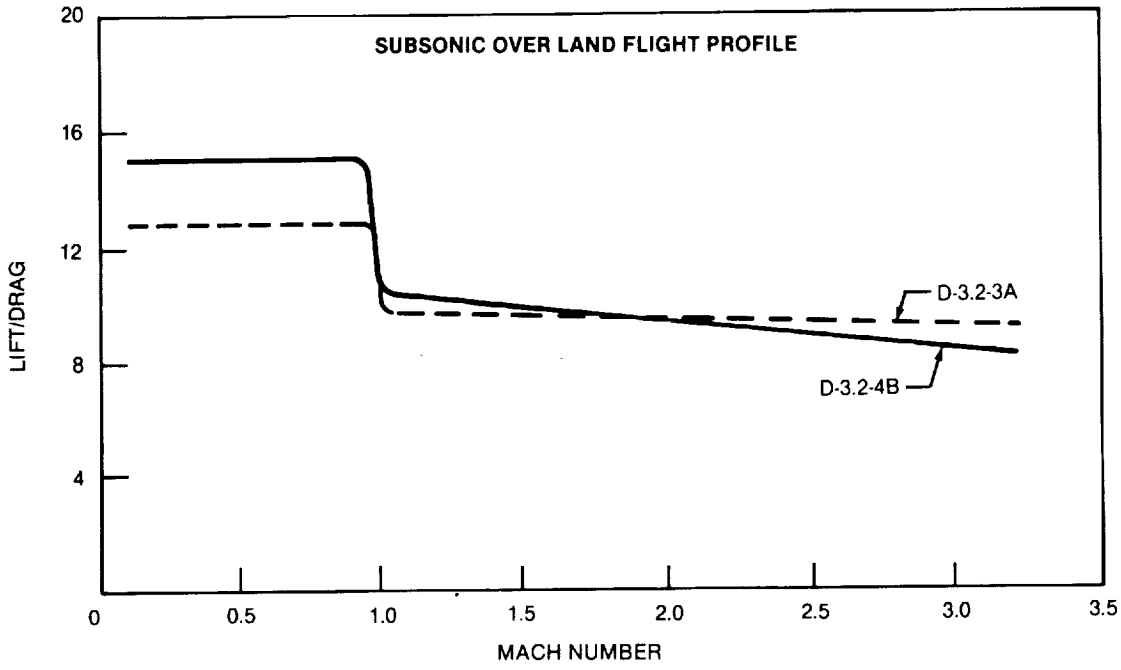

FIGURE 2-28. LIFT/DRAG VERSUS MACH NUMBER — D3.2-4B CONCEPT

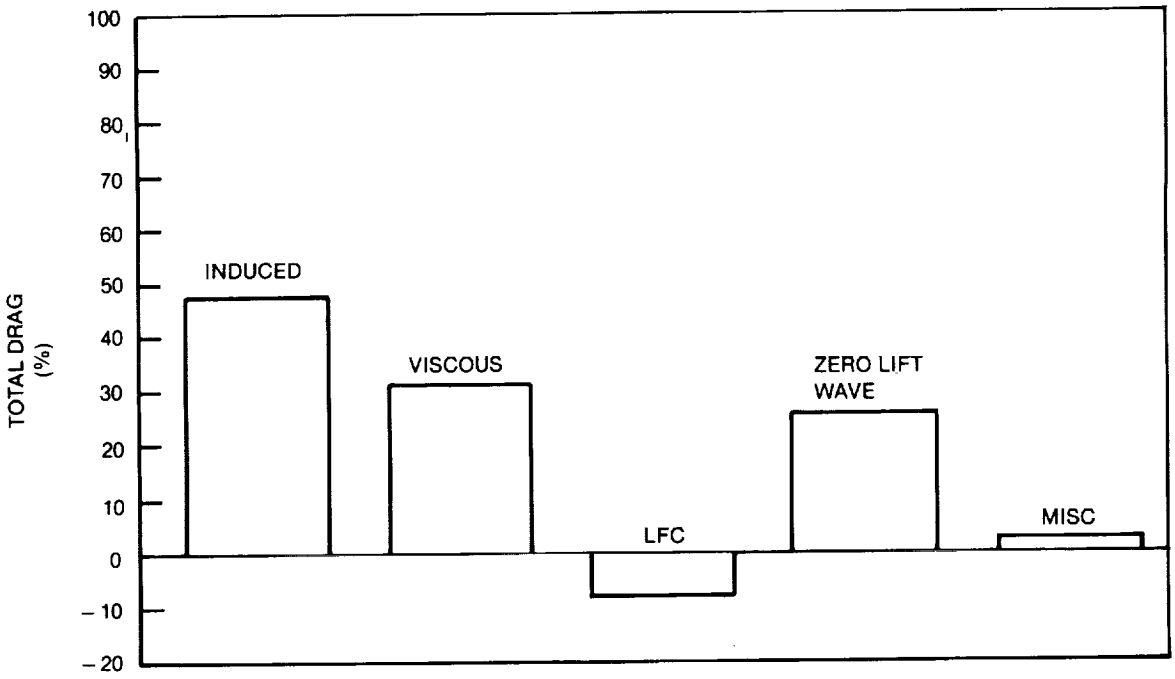

FIGURE 2-29. DRAG BREAKDOWN — D3.2-4B CONCEPT

typical wing-body configurations. During Phases I and II a development study was conducted to determine the potential performance improvements for hypersonic concepts by application of Computational Fluid Dynamics (CFD) and advanced graphics-based analysis. For Phase III, a detailed integration and analysis of the CFD-derived concepts resulted in D5.0-15A.

The fully blended wing-body had a reference area of 17,000 square feet, an aspect ratio of 1.1, and a taper ratio of 0.02. Inboard of the planform break, the leading-edge sweep was 80 degrees. The planform break was at 65 percent of the wing semi-span. Outboard of the planform break, the leading-edge sweep was 60 degrees. The vehicle slenderness factor, Tau ($\tau = Vol/S_{projected}^{3/2}$) is 0.069.

Initial Mach 4.0 and Mach 6.0 concepts for Phase I were based on data available from the 1960s and early 1970s. During Phase I, a detailed CFD concept refinement study was conducted. This study resulted in the fully blended Mach 4 and Mach 6 Phase I concepts and the fully blended Mach 5 Phase II concept, which was used as the baseline for the Phase III D5.0-15A configuration. The D5.0-15A spatular nose design was developed during the Phase I CFD study. The spatular nose also provided a blunted lift distribution, which helped reduce sonic boom (Reference 2-6).

The high-lift system on D5.0-15A consisted of plain trailing-edge flaps. There were no leading-edge devices. The blended-body, integrated engine/airframe concept was developed to enhance both aerodynamic and propulsion performance. Laminar flow control was not included in D5.0-15A.

Control surfaces required for the Mach 5.0 vehicle are illustrated in Figure 2-30. Longitudinal control and trim capabilities were achieved through a combination of elevons and totally movable tip controls. A nozzle flap was used to enhance trim capability. Elevons and movable tip controls were also used antisymmetrically to provide lateral control. Control authority was apportioned between the longitudinal and lateral axes to prevent overdeflection of the surfaces. Directional control was provided by rudders on the twin vertical tails. Each rudder was divided into two panels for redundancy. A fuel management system was used to aid longitudinal trimming. Control surfaces were sized according to McDonnell Douglas control-sizing guidelines. These guidelines are based on several wind tunnel tests, including the space shuttle, FDL-7 lifting body, AMI-X, and NASA wing-body and blended-body concepts. Both static and dynamic criteria were considered in sizing.

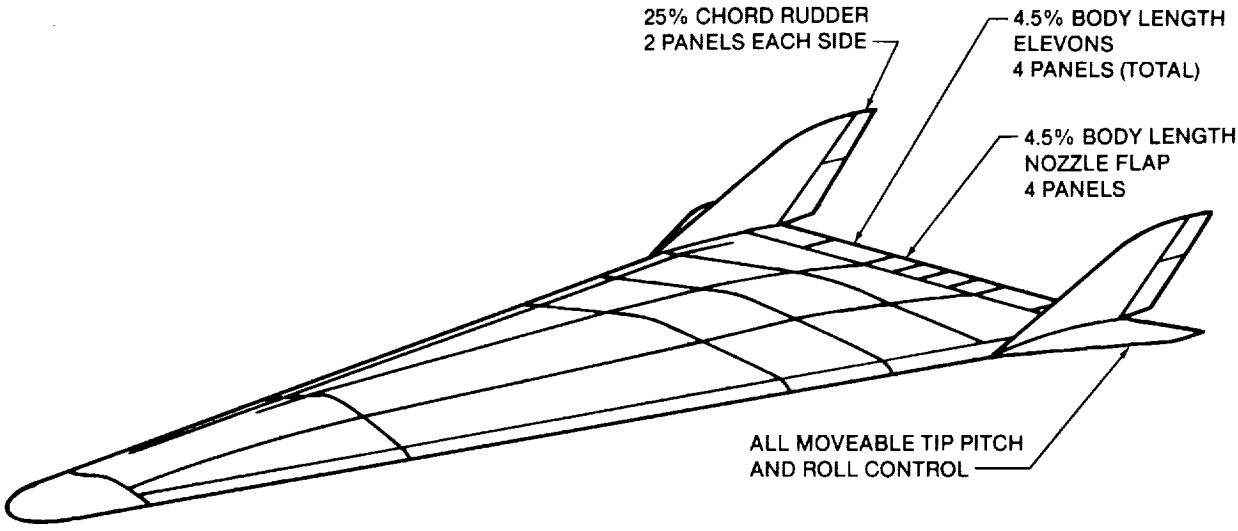

- STABILITY AND CONTROL AUGMENTATION ALL AXIS
- FUEL MANAGEMENT CONTROL

FIGURE 2-30. D5.0-15A CONCEPT CONTROL SYSTEM DESIGN FEATURES

The division of the airframe and propulsion system forces for D5.0-15A was as follows: inlet and nozzle forces were included with the engine, except for nozzle lift and moment, which were included in the airframe trim analysis; nacelle drag was included with the airframe forces.

Subsonic skin-friction analysis for D5.0-15A was based on Reynolds number and flat-plate skin-friction drag coefficients. Supersonically, viscous forces were calculated in HABP using the Mark III skin-friction option. The vehicle shape was represented by a simplified-geometry model composed of a number of flat surfaces; shear force for each surface was determined. Calculations used the reference temperature method for the laminar flow and the Spalding-Chi method (with temperature ratio) for the turbulent flow. The radiation equilibrium value (emissivity = 0.8) was used as the surface temperature.

D5.0-15A low-speed data was generated from analysis of the generic Mach 4.0 to Mach 6.0 concepts developed in Phases I and II. The trimmed lift curve slope was obtained from the data correlation for 75 degrees' leading edge sweep and an aspect ratio of 1.1 (Reference 2-7). The flap incremental lift coefficients for 0 to 30 degrees' flap deflections were obtained from the AST low-speed experimental data base, (Reference 2-1) clean leading edge configuration. Assessment of low-speed pitching moment characteristics was based on experimental data for the AMI-X blended body configuration. Studies of aircraft handling conducted as part of the Supersonic Cruise Aircraft Research (SCAR) program for the McDonnell Douglas AST concept, with similar pitching moment characteristics, showed that the augmented low-speed characteristics were acceptable (Reference 2-1).

The AMI experimental database was the basis for transonic aerodynamic parameters for D5.0-15A. The experimental values were scaled for aspect ratio, adjusted for skin friction, and trimmed using a nonplanar trim analysis including engine thrust effects.

Traditional aerodynamic analyses (HABP) as well as advanced CFD methods developed by McDonnell Douglas have been used in the present study. The results of the two methods were in close agreement, as shown in Figure 2-31. HABP is capable of handling more geometrically complex concepts than is currently possible with the CFD methods and therefore HABP has been used to evaluate the high-speed aerodynamic parameters for D5.0-15A. Leading-edge bluntness drag was evaluated from empirical data. Excrescence drag, an empirical drag term based on space shuttle data, was included in the miscellaneous drag terms.

The trimmed low-speed lift-to-drag ratios as a function of flap deflection angle are shown in Figure 2-32. The maximum trimmed lift-to-drag ratios for both flight profiles are shown in Figure 2-33 across the entire flight Mach range. Performance of D5.0-15A included the lift increment attributable to the underexpanded nozzle. The cruise drag breakdown is given in Figure 2-34.

2.3 Propulsion and Fuels

This section summarizes the results of the Phase III engine selection, engine/airframe integration, and the results of engine emissions and fuels studies. Engine data have been prepared through subcontracting arrangements with Aerojet TechSystems, General Electric Aircraft Engines, and Pratt & Whitney. All studies assumed an aircraft certification date of 2000/2010, with a corresponding technology availability date (TAD) of 1995-2000.

Engine Screening. During Phases I and II, a large number of candidate engine cycle/cruise Mach number/fuel combinations were evaluated as summarized in Table 2-2. Both military and commercial concepts were evaluated, ranging from preliminary designs developed for the high-speed propulsion (HSPA) studies for the Air Force, to commercial engines specifically tailored to the Douglas high-speed civil transport configurations. Engine screening was on the basis of takeoff gross weight (TOGW).

One important parameter for preliminary screening was engine cruise overall efficiency. Cruise overall efficiency is approximately equal to the product of the specific impulse times the flight velocity divided by the fuel heating value. It is a measure of fuel energy conversion to jet kinetic energy and is the product of

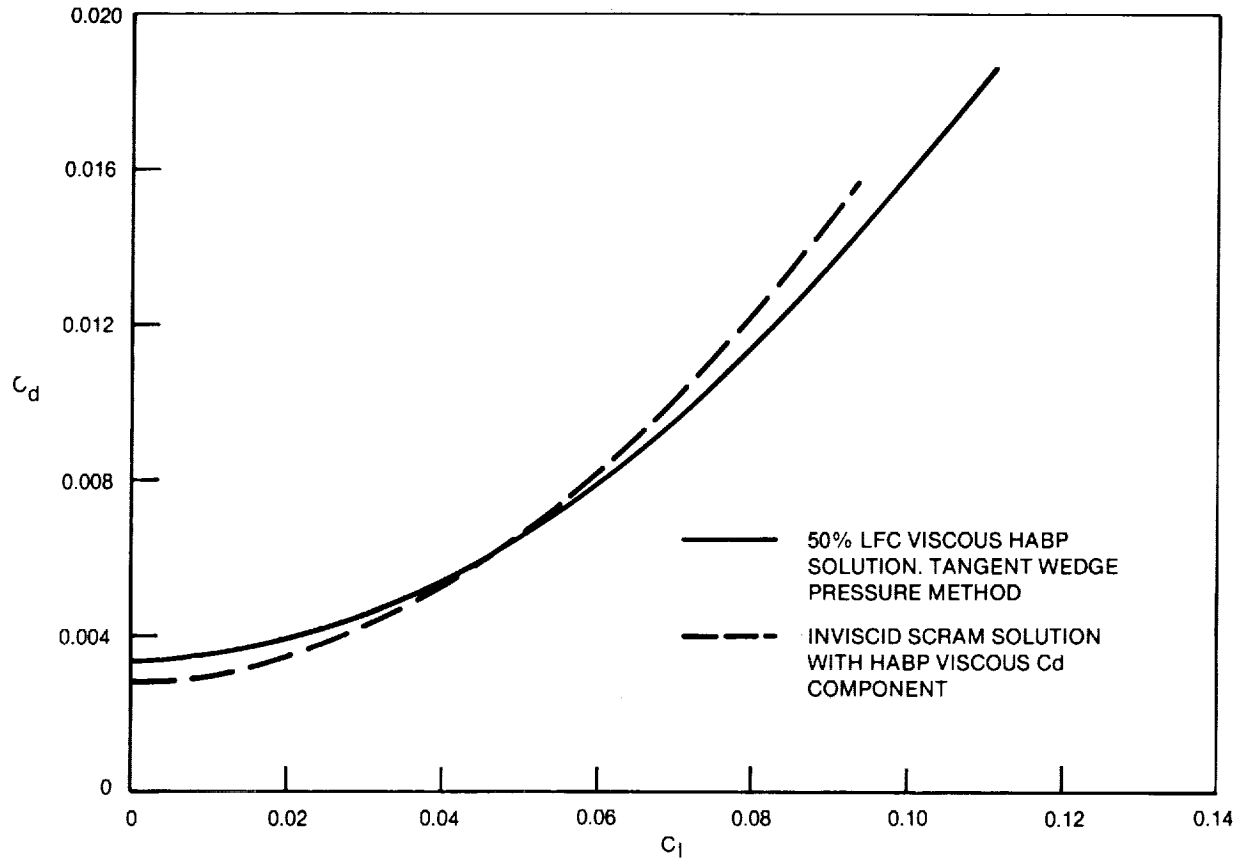

FIGURE 2-31. HABP — SCRAM COMPARISON AT MACH 5.0, D5.0-15A CONCEPT WITHOUT VERTICAL TAIL

the thermal efficiency times the propulsive efficiency. Specific impulse (I_{SP}) is used in lieu of specific fuel consumption (SFC). The conversion factor is I_{SP} = 3,600/SFC. Depending upon the design mission, fuel consumption during climb can amount to 25 percent or more of the total fuel weight at takeoff. In the event that sonic boom restrictions preclude supersonic flight over land, the aircraft may have to fly up to 40 percent of its design range at subsonic speeds. Thus the cycles with the best supersonic cruise overall efficiencies, generally turbojets, will not necessarily be the optimum for the vehicle.

Another major consideration is FAR Part 36, Stage 3 takeoff noise requirements, which also influence engine cycle selection. During Phase III, both P&W and GE addressed the takeoff noise problem. This section summarizes some of the engine company results. Section 4.3 discusses community noise in more detail and assesses the present status of takeoff noise estimates for both the Mach 3.2 and Mach 5.0 aircraft.

Independent of the engine screening process, the decision was made to evaluate two basic aircraft concepts during Phase III:

- Mach 3.2 using kerosene-based TSJF
- Mach 5.0 using LNG fuel

Also, the decision was made to evaluate one baseline and one alternate engine cycle at each of the two Mach numbers.

For the Mach 3.2 engine cycle selection, comparisons were made between several candidate engine cycles. These studies clearly showed the TOGW advantage of turbofan cycles over either turbojets and turbine-bypass engines when engine oversizing is used as one means of reducing jet velocity and, hence, jet noise at takeoff. Therefore, the choice narrowed to some variant of a turbofan cycle. Although the mixed flow turbofan had a very slight TOGW advantage over the variable stream control engine (VSCE) (duct burning turbofan), other Douglas and P&W studies showed the VSCE with a slight advantage.

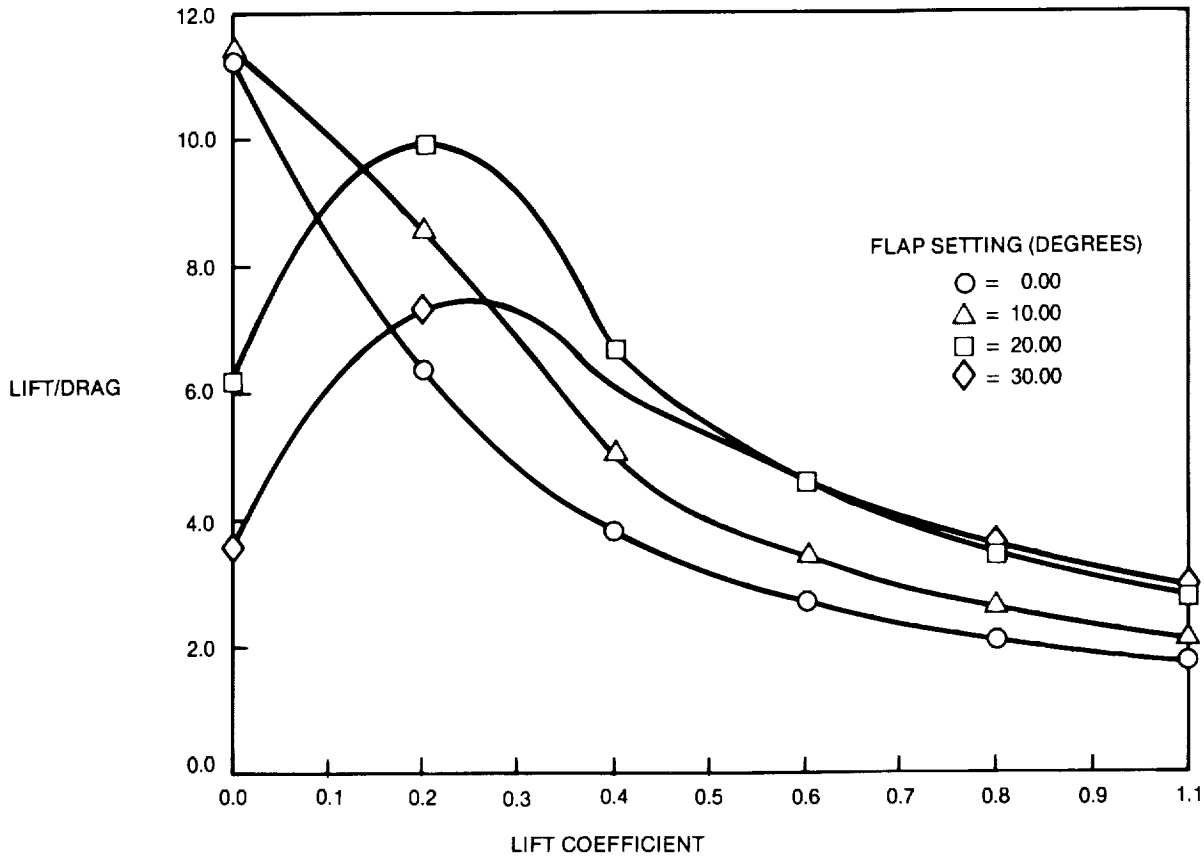

FIGURE 2-32. TRIMMED LOW-SPEED LIFT/DRAG — D5.0-15A CONCEPT

As for the choice between a P&W VSCE and a GE variable cycle engine (VCE), preliminary comparison showed little advantage of one over the other. Because of the timely availability of additional VSCE data and the engines' essentially equal TOGW values, the P&W VSCE was selected as the baseline Phase III engine. The GE VCE was retained as the alternate Mach 3.2 engine.

For the baseline Mach 5.0 engine selection, the results of the Phase I evaluations were used along with other quantitative and qualitative data provided by all three engine companies. These studies were inconclusive in identifying a clear choice, with the GE turbofan/ramjet (variable cycle hypersonic jet) having an edge; therefore, the decision was made to select the GE turbofan/ramjet (VCHJ) with LNG fuel as the baseline Mach 5.0 engine. The Aerojet TechSystems dual-regenerator air turboramjet (ATR) was selected as the alternate Mach 5.0 engine because preliminary data showed better supersonic cruise performance and lower weight than for the VCHJ.

Figure 2-35 shows the supersonic cruise overall efficiencies for the baseline Mach 3.2 and Mach 5.0 engines, including both uninstalled and installed data. These engine company data are compared with a goal value which represents optimistic assumptions of component performance. This goal value was developed from the data in References 2-8 through 2-10.

In addition, a P&W Advanced Ducted Prop was selected for the baseline subsonic (Mach 0.85) aircraft. This selection was based on results of studies of advanced engine cycles for MD-80/MD-11 derivatives.

Subsonic Baseline Engine – P&W Advanced Ducted Prop. For the subsonic baseline aircraft studies, the P&W Advanced Ducted Prop (ADP) engine has been selected as a representative advanced subsonic engine for long-range aircraft based upon studies of advanced MD80/MD-11 concepts.

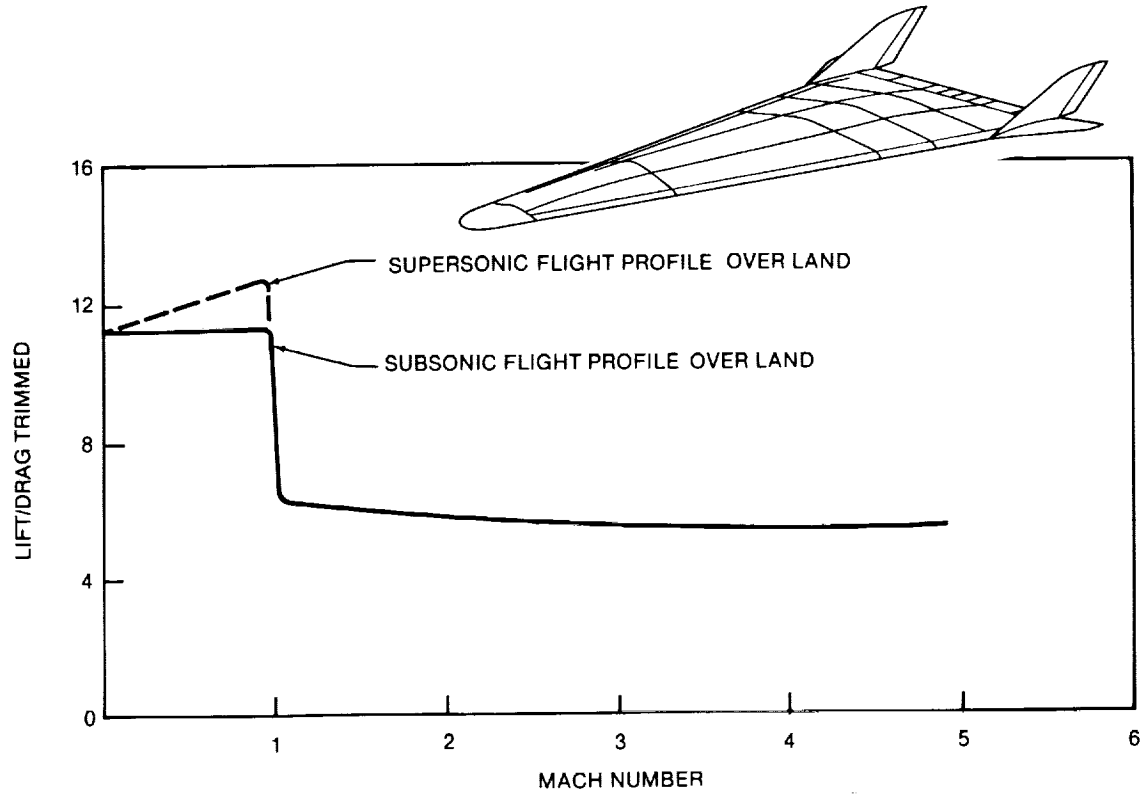

FIGURE 2-33. LIFT/DRAG VERSUS MACH NUMBER — D5.0-15A CONCEPT

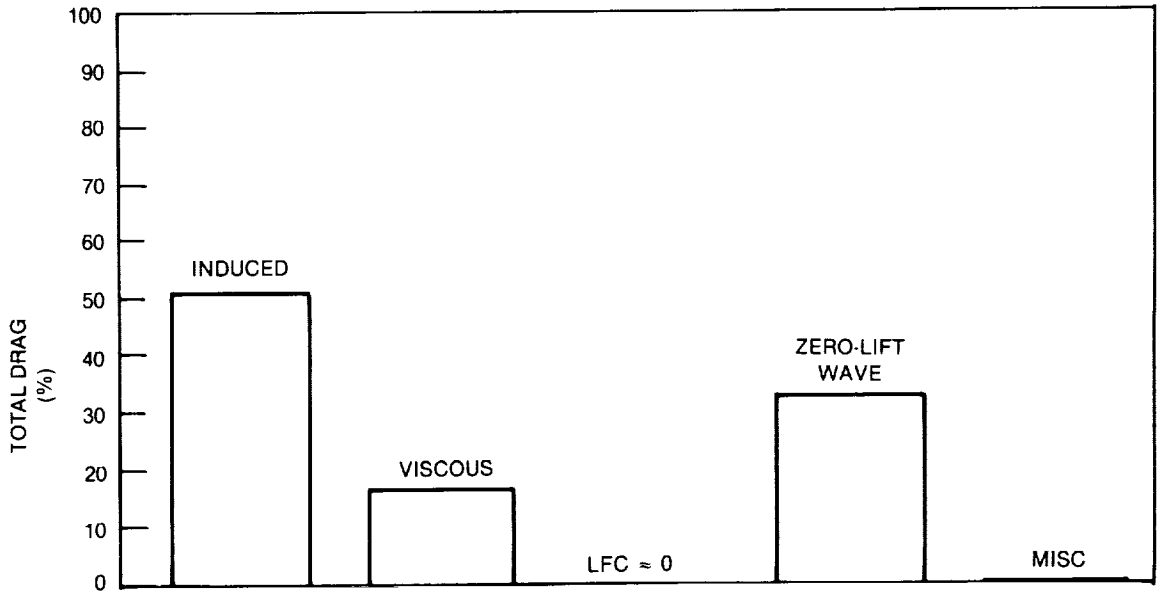

FIGURE 2-34. DRAG BREAKDOWN — D5.0-15A CONCEPT

TABLE 2-2
PHASE I AND PHASE II HSCT STUDY ENGINES

PHASE ONE — HIGH-SPEED PROPULSION ASSESSMENT (HSPA) ENGINES

- ENGINE CYCLES
  - — TURBOJETS
  - — TURBORAMJETS (TANDEM, TURBOFAN, OVER/UNDER)
  - — DUAL REGENERATOR AIR TURBORAMJET (ATR)
- CRUISE MACH NUMBERS — 3.5, 4.0, 4.5, 5.0, 6.0
- FUELS — KEROSENE-BASED, ENDOTHERMIC (MCH), LIQUID METHANE (LNG), AND LIQUID HYDROGEN

PHASE TWO — TAILORED ENGINE CYCLES

- MACH 2.2, JET A FUEL
  - — TURBINE BYPASS AND VARIABLE CYCLE ENGINE
- MACH 4.0, KEROSENE-BASED AND METHANE FUELS
  - — TURBOFAN RAMJETS
  - — AUGMENTED AND DRY TURBOJETS
  - — TURBINE BYPASS ENGINE
  - — MIXED FLOW TURBOFAN
  - — DUCT BURNING (NONMIXED FLOW) TURBOFAN
- MACH 6.0, LIQUID HYDROGEN FUEL
  - — TURBOFAN RAMJET

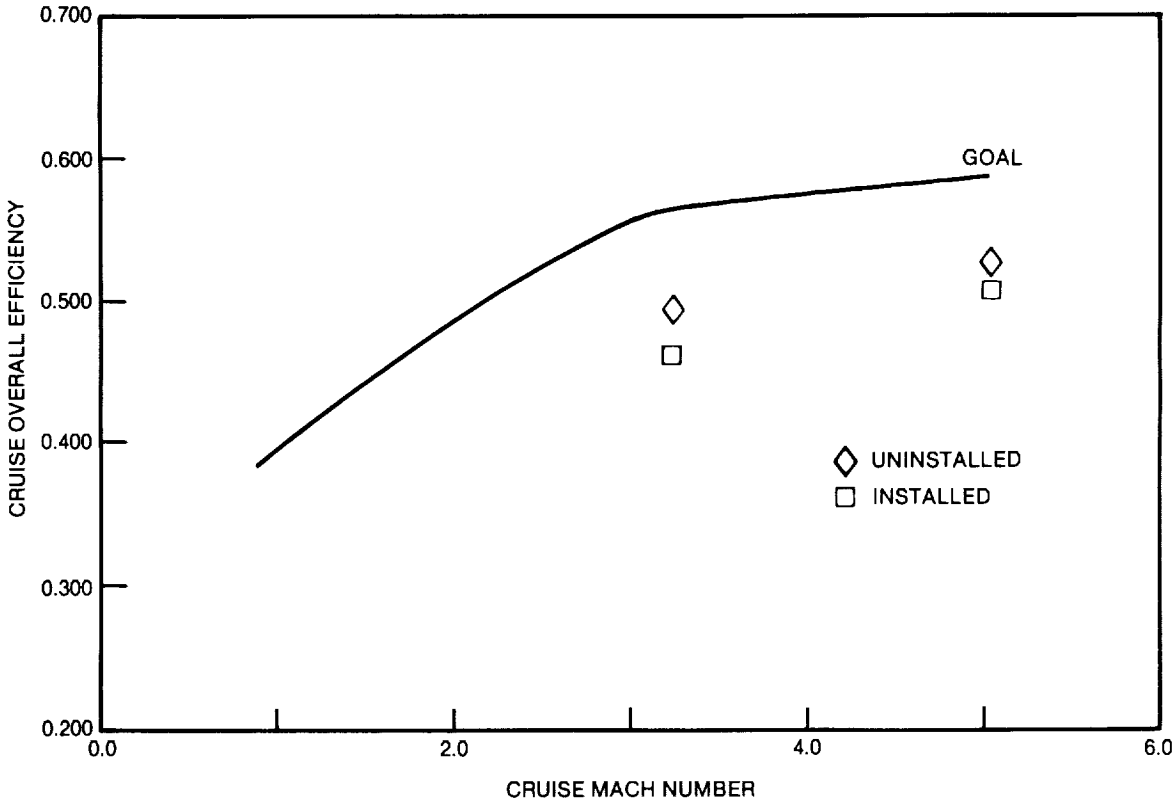

FIGURE 2-35. PEAK CRUISE OVERALL EFFICIENCY — PHASE III BASELINE ENGINES

The ADP (Figure 2-36) is a two-spool, geared high-bypass, high-pressure ratio, ducted prop engine with separate core (primary) and prop (duct or bypass) exhaust streams. One of its significant features is a variable pitch ducted prop that provides good operability as well as reverse thrust.

The cycle and component design parameters for this engine are as follows:

- Overall pressure ratio 36
- Fan pressure ratio 1.3
- Bypass Ratio 15
- Maximum combustor exit temperature 2,650°F

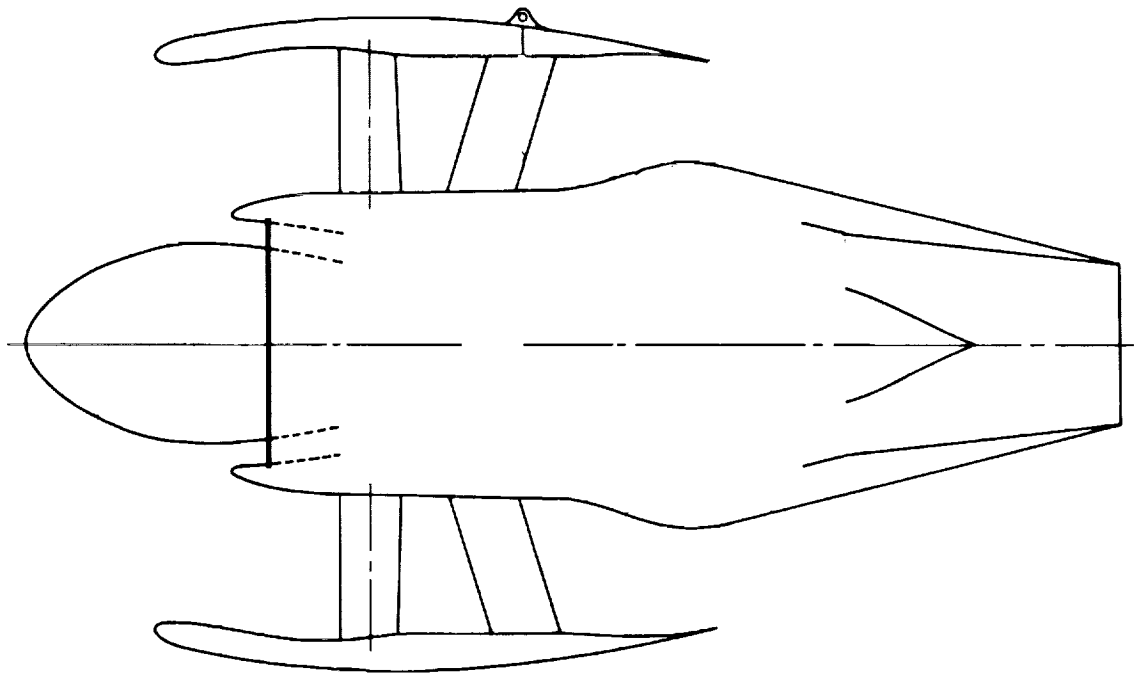

FIGURE 2-36. P&W MACH 0.85 ADVANCED DUCTED PROP

The ADP engine is rated at 28,300 pound sea-level static thrust, standard day + 27°F, with a design-corrected airflow of 1,450 pounds per second. Climb data at maximum rated thrust are shown in Table 2-3, while cruise specific fuel consumption data are shown in Figure 2-37.

All performance data include inlet and nozzle internal losses, as well as the core-cowl external drag for the P&W-designed nacelle. The nacelle design does not include intrusion of the pylon structure into the fan duct. Power extraction is 150 horsepower, and bleed flow is determined by the design-to-bleed concept to preserve the compressor stall margin. For the unscaled (1,450 pounds per second) engine, the estimated propulsion system weight, including prop duct, is 6,670 pounds.

Mach 3.2 Baseline Engine – P&W Variable Stream Control Engine. The Mach 3.2 baseline engine is the P&W Variable Stream Control Engine (VSCE) duct burning non-mixed flow turbofan using thermally stable jet fuel (TSJF). The unscaled engine has a design corrected airflow of 650 pounds per second, and maximum augmented and dry SLS thrust ratings of 61,901 and 29,694 pounds, respectively.

The VSCE (Figure 2-38) is an advanced, moderate-bypass-ratio, nonmixed-flow turbofan with duct burner augmentation and a coannular nozzle with inverted velocity profile for jet noise reduction. A distinctive operating feature is the independent control of both core and fan (duct) stream temperature and exit

TABLE 2-3
P&W MACH 0.85 ADVANCED DUCTED PROP SUMMARY PERFORMANCE

CLIMB AT 100-PERCENT RATED CLIMB THRUST

ALTITUDE (FT)	MACH NO. (–)	NET THRUST (LB)	SPEC FUEL CONSUMPTION (LB/IN./LB)	SPECIFIC IMPULSE (SEC)
0	0.20	18,500	0.288	12,495
10,000	0.40	11,900	0.378	9,520
20,000	0.50	9,400	0.399	9,024
30,000	0.60	6,800	0.429	8,384
36,089	0.85	5,200	0.521	6,908
42,000	0.85	3,800	0.526	6,840

NOTE: ALL DATA FOR UNSCALED ENGINE WITH DESIGN W_{CORR} = 1,450 LB/SEC

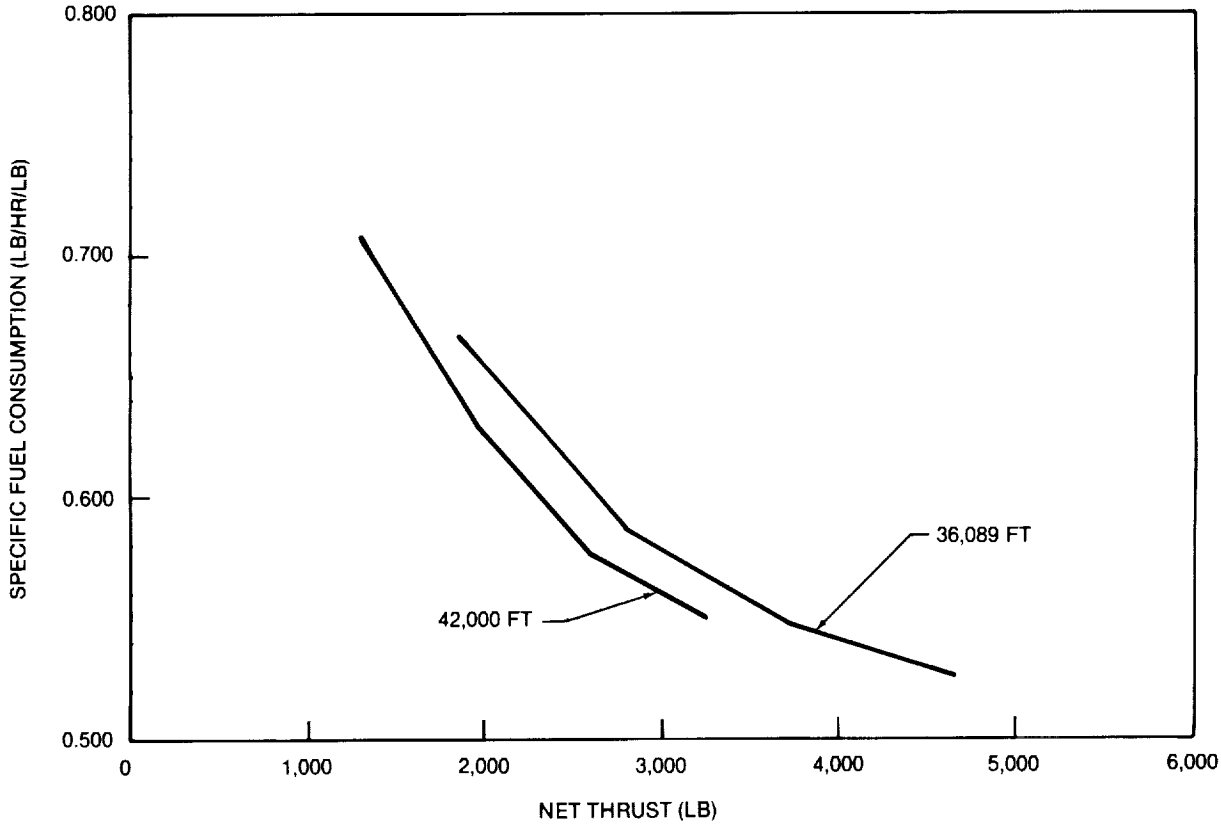

FIGURE 2-37. P&W MACH 0.85 ADVANCED DUCTED PROP — INSTALLED CRUISE SPECIFIC FUEL CONSUMPTION

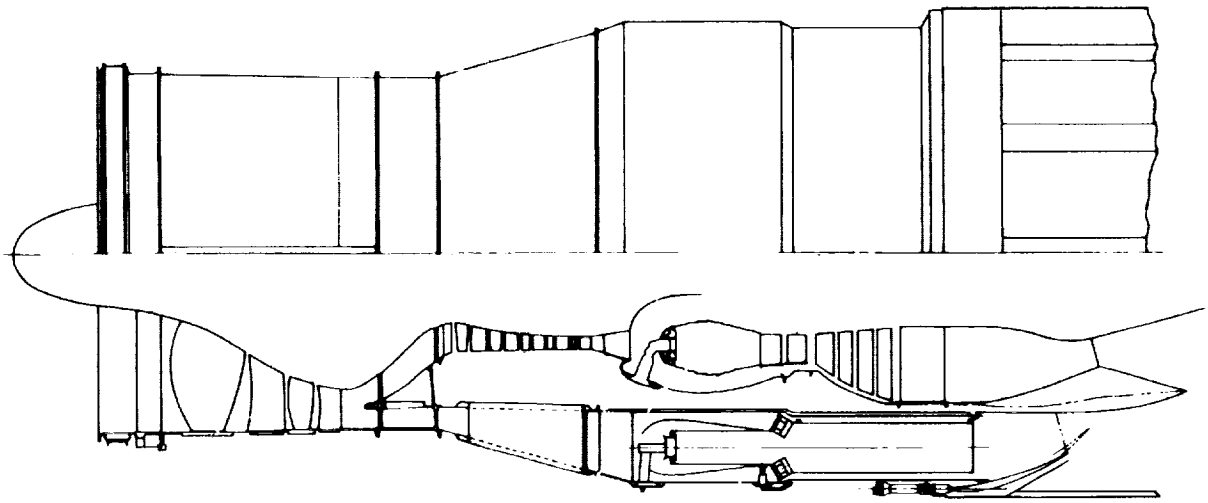

FIGURE 2-38. P&W MACH 3.2 VSCE DUCT BURNING TURBOFAN

velocity for in-flight cycle matching. Cycle matching is further enhanced by a P&W technique that offers the following advantages:

- Satisfies the unique thrust schedule requirements of advanced supersonic-cruise aircraft over the entire flight spectrum
- Provides low-core exhaust velocity at takeoff to obtain the noise benefit of an inverted velocity profile
- Minimizes specific fuel consumption at supersonic cruise by "high flowing" the core engine to control cycle bypass ratio

At takeoff, the main burner is throttled to an intermediate power setting to reduce the core contribution to jet noise. The duct burner is operated at a moderate temperature level to provide the required thrust and an inverted velocity profile. The thrust can be cut back for noise abatement after takeoff while still maintaining the inverted velocity profile.

During subsonic cruise, the VSCE operates as a moderate bypass turbofan engine. The main burner operates at a relatively low exit temperature, and there is no duct augmentation. Variable geometry components are matched to "high flow" the engine, i.e., maintain maximum constant corrected airflow down to 10-20 percent of maximum rated thrust and well below the sfc "bucket," to reduce inlet spillage and bypass losses.

During supersonic cruise, the main burner temperature is increased (relative to takeoff), and the high spool speed is increased to maintain high flow condition. This high flow condition reduces the cycle bypass ratio and the amount of duct augmentation required. At the specific impulse peak, i.e., the sfc "bucket," the core and the duct exit temperatures and velocities are approximately equal to maximize propulsive efficiency.

The cycle and component design parameters for this engine are:

- Overall pressure ratio 14.3
- Fan pressure ratio 3.67
- Design bypass ratio 1.30
- Maximum compressor discharge temperature 1,860°R
- Maximum rotor (turbine) inlet temperature 3,960°R

A variable geometry bicone inlet was selected for the Mach 3.2 baseline engine based on the results of Douglas supersonic transport studies conducted in the late 1970s. The inlet system is designed for Mach 3.2 cruise at an altitude of 70,000 feet. The inlet capture area is sized to satisfy engine, inlet bleed, and miscellaneous airflow requirements. The local flow conditions ahead of the inlet were determined by assuming a wing-leading edge precompression resulting from six degrees flow deflection.

All performance data used in Phase III are installed data and account for inlet drag and recovery factor variation with freestream Mach numbers. Inlet drags include bypass, boundary-layer bleed, and spillage drags, as well as miscellaneous drag due to inlet leakage, engine cooling, and the like. Inlet drag also includes nacelle external skin friction.

The raw P&W data were computed using MIL-E-5007D inlet total pressure recovery, since better estimates of inlet pressure recovery were not yet available. For Mach numbers above the inlet starting Mach number of 1.95, inlet recovery is greater than the MIL-E-5007D value and is based on MIL-E-5007D but using local total pressure and Mach number ahead of the inlet. Below Mach 1.95, the pressure recovery is lower than the MIL-E-5007D value and is based on leading edge shock losses, inlet shock losses external to the inlet, viscous losses, and the effect of the normal shock ahead of the inlet.

The nozzle for the Mach 3.2 baseline engine is discussed later in this report. All P&W performance data assumed a velocity coefficient (C_v) of 0.985 that also accounts for losses in the nozzle cone. In comparison, GE provided data for an axisymmetric plug nozzle, with a C_{fg} of 0.986 at Mach 3.2 cruise. In view of the agreement between the GE and P&W data, the P&W data was used for baseline Phase III analyses.

Installed engine performance data are summarized in Figures 2-39 and 2-40. Figure 2-39 is a plot of engine jet velocity versus net thrust for sea level static (SLS) takeoff and clearly shows the magnitude of the inverted velocity profile.

During climb, installation losses reduce maximum available climb thrust approximately 5-10%, the lower figure when the inlet is started, while the decrease in specific impulse (I_{SP}) at top of climb is approximately 80 seconds. Figure 2-40 compares uninstalled and installed specific impulse during supersonic cruise. Installation losses reduce maximum cruise I_{SP} by approximately 10 percent.

The engines are individually mounted in nacelles located on the aft section of the wing. Wing-mounted pylons support the nacelles. A schematic of the nacelle, including the inlet, engine, and nozzle installation, is shown in Figure 2-41. The semi-angle of the bicone inlet tip cone is fixed at 7.10 degrees. To maintain an approximate throat Mach number of 1.3 to 1.5 for started inlet operation, the diameter of the second cone varies so that the inlet throat area can be increased for off-design Mach numbers. The semi-angle of the second cone varies from 11.4 degrees for cruise down to 7.1 degrees for the completely retracted configuration that is used for flight Mach numbers below the inlet starting Mach number of 1.95. The resulting maximum throat area available for Mach numbers below 1.95 is sufficient to accommodate engine airflow demands.

Table 2-4 shows the estimated weights of the engine and major components. The P&W estimated weight of the engine, not including the nozzle, is 4,684 pounds. The nozzle weight of 600 pounds does not include the weight of the nozzle exhaust cone, thrust reverser, or suppressor. For screening studies, a nozzle weight of 3,340 pounds was assumed based on previous Douglas studies. The scaling exponent for bare engine weight with corrected airflow is 1.02. All engine scaling is on the basis of engine corrected airflow from the baseline SLS value. For scaling purposes, it is assumed that thrust varies directly with corrected airflow.

The nozzle concept (Figure 2-42) is based on engine and acoustic studies performed by Douglas and incorporates a combination of suppression techniques to meet FAR 36, Stage 3. Inlet bleed air will be used for nozzle/engine cooling and then injected into the engine exhaust to aid in noise reduction. The duct-burning section of the nozzle has been sized for a passive thermal protection system.

Ancillary equipment for generating secondary power is clustered below the engine for easy access and safety. Conventional access concepts should enhance maintainability. Clam-shell doors provide unlimited access to engine and nozzle components. The inlet cowl can be moved forward for bicone inlet and engine

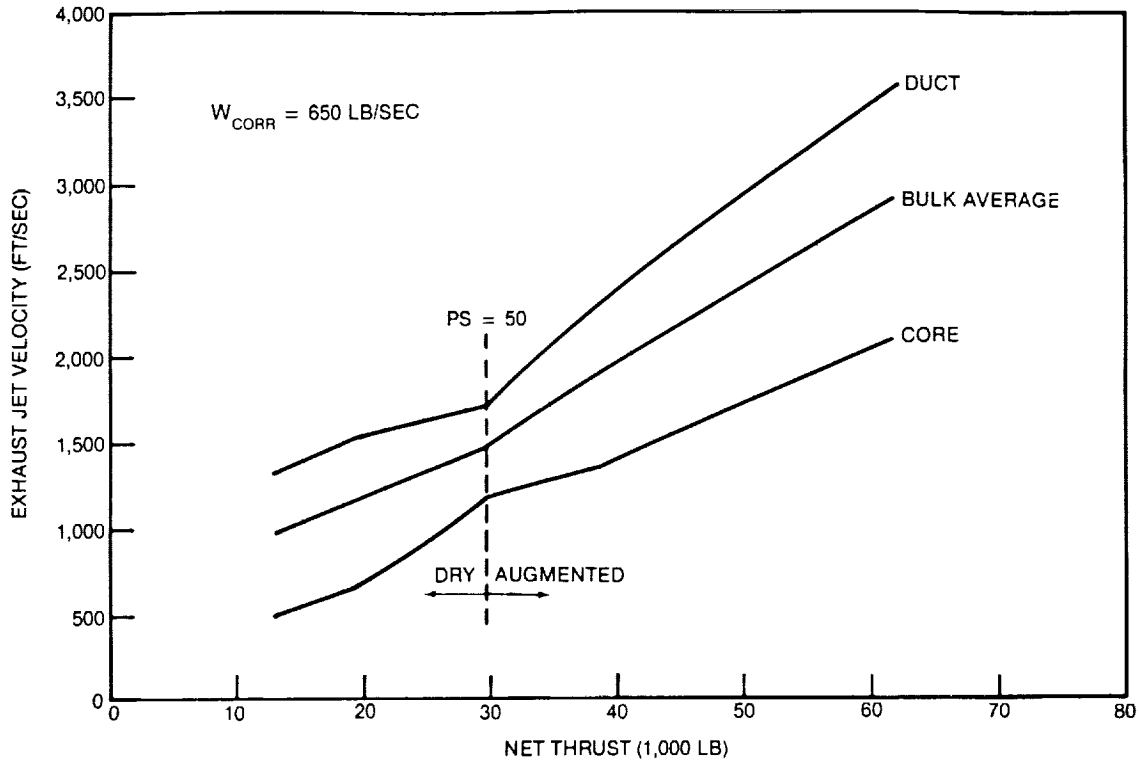

FIGURE 2-39. P&W MACH 3.2 VSCE DUCT BURNING TURBOFAN, JET VELOCITY, SEA LEVEL STATIC TAKEOFF

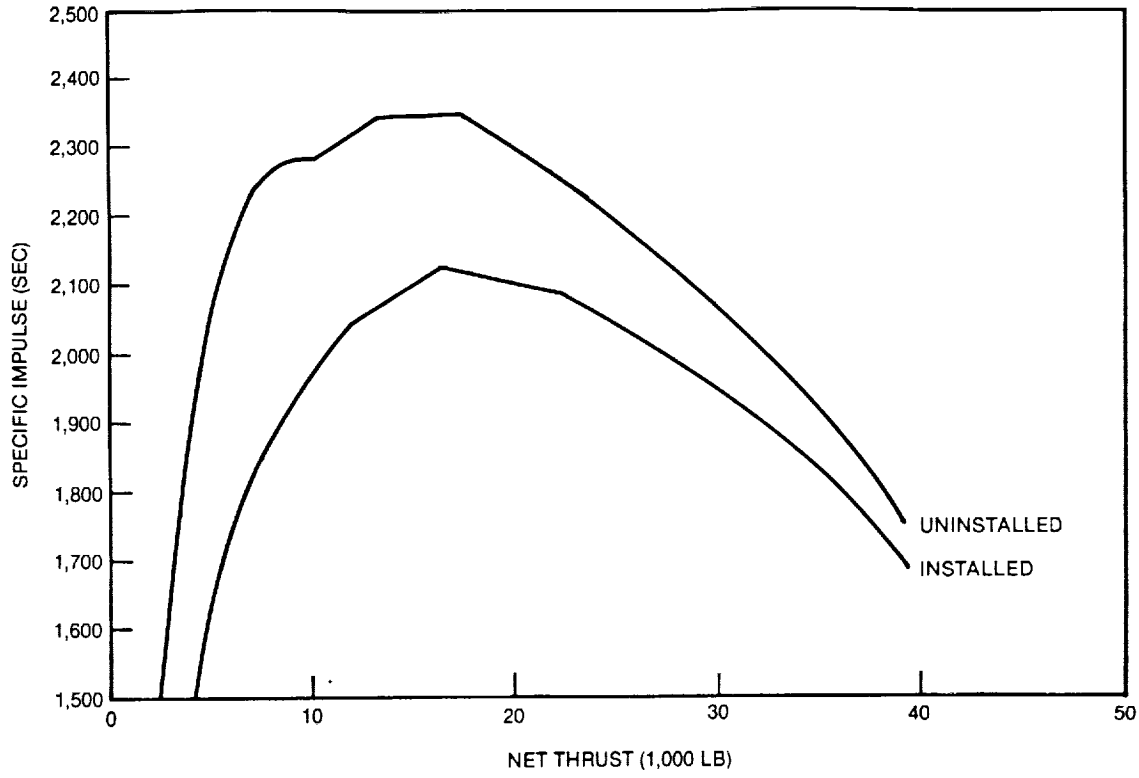

FIGURE 2-40. P&W MACH 3.2 VSCE DUCT BURNING TURBOFAN, MACH 3.2 CRUISE SPECIFIC IMPULSE AT 65,000 FEET

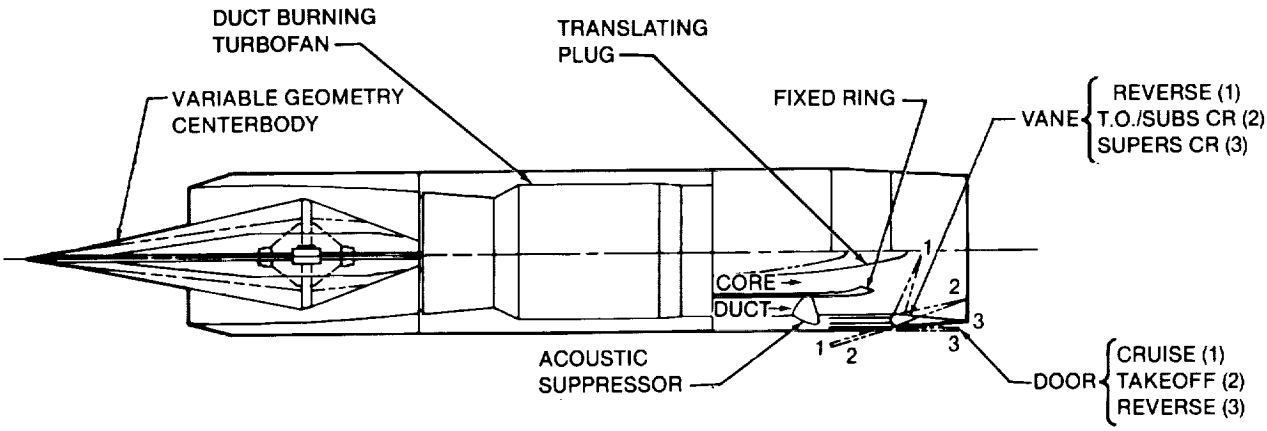

FIGURE 2-41. MACH 3.2 NACELLE FEATURES, P&W VSCE DUCT BURNING TURBOFAN

TABLE 2-4
P&W MACH 3.2 VSCE DUCT BURNING TURBOFAN, MAJOR ENGINE COMPONENT WEIGHTS

DESIGN CORRECTED AIR FLOW = 650 LB/SEC

COMPONENT	WEIGHT (LB)
BARE ENGINE	4,114
MOUNTS	70
NOZZLE	600
CONTROL/PLUMBING	500
TOTAL	5,284

access. Maintenance can be performed using ground access stands and conventional equipment. Firewalls, fire detectors, and fire extinguishers in each nacelle provide fire protection. Dual fire detection sensors are used to signal both overheat and fire. A fire signal will automatically shut off fuel to the affected engine and discharge the stored extinguishing agent. The system must be designed to protect the primary structure.

Fuel will be supplied in shrouded lines to the engine by routing it through the pylon. Pressure relief and drainage is provided. Shut off valves and flow metering devices are located for easy access.

P&W has provided a preliminary assessment of takeoff noise reduction which identified the VSCE and the turbine bypass engine as having the greatest potential for satisfying FAR Part 36, Stage 3 requirements, with the VSCE having the edge. One element favoring the VSCE is the inherent inverted velocity profile (IVP).

Use of independently variable fan and core jet areas is a key feature of the variable stream control engine. This allows optimization of the takeoff part power airflow and enables "high flowing" the engine i.e., maintaining maximum design flow, over a range of takeoff power conditions. The engine thereby maintains maximum airflow and achieves thrust variation primarily through changes in jet velocity.

The VSCE with a suppressor nozzle would normally have a fixed duct stream (suppressor) jet area when deployed over the sideline and community noise monitors. For purposes of this sideline noise study, however, a variable area suppressor was assumed. This will allow optimization of jet noise at the sideline

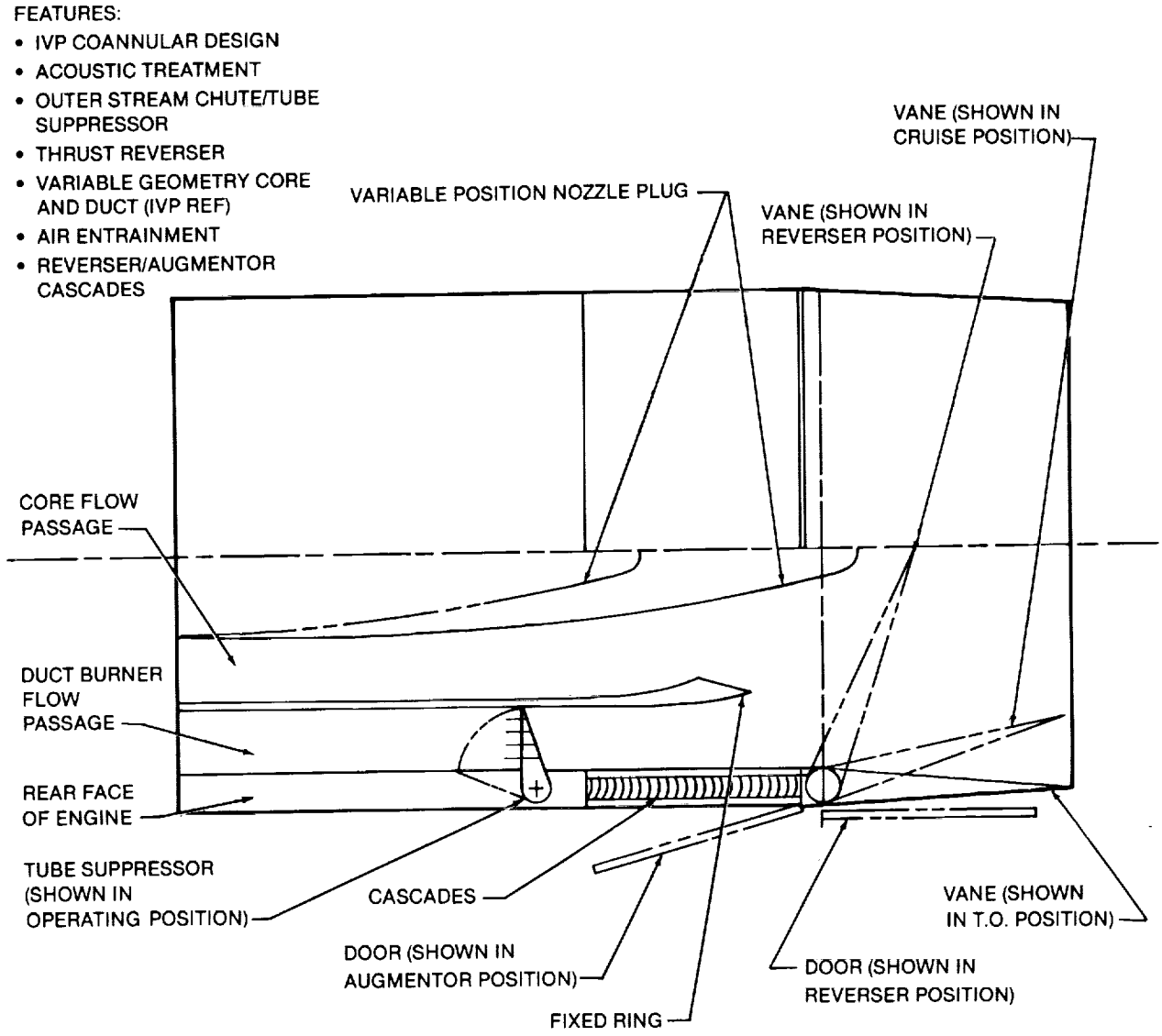

FIGURE 2-42. MACH 3.2 NOZZLE WITH ACOUSTIC SUPPRESSION FEATURES

condition. Once the amount of engine scaling/oversizing for sideline noise has been determined (along with the associated suppressor jet area), that suppressor jet area would then be held fixed at that design duct jet area for future studies such as cutback noise. Full two-stream nozzle variability is still available at all other flight conditions with the suppressor in the stowed position.

Figure 2-43 shows P&W estimates for sideline EPNdB as a function of bulk average jet velocity at takeoff. These data are for the unscaled (650 pounds per second) engine at all jet velocities (i.e., the effect of decreasing jet velocity on engine and aircraft size was not accounted for). The data do, however, account for four engines. These data were developed by correlating engine jet velocity against engine thrust. Both unsuppressed and suppressed data are shown, with and without a thermal acoustic shield.

All data in Figure 2-43 assume use of an acoustically treated ejector nozzle with a length/diameter ratio of 1.5 and a 1.5-inch thick acoustic treatment. The estimated weight of this nozzle (without suppressor) for an engine corrected airflow of 650 pounds per second is 2,390 pounds based upon previous Douglas supersonic transport studies.

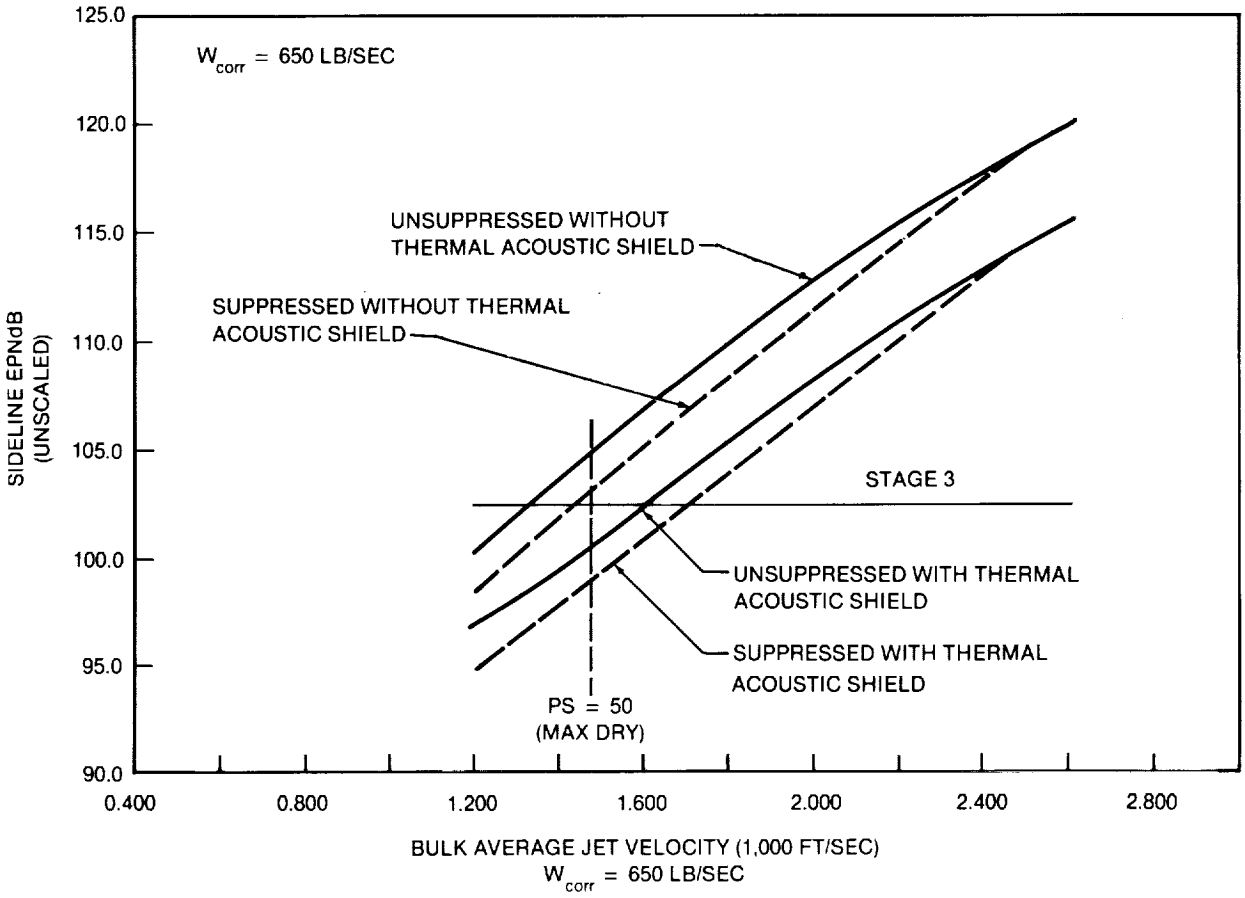

FIGURE 2-43. P&W VSCE SIDELINE NOISE AT TAKEOFF

The suppressed data assume a stowable mechanical suppressor deployed in the duct stream. This suppressor features 12 chutes with 24 tubes at the outer rim, with a base area to jet area ratio of 2.6. The estimated weight of the suppressor for an engine corrected airflow of 650 pounds per second is 670 pounds.

The thermal acoustic shield is a relatively low velocity, high-temperature, partial-annular (180 degrees) shielding stream. It reduces the noise on the shielding side (toward the observer) by both reducing the shear on that side (reduced source) and by redirecting the generated noise away from the observer (shielding). A noise reduction of approximately 4 PNdB is projected for this concept. The estimated weight of a thermal acoustic shield for an engine corrected airflow of 650 pounds per second is 810 pounds.

Figure 2-43 shows that, theoretically, Stage 3 requirements can be satisfied by oversizing the engine to permit throttling the engine and still maintain the same thrust while reducing jet velocity to an appropriate level. However, this may not be the case, since preliminary analyses have indicated that the resulting growth in aircraft and engine size produces a noise increase that more than offsets the noise reductions due to lower exhaust velocities. Thus, it is imperative that the development of low noise nozzles be a prime area for further study.

Mach 5.0 Baseline Engine – GE Turbofan/Ramjet Engine. The Mach 5.0 baseline engine is the GE variable cycle turbofan/ramjet engine (also referred to as a variable cycle hypersonic jet or VCHJ) using LNG fuel. The unscaled engine has a design corrected airflow of 748 pounds per second, and a design maximum dry SLS thrust rating of 72, 183 pounds. Although the engine is augmented, it has been sized to take off partially dry, and the augmented SLS rating is not specified.

The VCHJ is a new engine concept defined by GE in 1985 from variable cycle concepts originally studied during the NASA-sponsored AST/SCAR supersonic transport studies during the late 1970s. The basic engine configuration is shown in Figure 2-44. The engine is an after-burning dual-rotor turbofan that

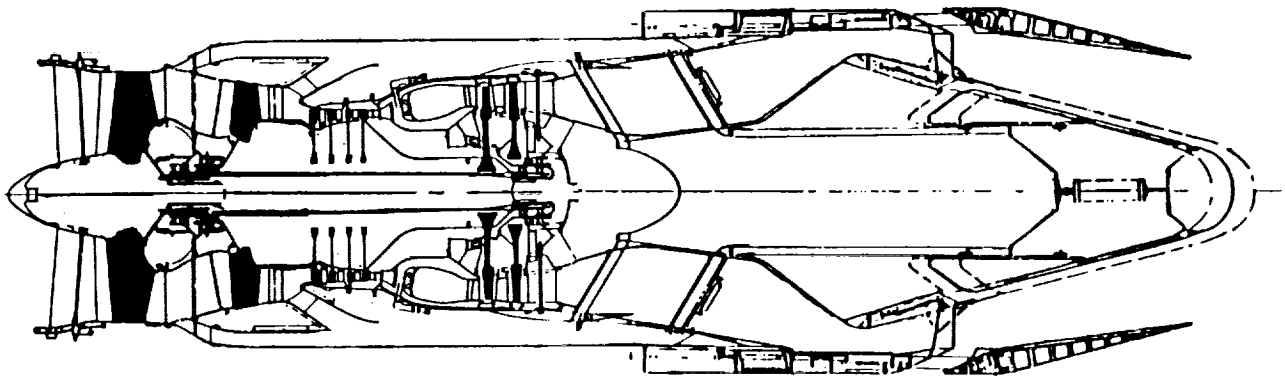

ENGINE SHOWN WITH AXISYMMETRIC COANNULAR NOZZLE

FIGURE 2-44. GE MACH 5.0 VCHJ

combines double-bypass, variable-cycle engine features with high Mach flow enhancement concepts. Several smooth transitioning engine operational modes are made possible by these features:

- Low specific thrust takeoff for noise reduction, with high thrust capability via augmentation, if required
- Maximum climb and acceleration thrust during subsonic cruise and transonic engine operation
- High thrust windmilling (ramjet) operational modes plus efficient hypersonic cruise capabilities
- Very good part-power subsonic cruise and loiter capabilities

The turbofan core engine of the VCHJ is based on the double bypass, variable cycle engine (VCE) developed by GE during studies of supersonic propulsion technology conducted as part of the NASA-sponsored Supersonic Cruise Research (SCR) program. The VCE core employs a low-temperature augmenter for supersonic acceleration. Noise constraints preclude the use of the augmentor at takeoff; therefore, the fan has been sized to satisfy takeoff and subsonic cruise requirements without augmentation.

The variable cycle features that give the VCE core improved flexibility over conventional mixed flow turbofans are:

- Split fan (outer) bypass duct between the high flow front block and the rear block with variable inlet guide vanes
- Fan variable area bypass injector (forward VABI)
- Exhaust variable area bypass injector (rear VABI)
- Variable area low pressure turbine
- Core driven rear fan block
- Variable area exhaust system with inverted velocity profile during takeoff

The turboramjet essentially phases out the turbomachinery during very high-speed operation. A ram air bypass duct is located around the basic engine, and a special stream control valve functioning in a manner similar to a GE patented variable area bypass injector (VABI) is employed to allow smooth transition from pure turbojet mode to pure ramjet mode as flight speed increases above Mach 3. If compressor windmilling cannot provide enough shaft power for power generation, a ram air turbine auxiliary power unit will supply airframe requirements.

The cycle and component design parameters for this engine are:

- Overall pressure ratio 25
- Turbine rotor inlet temperature 4,000°F maximum

- Bypass ratio 1.50
- Fan pressure ratio 5.5

For the Mach 5.0 baseline engine, a variable geometry two-dimensional inlet was selected. The inlet and nozzle are designed for Mach 5.0 cruise at an altitude of 83,000 feet, which is the midpoint altitude between start of cruise and end of cruise. The inlet capture area is sized to satisfy engine, inlet bleed, and miscellaneous airflow requirements. The local flow conditions ahead of the inlet were determined by assuming a wing leading edge precompression resulting from six degrees flow deflection.

All performance data used in Phase III are installed data, and account for inlet drag and recovery factor variation with freestream Mach numbers. Inlet drags include bypass, boundary-layer bleed, spillage drags, as well as miscellaneous drag due to inlet leakage, engine cooling, and the like. Inlet nacelle external skin friction drag is not included, as it is accounted for in the airframe drag.

The raw GE data were computed using MIL-E-5007D inlet total pressure recovery, since better estimates of inlet pressure recovery were not yet available. For Mach numbers above the inlet starting Mach number of 1.50, inlet recovery is generally greater than the MIL-E-5007D value and is based on MIL-E-5007D but using local total pressure and Mach number ahead of the inlet. Below Mach 1.50, the pressure recovery is lower than the MIL-E-5007D value and is based on leading edge shock losses, inlet shock losses external to the inlet, and viscous losses, and the effect of the normal shock ahead of the inlet.

Figure 2-45 shows the Single Expansion Ramp Nozzle (SERN) that has been incorporated into the Mach 5.0 concept. The SERN allows for a high degree of propulsion system integration, since the contoured upper nozzle surface is formed by the aircraft lower surface. The nozzle used is minimum length, with a point expansion fan in the nozzle throat and isentropic flow turning along the upper nozzle contour. The exact nozzle geometry was developed from nozzle throat and ambient conditions for cruise.

In contrast, the raw GE data are based on performance characteristics of a symmetrical two-dimensional convergent-divergent (2D-CD) nozzle. Research revealed that the Douglas-designed SERN performance equaled or exceeded the GE estimates. Therefore, no correction factors were applied to the raw GE data to account for nozzle performance.

As part of their Phase III effort, GE investigated adapting their acoustic control nozzle with the two-dimensional SERN, with the results shown in Figure 2-46. The primary change to the basic SERN was the addition of a centerbody, which is axisymmetric at the engine face and transitions to two-dimensional upstream of the nozzle throat. At the throat, the two-dimensional centerbody pivots to provide equal area ratios on the upper and lower surfaces of the centerbody to minimize mixing losses at the centerbody trailing edge. Because of the SERN installation, the GE nozzle design does not include an ejector, and hence it resembles a chute suppressor nozzle but without an ejector.

GE estimated a sideline noise of 109.7 EPNdB. This estimate was based on a four engine operation but did not include aircraft scaling effects. The scaling factor for the baseline Mach 5.0 concept is 1.842 based upon a TOGW of 1,213,000 pounds. The scaled noise estimate would be approximately 112 dB, or approximately 10 dB in excess of the Stage 3 limit.

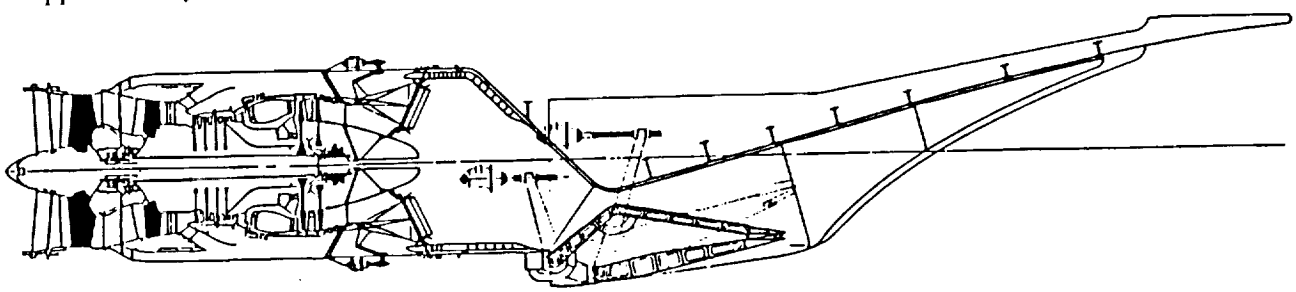

FIGURE 2-45. MACH 5.0 SINGLE EXPANSION RAMP NOZZLE

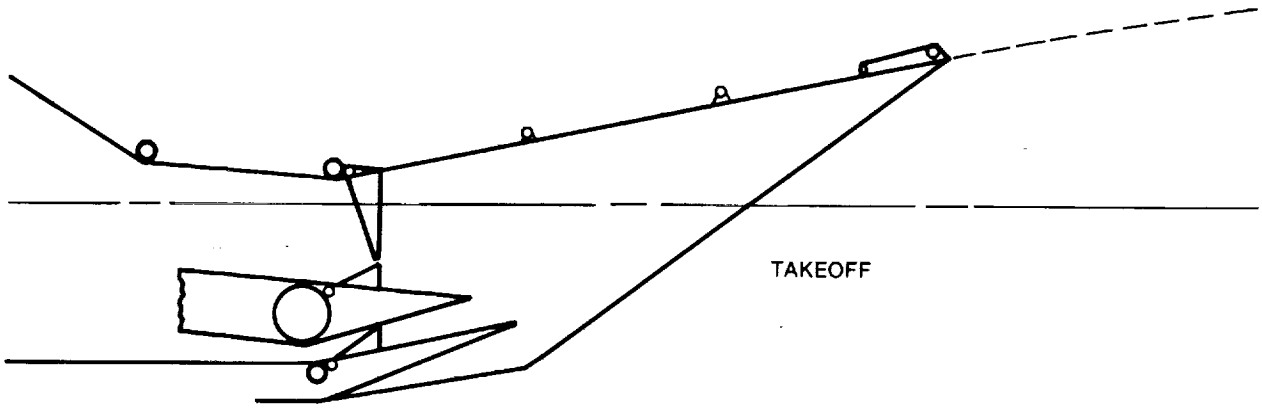

FIGURE 2-46. GE MACH 5.0 WEDGE SUPPRESSOR NOZZLE CONCEPT

Installed engine performance data are summarized in Figures 2-47 and 2-48. Figure 2-47 is a plot of bulk average jet velocity versus SLS net thrust for the unsuppressed and suppressed modes, with no jet velocity reduction due to entrainment of ambient air. Figure 2-48 shows that jet velocity is not substantially different for unsuppressed and suppressed mode operation.

During climb, installation losses reduce maximum available climb thrust approximately 2-5%. The decrease in specific impulse (I_{SP}) at the top of the climb is approximately 40 seconds.

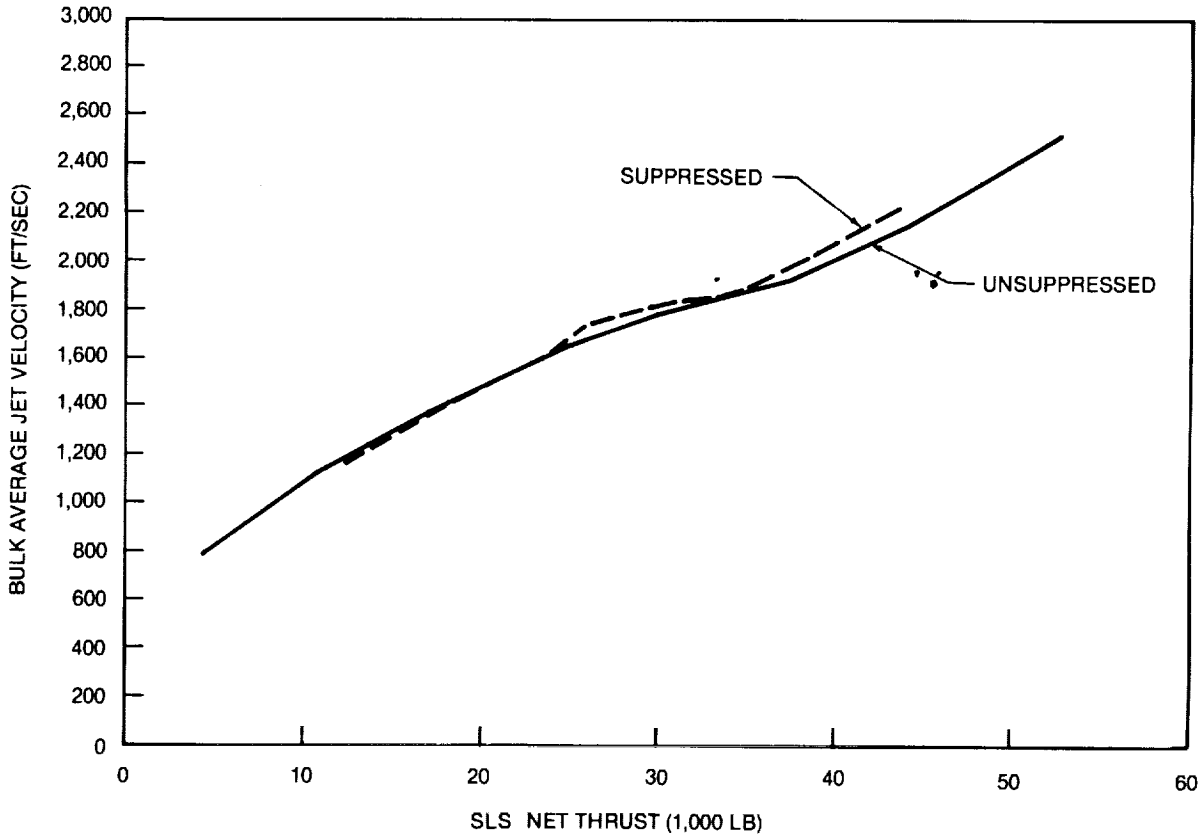

FIGURE 2-47. GE MACH 5.0 VCHJ

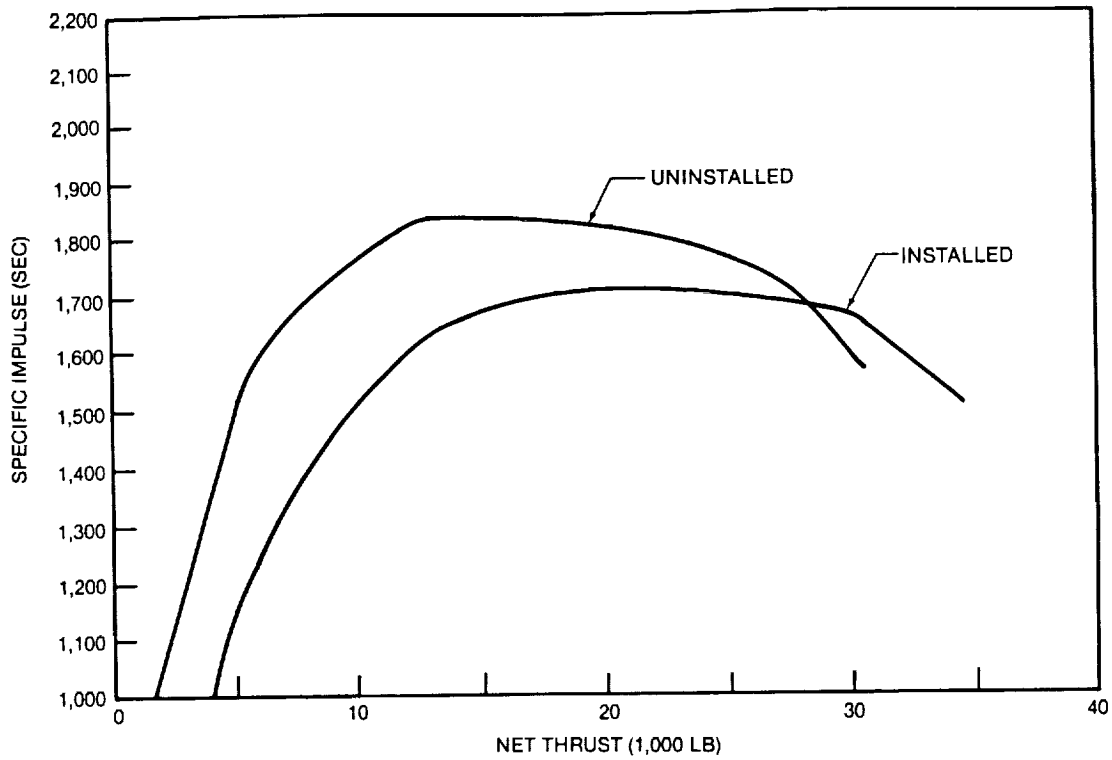

FIGURE 2-48. GE MACH 5.0 VCHJ — INSTALLED I_{SP} AT 80,000 FEET

Figure 2-48 compares uninstalled and installed supersonic cruise specific impulse. Installation losses are seen to reduce the maximum I_{SP} by nearly 10 percent.

The four engines are mounted in a Quad Pod propulsion module on the fuselage lower centerline. Thus the engine installation is aerodynamically integrated with the fuselage. The propulsion system Quad Pod is comprised of three different modules with two transition sections. Depending on the final configuration of the aircraft, engine removal will either be from below or, if there is insufficient ground clearance, on rails from the rear after removing the nozzle transition/variable throat module. The Quad Pod inlet is divided into two modules; the inlet with individual movable ramps and the transition section including both bypass air and pressure surge dumps.

The capture area for the unscaled engine inlet is 18.92 square feet. The inlet width for the unscaled engine is 78.00 inches, and the inlet height measured with respect to the initial point of the forward inlet ramp is 34.94 inches. The inlet width exceeds the maximum engine diameter by six inches to allow enough clearance between adjacent engines for mounting and ducting hardware.

The variable inlet throat area is increased for off-design Mach numbers so that a throat Mach number of approximately 1.3 to 1.5 is maintained. At cruise speed, the inlet ramp deflects the aircraft forebody flow by a maximum of 12 degrees; at off-design Mach numbers, the inlet ramp flow deflection decreases down to a value of zero for Mach numbers below the inlet starting Mach number of 1.5.

The inlet incorporates localized porous bleed in areas around the shock impingement points in the supersonic diffuser. Flow is bled in the terminal normal shock area through the slot formed by the inlet moveable ramp surfaces. Some sidewall bleed will be provided, if required.

A segment of the upper nozzle surface is moveable allowing for variation of nozzle throat area. Nozzle mass flow variations with flight altitude and Mach number, as well as engine throttle setting, mandate the need for a variable throat area. The lower nozzle ramp can rotate about a pivot point located upstream of the throat, allowing control over the exit area of the ducted portion of the nozzle flow. This alleviates the

amount of nozzle flow overexpansion occurring for the higher back-pressure cases. Entrainment chutes are located in the lower nozzle ramp to alleviate take-off noise and exit flow overexpansion.

The thrust reverser, shown in Figure 2-49, employs a simple drop bucket, or chute, to direct the thrust from the outboard engines forward and slightly outboard from the sides of the propulsion pod. Turning vanes will be provided as required in the bucket to properly direct the airflow direction. During reverser operation, the center engines will be reduced to idle.

The engine compartment will house four separated engines and contain provisions for fuel lines, secondary power generating equipment, cooling air ducting, compartment ventilation, and fire protection. The preferred method for mounting the engines will be by using trunions on the engine center line and by using sliding trunions at the forward end of the engine. Engines will be sealed to the inlet and nozzle ducts with flexible metal bellows secured with band clamps.

All engine scaling is on the basis of engine-corrected airflow, with the baseline SLS value being 748 pounds per second. For scaling purposes, it is assumed that thrust varies directly with corrected airflow. The heat exchanger and miscellaneous items are located outside the engine envelope. The fuel/air heat exchanger used for engine cooling is the only significant item. The ram air that is cooled by the heat

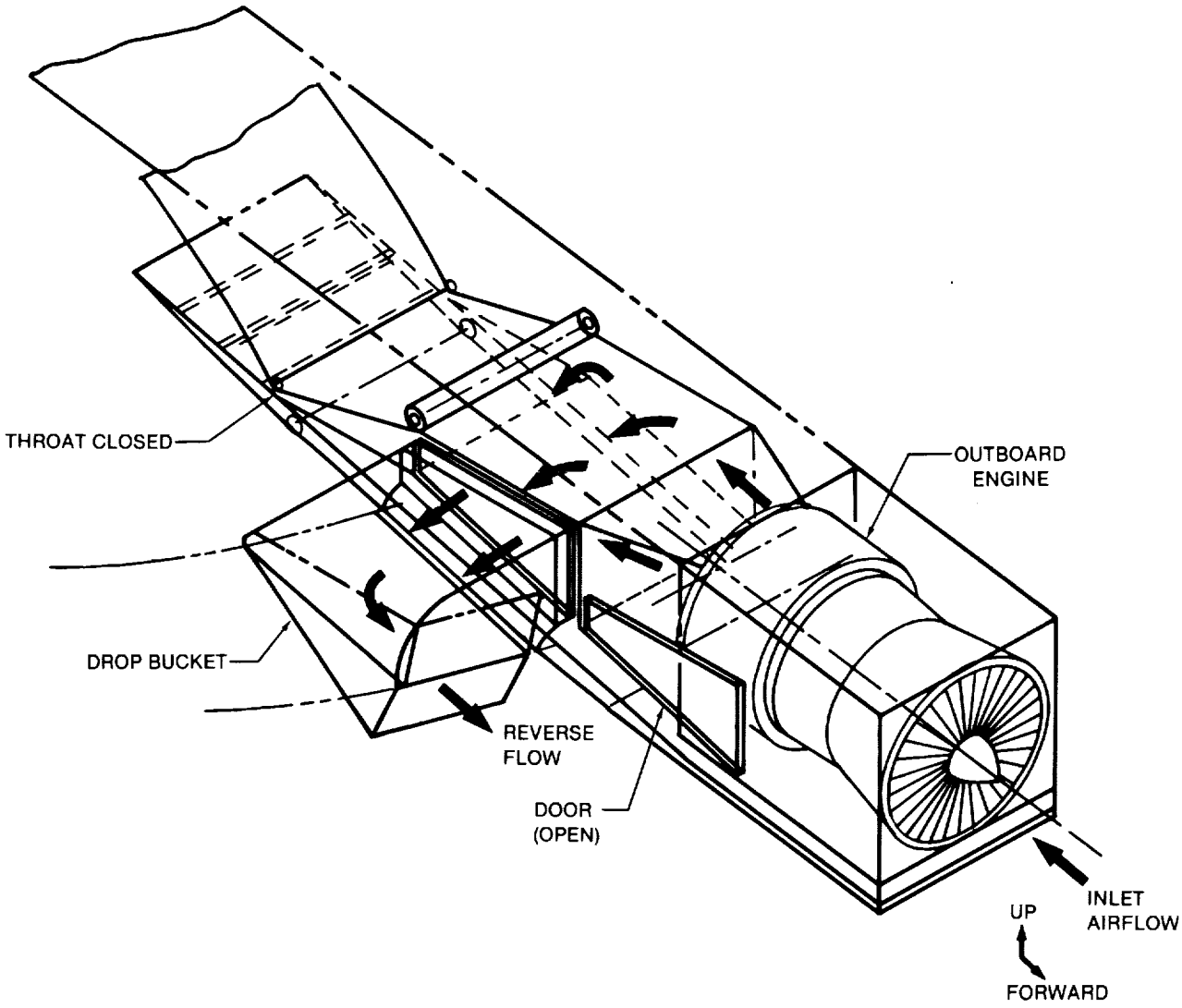

FIGURE 2-49. MACH 5.0 THRUST REVERSER SYSTEM

exchanger used for engine cooling is the only significant item. The ram air that is cooled by the heat exchanger is taken off the engine shell approximately 60 inches aft of the engine face, with the cooled air injected into the vicinity of the engine-nozzle interface.

GE's weight estimates are based on a materials availability date (MAD) of 2000 (2010 IOC), which would suggest that the data represent today's best estimates of future materials development. However, the weight data do include a 5- to 10-percent margin. The heat exchanger weight is a function of the cooling load, and this, in turn, depends upon the materials used. Use of lighter materials with higher temperature capability would reduce the weight of the engine and the size and weight of the heat exchanger.

Alternate HSCT Engines. The alternate Mach 3.2 engine is the GE Variable Cycle Engine (VCE) using thermally stable jet fuel (TSJF). The basic engine configuration is shown in Figure 2-50. The unscaled engine has a design-corrected airflow of 737 pounds per second, and a maximum dry SLS thrust rating of 65,167 pounds. The engine is not augmented.

The engine is essentially the core engine of the GE Mach 5.0 VCHJ. The VCE is twin spool, with double bypass variable geometry to optimize fan/compressor/turbine match over the entire flight spectrum to maximize subsonic and supersonic cruise performance. Unlike the Mach 5.0 engine, the Mach 3.2 VCE incorporates a GE-designed axisymmetric nozzle with translating nozzle shroud and inner plug to vary the nozzle throat area. During takeoff, the bypass flow is diverted through struts. This forces the flow along the inner plug to achieve an inverted velocity profile for jet noise reduction.

The cycle and component design parameters for this engine are:

- Overall pressure ratio 22
- Fan pressure ratio 4.8
- Bypass ratio 0.5
- Maximum rotor inlet temperature 4,000°F

All engine scaling is on the basis of engine-corrected airflow, with the baseline SLS value being 737 pounds per second. For scaling purposes, it is assumed that thrust varies directly with corrected airflow.

Engine performance data are presented in Figures 2-51 and 2-52. Inlet installation drag and total pressure recovery data were determined using the procedure summarized earlier in this report, but using GE airflow schedules. GE estimated the nozzle performance data for an axisymmetric nozzle with translating inner nozzle plug.

The alternate Mach 5.0 engine is the Aerojet TechSystems, two-spool air turboramjet (ATR) using LNG (Figure 2-53). Initially, Aerojet proposed a conventional dual regenerator ATR where the incoming fuel is heated regeneratively in the combustor and nozzle walls to drive the turbine while providing cooling for these areas. The result was an engine that yielded estimated Mach 5.0 cruise performance equal to or better than that of the GE VCHJ. However, the subsonic performance was significantly less that that of the VCHJ (1,872 seconds specific impulse at Mach 0.95 cruise versus 4,352 seconds for the VCHJ, with corre-

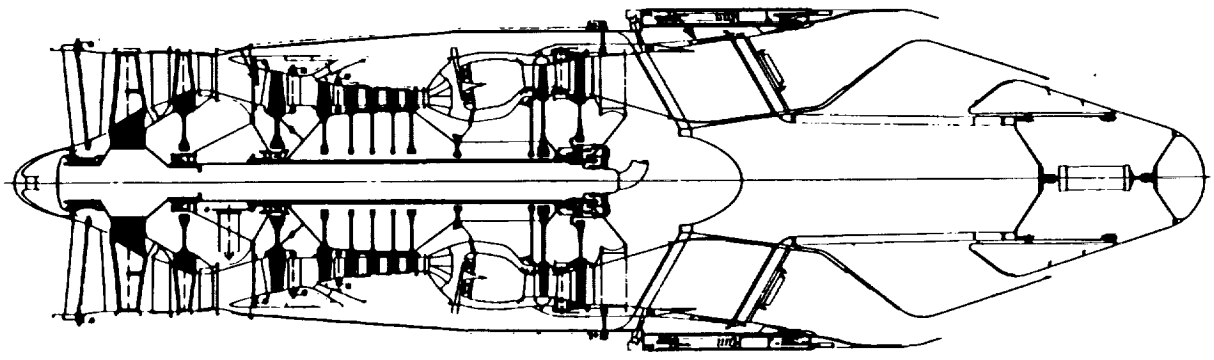

FIGURE 2-50. GE MACH 3.2 VCE

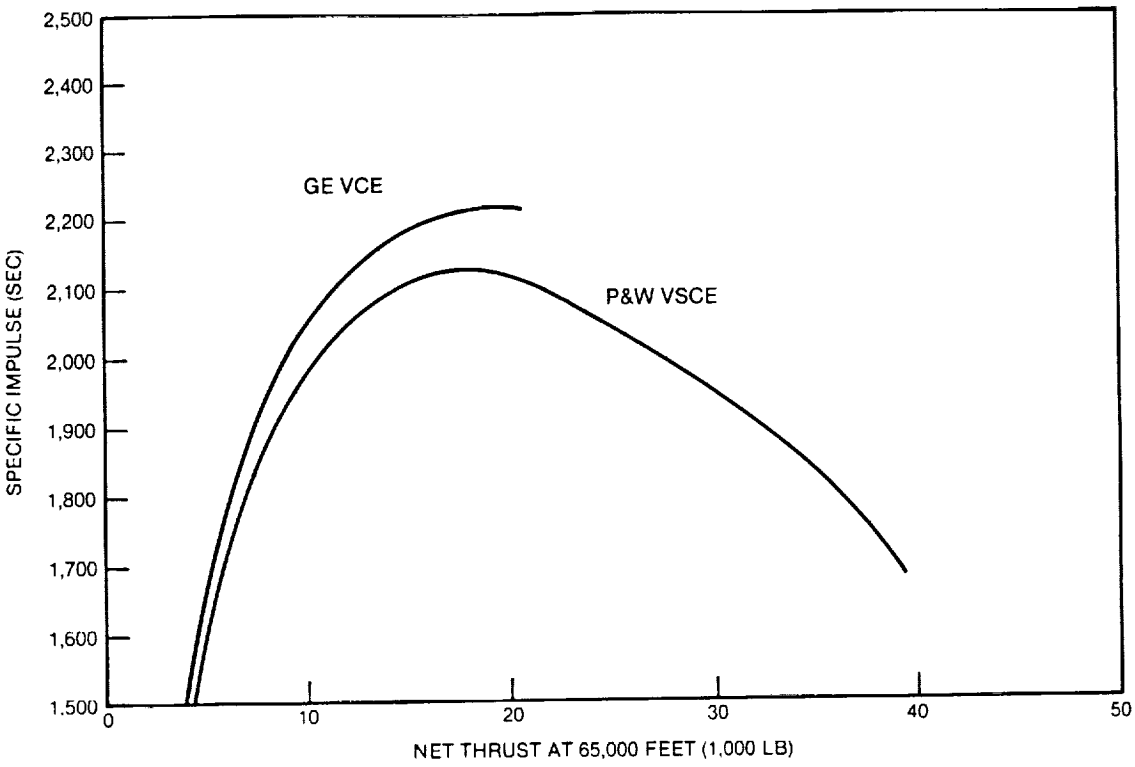

FIGURE 2-51. COMPARISON OF INSTALLED CRUISE SPECIFIC IMPULSE FOR MACH 3.2 ENGINES

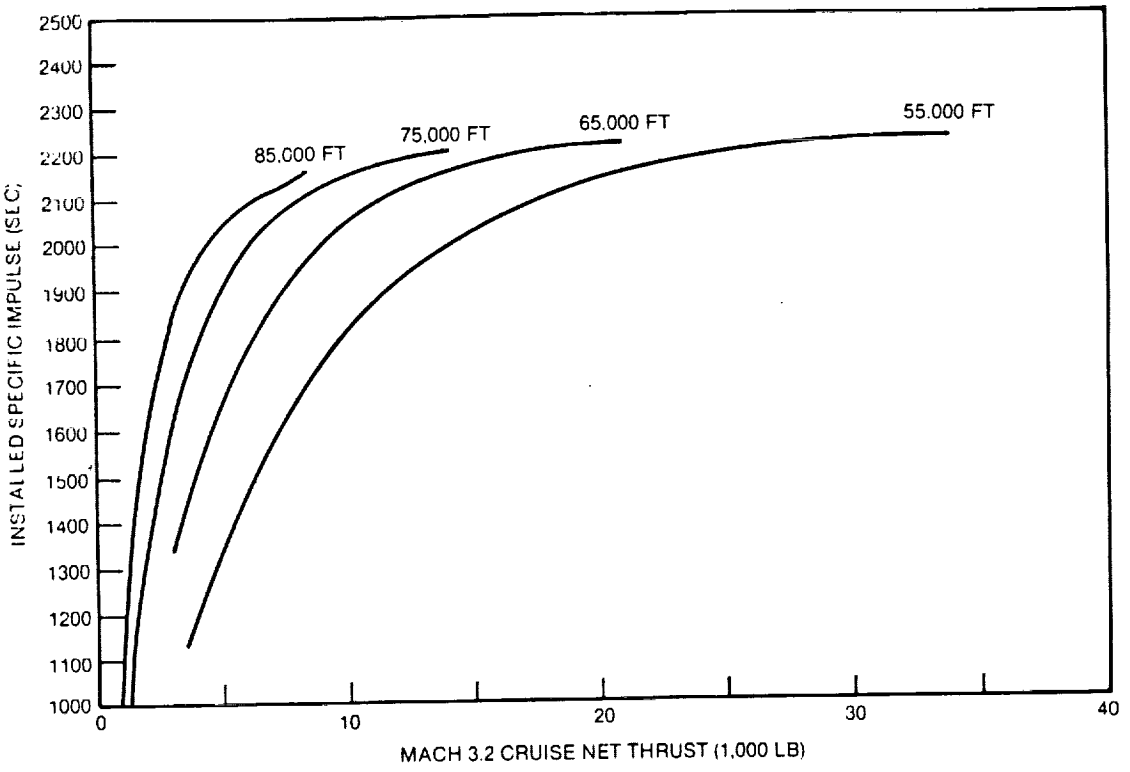

FIGURE 2-52. GE MACH 3.2, VCE — INSTALLED CRUISE SPECIFIC IMPULSE

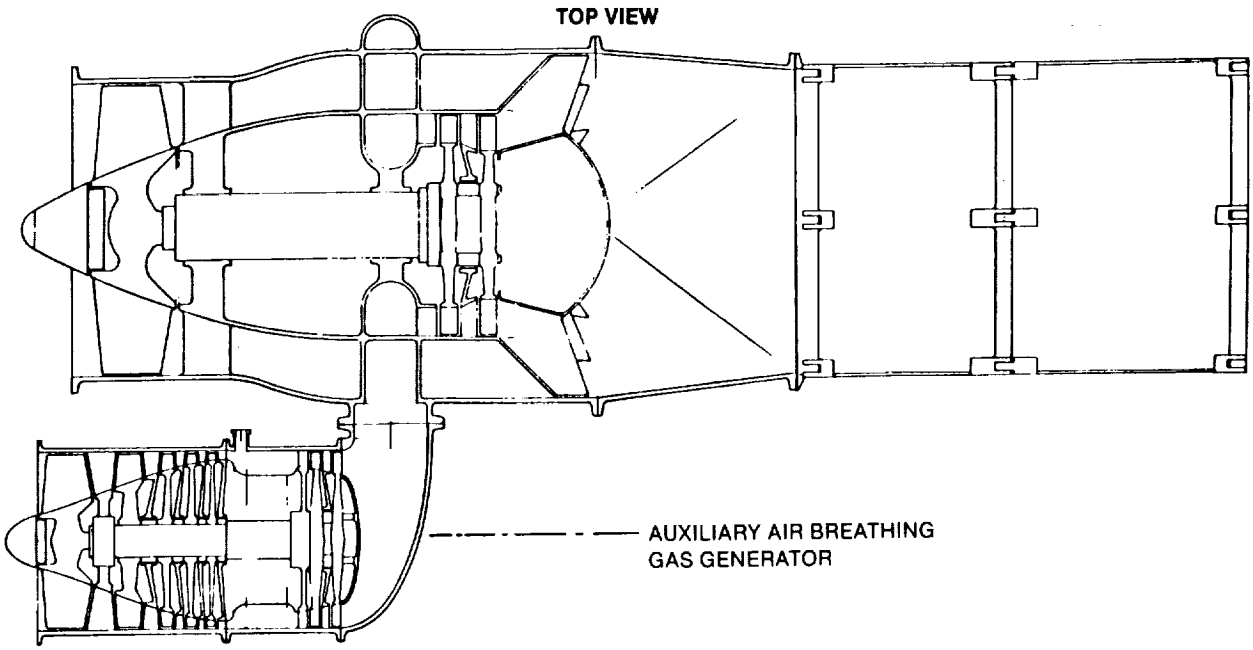

FIGURE 2-53. AEROJET TECHSYSTEMS MACH 5.0 TWO-SPOOL ATR ENGINE

sponding reduced performance during climb, especially below Mach 3.0). When these data were used to estimate aircraft takeoff gross weight, the results showed the VCHJ with a significant advantage, even for the all-supersonic cruise mission.

During Phase III, Aerojet proposed a two-spool ATR, where a separate auxiliary airbreathing gas generator provides the motivating force for the turbine at flight speeds below Mach 3.0. The result is significantly improved subsonic performance (specific impulse greater than 5,300 seconds at Mach 0.95 cruise), but at the expense of additional weight.

Although the latest Aerojet TechSystems data show potential for lower takeoff gross weights than for the VCHJ, no comparative analyses were accomplished due to resource limitations.

Baseline Engine Performance Improvement. A prime objective of the HSCT program is to identify the key propulsion-related technologies that limit HSCT potential and those technological areas that offer the greatest potential for achieving HSCT economic viability and environmental acceptability. All three engine companies (GE, P&W, and Aerojet TechSystems) provided inputs and projections for future improvements. For the baseline discussions, an FAA certification date of 2005/2010 was assumed, with projections beyond that to an FAA certification date of 2015/2020. This section discusses those technology areas that could result in reduced TOGW.

For this study, the critical technologies are:

- Improved cycle performance, both at subsonic and supersonic cruise
- Reduced engine weight (increased thrust/weight)

The two items are directly related to economic viability, with advanced hot section design critical to both.

The baseline Mach 3.2 engine is the P&W variable stream control engine (VSCE) and the alternate Mach 3.2 engine is the GE variable cycle engine or (VCE). Both engines use kerosene-based, thermally stable jet fuel, or TSJF. Both these engines were used by the respective engine companies as the baseline Mach 3.2 engine for technology projections.

Sizing studies have shown that mission total fuel comprises over 60 percent of the TOGW, and that TOGW is sensitive to cruise specific impulse (specific fuel consumption). Of particular concern is subsonic specific fuel consumption in view of the potential for subsonic cruise over land to prevent sonic boom and

the correspondingly large fuel fraction required for the subsonic cruise segment over land.

P&W performed a subsonic performance improvement study for the VSCE in which the effects of changes in major cycle parameters – fan pressure ratio, bypass ratio, overall pressure ratio, and design combustor exit temperature – were evaluated. The study results showed that increasing overall pressure ratio by 10% (to 15.8) offered the best potential for improvement in subsonic SFC, but the improvement was only 1.4 percent.

Sensitivity studies for the subsonic cruise over land case show that the corresponding reduction in TOGW would be approximately 2 percent, not including any allowance for a corresponding engine weight increase which could negate any TOGW savings. It is concluded, therefore, that these data show little promise in substantially reducing TOGW.

GE performed a similar study for its Mach 3.2 VCE. However, GE took a different approach examining the effects of control schedules. In its study, engine control schedules were optimized for Mach 0.95 cruise at 30,000, 35,000, and 40,000 feet, assuming dry thrust. The results of this study indicated a potential reduction in SFC from 0.5 to 2.0 percent through control schedule modification. The corresponding TOGW decrease would be approximately 0.7 to 3.0 percent.

From the above data, it is concluded that there is little or no promise in substantially reducing subsonic specific fuel consumption using the techniques discussed above. This is underscored by the different approaches investigated at the two engine companies and the small differences between the P&W and GE results. Other approaches must be taken to reduce aircraft subsonic specific fuel consumption.

Both engine companies were requested to provide projections of SFC improvements assuming better technology to determine the potential for performance improvements. GE provided the following SFC reduction projections for their Mach 3.2 variable cycle engine:

- Mach 0.9 at 36,089 feet – 5.2% Δ SFC
- Mach 3.2 at 65,000 feet 3.0% Δ SFC

These improvements would be achieved through component efficiency increases, reductions in cooling air requirements, improvements in burner efficiency, and reductions in nozzle unburned air. Increased material temperature capability and better flow modeling to reduce losses and better heat transfer formed the bases for these projections. These techniques would increase engine thrust/weight, further reducing TOGW.

To assess the effect of SFC and engine weight reductions on aircraft TOGW, sensitivity analyses were performed for two 6,500 nautical mile missions assuming

- All supersonic cruise
- 2,000 nautical mile subsonic cruise segment over land

Using these sensitivity data, these SFC reductions would result in an approximate 6-percent TOGW reduction for the all supersonic cruise mission and 11-percent TOGW reduction for the mission with 2,000-nautical-mile subsonic cruise segment over land.

The GE projections are consistent with the P&W goal of 5-percent reduction in SFC, and it is reasonable to assume that comparable improvements would be achieved with the P&W VSCE.

Another key technology area affecting TOGW is engine thrust-to-weight (T/W) ratio. P&W has established a goal of a 10- to 15-percent improvement in engine T/W and discusses three major improvement areas:

- Materials technology
- Turbine technology
- Cooling system technology

This information was based upon results of a series of Air Force funded (e.g., IHPTET), NASA, and engine company in-house studies. Figure 2-54 shows projected thrust/weight trends for the GE Mach 3.2 variable cycle engine (VCE) and the Mach 5.0 variable cycle turbofan ramjet (VCTJ) along with the current GE estimates for these engines. The sea level static takeoff jet velocity was arbitrarily limited to approximately 2,500 feet per second to reduce jet noise.

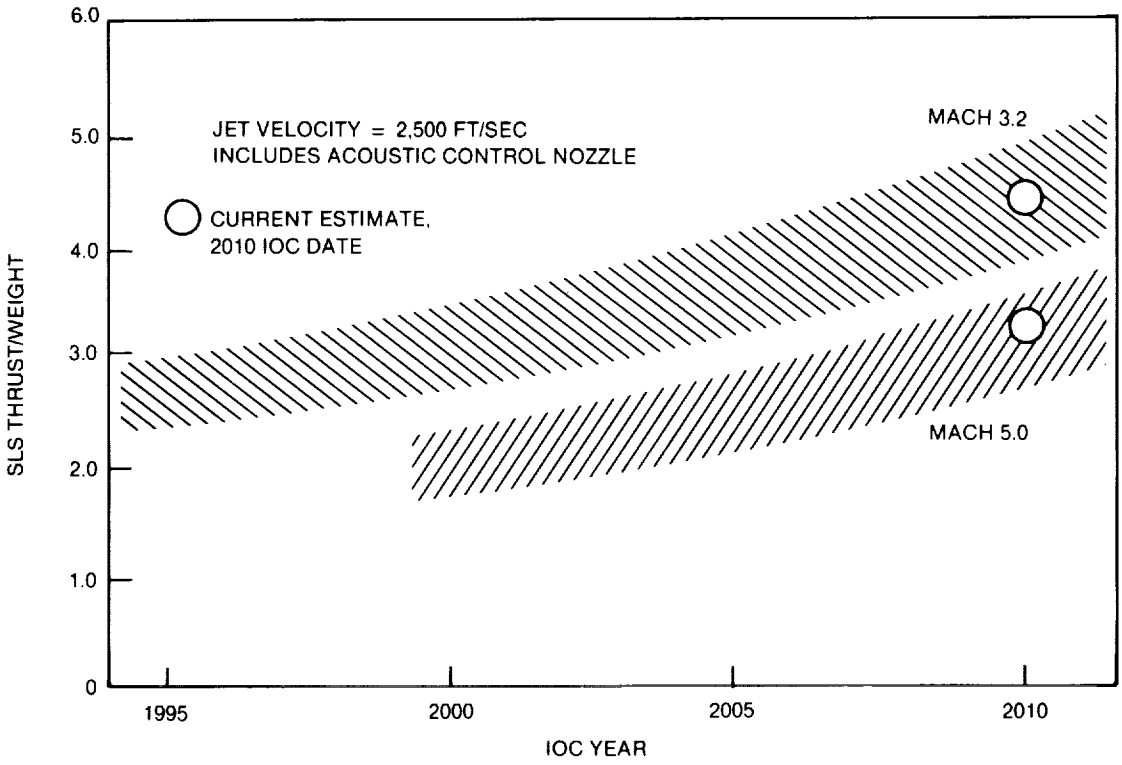

FIGURE 2-54. GE TECHNOLOGY PROJECTIONS

Figure 2-54 shows that there is a wide band in the projections for thrust/weight improvements. However, the data would indicate that a 15- to 20-percent improvement in thrust/weight is not unrealistic. An additional 10-percent improvement would be achieved if the design jet velocity could be increased to 2,800 feet per second and still satisfy FAR Part 36 Stage 3 noise requirements, assuming no additional nozzle weight penalty for suppression devices. Combining these two projections and including an allowance for additional noise suppression devices, an overall projection for increased thrust/weight of 20 to 25 percent appears reasonable. From sensitivity analyses, the corresponding TOGW reductions would be approximately:

- 9 to 11 percent for the all supersonic cruise mission
- 14 to 17 percent for the mission with 2,000 nautical mile subsonic cruise segment over land

It is concluded that, although engine weight is only approximately 10 percent of TOGW, there is the potential for TOGW reductions of 10 percent or more from increasing engine thrust/weight. It is thus recommended that emphasis be placed upon reducing engine weight as a means of reducing TOGW. When combined with the projections for SFC reduction, these data indicate potential TOGW reductions of:

- 15 to 17 percent for the all supersonic cruise mission
- 25 to 28 percent for the case with 2,000 nautical mile subsonic cruise segment over land

The baseline Mach 5.0 engine is the GE variable cycle turbofan ramjet with LNG fuel, while the alternate is the Aerojet TechSystems two-spool dual-regenerator air turboramjet. GE and Aerojet TechSystems have addressed the technology needs and projections for their respective Mach 5.0 engines.

GE showed an SFC improvement of 0.5 percent for its variable cycle turbofan ramjet engine through control schedule optimization. From the results of sensitivity studies, the corresponding reduction in TOGW would be 1 percent or less for both the all-supersonic cruise and subsonic cruise missions over land. Other means of reducing TOGW must be explored.

GE provided projections of SFC improvements assuming better technology. The SFC reduction projections for the Mach 5.0 variable cycle turbofan ramjet engine are:

- Mach 0.9 at 36,089 feet – 5.2% Δ SFC
- Mach 5.0 at 85,000 feet 2.2% Δ SFC

These improvements would be achieved through component efficiency increases, reductions in cooling air requirements, improvements in burner efficiency, and reductions in nozzle unburned air. Increased material temperature capability and better flow modeling to reduce losses and better heat transfer formed the bases for these projections.

Using sensitivity study results, these SFC reductions would result in an approximate 5-percent TOGW reduction for the all supersonic cruise mission and 12-percent TOGW reduction for the 2,000-nautical-mile subsonic cruise mission over land.

Engine weight can be reduced through the use of higher stage loadings and advanced materials. It is projected that engine thrust/weight could be as high as 10, which is more than twice the present values. In contrast, GE (Figure 2-54) projections are more modest. Following the same logic as for the Mach 3.2 engine, projections of 20- to 25-percent improvement in Mach 5.0 engine thrust/weight appear reasonable. From sensitivity studies, the potential TOGW reductions are approximately:

- 12 to 14 percent for the all supersonic cruise mission
- 24 to 27 percent for the mission with 2,000 nautical mile subsonic cruise segment over land

Similar to the Mach 3.2 aircraft results, there is the potential for TOGW reductions of 12 to 25 percent from increasing engine thrust/weight even though engine weight is only approximately 10 to 15 percent of TOGW. Thus, it is recommended that in future studies emphasis be placed upon reducing engine weight as a means of reducing TOGW.

When combined with the projections for SFC reduction, these data indicate potential TOGW reductions of:

- 16 to 18 percent for the all supersonic cruise mission
- 33 to 36 percent for the case with 2,000 nautical mile subsonic cruise segment over land

Thus, there appears to be a basis for concluding that assuming reasonable technology advances, there is the potential for substantial reductions in the takeoff gross weight of the Mach 5.0.

Fuels. Fuels were evaluated from the standpoint of energy content, thermal stability, heat sink capability, availability, logistics, safety, and cost. Conventional aircraft kerosene-based fuels, Jet A and the JP series, have been universally used in both commercial and military applications.

For high-speed applications, the choice of fuel is of broadened importance: the fuel energy content influences the size and weight of the airplane; the heat sink capability and thermal stability limits of the fuel influence the Mach number achievable; and the cost of the fuel becomes a more predominant factor in the operating economics.

The initial evaluations of candidate fuels for high-speed applications resulted in the elimination of both liquid hydrogen and endothermic hydrocarbon. Both fuels have technical merits, but are not competitive on a economic basis, for near-term commercial application.

Commercial airplane operations beginning in the 2000-2010 time period focus these studies to kerosene-based jet fuels and LNG. It is generally agreed that the thermal stability of Jet A is a limiting factor in high Mach number applications. Some of today's fuel supply has been shown to have thermal stability limits above that of Jet A. This indicates that kerosene-based fuels can be produced with enhanced thermal capability. Based on inputs from refiners and engine manufacturers, Douglas chose the JP-7 as the reference fuel for the Mach 3.2 studies. The properties of JP-7 that are desirable from the standpoint of commercial

application are related to thermal stability; however, some of the properties of JP-7 may not be required.

Aircraft gas turbine engines have been designed and operated routinely on kerosene fuels in both commercial and military airplane service, and also have involved millions of hours on natural gas fuel in dual fuel marine and industrial applications.

HSCT fuel system design is similar to that of the conventional subsonic airplane for cruise speeds up to Mach 2.0 or 2.5. At higher cruise speeds, the requirements for an enhanced thermal stability kerosene fuel or for LNG fuel may require extensive changes in the fuel system configuration. Fuel nozzle coking is the specific problem leading to the concern about thermal stability. Commercial jet engines experience fuel temperature on the order of 325°F at the inlet of fuel nozzles. The SR-71, using JP-7 fuel, is able to accommodate fuel temperatures as high as 600°F.

Successful use of LNG in a high-speed aircraft propulsion system is primarily an issue of system design. LNG does not adapt well to a kerosene-fuel engine system design. Engine fuel system optimization cannot be successful without considering aircraft tank system optimization. Structural studies of typical fuel tank designs for subsonic, supersonic, and hypersonic aircraft have shown that minimum weight designs are achievable when 2219 aluminum alloy is used in connection with the minimum pressure at which the LNG tank should be allowed to operate.

NOx is formed in the combustion process with any fuel when oxygen molecules, which are not involved in reaction with the fuel, combine with nitrogen from the air under the high temperature conditions which exist in the combustor. Since LNG produces lower adiabatic flame temperatures than Jet A, there will be less NOx generated per pound of fuel burned when LNG is used as the fuel. Mixing of fuel in a gaseous state with air has been shown to occur more rapidly and completely than when the fuel is injected in liquid form. Accordingly, there will be more rapid and complete mixing with methane than with Jet A.

However, this desirable end goal can be more nearly achieved if the fuel is introduced in a gaseous state rather than in a liquid state. The more complete mixing from use of methane produces two additional benefits:

- Production of NOx is minimized if mixture is lean
- Engine life is extended and maintenance requirements are reduced

High-temperature emissions associated with nitrogen-oxygen reactions and NOx formation will depend on combustion temperatures and, particularly, the uniformity of these temperatures in the combustor. Gas injection and uniform air/fuel mixing lessen the possibility for NOx formation. From an emissions standpoint, LNG with a high (4:1) hydrogen-to-carbon ratio, is a clean-burning fuel. Only NOx or other exhaust chemistry which could affect the ozone layer are of major concern relative to the use of LNG.

Another important aspect of fuel selection involves the use of the fuel heat sink to enhance engine performance. Figure 2-55 shows several ways fuel can be used to cool structure and return thermal energy to the propulsion cycle. Engine combustor and nozzle heat is recycled via the fuel. Airframe heat is added to the fuel heating value. Engine turbine cooling air is cooled by fuel, enabling less bleed air extraction and higher engine turbine temperature. Bleed air is cooled by fuel, avoiding the need for parasitic fan air cooling.

Natural gas is a mixture of methane and primarily ethane as a secondary component. There are three different forms of the liquid state of pure methane which can be considered. The major properties are listed below.

	NORMAL BOILING POINT (NBP)	TRIPLE POINT (TP)	SLUSH (50 PERCENT SOLID)
Vapor Pressure, psia	14.7	1.7	1.7
Temperature, °R	201.0	163.0	163.0
Density, lb/ft^3	26.4	28.4	30.2
Heat of Vaporization (BTU/lb) at 15 psia	220.0	250.0	263.0

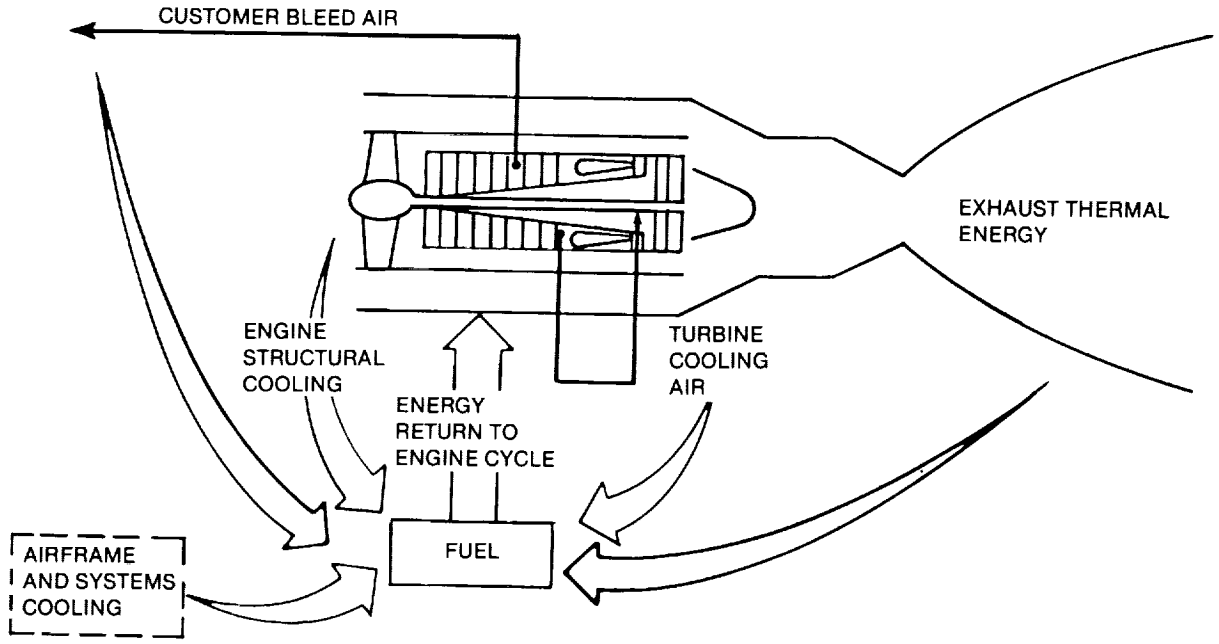

FIGURE 2-55. WASTE HEAT RECOVERY CONCEPTS BENEFIT THE TOTAL AIRCRAFT/ENGINE

Another form of methane as a candidate fuel is gelled methane. Advantages of gelled methane are (1) reduction in sloshing, heat transfer (wall contact), and boiloff in fuel tanks, (2) reduction in dissolution and heat transfer from tank pressurization gases (GN_2or LNG), (3) reduction in leakage through small holes or cracks, and (4) reduction in thermal stratification and solid settling in slush fuel tanks. Gelled methane also may reduce the fire hazard associated with methane spills and pool fires since it reduces vaporization. Gelled methane might not be effective in a high wind shear spill scenario since the fluid does not shear-thicken as does antimisting kerosene.

Removal of oxygen significantly improves fuel stability. The chemistry involves primarily free radials, but polymerization, addition, and condensation reactions are also important. Deposit formation rate depends on temperature with the process starting at approximately 100°C (212°F). The rate is also affected by flow parameters (velocity, Reynolds number, residence time). Dissolved and surface metals have a significant effect on deposit formation. The thermal decomposition of hydrocarbons can be generally classified in three temperature regimes:

- Low temperature (below 300°C/572°F) – deposition by autoxidation
- High temperature (above 500°C/932°F) – decomposition by direct pyrolysis
- Intermediate temperature – combination of both autoxidation and pyrolysis mechanisms

Thermal stability is an important aspect of fuel chemistry for high Mach aircraft propulsion systems. However, thermal stability is not a property which alone determines the limiting use of the fuel. Collectively, four issues are of primary importance:

- The range of fuel properties which must be considered
- Kinetic and thermodynamic conditions
- Thermal decomposition
- Design of the fuel handling system

Methane contains constituents, which at their extreme would promote thermal instability. However, absence of oxygen, aromatic molecules, and long-chain alkanes, probably make methane the most thermally stable of any fuel being considered for high-speed aircraft.

All engine and aircraft thermal energy should enter the fuel downstream of the engine high pressure pump and upstream of the pump drive turbine. This results in less likelihood of gas-phase thermal decomposition (pyrolysis) because the fuel is at maximum pressure and does not boil. Routing of high-pressure (3,000 psia) fuel throughout the aircraft would be unacceptable.

Turbojets, turbofans, afterburners, and ramjets of the future will continue to require the highly advanced control valve design and technology which has been developed for gas turbine engines. These engines are often configured to run on either kerosene or gaseous fuel via dual-passage fuel nozzles. The gas injection nozzles are very simple in design, requiring only an arrangement of showerhead holes since fuel atomization is not required. Fuel thermal stability is not an issue. Deposits do not form in either the nozzles or combustor, regardless of the chemistry of the natural gas.

It may be difficult to ignite and burn cold methane. Combustion instability could occur and affect turbine temperature and compressor stall/surge margin during acceleration to idle. Windmill relight also could be a problem. It is anticipated, therefore, that provisions may be needed to ensure uniform liquid methane vaporization/atomization. At idle power and above, the main engine combustor is intended to run on gaseous fuel.

Fuel injection during the afterburner and ramjet modes involves similar consideration. Afterburner fuel must be uniformly distributed to avoid generating unsymmetrical backpressure for the engine fan, which could affect fan stall margin. Ramjet fuel injection is a critical issue. Because of air temperature rise across the inlet normal shock wave, ramjet combustor gases can be extremely hot (over 4,000°F). Therefore, the fuel injector design must consider fuel instability and possibly special means for cooling.

Material selection is also important relative to fuel nozzle coking. From a design standpoint, there are numerous ways to avoid nozzle problems associated with fuel decomposition while operating the engine at temperatures which might otherwise cause problems. The airplane weight increments associated with the fuel system components are fully accounted for in both the Mach 3.2 and the Mach 5.0 concept studies.

All of the fuel system components and their integration into an airplane were determined to be technically feasible. Technology availability in the mid-1990s was determined to be achievable for both Mach 3.2 and Mach 5.0.

2.4 Aircraft Thermal Management

The thermal management studies analyzed the requirements for maintaining energy balances of the Mach 3.2 (D3.2-3A) and Mach 5.0 (D5.0-15A) concepts. Sources of heat generated within as well as entering the aircraft and requiring dissipation were considered. Fuel was used as the primary heat sink for absorbing energy loads.

The term "thermal protection system" is used to denote both a passive (insulation) and an active (cooling fluid) cooling system. Except for the engine inlet and nozzle, the aerodynamic heating of the aircraft was regulated by passive thermal protection systems (TPS). Criteria for sizing such insulation included insulation weight, fuel boil-off (in the case of LNG for the Mach 5.0 concept), heat flux, and fuel temperature (in the case of TSJF for the Mach 3.2 concept).

Various insulating materials were investigated, and factors such as space available for the required thickness and the corresponding weights were considered. The fuel tanks and cabin were sized for the insulation on both the Mach 3.2 and Mach 5.0 concepts. The Environmental Control System sizing took into account the heat generated by personnel, avionics equipment, and aerodynamic heating.

Modularized Multilayer Insulation (MMLI), which consists of an evacuated nickel foil jacket covering alternate layers of nickel reflector foils and wire mesh separators, was selected for the Mach 3.2 and Mach 5.0 concepts. The purpose of the wire mesh is to separate the foils, which act as radiation shields. The effective thermal conductivity of the MMLI varies with temperature as well as the surrounding pressure – at higher pressures the foils and separators are compressed together. Due to the resulting increased points

of contact between the layers, heat is transferred more readily by conduction. This is the case of the Mach 3.2 concept cabin where the MMLI experiences the 11 psia cabin pressure.

At lower surrounding pressures, there is less compression of the layers and, hence, less heat transfer by conduction. Consequently, the effective conductivity is lower in this case. This is the situation for the Mach 5.0 concept.

In the Mach 5.0 concept (Figure 2-56), the nonpressurized air gap external to the MMLI of the cabin and fuel tanks (and internal to the outer honeycomb skin) experiences the low atmospheric pressure (.25 psia) associated with flight at high altitudes. Consequently, the Mach 5.0 concept cabin requires less insulation than the cabin of the Mach 3.2 concept. The corresponding unit weights (lbm/ft^2) for the insulation do not include installation fasteners, restraints, or support structures. Margins to account for installation are reflected in weights quoted in Table 2-5. An additional criterion for the MMLI sizing was the requirement that a minimum of five reflector foils, including the outer jacket, were needed to ensure sufficient rigidity of the foil packet.

The temperature-dependent thermal resistance of the honeycomb was based on an effective conductivity that was modeled analytically. This conductivity included the effects of both conduction and radiation across the core and was based on known thermal material properties as well as specified honeycomb core dimensions and operating temperature ranges.

Aerodynamic heating data were incorporated as input to the HEATRAN thermal analysis program to compute transient structural temperatures. The Mach 3.2 concept wing tank insulation was sized to minimize the fuel tank temperature rise due to aerodynamic heating. The governing constraint was a maximum limit value of 200°F for the temperature of this fuel. A typical cross section of the wing structure tank and insulation is shown in Figure 2-57. The external surface of the tank is covered with MMLI. Between this insulation and the outer honeycomb, the air gap is 1/2-inch wide. Aerodynamic heating is transferred across this gap by radiation and free convection, followed by conduction across the insulation and tank wall, and hence, by free convection into the fuel.

An average value of the wing-heat-transfer coefficient was used for both the top and bottom surfaces. The increase in fuel temperature due to this heating is shown in Figure 2-57 and corresponds to various thicknesses of MMLI. Each thickness is composed of a different number of reflective foil and wire mesh separators. Computation of the fuel temperature is based on the amount of fuel remaining in the tank, the fuel flow to the engine and the aerodynamic heating at various times.

During descent, the fuel used to absorb the environmental control system heat loads (aerodynamic heating to the cabin, avionic cooling, and personnel heat loads) is recirculated into the fuel tanks. The effects of this recirculation on the temperature of the fuel in the tank are not included — preliminary analysis have shown them to be negligible (25°F higher temperature at landing). Consequently, the use of 0.204 inch of MMLI on the upper and lower surfaces of the fuel tanks was selected to keep the fuel temperature below the 200°F limit. The location of the fuel tanks, the MMLI thicknesses, and the corresponding unit weights are shown in Figure 2-58.

The Mach 3.2 concept cabin insulation was sized with constraints on both heat flux and cabin air temperature. A typical fuselage cross section is shown in Figure 2-59. The net aerodynamic heat flux through the cabin walls was limited to 30 $BTU/hr/ft^2$ to fit the capacity of the environmental control system. The cabin air temperature was held constant at 70°F. Consideration was given to radiation and free convection across the air gap, with forced convection along the inner surface of the cabin liner where the film coefficient was 3.0 $BTU/hr/ft^2$ °R. The results of the MMLI sizing are shown in Figure 2-58.

The arrangement of the LNG fuel tanks and the pressurized cabin for the Mach 5.0 concept is shown in Figure 2-60. Figure 2-56 depicts a typical cross section of the cabin and fuel tanks. The outer skin is composed of 1-inch RSR titanium honeycomb with supporting structures. The cabin wall consists of a NOMEX honeycomb core with poly ether-ether ketone (PEEK) face sheets as the pressure shell. The external surfaces of the cabin pressure shell and the PEEK fuel tank walls are covered with MMLI.

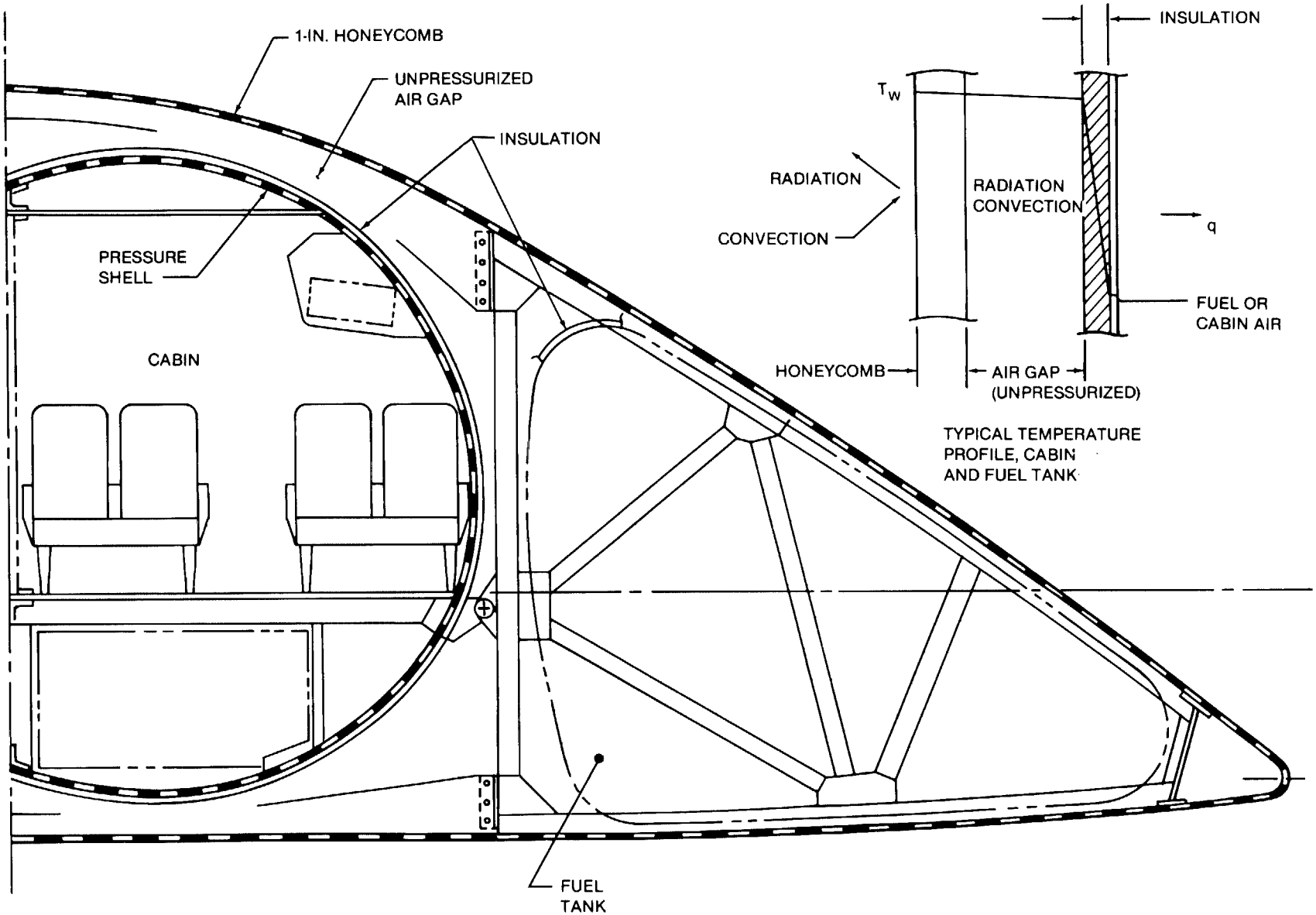

FIGURE 2-56. TYPICAL CABIN AND FUEL TANK SECTIONS — MACH 5 CONCEPT

TABLE 2-5
THERMAL PROTECTION SYSTEM — AVERAGED INSTALLED UNIT WEIGHT

UNIT WEIGHTS BASED ON WETTED AREA	D-3.2-3A LB/FT^2	D-5.0-15A LB/FT^2
PASSIVE TPS		
PASSENGER CABIN	0.827	0.712
FUEL TANK	0.377	0.526
ENGINE EXHAUST	0.630	
ACTIVE TPS		
ENGINE INLET	N/A	2.80
ENGINE EXHAUST	N/A	3.65

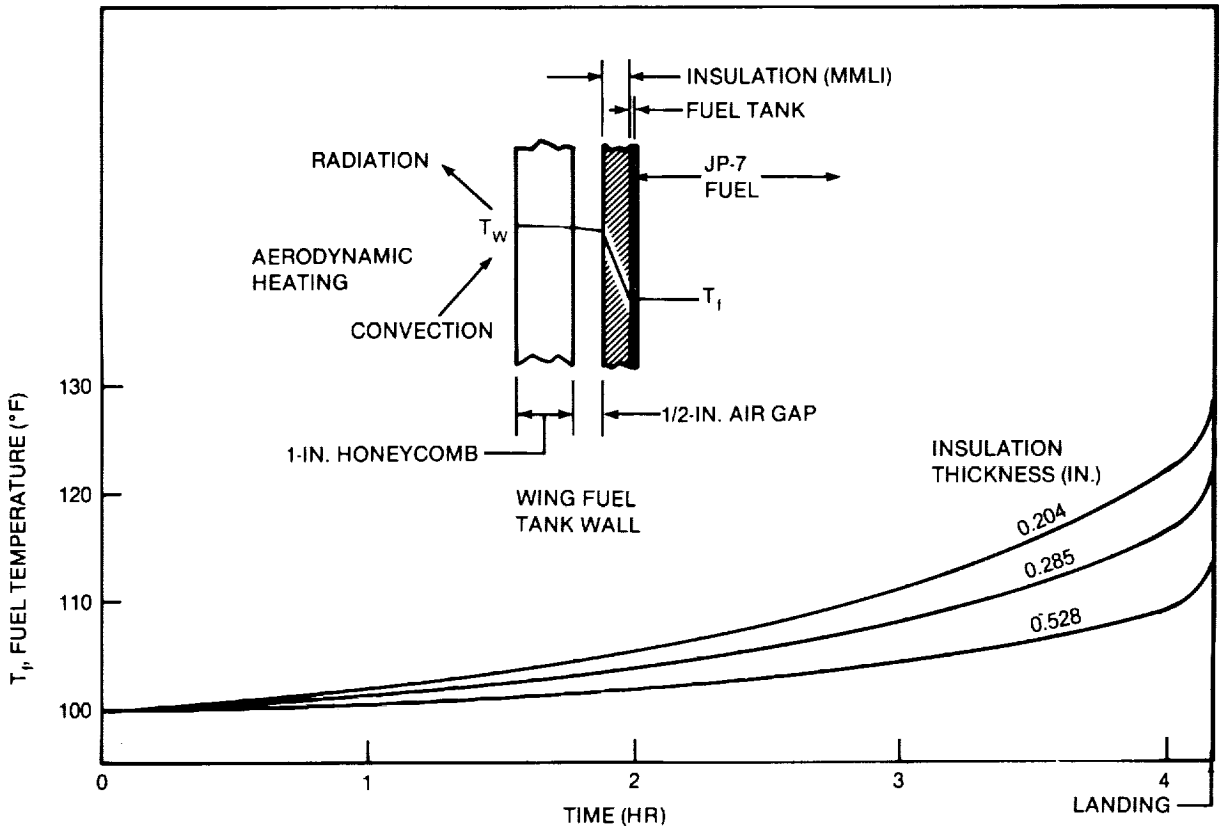

FIGURE 2-57. MACH 3.2 VEHICLE FUEL TEMPERATURES, MMLI TANK INSULATION

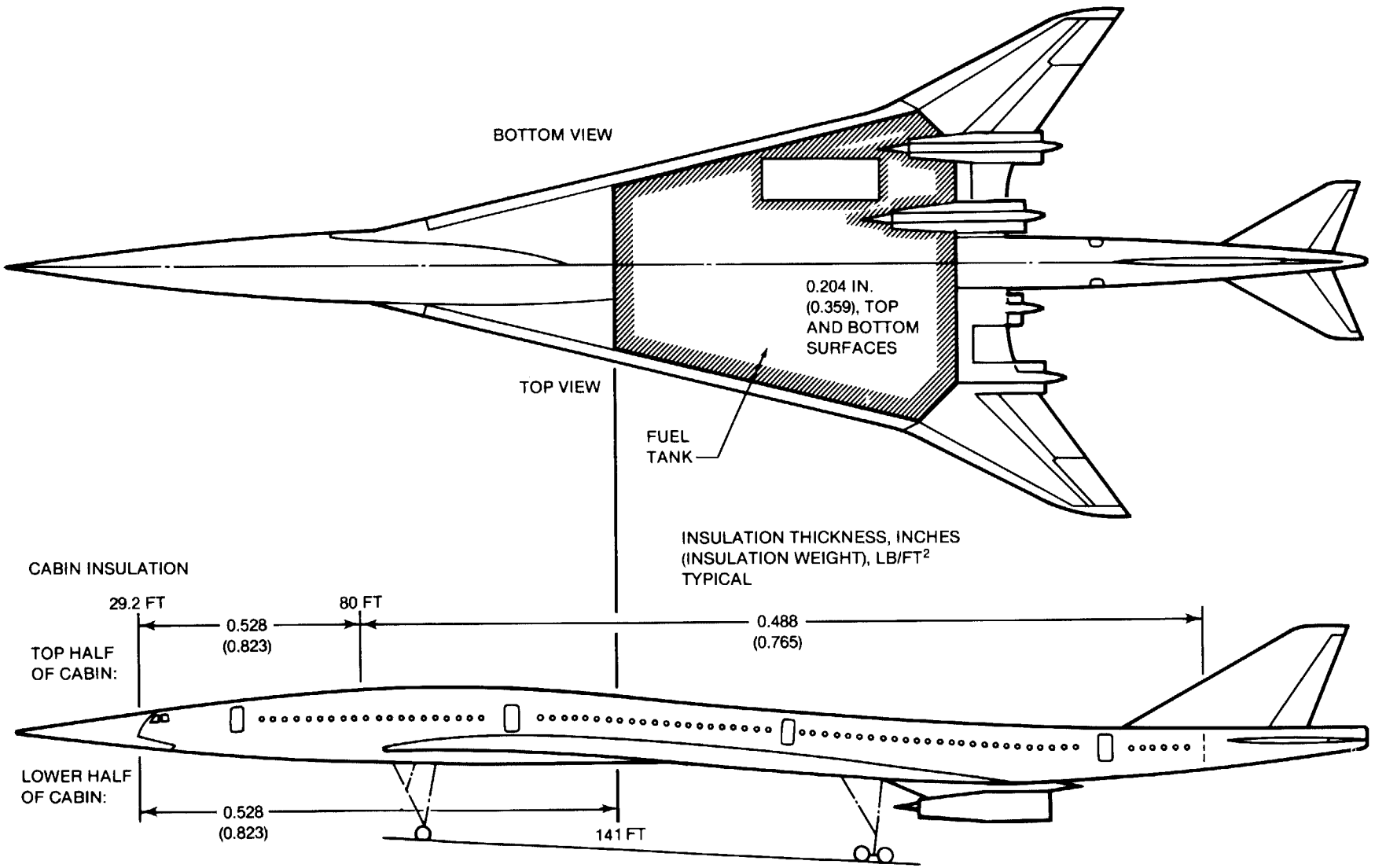

FIGURE 2-58. MACH 3.2 CABIN AND WING TANK MMLI INSULATION THICKNESSES

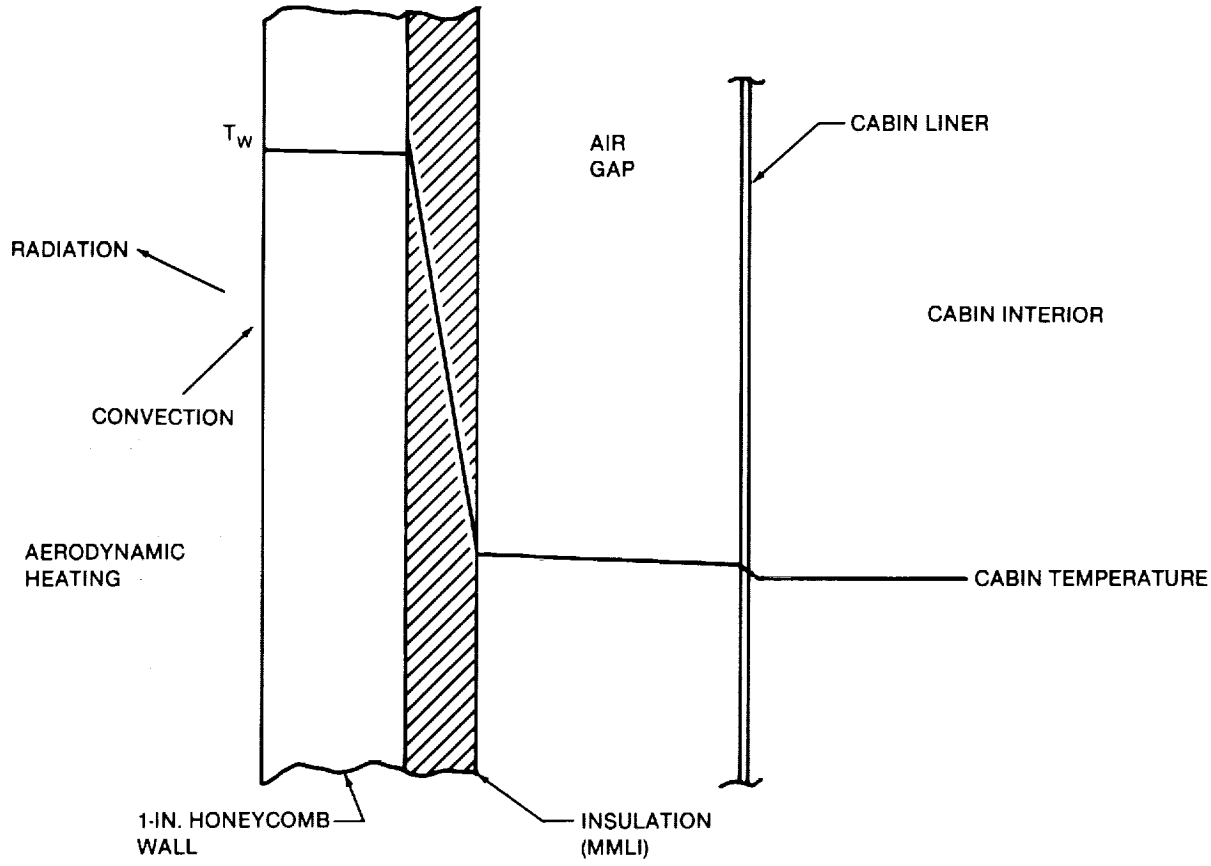

FIGURE 2-59. MACH 3.2 FUSELAGE INSULATION DESIGN

The MMLI thickness was optimized for the upper and lower surfaces of each fuel tank (except the lower surfaces of tanks No. 3 through 5). This optimum thickness corresponded to the minimum total weight composed of the boiloff, insulation, and tank structure. Variations of these weights with insulation thickness as well as the selection of the optimum insulation thickness are shown in Figure 2-61 for a typical case. The results of the MMLI thickness optimization for the upper and lower tank halves are shown in Figure 2-62, indicating the unit weights (lbm/ft^2).

The criteria for sizing the cabin insulation included a 70°F cabin air temperature, an 80°F cabin liner temperature and a cabin film coefficient of 2.5 $BTU/hr/ft^2$ °R. Net aerodynamic heating is transferred across the outer honeycomb and across the air gap to the MMLI by radiation and free convection. A typical cross-section is shown in Figure 2-56. This heat is then conducted across the insulation and convected from the cabin wall by the environmental control system where it is ultimately absorbed by the fuel. The results of the insulation sizing for the cabin are summarized in Figure 2-63.

Transient temperature profiles for both the Mach 3.2 and Mach 5.0 fuselages and wings were generated to enable determination of temperature gradients, thermal stresses, and thermal expansions. Two examples of such profiles are provided in Figures 2-64 and 2-65. Figure 2-64 represents the Mach 3.2 fuselage bottom 20 feet behind the nose. Figure 2-65 represents the Mach 5.0 wing tank bottom 42 feet behind the wing leading edge.

A vapor cycle environmental control system has been selected for the Mach 3.2 and 5.0 concepts. Performance numbers are at the top of descent were chosen, since the aero cooling load is maximum at this flight condition. A chart of fuel tank temperature rise during descent (Figure 2-66) is given for the Mach 3.2 aircraft. A coefficient of performance (COP) comparison is given in Table 2-6. A vapor cycle system was chosen over an air cycle system because of the large difference in COPs.

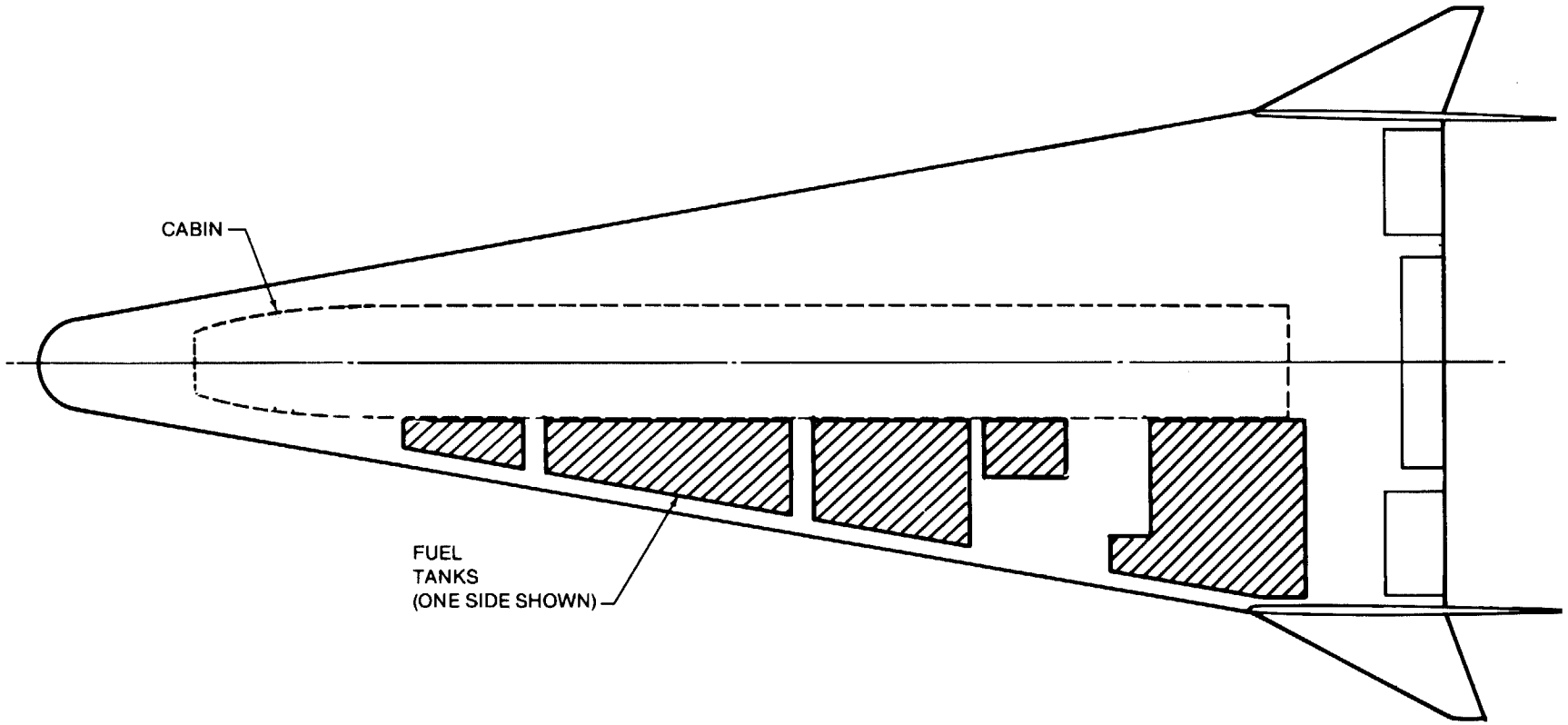

FIGURE 2-60. D5.0-15A CONCEPT CABIN AND FUEL TANK ARRANGEMENT

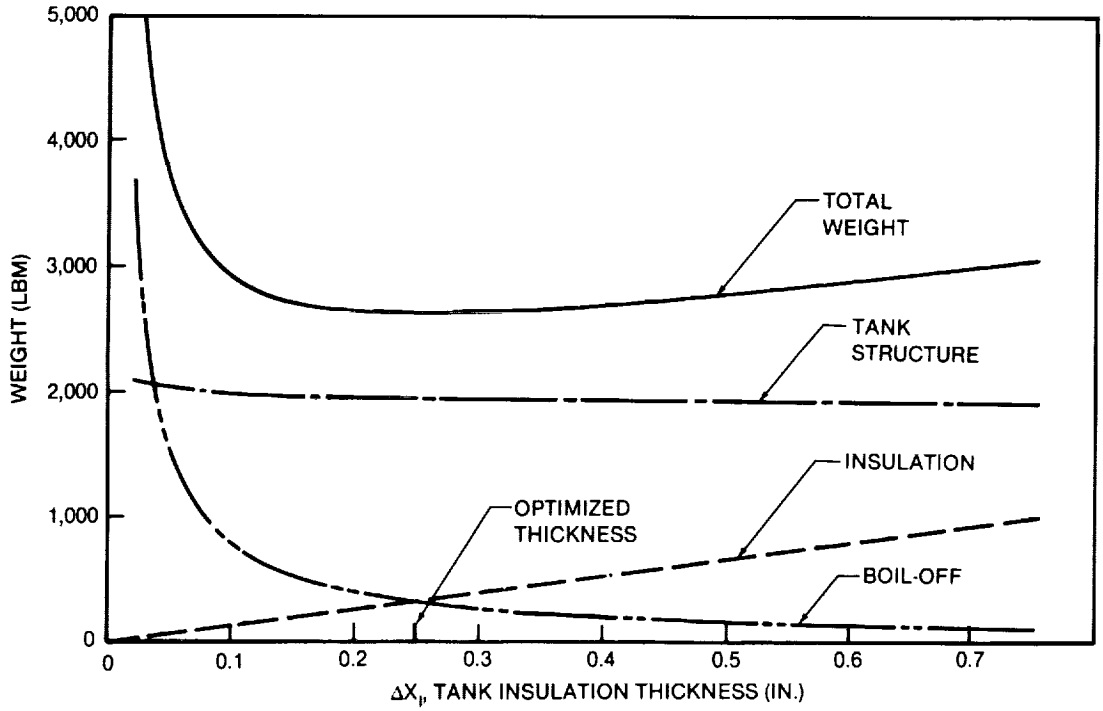

FIGURE 2-61. FUEL TANK INSULATION OPTIMIZATION, MMLI — TANK NO. 2, LOWER SURFACE, D5.0-15A CONCEPT

The initial fuel tank temperature at the top of descent is 205°F per a thermal management fuel tank model (Figure 2-66). The fuel tank temperature increases to 259°F at landing, which is well below the boiling point and thermal stability limit assumed for TSJF. This analysis assumed that all of the fuel required for the air conditioning system is recirculated to the tank. Fuel tank temperature rise due to aerodynamic heating of the fuel tank is included.

The Mach 3.2 concept engine inlet needs additional analysis to determine whether any active or passive TPS is required. For the nozzle, the duct-burning section was sized for a passive TPS. Low-Q all-metal insulation was used with the criterion that the adjacent nacelle structure temperature be limited to 1,000°F. Gas radiation as well as convection was considered. The insulation thickness to meet this criterion is 0.34 inch.

Active cooling of the throat regions of the Mach 5.0 concept nozzle and inlet will be required. Based on McDonnell Douglas studies, a wall structure comprised of honeycomb and a skin heat exchanger is recommended. The coolant circulated through these heat exchanger tubes should be an intermediate medium, transferring inlet air and engine exhaust heat to the fuel.

The amount of LNG fuel boil-off due to solar irradiation was small, both in cases where the aircraft was assumed parked in the sun on a 100°F day for one hour and where the aircraft was in flight. In these cases the fuel tank insulation consisted of MMLI of the thicknesses found in the insulation optimization study discussed previously.

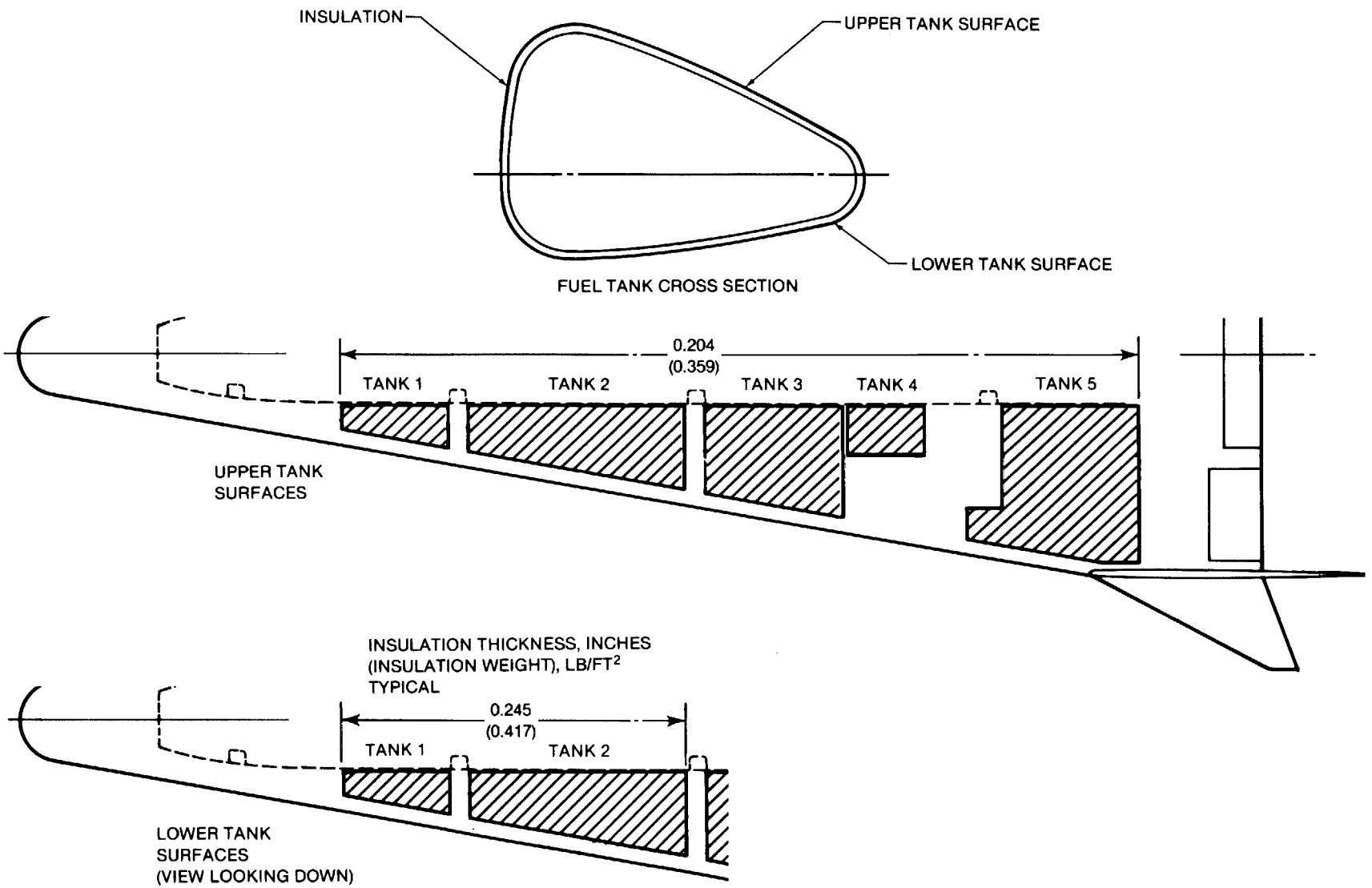

FIGURE 2-62. LNG FUEL TANK INSULATION THICKNESSES — D5.0-15A CONCEPT

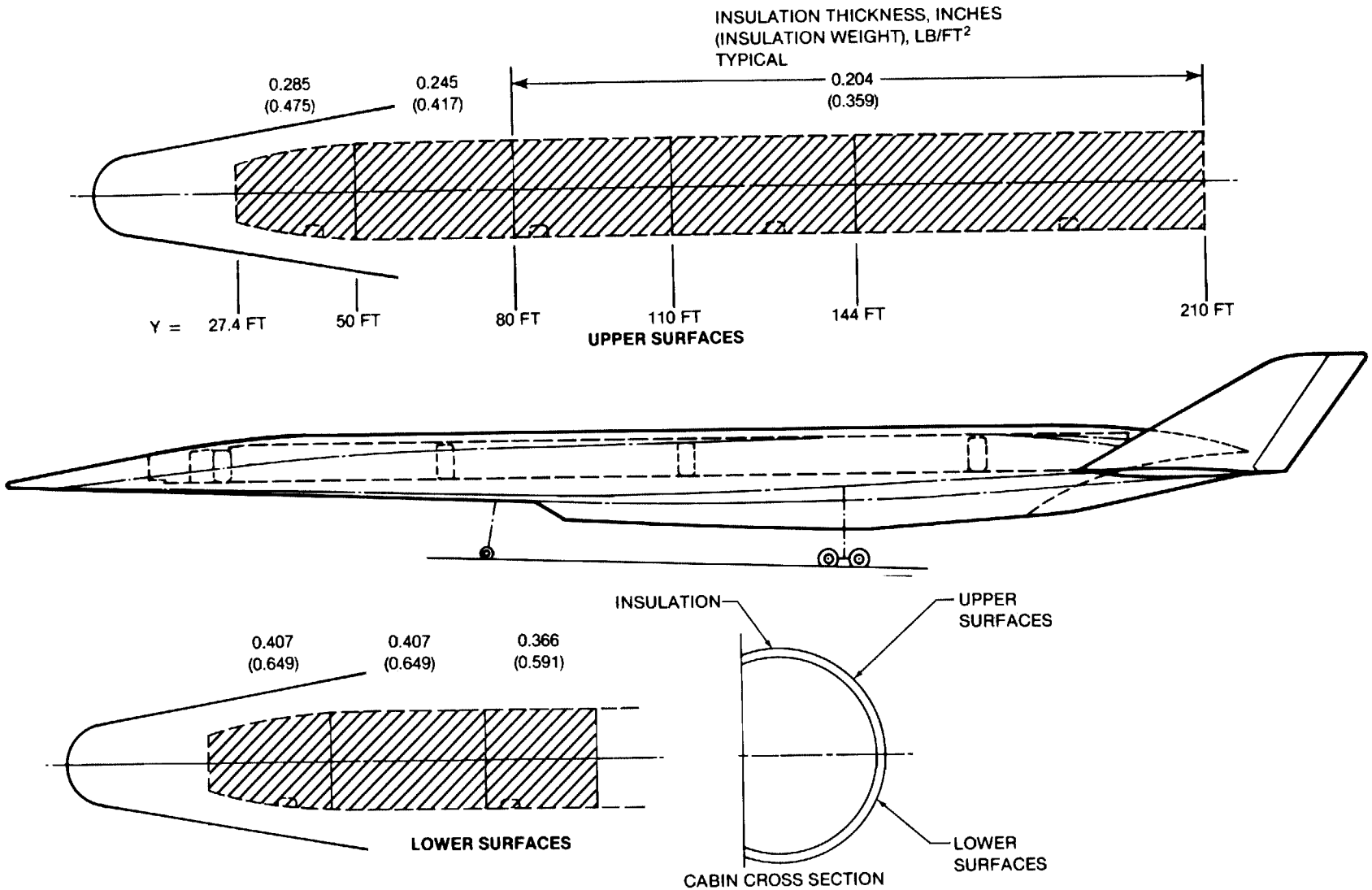

FIGURE 2-63. CABIN INSULATION THICKNESSES — D5.0-15A CONCEPT

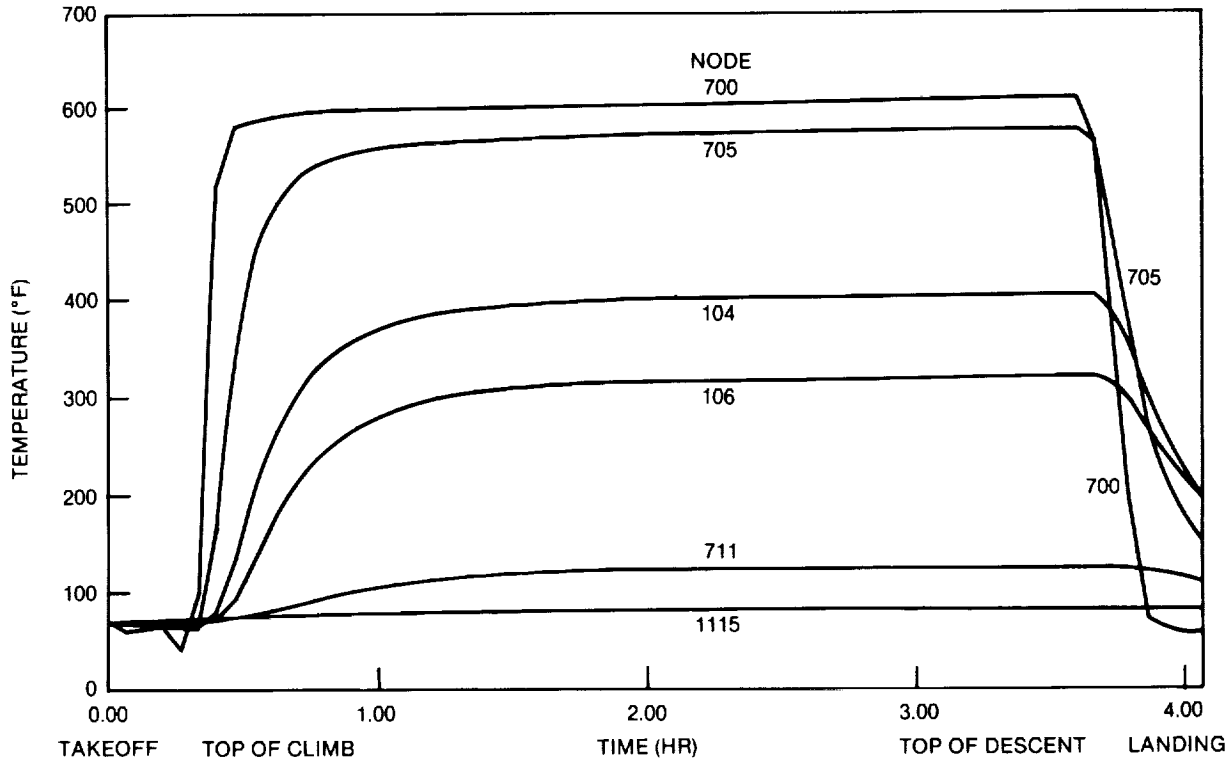

A. FUSELAGE LOWER SURFACE TEMPERATURES AT X = 20 FT

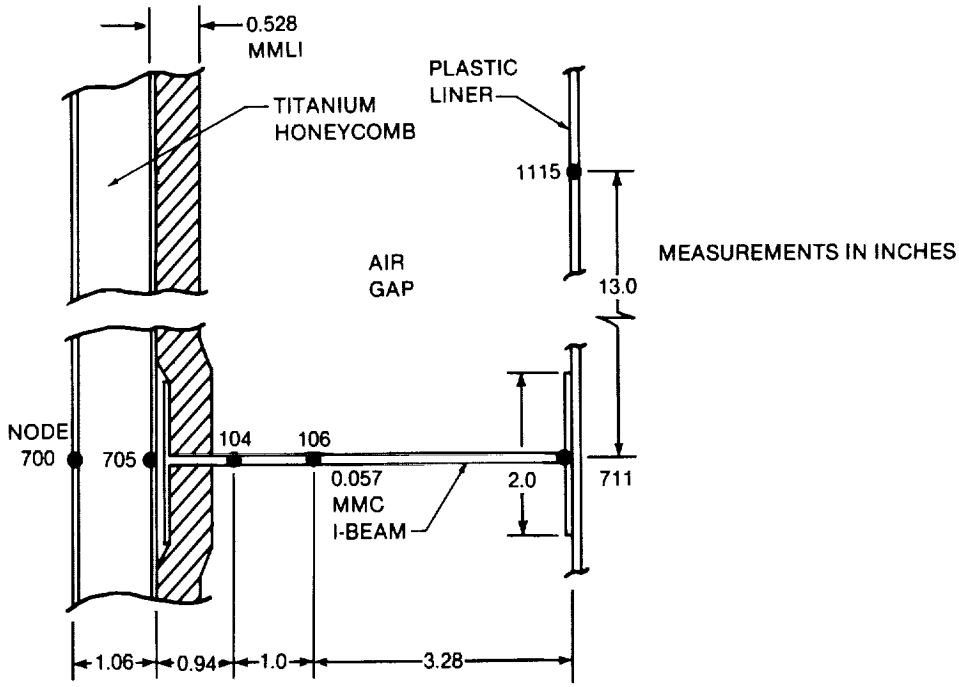

B. THERMAL MODEL FOR LOWER FUSELAGE AT X = 20 FT

FIGURE 2-64. MACH 3.2 THERMAL MODEL AND TEMPERATURES

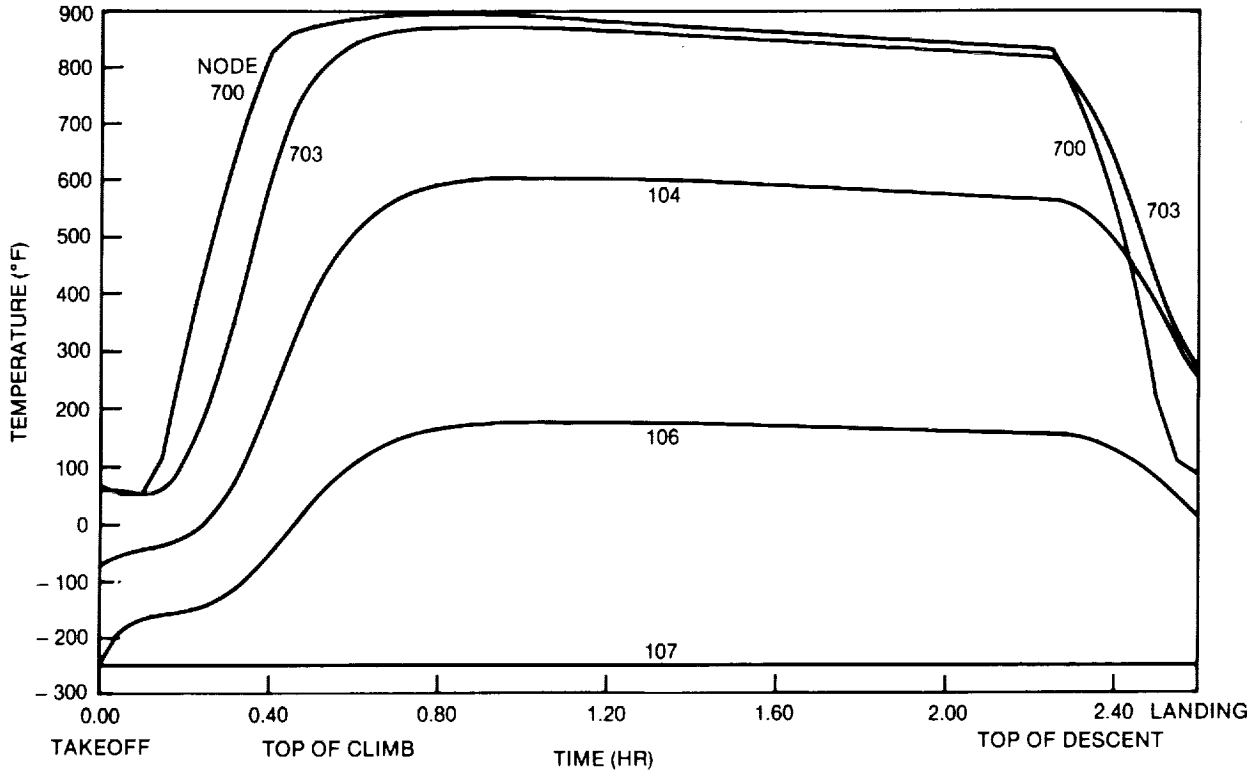

A. WING LOWER TANK SURFACE TEMPERATURES AT X = 42 FT

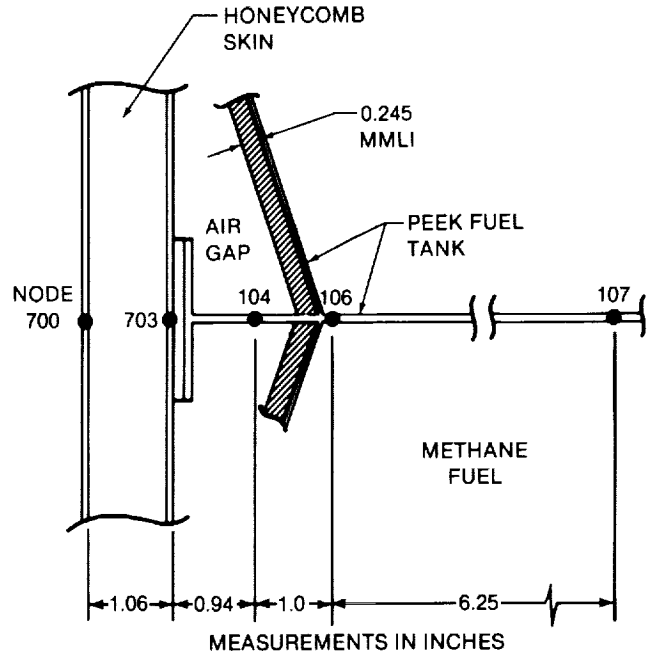

B. THERMAL MODEL FOR LOWER FUEL TANK AT X = 42 FT

FIGURE 2-65. MACH 5.0 THERMAL MODEL AND TEMPERATURES

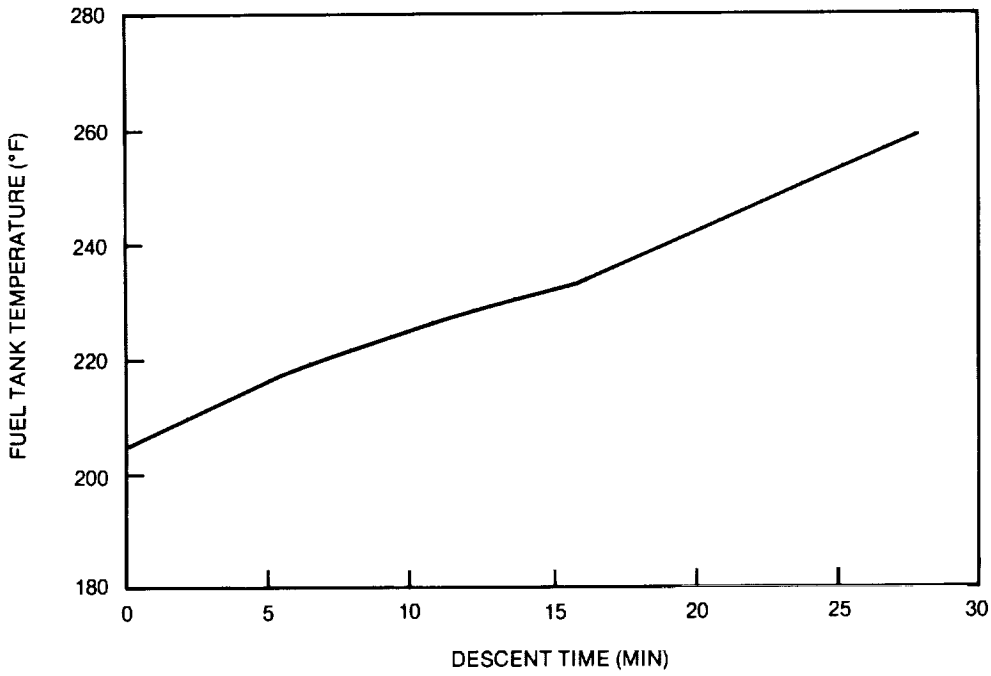

FIGURE 2-66. MACH 3.2 FUEL TANK TEMPERATURE ON DESCENT

TABLE 2-6
OPEN AIR CYCLE VERSUS VAPOR CYCLE COP COMPARISON

MACH NO.	COP OPEN AIR CYCLE	COP VAPOR CYCLE	Δ — PERCENT
3.2	0.3110	0.7931	+ 155.0
5.0	0.2974	2.6750	+ 799.5

2.5 Structures and Materials

This section presents the evaluation of the major structural components of the Mach 3.2 (D3.2-3A) and the Mach 5.0 (5.0-15A) concepts. The major components examined consisted of the fuselage, wing, empennage, nacelle, fuel tanks, and passenger cabin. In addition, landing gear frames, fuel tank bulkheads, truss members, and nose/leading edge areas were examined, as well as the wing leading edge and laminar flow control (LFC) structural elements for the Mach 3.2 aircraft concept. Finite element models (FEM) of the concepts were constructed and run with the critical loading cases and associated temperatures. With these loading conditions, aircraft structure was sized.

The objectives of this study are to (1) provide fail-safe, maintainable, and reliable structural concepts that meet minimum weight, volume, and cost considerations, (2) perform a preliminary structural analysis in order to conduct a weight analysis of the vehicles, and (3) delineate problem areas.

The structural concepts used on the aircraft consisted of fail-safe and safelife designs. The fail safe design consists of two shells. The outer shell is the load-carrying structure, and the inner shell, which is

isolated from the effects of the loads on the outer shell structure, only reacts to cabin pressure and inertia loads. In the safelife design, the outer shell is the load-carrying structure and reacts to passenger cabin loads. The fuel tanks only react to internal pressure and inertia loads. Passive insulation systems were used for both the passenger cabin and the fuel tank areas. Structure used for the empennage, nose, and leading edges were required to endure the highest temperatures.

Structural definition resulted from strength analysis including the effects of combined force and thermal loads for critical loading conditiong. Various structural concepts were investigated to determine weight. Materials considered ranged from those currently available to those still under development. Extensive work is being done in industry and government to develop materials for high-speed flight – the SCS-8/RSR Al for the Mach 3.2 concept and SCS-6/RSR Ti for the Mach 5.0 concept. The materials need to be fully characterized to become operational. Designs have been established that provide workable systems with feasible weight/volume/cost relationships. Additional analytical work is required to verify this conclusion, especially in the areas of high temperature damage tolerance and durability assessment. In addition, technology needs in certification, material allowables, and fabrication techniques and processes are required.

Mach 0.85. The Mach 0.85 concept is an advanced subsonic aircraft consisting of a wing-body configuration and empennage. The evaluation of the Mach 0.85 configuration, consisted of application of newer materials and fabrication techniques to the configuration shown in Figure 2-1. Suitable materials are shown in Figure 2-67. The materials include metal matrix composites, graphite-epoxy composites, and standard aluminums. As shown in these figures, SCS-8/Al 6061 is the most efficient material, having a specific moduli of 230 and a specific compressive yield of 1,160 at room temperature. It was used for the structural evaluation for the concept. The following three materials on the figure are graphite laminates: T300/N5208, IM6/1808I, and Celion 6K/PMR-15. The remaining four materials are aluminum, with Al 2618 being equivalent to the aluminum material used on the Concorde.

To further reduce the weight for the advanced subsonic aircraft, honeycomb construction was used for the load-carrying skins instead of traditional skin-stringer design. It was estimated that honeycomb construction would result in an approximate 15-percent weight reduction.

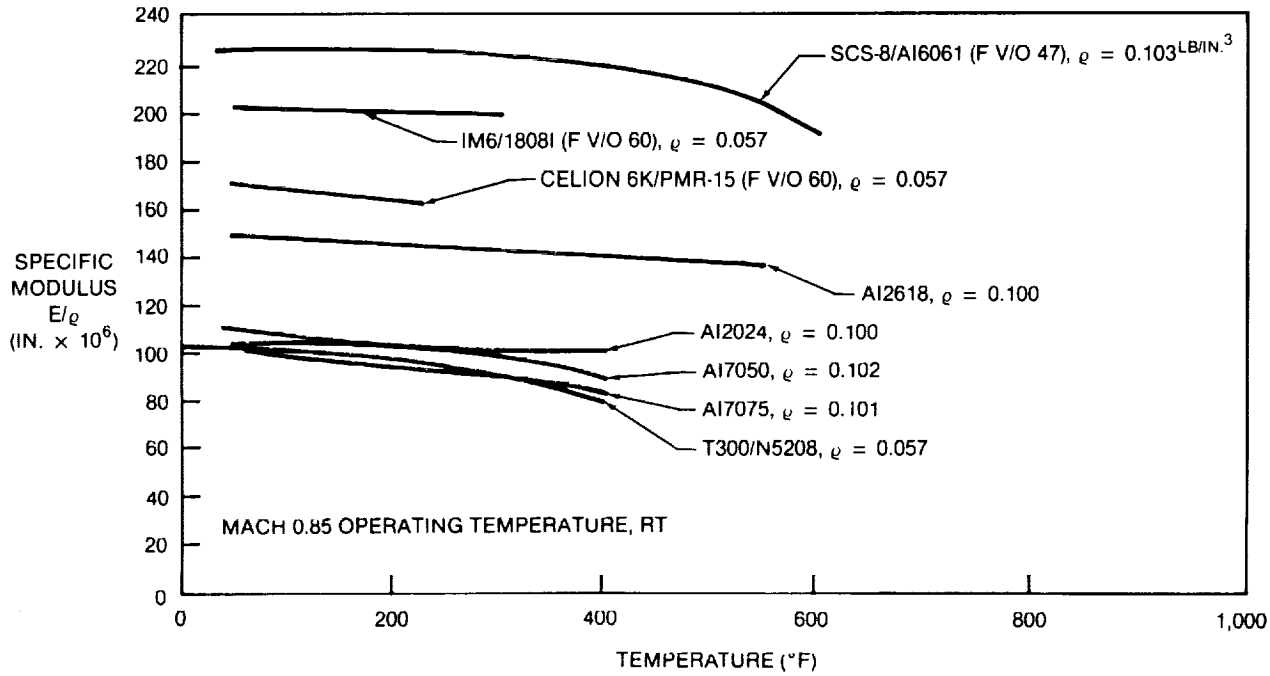

FIGURE 2-67. SPECIFIC MODULUS OF MACH 0.85 CANDIDATE MATERIALS

Mach 3.2. The Mach 3.2 concept is a wing-body configuration. It consists of honeycomb load-carrying skins for the outer fuselage shell, wing, and empennage. The substructure consists of frames, ribs, and spars. The honeycomb skins carry all the body bending loads and internal pressure of the passenger cabin for the safelife design as previously described. The fuel tanks only react to internal loads.

Figure 2-68 presents the maximum temperatures the aircraft will experience. This is a temperature range of 400°F to 680°F. The maximum temperature on the fuselage nose is 680°F; the leading edge temperatures are 625°F for the wing and 530°F for the empennage. Fuselage lower surface temperatures range from 525°F to 590°F, and the upper fuselage surface temperatures range from 400°F to 460°F. Materials that can endure these temperature regimes are shown in Figure 2-68. The Al MMC listed in the figure refers to SCS-8/RSR-Al.

Figures 2-69 and 2-70 present comparisons of the candidate materials in terms of specific moduli and specific yield strength as a function of temperature. The higher these parameter values, the more efficient the material is working; and, therefore, a lower structural weight structure will result with its usage.

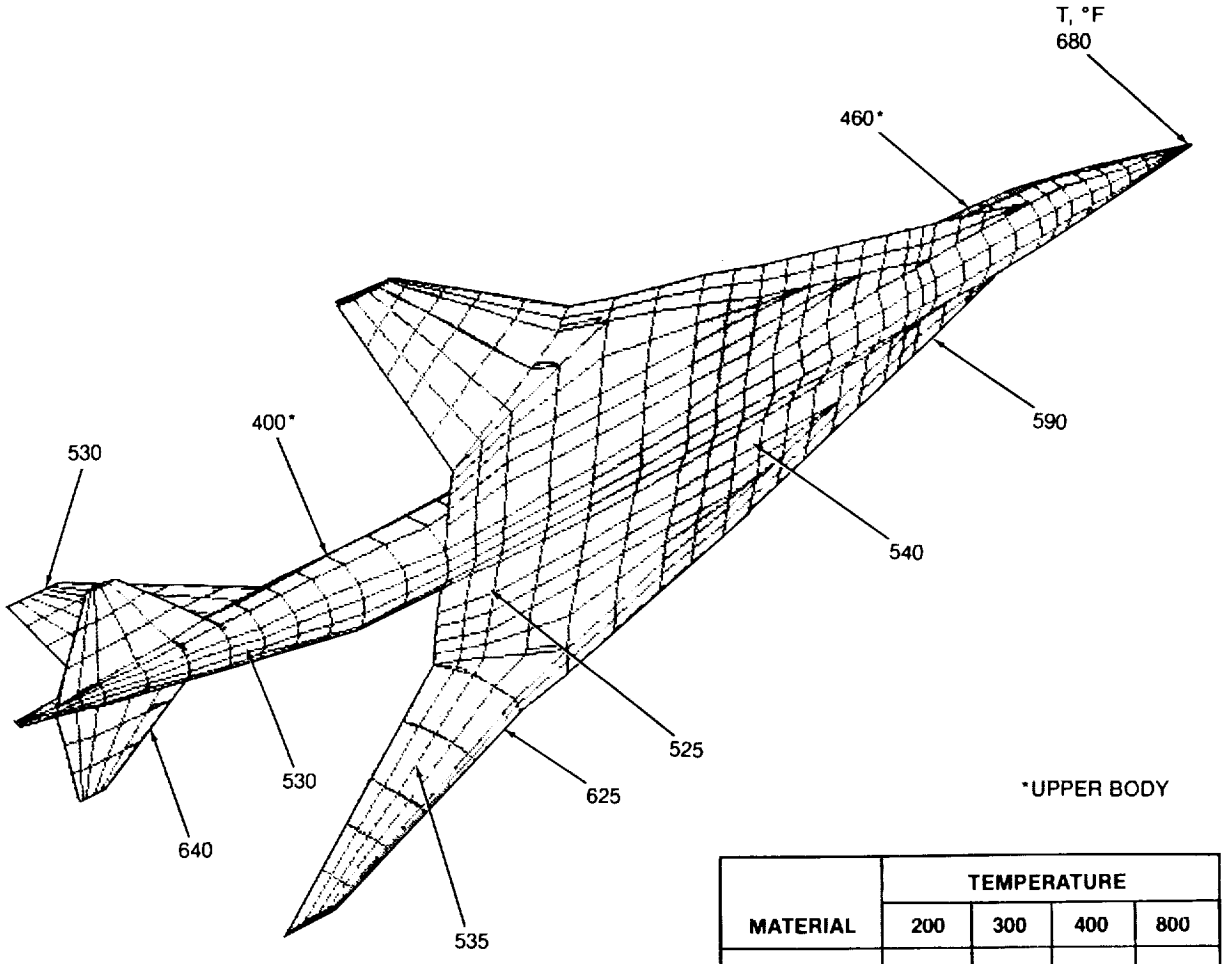

MATERIAL	TEMPERATURE			
	200	300	400	800
Al	•			
G/E_p		•		
Al-Li			•	
G/PI			•	
Al MMC				•

FIGURE 2-68. MAXIMUM TEMPERATURES — CANDIDATE MATERIALS — MACH 3.2

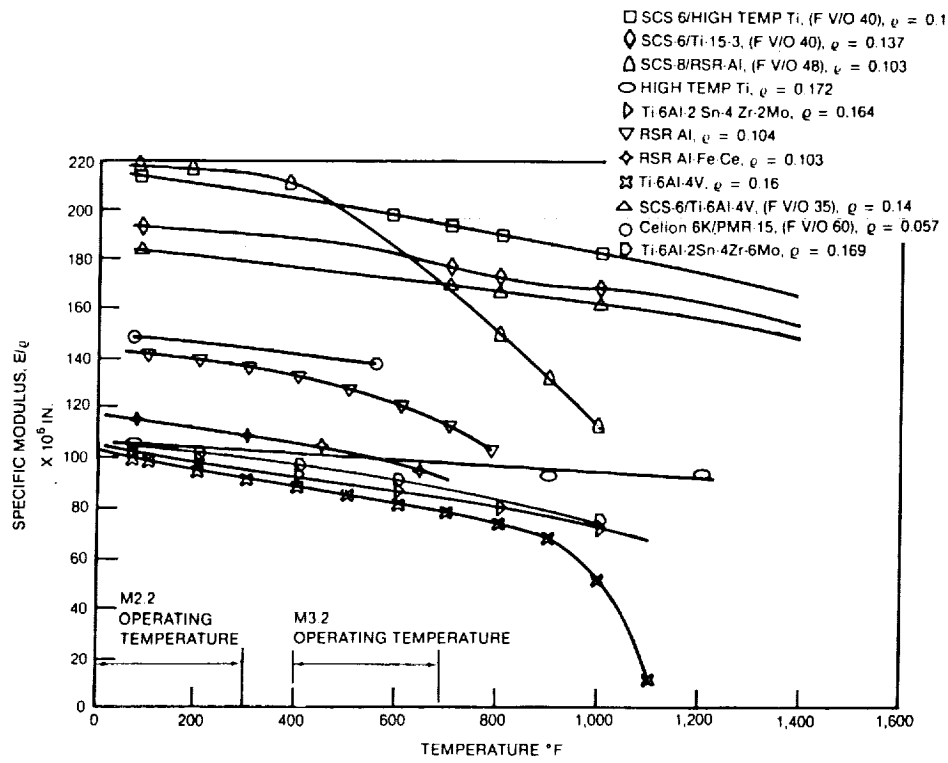

FIGURE 2-69. SPECIFIC MODULUS OF MACH 3.2 CANDIDATE MATERIALS

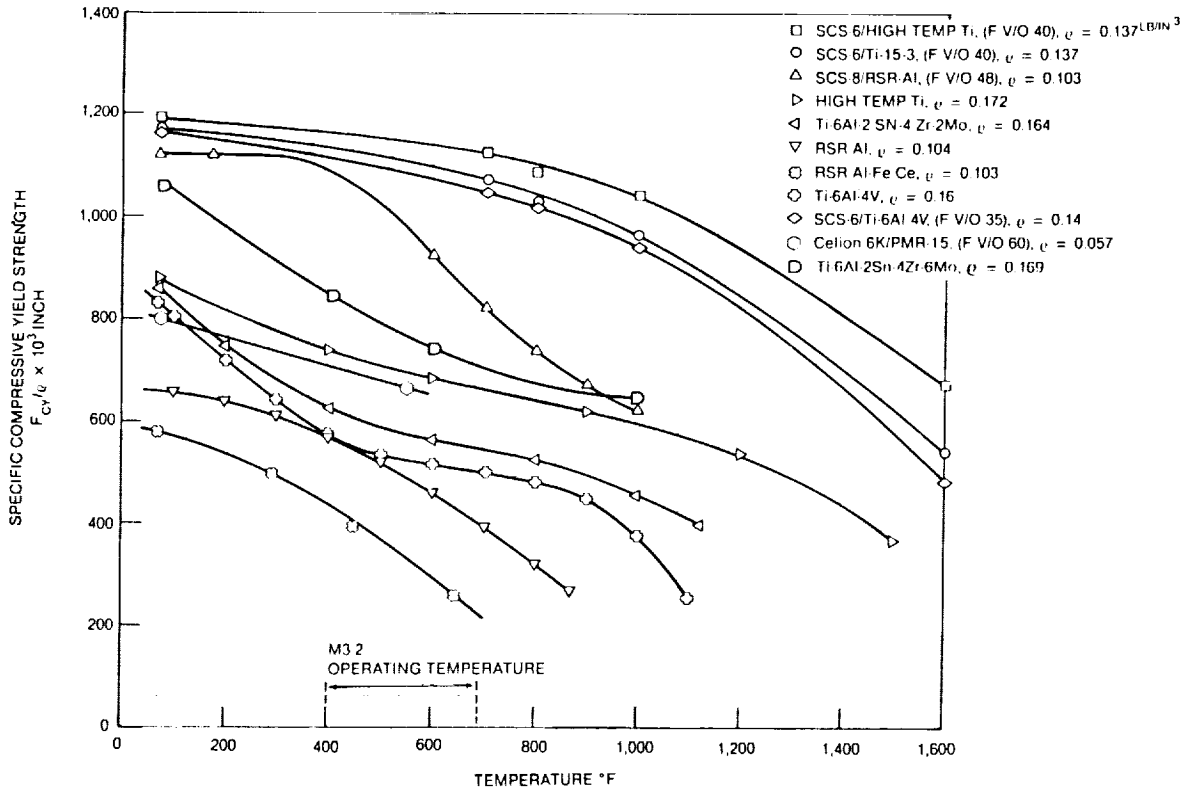

FIGURE 2-70. SPECIFIC COMPRESSIVE YIELD STRENGTH OF MACH 3.2 MATERIALS

C-2

The materials listed consist of aluminum, titanium, Al metal matrix composites (Al MMC), Ti metal matrix composites (Ti MMC), and polymetric composites (PC). For room temperature and up to 480°F the Al MMC, SCS-8/RSR Al, has the best specific moduli value and the specific yield strength is relatively high. The next three materials, i.e., SCS-6/RSR Ti, SCS-6/Ti-15-3-3-3, and SCS-6/Ti-6Al-4V, are superior at the higher temperatures and thus, more suitable structural materials for higher speed concepts. The next material is a PC, Celion 6K/PMR-15, which together with RSR Al rank above the titaniums and are thus possible candidates for the Mach 3.2 concept; however, they do not offer the weight savings potential of Al MMC. The remaining four materials are RSR Al and three titaniums, including the Ti 6-4. These materials would result in a less efficient and heavier structure. Their properties are approximately 50 percent lower than the aluminum metal matrix composite.

In addition to these types of comparisons, surveys were made of industry and government centers to determine production readiness. For example, RSR Al has been tested to 900°F for 100 hours and maintains a Rockwell Hardness B value nearly equal to that of the material at room temperature. (The higher temperature capability was explored as a safety factor in case the aircraft overshoots its predicted temperature.) By combining this RSR Al matrix material with the silicon fiber, SCS, an aluminum material suitable for the Mach 3.2 concept is identified.

Buckling, crippling, stiffness, tension, and other failure modes play important roles in the selection of materials for the primary structure of an aircraft. Figure 2-71 shows the failure mode weight distribution for the primary structure for a variety of aircraft. Buckling and crippling account for approximately 75 percent of the primary structural weight. Failure mode ranking for HSCT material candidates is shown in Table 2-7. SCS-8/RSR Al is the most efficient material from the buckling-crippling standpoint even though the rating of tension and stiffness of the Al MMC falls below the Ti MMC. Thus, SCS-8/RSR Al was used for the structural evaluation of the Mach 3.2 concept.

The loading conditions examined consisted of the following:

- Mach 0.9 climb
- Mach 0.9 descent
- Pressure loading including flutter
- Supersonic cruise
- Landing
- Lateral pressures

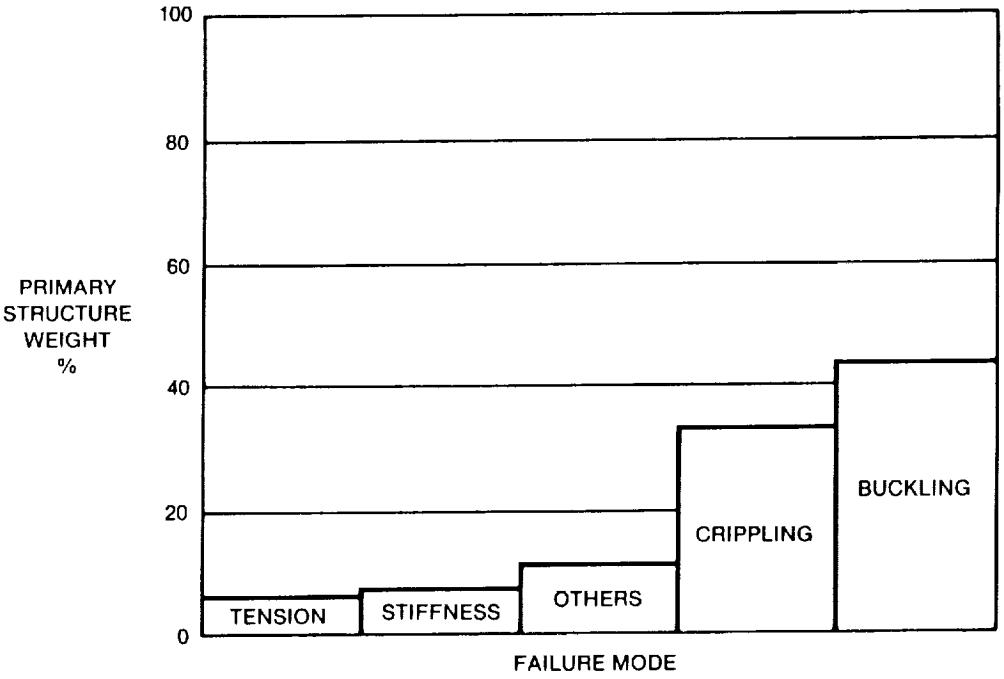

FIGURE 2-71. FAILURE MODE WEIGHT DISTRIBUTION

TABLE 2-7
EVALUATION OF CANDIDATE MATERIALS — MACH 3.2 CONCEPT

CANDIDATE MATERIALS	COMPRESSION (CRIPPLING AND BUCKLING) RATING	TENSION AND STIFFNESS RATING
Ti-6Al-4V (BASELINE)	12	7
RSR-Ti	10	5
SCS-6/Ti-15-3	3	2
SCS-6/RSR-Ti	2	1
SCS-6/RSR-Al	1	3
Ti-6-2-4-2	11	6
RSR-Al	8	10
RSR-Al-Fe-Ce	14	14
SIC_W/Al 2124	6	9
IM6/1808I	5	8
C6K/RPMR-15	7	12
T300/N6206	4	11
Al-7075-T6	13	13
Ti-6-2-4-6	9	4

Based on these loading conditions, the maximum load at temperature, the maximum temperature at load, and other pertinent conditions (flutter and landing) were examined to verify structural integrity of the components. A safety factor of 1.5 was used with the loads examined.

An FEM of the Mach 3.2 (D3.2-3A) concept was constructed (Figure 2-72). The FEM represents the wing skins, spars, and ribs; fuselage skins, frames, and longerons; and the empennage skins, ribs, and spars of the aircraft. Shear members were included in the spars, ribs, and frames. The FEM consists of 992 nodes, 3,286 elements, and 3,390 degrees of freedom. The FEM included the temperatures, materials, and loading conditions described above. Both stresses and deflections were checked for the various loading cases examined. The critical flight condition occurred at Mach 0.9 climb.

The maximum stress occurs at the outboard root intersection for the critical Mach 0.9 climb condition. Actual stresses are compared to the allowable stresses to ensure structural integrity, and skin gages adjusted accordingly. The aircraft also is examined for low stress areas in order to use minimum gage materials as much as possible. Most of the fuselage and the forward portion of the wing fall into that category. Figure 2-73 depicts the aircraft under limit-load critical design case. This condition is examined to ensure that there are no structural deformations or deflections that would inhibit movement of the control surfaces, such as the ailerons or flaps. The wing tip deflection under critical limit loads is 114 inches. Internal, structural configuration changes to increase moment-of-inertia alleviates this condition without significant weight penalty; detailed design analysis would include tradeoffs with wing thickness and load alleviation devices.

Based on the internal loads from the FEM and the materials previously discussed, parametric trades were conducted for the major structural components consisting of the wing, fuselage, and empennage. In Phase I, six structural concepts were analyzed for the wing and seven for the fuselage. From that analysis,

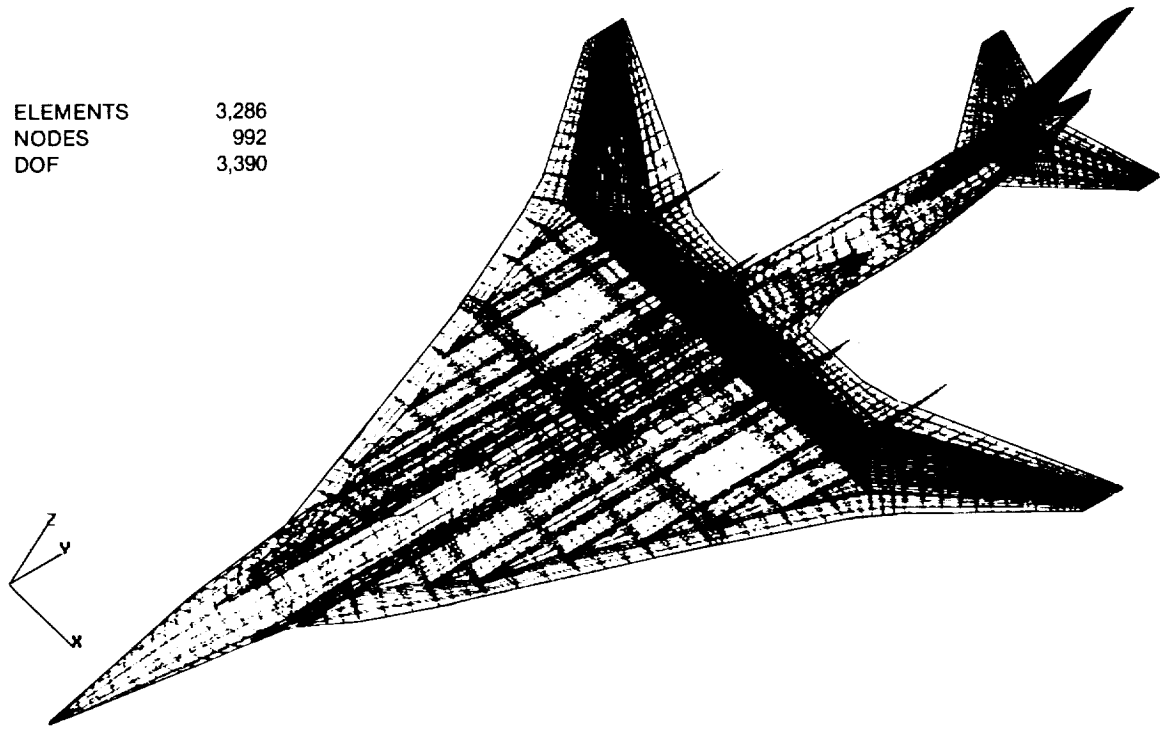

FIGURE 2-72. FINITE ELEMENT MODEL — MACH 3.2 CONCEPT

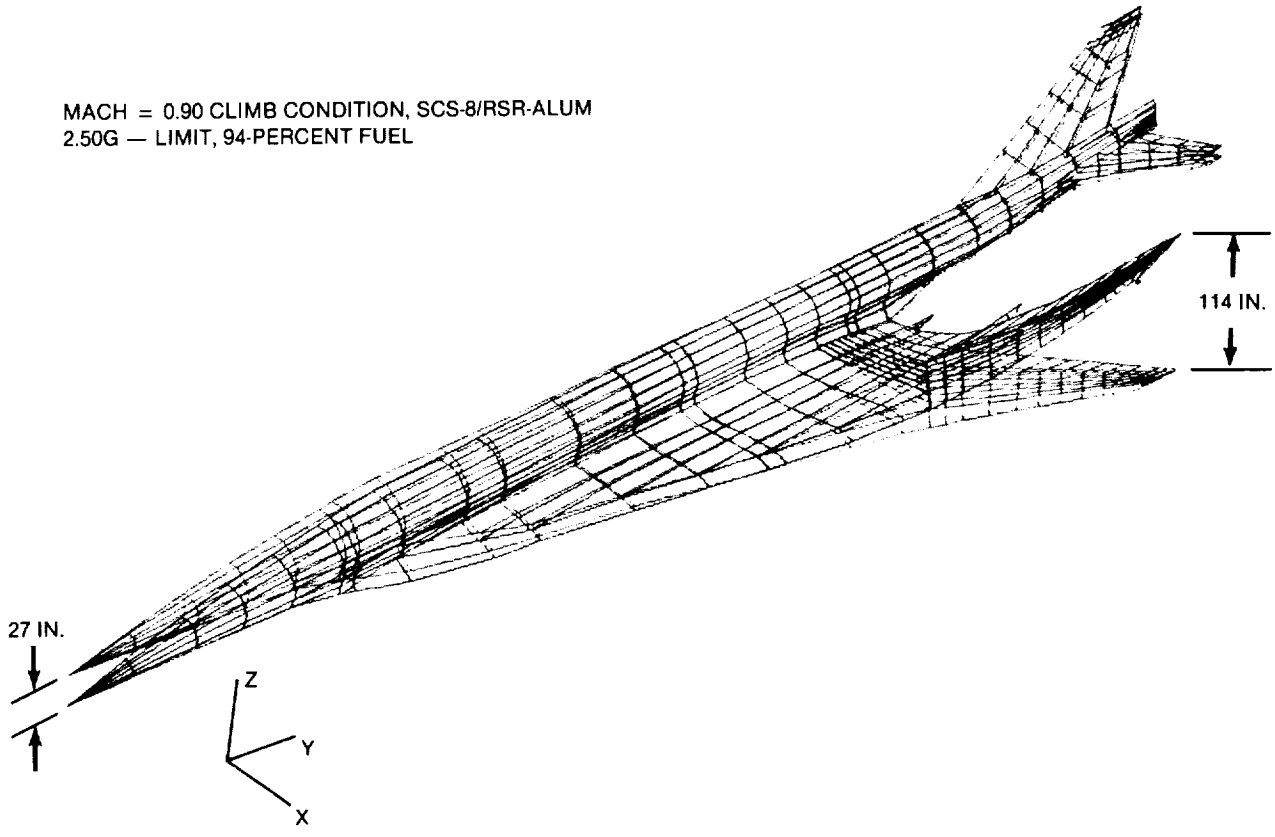

FIGURE 2-73. DEFLECTIONS — MACH 3.2

three structural concepts were selected for minimum weight, volume, cost considerations. These were (1) the conventional skin-stringer design, (2) super-plastically formed, concurrently diffusion bonded (SPF/DB) structure, and (3) the traditional honeycomb construction. In performing an optimization analysis of these three concepts, the honeycomb SCS-8/RSR Al system was selected as the preliminary structural configuration. Typical values for the outer skin are shown on Figure 2-74. The optimization analysis included strength, stability, crippling, and thermal stresses. These sizes are used in the weight analysis of the aircraft.

The optimization conducted using SCS-8/RSR Al honeycomb construction for the load-carrying members, resulted in a structural weight reduction of 35 percent relative to mid-1970s technology studies of high-speed commercial aircraft. This reduction achieved an important improvement in fuel efficiency. Section 2.6 presents detail weight statements and weight breakdown of structures, fuel, power plant, payload, and systems.

Mach 5.0. Mach 5.0 concept is a blended-body configuration. Its entire outer structure is fabricated from honeycomb, and the substructure consists of frames, spars, and ribs. Figure 2-75 presents the maximum temperatures the aircraft will experience, along with candidate materials. The maximum temperatures are 1,580°F on the nose, 1,200°F on the leading edge of the wing, 1,425°F on the empennage, 920°F on the upper fuselage, and 1,020°F on the lower fuselage.

Figures 2-76 and 2-77 represents an evaluation of the materials based on the specific moduli and specific compressive yield strength. The materials listed consist of titanium, René 41, and TD Ni Cr. The best materials are the upper three titaniums, all metal matrices consisting of RSR-Ti, Ti-15-3, and Ti 6-4. SCS-6/RSR-Ti being the most efficient was used for the structural evaluation of the concept. The next two materials consist of RSR Ti and René 41. René 41 has the highest temperature capability of the group and was used for the wing leading edge. The remaining three materials are two titaniums and TD Ni Cr. The

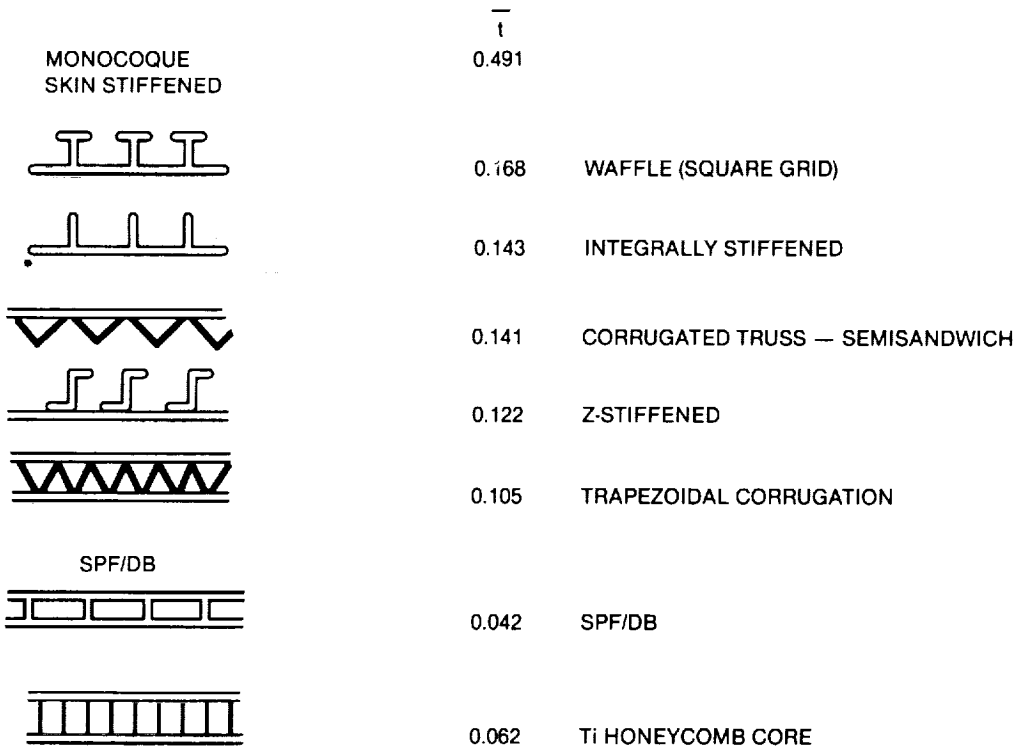

FIGURE 2-74. PARAMETRIC TRADES — FUSELAGE MIDBODY

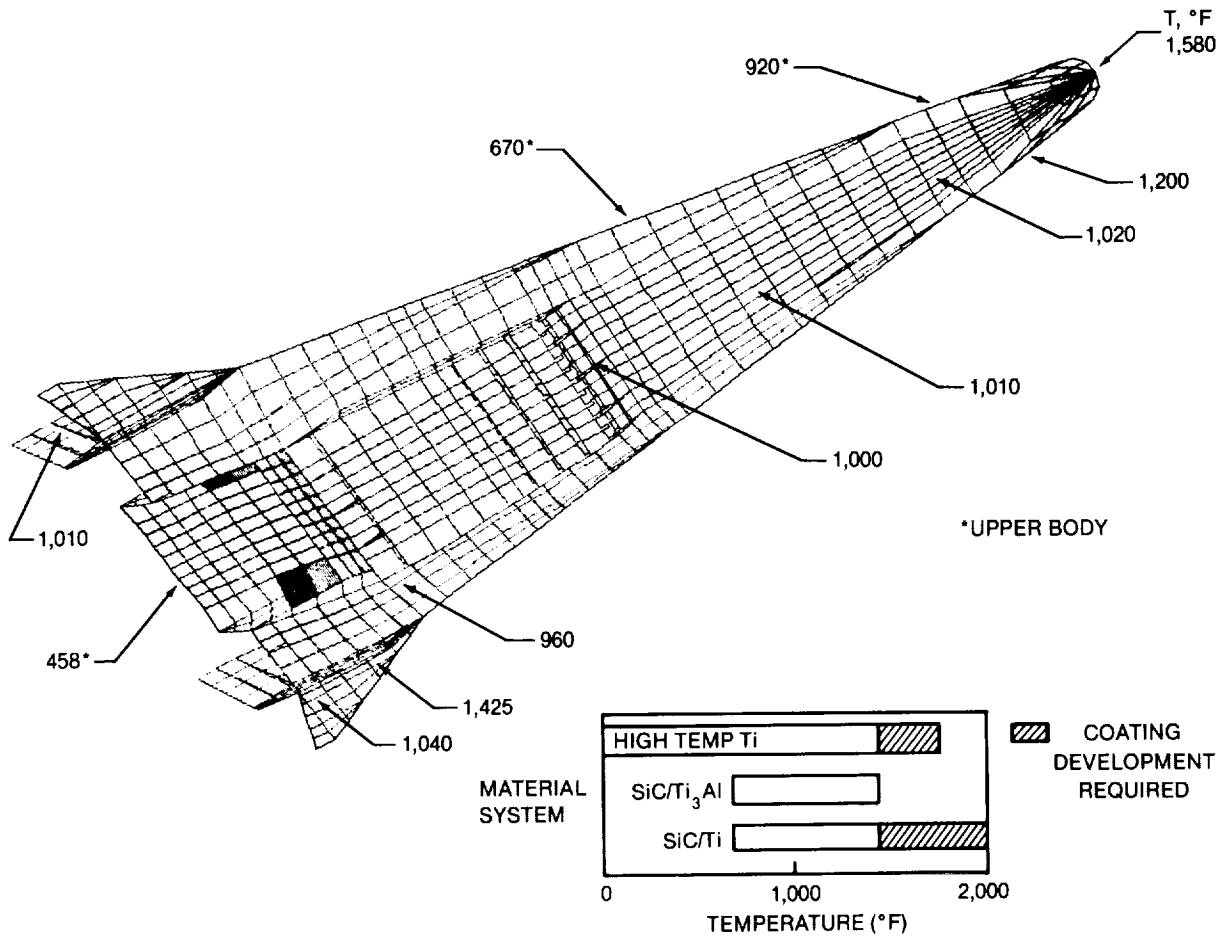

FIGURE 2-75. MAXIMUM TEMPERATURES — CANDIDATE MATERIALS — MACH 5.0 CONCEPT

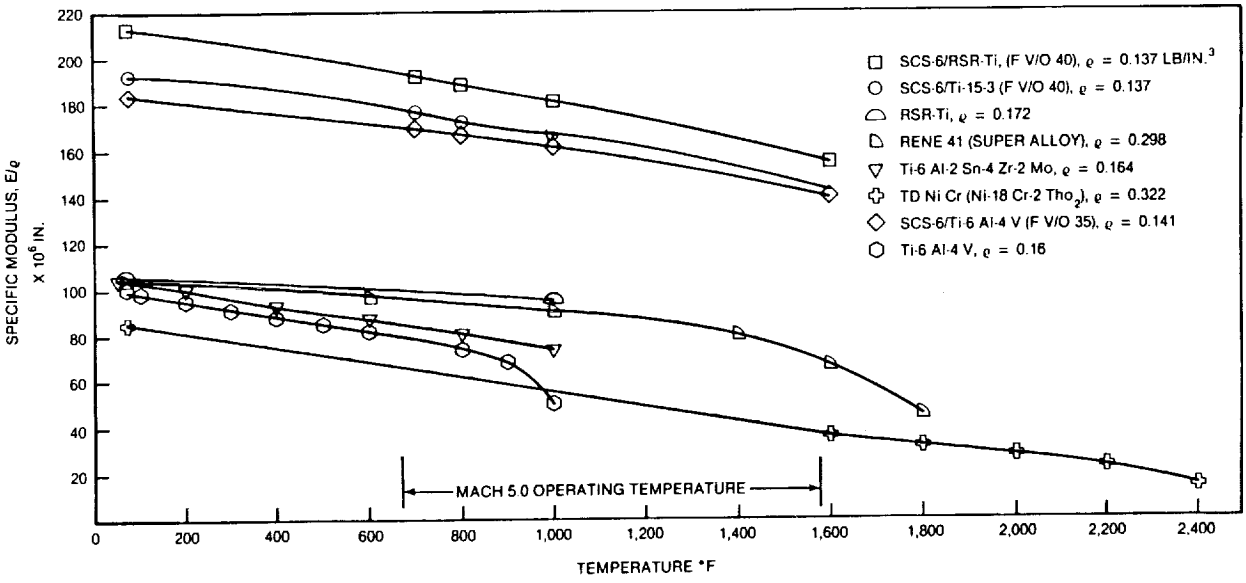

FIGURE 2-76. SPECIFIC MODULUS OF MACH 5.0 CANDIDATE MATERIALS

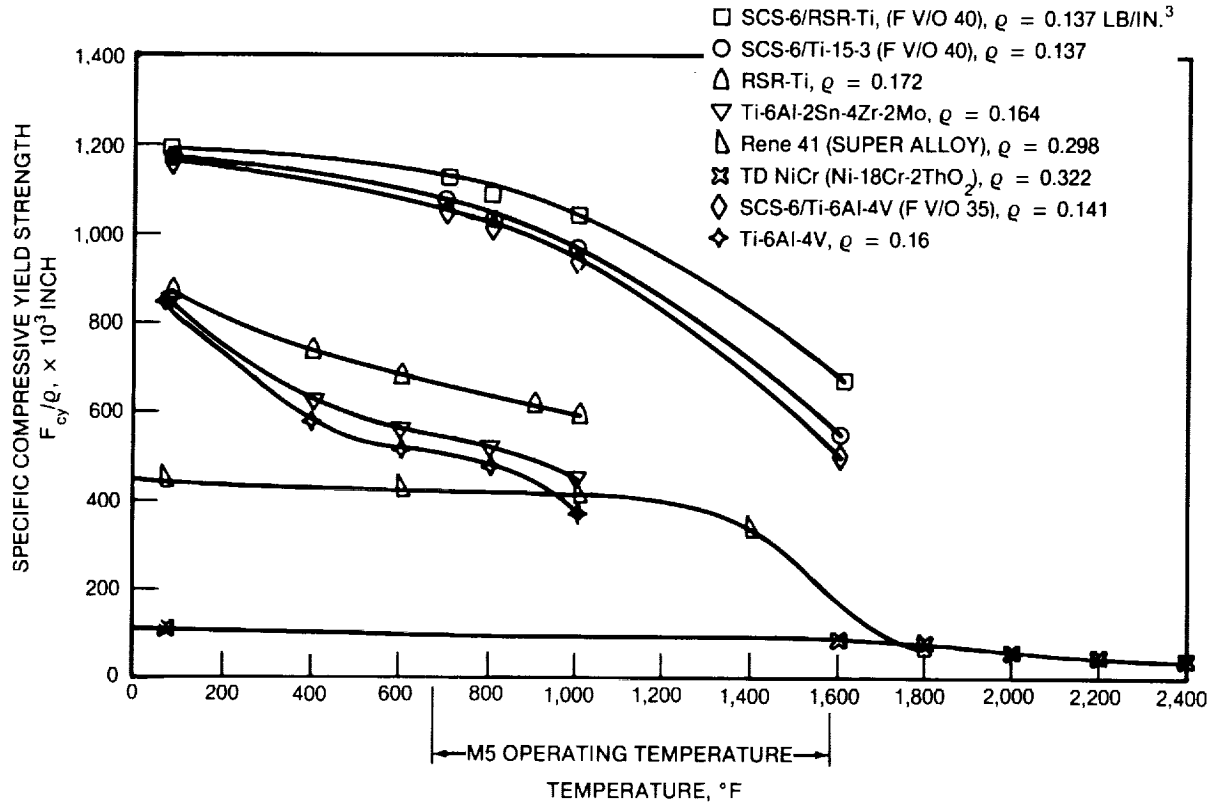

FIGURE 2-77. SPECIFIC COMPRESSION YIELD STRENGTH OF MACH 5.0 CANDIDATE MATERIALS

TD Ni Cr was used for the leading edge of the empennage because of its greater temperature overshoot capability. Considerable work is being done in industry and government, especially NASA's Langley Research Center and Lewis Research Center, to develop these and other advanced materials. TD Ni Cr is no longer offered commercially and would only be considered if the R&T program was not successful in developing an advanced material to meet temperature overshoot conditions. McDonnell Douglas has performed high-temperature tests on titanium metal matrix composites with success in the Mach 5.0 temperature range.

Table 2-8 shows the Mach 5.0 candidate materials and their evaluation. As shown, SCS-6/RSR-Ti is the highest ranked not only from the buckling and crippling standpoint, but also from a tension and stiffness consideration; consequently it was used for structural evaluation of the Mach 5.0 concept. The materials were evaluated at 880°F since that temperature is representative of most of the aircraft surface at cruise conditions; the critical design case under consideration.

In addition to the materials for the major components, materials investigation were performed for the major structural elements of the propulsion system, including the inlet ramps, nacelle, exhaust, and exhaust ramps. The candidate materials are shown in Figures 2-78. The Lewis Research Center has developed a ceramic-ceramic material far superior to the others, as shown in the figure. Consequently, it was chosen for the internal structural applications. The external shell of the inlet and nacelles is SCS-6/RST Ti, and GRAPHITE/HFC,TZM was used for the engine/nozzle transition structure.

The same type of loading conditions were examined for the Mach 5.0 concept as for the Mach 3.2 concept. In this case, however, the cruise condition was the critical design case. All other similar conditions were examined. An FEM was constructed for the Mach 5.0 (D5.0-15A) concept and is shown in Figure 2-79. The FEM represents all the structural elements of the aircraft: the spars, ribs, frames, longerons, and

TABLE 2-8
EVALUATION OF CANDIDATE MATERIALS — MACH 5.0 CONCEPT

CANDIDATE MATERIALS	COMPRESSION (CRIPPLING AND BUCKLING) RANK	TENSION AND STIFFNESS RANK
Ti-6Al-4V BASELINE	5	5
RSR-Ti	4	3
SCS-6/Ti-1S-Ti	2	2
SCS-6/RSR-Ti	1	1
SCS-8/RSR-Al	3	4

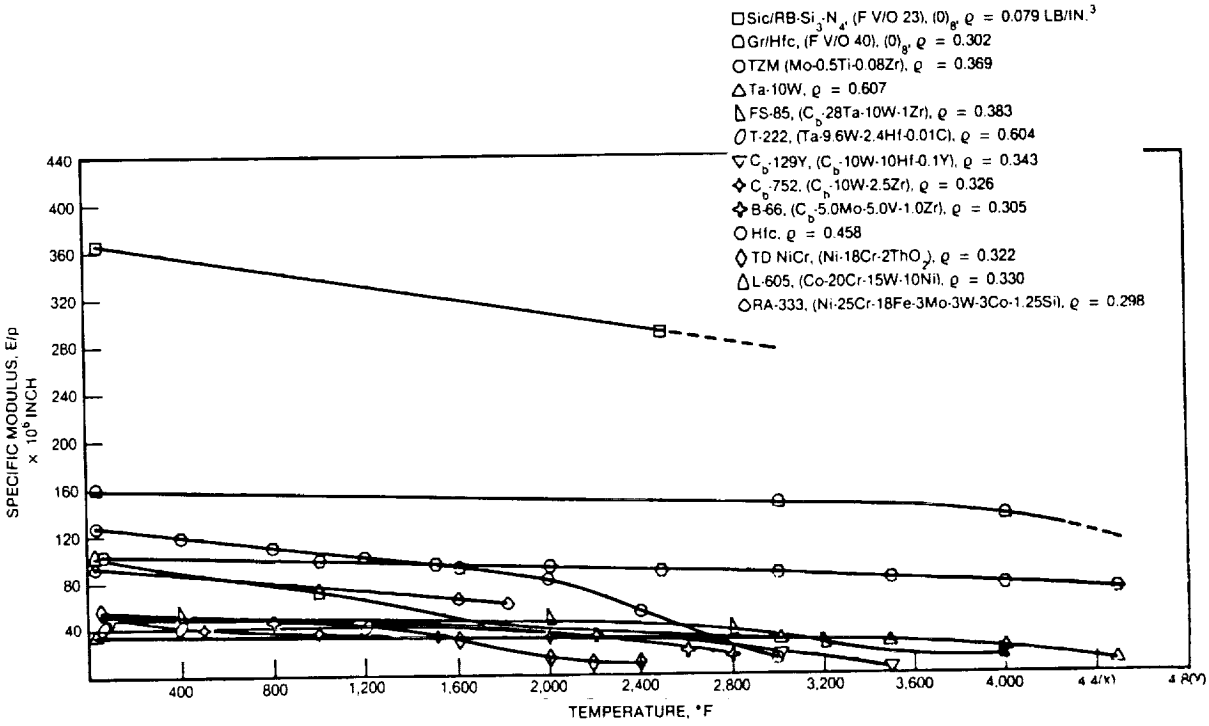

FIGURE 2-78. SPECIFIC MODULUS OF MACH 5.0 PROPULSION SYSTEM CANDIDATE MATERIALS

shear webs for the major components. The passenger cabin and propulsion system, including inlet, nacelle, and exhaust also are modeled. The FEM consists of 1,616 nodes, 4,184 elements, and 9,206 degrees of freedom. The FEM included temperatures, materials, and loading conditions specified in the previous paragraphs. Of the three flight conditions examined (transonic at climb, descent, and cruise), the cruise condition, with its associated maximum temperatures, became the critical design case for most of the structure. Both deflection and stress were checked to ensure structural integrity. Stress levels, as well as deflections (Figure 2-80), were within structural allowables.

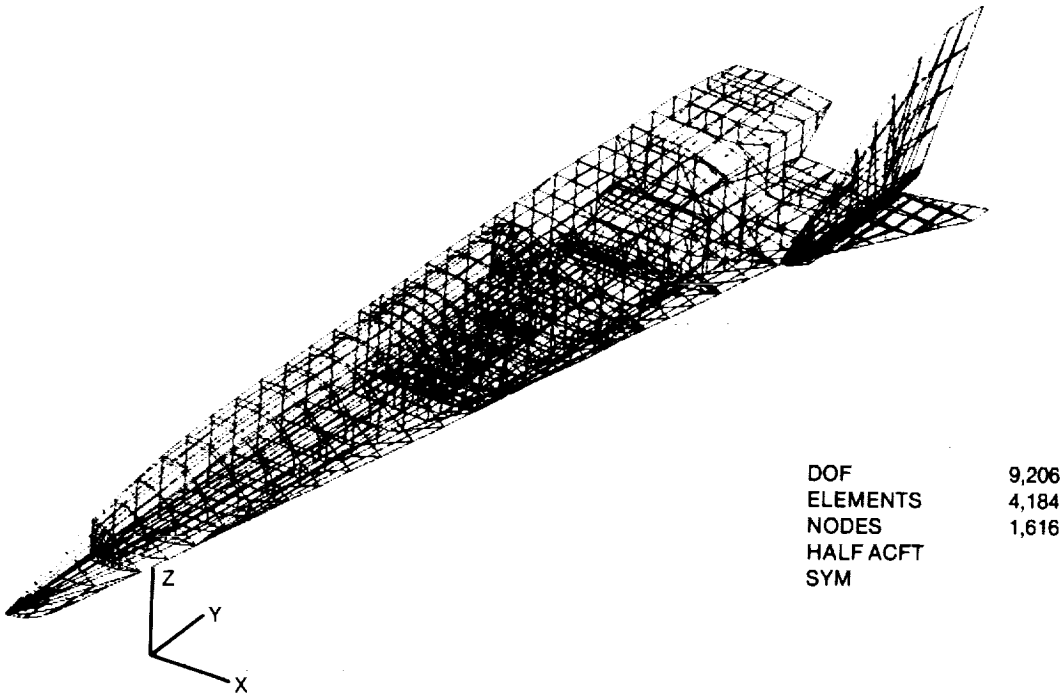

FIGURE 2-79. FINITE ELEMENT MODEL — MACH 5.0 CONCEPT

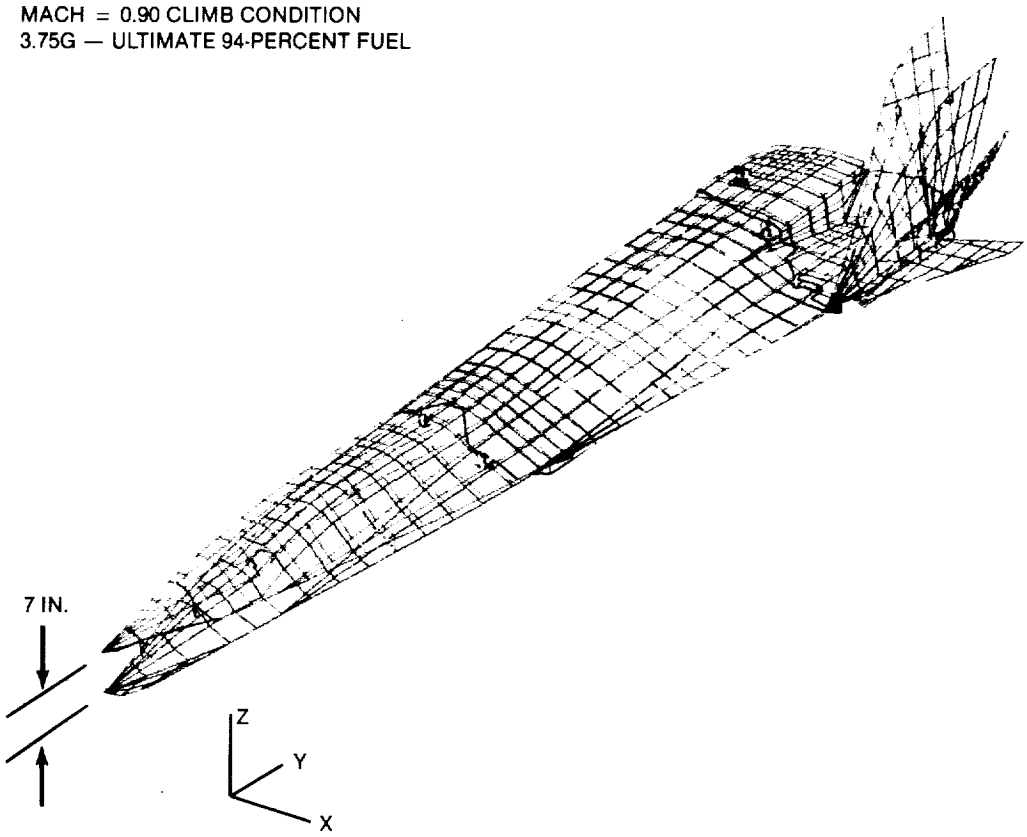

FIGURE 2-80. DEFLECTIONS — MACH 5.0 CONCEPT

Based on the internal loads from the FEM for the three conditions and the candidate materials, parametric trades were conducted. As in the case of the Mach 3.2 concept, the same structural concepts were examined and reduced to three: (1) the skin-stringer, (2) superplastic formed/diffuser bonded, and (3) honeycomb constructions. The trades were performed on these three structures, and the results shown in Figure 2-81. The honeycomb panel, constructed of SCS-6/RSR Ti, results in the lightest weight structure. Conventional materials such as Ti 6-4 and Ti 6-2-4-2 are significantly heavier in weight. This optimization was performed for the entire aircraft, and typical results are depicted in Figure 2-82. Also shown in the figure are the sized members for the passenger cabin, fuel tanks, and sub-structure. These sizes were used in the weight analysis of aircraft.

The selection and optimization of the SCS-6/RSR Ti honeycomb construction, resulted in a structural weight reduction of 15 percent relative to the mid-1970s technology studies of high-speed commercial aircraft. This structural weight reduction achieved an important improvement in fuel efficiency. Section 2.6 presents a discussion of these results and detail weight statements.

Supporting Technology. Other significant work is being conducted in industry and the government to develop the technology for high-speed aircraft. This work is briefly noted here since it helped formulate the direction and analysis performed in this study. Laminar Flow Control: Extensive studies have been conducted to evaluate laminar flow control on test aircraft with actual flight hardware systems (Reference 2-11). Various structural concepts have been built and tested using SPF/DB. Electron beam technology performed the perforation in the titanium for the laminar flow suction. These results were used in the analysis of laminar flow control structures of the Mach 3.2 concept. NASP: A concerted, high temperature/lightweight materials development program is being performed in parallel to configuration development. This activity together with structural configuration and thermal studies has aided in the Mach 5.0 concept definition and evaluation.

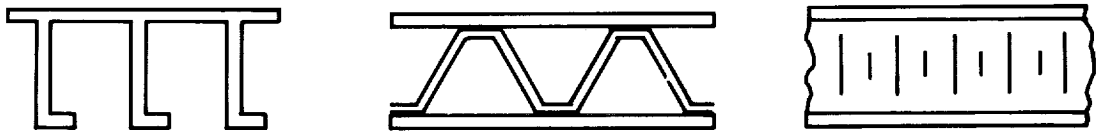

	STIFFENED SKIN	FOUR-SHEET SPF/DB	HONEYCOMB
	WEIGHT (LB/FT^2)	WEIGHT (LB/FT^2)	WEIGHT (LB/FT^2)
Ti-6-4	3.08	3.82	1.90
Ti-6-2-4-2	2.86	3.58	1.89
RSR-Ti	2.77	3.50	1.87
SCS-6/Ti-6-4	1.77	2.79	1.49
SCS-6/Ti-15-3	1.72	2.71	1.46
SCS-6/RSR-Ti	1.72	2.71	1.45

FIGURE 2-81. STRUCTURAL PANEL WEIGHTS FOR MACH 5.0 AIRCRAFT WING

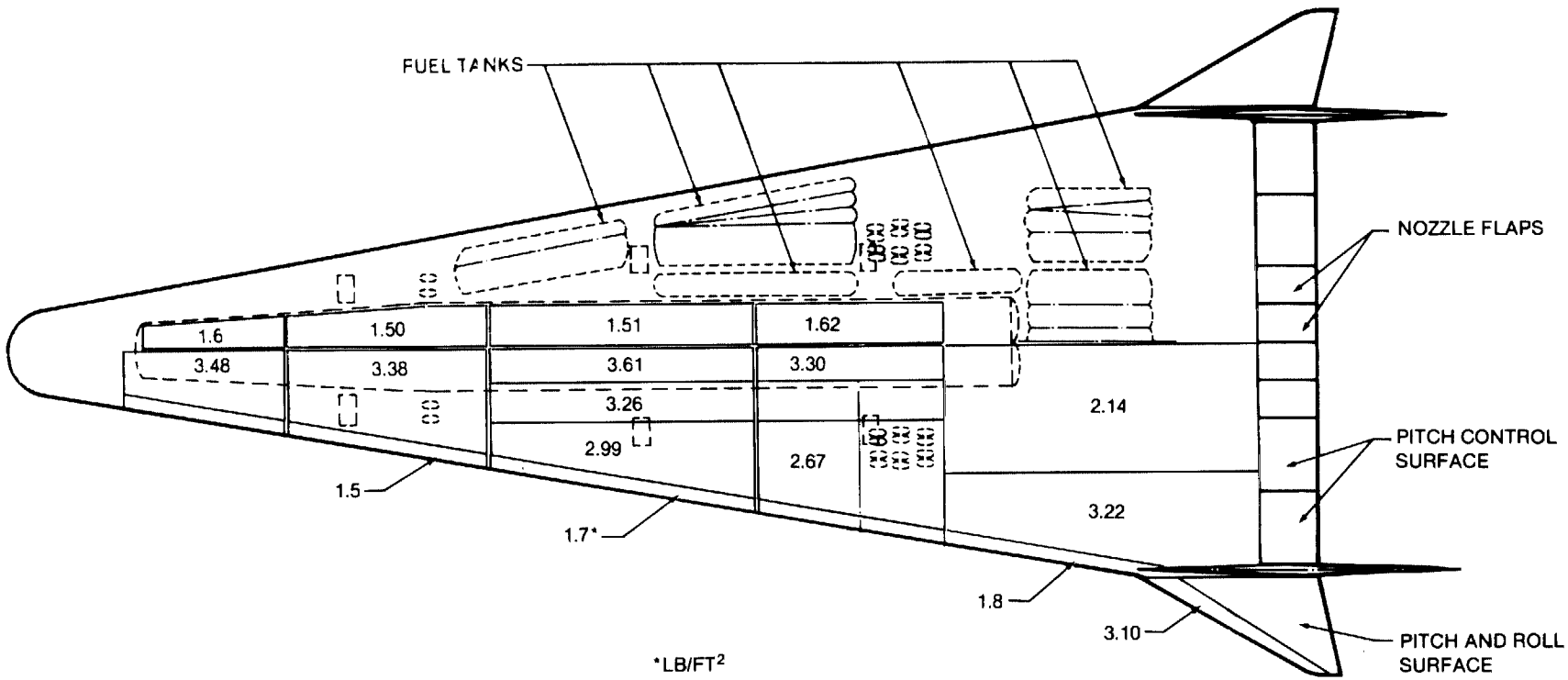

FIGURE 2-82. MACH 5.0 CONCEPT STRUCTURAL UNIT WEIGHTS/PASSENGER CABIN AND OUTER SHELL

2.6 Weights

This section summarizes the weight analysis that includes the derivation and utilization of consistent conceptual design level weights. Technology improvements assumed achievable by the year 2000 have been identified and included.

Parametric weights were determined in Phase III for aircraft sizing to meet specific mission requirements. Following this, group weights were developed for the final Mach 3.2 (D3.2-3A) and Mach 5.0 (D5.0-15A) baseline concepts. Parametric weights were derived from the conceptual MAPES (mass properties estimation system) computer program based on Phase I and II statistical weights. Adjustments based on results of Phase III detail structural analysis and optimization were made to these earlier statistical weights.

Operational Empty Weight. Operational empty weight (OEW) is a measure of the weight efficiency of the aircraft. The OEW consists of the manufacturer empty weight (MEW) plus operator items. MEW component weight considerations are described below.

The structures weights for the Mach 3.2 and Mach 5.0 concepts, which includes the wing (Mach 5.0 wing weight also includes the movable tips), fuselage, and tail sections, were derived from unit weights (pounds per square feet) in the structural optimization analysis. The structural optimization analysis includes considerations of external aerodynamic loads and thermal heating, year-2000 technology material properties, structural arrangements, benefits of a passive thermal protection system (TPS), and commercial aircraft design criteria and standards.

Aircraft systems weights excluding the TPS, and the Mach 5.0 liquid methane fuel tank, and systems installation weights were based on weight data from the Concorde and past NASA/McDonnell Douglas high-speed commercial aircraft studies conducted in the mid-1970s. Assumed year-2000 system technology weight improvements over the mid-1970 weight base are shown in Table 2-9.

The landing gear technology weight improvement factor of 15 percent is based on a Douglas study, Technology Alternatives for Airlift Deployment (1982).

The inlet, nacelle, mounting, and engine system installation technology weight improvement of 20 percent for the Mach 3.2 and Mach 5.0 concepts are established from structural analysis results. The variable inlet geometry mechanism and system weight improvements, which are included above, are based on lighter weight structure and innovative variable geometry mechanism design. The engine exhaust, sound suppressor, thrust reverser, and accessory drive system technology weight improvement factor of 10 percent is based on engineering judgment in view of lighter weight high-temperature materials and innovations in design for weight reduction. The Mach 5.0 engine exhaust system weight includes the single expansion ramp nozzle.

TABLE 2-9
SYSTEMS TECHNOLOGY WEIGHT IMPROVEMENTS

YEAR 2000 CONCEPT MACH 3.2 AND MACH 5.0 SYSTEMS	% WEIGHT IMPROVEMENTS FROM MID 1970 WEIGHT BASE
LANDING GEAR	-15
INLET, NACELLE, MOUNTS	-20
ENGINE EXCHANGE, SOUND SUPPRESSOR, THRUST REVERSER	-10
FUEL SYSTEM	-5
FLIGHT GUIDANCE AND CONTROLS	-30
CABIN FURNISHINGS	-20
INSTRUMENTS	+5
ELECTRICAL POWER	-10
AVIONICS	-10
ICE PROTECTION	-15

The fuel system weight for the Mach 3.2 concept reflects an integral fuel system. The fuel system technology weight improvement factor of 5 percent is based on engineering judgment taking into account improvements in technology for lighter weight pumps, valves, and plumbing. The installation weight of the Mach 5.0 LNG fuel tank structure is based on optimized structural analysis unit weights (pounds per square foot of wetted tank area) derived during Phase III. The averaged optimized tank structural installed unit weight is 1.01 pounds per square foot.

The passenger and crew (cabin) furnishings group technology weight improvement factor of 20 percent is based on engineering judgment taking into account improvements for the lighter weight materials and construction for such items as passenger seats, cabin ceiling and sidewalls, overhead stowage racks, galley structure and inserts, and lavatory installations. The all-electric vapor cycle cabin air conditioning and pressurization system weights are established from results of the environmental controls system analysis. The TPS weight is determined from a thermal management system analysis. This analysis concludes that the use of a passive modularized multilayer insulation (MMLI) TPS for the passenger cabin and fuel tanks for both the Mach 3.2 and 5.0 configurations is feasible. The TPS weight also includes a passive system for the Mach 3.2 engine exhaust nozzle. The Mach 5.0 TPS weight includes an active TPS for the engine inlet and exhaust nozzle. Table 2-10 shows the averaged TPS unit weights.

TABLE 2-10
THERMAL PROTECTION SYSTEM — AVERAGED INSTALLED UNIT WEIGHT

UNIT WEIGHTS BASED ON WETTED AREA	D-3.2-3A LB/FT^2	D-5.0-15A LB/FT^2
PASSIVE TPS		
PASSENGER CABIN	0.827	0.712
FUEL TANK	0.377	0.526
ENGINE EXHAUST	0.630	
ACTIVE TPS		
ENGINE INLET	N/A	2.80
ENGINE EXHAUST	N/A	3.65

The advanced technology glass cockpit instrument system (two-person cockpit crew) has a positive technology factor of 5 percent. The increase in weight is based on a Douglas/IRAD study that includes flat panel displays and multiplexed digital data bussess. The flight guidance and control technology weight improvement factor of 30 percent is established from the use of an all-electric and fly-by-light flight guidance and controls system. The avionics system technology weight improvement factor of 10 percent is based on a Douglas study that includes component repackaging and the utilization of light-weight wiring. A weight improvement factor of 10 percent for the electrical power system is established from the use of an advanced technology all-electric secondary power system. The 10-percent weight improvement reflects engineering judgment and a weight penalty for higher power demands from the electric cabin air conditioning system due to the increased cabin thermal gradient produced by aerodynamic heating which occurs at higher Mach numbers. Hydraulic and pneumatic power systems are eliminated as a result of the all-electric secondary power system and, thus, have a technology weight improvement of 100 percent.

The laminar flow control system weight, which includes suction pumps, motors, ducting, control valves, engine pneumatic bleed system, and installation, is based on an laminar flow control power requirement and the system weight analysis results. The ice protection system technology weight improvement factor of 15 percent is established by replacing a conventional hot-air pneumatic anti-ice system with an all-electric anti-ice system. Ice protection is assumed for the cockpit windshield, pitot and static ports, and engine inlets.

The load and handling weight includes weight penalties for hard points and receptacles required for jacking, leveling, and mooring the airplane. The deletion of the auxiliary power unit system is based on studies to reduce the aircraft OEW with improvements in aircraft maintainability and reliability.

The Mach 3.2 dry engine weight (excluding the nozzle) is based on data received from P&W. The TSJF P&W duct burning turbofan engine has a reference maximum dry sea level static takeoff thrust rating of 29,686 pounds per engine and a bare engine weight of 4,114 pounds.

The Mach 5.0 dry engine weight (excluding the nozzle) is based on data received from GE for the LNG-fueled GE VCHJ engine. The engine reference maximum dry sea level static takeoff thrust is 72,183 pounds per engine with an engine weight of 6,692 pounds.

The operator items weight represents passenger and galley service to accommodate a three class, 300-passenger cabin for flights of up to 4 hours. The weights are based on subsonic and past high-speed study weight data and engineering judgment to reflect speeds up to Mach 5.0.

Payload. The payload weight is derived as follows:

- 165 pounds per passenger × 300 passengers = 49,500 lb
- 40 pounds of baggage per passenger × 300 passengers = 12,000 lb
- Mission payload weight = 61,500 lb
- Lower cargo weight at 10 pounds per cubic feet = 5,000 lb
- Maximum space limited payload weight = 66,500 lb

Mach 0.85. The Mach 0.85 subsonic baseline airplane weight analysis was performed in Phase I (see Figure 2-1 for geometry data). The weight methodology included the utilization of the conceptual design subsonic MAPES module that contains empirical subsonic weight equations. The emperical equations were modified to reflect the MD-11 weights.

Since the wing, tail, and fuselage emperical weight equations reflect the MD-11 technology level, a year-2000 technology weight improvement factor of 22 percent was incorporated, taking into consideration the use of advanced structural materials such as graphite composites and aluminum metal matrix. The systems weight reflects year-2000 weight improvements as shown in the Table 2-9, including an all-electric secondary power system, hybrid laminar flow control, and a wet horizontal tail center-of-gravity control system.

The propulsion system weight is based on data from the proposed P&W Advanced Ducted Prop study conducted by Douglas in late 1986. The propulsion system weight includes the dry engine, propellers and gear box, nacelle, exhaust, engine systems, and pylon structures.

Parametric weights were generated for the aircraft mission performance and sizing analysis. The resultant weights and geometry produced from the aircraft mission performance (6,500 nautical miles) and sizing analysis are as follows:

- Takeoff gross weight = 397,000 lb
- Operational empty weight = 189,000 lb
- Mission payload weight = 61,500 lb
- Reference wing area = 2,680 ft^2
- Maximum TOSLS engine thrust/engine = 34,600 lb
- Number of passengers = 300

Mach 3.2. The geometry and functional group weights for the final D3.2-3A baseline concept is presented in Table 2-11 and corresponds to a takeoff gross weight of 769,000 pounds and a range of 6,500 nautical miles.

The weight analysis for the D3.2-4B concept, a compromised configuration for subsonic flight is based on Figure 2-7. The weight analysis uses the D3.2-3A concept weight as a base. The -4B weight analysis accounts for only geometry changes to the wing – an increase in aspect ratio combined with a decrease in sweep. The remaining structure and system weights were assumed identical to the D3.2-3A concept.

TABLE 2-11
D3.2-3A CONCEPT GEOMETRY AND WEIGHT DATA

GEOMETRY DATA	
MACH NUMBER	3.2
RANGE (N MI)	6,500
FUEL TYPE	TSJF
NUMBER OF PASSENGERS	300
TAKEOFF GROSS WEIGHT (LB)	769,000
MAXIMUM ZERO FUEL WEIGHT (LB)	297,800
MAXIMUM SPACE LIMITED PAYLOAD (LB)	66,500
WING AREA — TOTAL PLANFORM (FT^2)	9,500
HORIZONTAL TAIL AREA — TOTAL PLANFORM (FT^2)	733
VERTICAL TAIL AREA — TOTAL PLANFORM (FT^2)	670
NUMBER OF ENGINES	4
MAXIMUM SEA LEVEL STATIC DRY THRUST PER ENGINE	29,500
WEIGHT DATA (LB)	
STRUCTURES	98,054
POWER PLANT	35,115
SYSTEMS	91,066
MANUFACTURE EMPTY WEIGHT	224,235
OPERATOR ITEMS	7,100
PAYLOAD	61,500
ZERO FUEL WEIGHT	292,835
FUEL	476,165
TAKEOFF GROSS WEIGHT	769,000

Parametric weights of the D3.2-4B concept were generated for the mission performance and sizing analysis. The results from the aircraft mission performance (6,500 nautical miles) and sizing analysis are as follows:

- Takeoff gross weight = 880,000 lb
- Operational empty weight = 250,000 lb
- Mission payload weight = 61,500 lb
- Reference wing area = 9,500 ft^2
- Maximum dry TOSLS engine thrust/engine = 30,645 lb
- Number of passengers = 300

The results from the mission performance and sizing analysis shows an increase of 19,000 pounds in OEW and 111,000 pounds in takeoff gross weight relative to the D3.2-3A baseline.

Mach 5.0. The geometry and functional group weights for the final D5-15A baseline concept is presented in Table 2-12 and corresponds to a takeoff gross weight of 1,213,000 pounds and range of 3,900 nautical miles.

Fail-Safe Versus Safelife Fuselage Concepts. A first-order conceptual weight comparison between the D3.2-3A baseline safelife fuselage and a fail-safe fuselage concept (shown in Figure 2-8) was developed to determine resulting aircraft performance affects. The fail-safe -3A fuselage weight was assessed by using the weight relationships derived from analysis of the D5.0-15A fail-safe fuselage weight.

The D3.2-3A fail-safe nonbending load-carrying inner pressure shell weight was determined by first estimating a safelife fuselage weight based on Phase II statistical weight methodology. The safelife fuselage weight was estimated at 44,150 pounds. The fail-safe fuselage weight corresponds to 42 percent of the safelife

TABLE 2-12
D5.0-15A CONCEPT GEOMETRY AND WEIGHT DATA

GEOMETRY DATA	
MACH NUMBER	5.0
RANGE (N MI)	3,900
FUEL TYPE	METHANE
NUMBER OF PASSENGERS	300
TAKEOFF GROSS WEIGHT (LB)	1,213,000
MAXIMUM ZERO FUEL WEIGHT (LB)	540,300
MAXIMUM SPACE LIMITED PAYLOAD (LB)	66,500
WING AREA — TOTAL PLANFORM (FT^2)	17,000
HORIZONTAL TAIL AREA — TOTAL PLANFORM (FT^2)	0
VERTICAL TAIL AREA — TOTAL PLANFORM (FT^2)	1,682
NUMBER OF ENGINES	4
MAXIMUM SEA LEVEL STATIC DRY THRUST PER ENGINE	132,955
WEIGHT DATA (LB)	
STRUCTURES	143,586
POWER PLANT	200,236
SYSTEMS	123,413
MANUFACTURE EMPTY WEIGHT	467,235
OPERATOR ITEMS	6,570
PAYLOAD	61,500
ZERO FUEL WEIGHT	535,305
FUEL	677,695
TAKEOFF GROSS WEIGHT	1,213,000

fuselage weight. This was applied to the safelife fuselage weight of 44,150 pounds, which resulted in an inner fail-safe pressure shell weight of 18,500 pounds.

The fail-safe outer load-carrying fuselage shell weight was estimated by using an averaged, unpressurized, outer shell structural unit weight of 2.7 pounds per square foot. This is based on the -15A optimized center wing structure weight average. This unit weight was applied to an outer fuselage shell area of 12,955 square feet (14.8 percent greater in wetted area than the safelife fuselage) to produce an outer shell weight of 35,000 pounds.

The combined weights of the fail-safe inner and outer fuselage shells is 53,500 pounds, compared to the safelife fuselage weight of 44,150 pounds. The result is a weight gain of 9,350 pounds. Weight analysis was performed to account for the reduction in passenger cabin TPS weight. The result of the analysis shows a 55-percent reduction in passenger cabin TPS weight which yields a weight reduction of 3,870 pounds. The net delta OEW weight penalty, of structure (increase) and cabin TPS (decrease) is 5,480 pounds. This results in the following aircraft weight and sizing necessary to maintain the 6,500-nautical-mile range.

- Takeoff gross weight = + 2.4 percent
- Block fuel weight = + 1.8 percent
- Operational empty weight = + 3.8 percent
- Wing area = + 1.6 percent
- Engine thrust = + 2.8 percent

Weight Summary. Takeoff gross weight impacts the HSCT concepts in many ways, including the quantity of engine emissions, sonic boom and community noise levels, economic viability, and airport compatibility.

The takeoff gross weight is divided into five major parts (Figure 2-83, also Table 2-11 and 2-12) to show the major weight items. The dominating weight fraction is the fuel. To reduce the takeoff gross weight and making the HSCT more viable and competitive, the fuel fraction must be reduced considerably. Future HSCT studies should address topics such as innovative drag reduction, propulsion system inlet, nozzle design, engine cycle, and structural concepts that provide fail-safe, maintainable, and reliable components that meet minimum weight requirements and reduce fuel fraction.

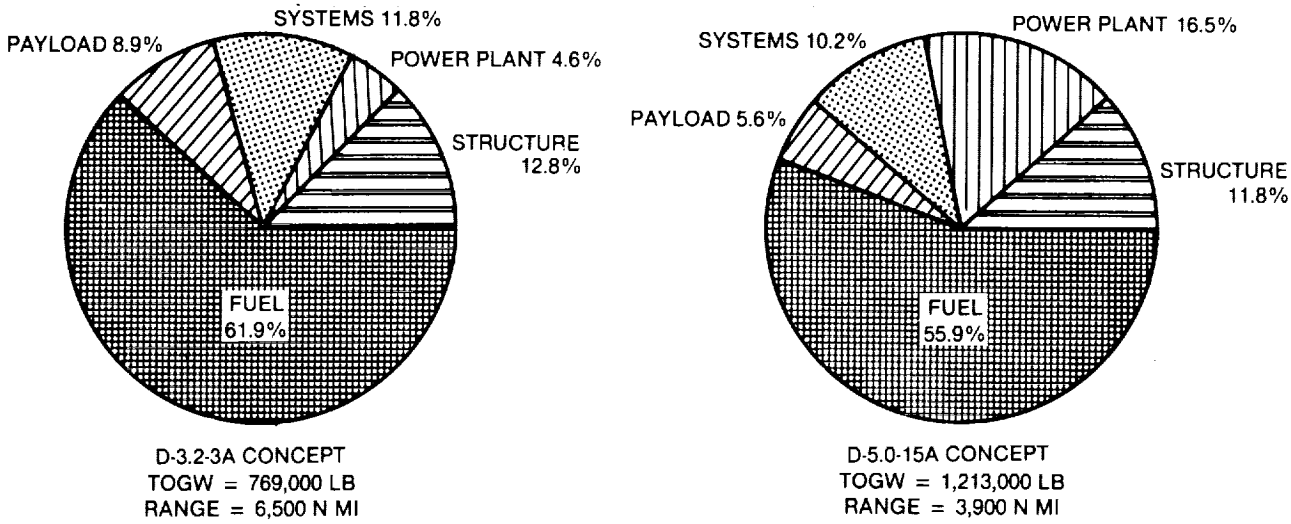

FIGURE 2-83. HIGH-SPEED CIVIL TRANSPORT CONCEPT DESIGN WEIGHT BREAKDOWN

3.0 ASSESSMENT

3.1 Performance

The HSCT performance was analyzed according to commercial domestic and international aviation rules and practices. The analysis included takeoff and landing performance, mission analysis, and determination of takeoff and approach flight paths.

Mission Definition. The mission profile is depicted in Figure 3-1 and begins with conventional takeoff and climb out to 10,000-feet altitude. This is followed by an accelerating climb to the cruise Mach number. The climb is continued at cruise Mach number until optimum cruise altitude is reached. During Phase I, it was shown that variation of the speed-altitude schedules had only minor influence on aircraft size, and true optimization was beyond the scope of available engine data. The main limitations in climb are the cabin rate of climb and the aircraft excess thrust over drag at the top of climb. Conventional cabin pressure altitude at cruise is 8,000 feet, and the limiting rate of pressurization change is equivalent to 300 feet per minute at sea level. This requires that the climb takes at least 23.5 minutes. A requirement of 4,000-feet-per-minute potential rate of climb was assumed to ensure sufficient acceleration and rate of climb to reach cruise altitude.

Cruise is flown at constant Mach number and optimum altitude to maximize range factor, which is mainly a function of the maximum lift-to-drag ratio. During fuel burn-off the aircraft is allowed to cruise-climb to remain at optimum conditions. The descent is at idle power and constant airspeed, as is the current convention. The cabin rate of descent is limited to 300 feet per minute with idle power.

Below 10,000 feet altitude, regulation specified speeds of 250 knots are maintained until landing approach at conventional speeds of 140 knots or less. Fuel reserves based on international rules are maintained: 5 percent of block fuel, fuel to fly to an alternate destination of 200 nautical miles, and fuel for a half-hour hold at the 2,000-foot altitude. Sufficient taxi, takeoff, and landing allowances for time and fuel determinations are included.

Winds aloft at the 60,000- to 90,000-foot cruise altitudes of the Mach 3.2 and Mach 5.0 concepts are considerably less than those at the cruise altitudes of subsonic aircraft (35,000 to 43,000 feet). With supersonic vehicle speeds of 4 to 6 times the subsonic airplane speed, wind influence on still-air range is less than a tenth of that of subsonic airplanes. Therefore, wind effects are only used for the subsonic reference airplane.

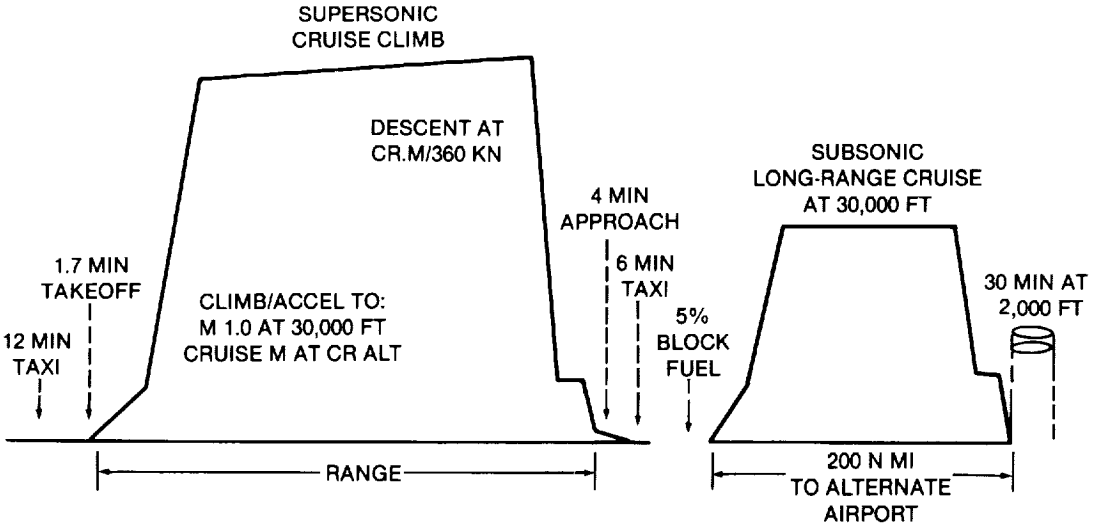

FIGURE 3-1. MISSION PROFILE

The effects of earth's rotation are incorporated in the mission computation program. These effects are illustrated for an early Mach 5.0 concept in Figure 3-2 showing average cruise-specific range (miles per pound of fuel) of 10 city-pairs in reciprocal directions. The figure shows that aircraft flying in an easterly direction have a greater advantage in specific range due to the centrifugal forces of combined earth rotation and cruise speed than aircraft flying in a westerly direction. Missions sizing was based on a neutral north-south route across the equator. HSCT takeoff, cruise, and landing segments can be flown much as a conventional aircraft, including diversions or delays.

Concept Sizing. Sizing was accomplished using the Computer Aided Sizing and Evaluation system (CASES), which consists of interacting modules of stability and control, aerodynamic design, weight and balance, propulsion and systems, and airplane performance. By varying wing reference area and engine size, the optimum configuration is determined, taking into account constraints and margins as considered appropriate.

During Phase II, drag variation with wing area was included to enable sizing of wing area and engine thrust to satisfy all constraints. These constraints are: (1) takeoff field length of 11,000 feet or less, (2) landing approach speed of 140 knots or less, and (3) cruise at optimum altitude or at the operationally determined ceiling (4,000-feet-per-minute potential rate of climb).

These constraints do not necessarily determine the lowest cost airplane. For the preliminary screening, the maximum takeoff gross weight was selected as representative of the overall cost, with empty weight representing capital cost and fuel burned representing operational cost. Therefore, the minimum value of design takeoff gross weight satisfying the 11,000-foot takeoff field length determined the wing/engine size combinations. As shown in Figure 3-3, the takeoff gross weights were 684,000 pounds and 984,700 pounds, respectively, for the Phase II Mach 3.2 and Mach 5.0 concepts.

For the Phase III sizings, the Phase II reference wing areas were retained at 9,500 and 17,000 square feet, respectively, for the Mach 3.2 and 5.0 concepts. The engine sizes for both vehicles were revised for the 11,000-foot takeoff field length requirement, and the takeoff gross weights were updated based on revised inputs.

Mach 0.85. Economic analysis included an advanced subsonic transport. This design included a wing with a high aspect-ratio, 11.4, a hybrid laminar flow system, riblets, wet tail for center-of-gravity control, advanced structures, metallic and nonmetallic, and three very high bypass ratio ducted fan engines. The

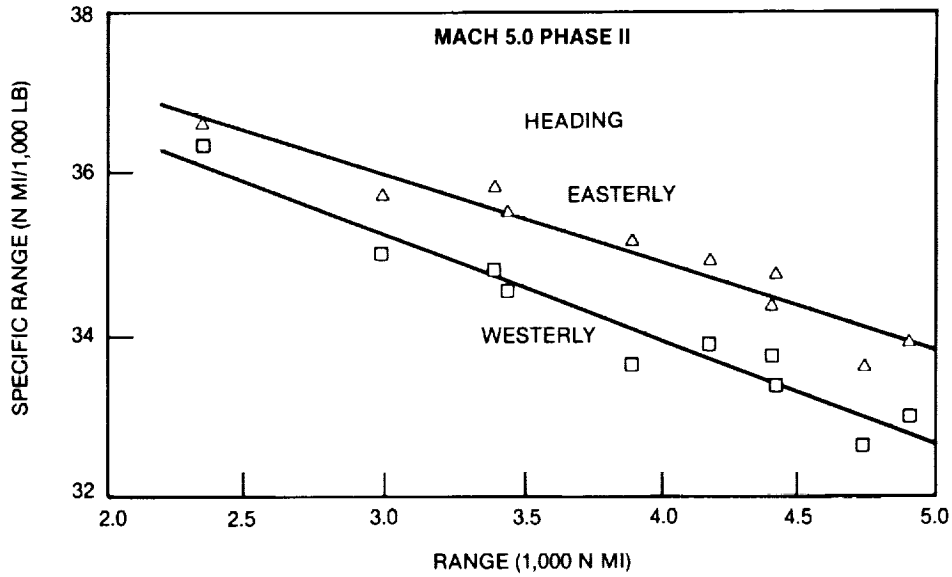

FIGURE 3-2. EFFECT OF EARTH'S ROTATION — WORLD ROUTES STUDY

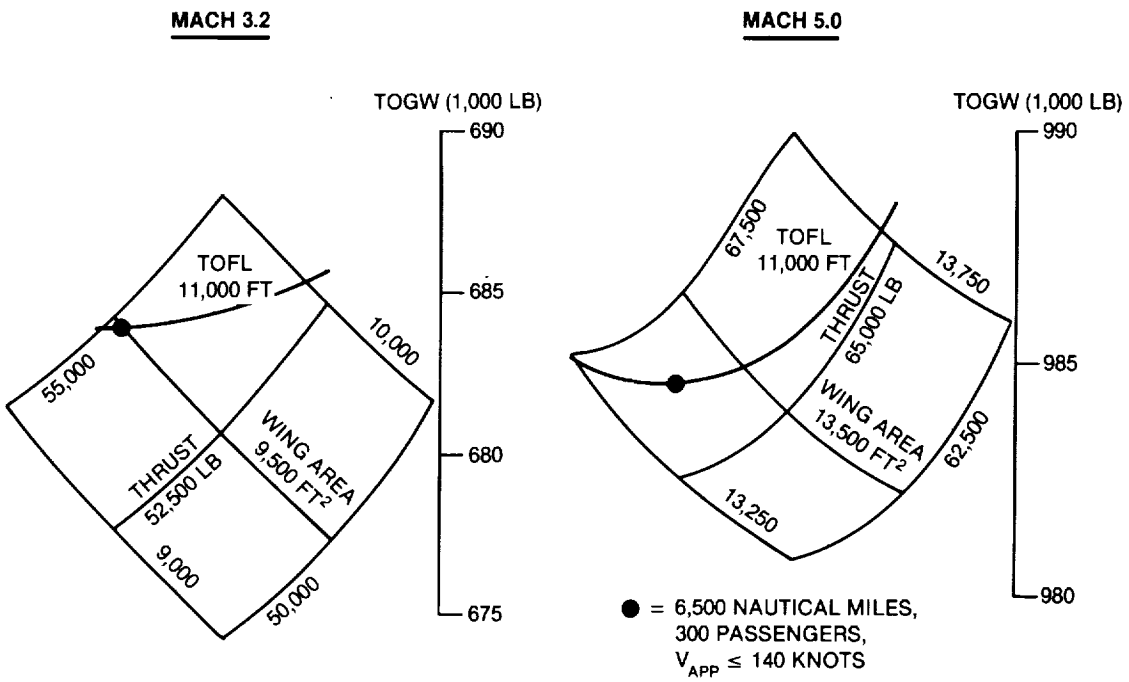

FIGURE 3-3. HSCT SIZING

airplane was sized for 300 passengers and 7,400-nautical-mile still-air range. (The design range of 6,500-nautical-mile geometric distance was corrected for prevailing westerly headwinds across the northern Pacific. HSCTs are assumed to fly above the weather and the relatively small headwinds relative to the cruise speeds are negligible.) The wing and engine were sized by an initial cruise altitude for maximum range and cruise-power ceiling altitude (Figure 3-4). The maximum takeoff gross weight is 397,000 pounds, with a takeoff field length of approximately 7,000 feet and landing approach speed of 130 knots.

Mach 3.2. Two configurations were developed for Mach 3.2. The D3.2-3A configuration was optimized for supersonic flight with minor compromises for low-speed flight (takeoff and landing). The D3.2-4B configuration was compromised for subsonic flight over land. The wing design differences are typified by the increase in aspect ratio from 1.55 to 2.21.

The P&W duct burning turbofan used on the Mach 3.2 concept features several power settings including Power Code (PC) 50, the maximum dry thrust, and PC 100, the maximum augmented thrust. As jet velocities and corresponding noise increase with PC, it is advantageous from a community noise standpoint to use the lowest power code during takeoff. The influence of takeoff power codes on gross weight versus range are shown in Figure 3-5. A heavy weight or range penalty results from decreasing power codes. The selected Mach 3.2 (D3.2-3A) sizing point is PC 100, which results in a maximum takeoff gross weight of 769,000 pounds for the 6,500-nautical-mile range.

The New York-Tokyo market is second in terms of international revenue passenger miles (rpm) and thus presents an aircraft sizing focal point. This route has an overall distance of 6,236 nautical miles with a 2,518-nautical-mile subsonic flight segment (40 percent) if diverted from the great-circle route to allow minimum flight over land (Figure 3-6).

To study the effect of subsonic flight segments, the -3A and the -4B concepts were sized to 6,500-nautical-mile range with up to 40-percent subsonic legs. Figure 3-7 shows the increased maximum takeoff gross weight for the -4B concept for the all-supersonic design mission. This is a result of greater structural weight due to the larger aspect ratio and the lower aerodynamic efficiency at supersonic cruise. However, with increasing subsonic flight distances, the supersonic design is penalized with increased max-

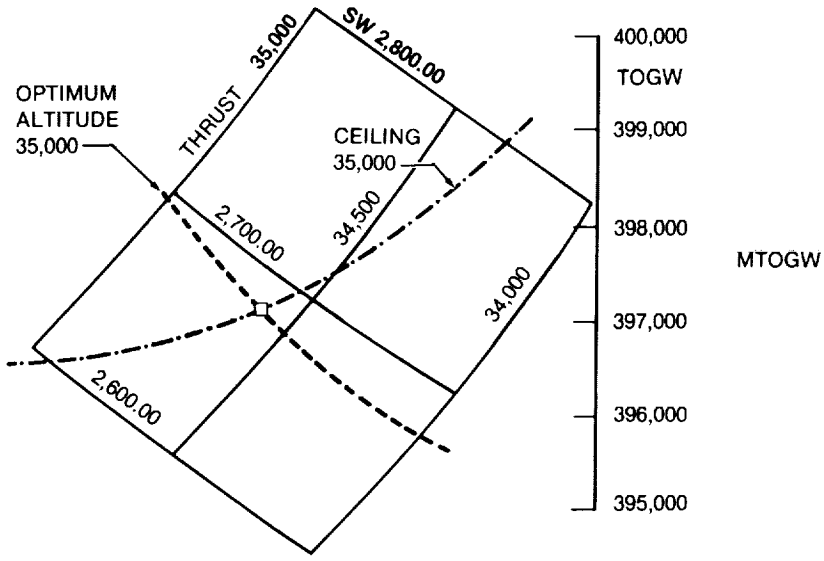

FIGURE 3-4. SIZING FOR SUBSONIC AIRPLANE

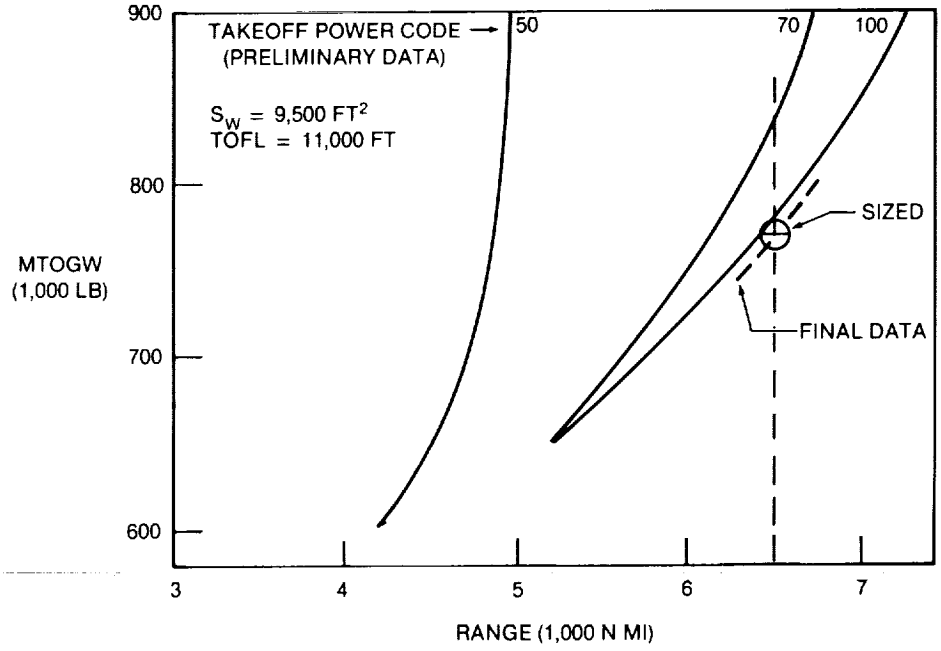

FIGURE 3-5. D3.2-3A PHASE III CONCEPT DESIGN RANGE VERSUS POWER CODE

imum takeoff gross weight as opposed to the improved subsonic configuration. Consequently, for subsonic legs greater than 27 percent of the total range (approximately 1,750 nautical miles), the -4B concept is lighter than the -3A configuration.

Mach 5.0. The Mach 5.0 concept was developed without laminar flow control. The best range was obtained with the takeoff Power Code 40 of the GE VCHJ engines. The resulting range predicated on the takeoff field length requirement of 11,000 feet is 3,903 nautical miles with a maximum takeoff gross weight of 1,213,000 pounds.

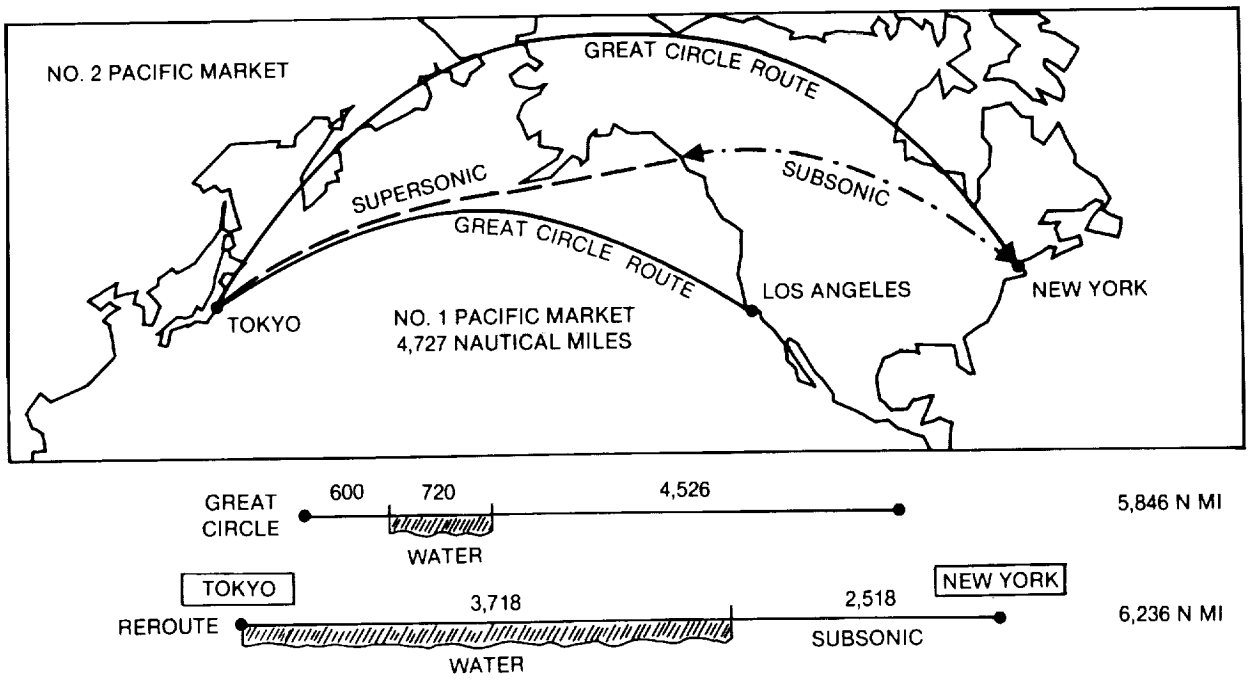

FIGURE 3-6. KEY OVERLAND MARKET: NEW YORK-TOKYO

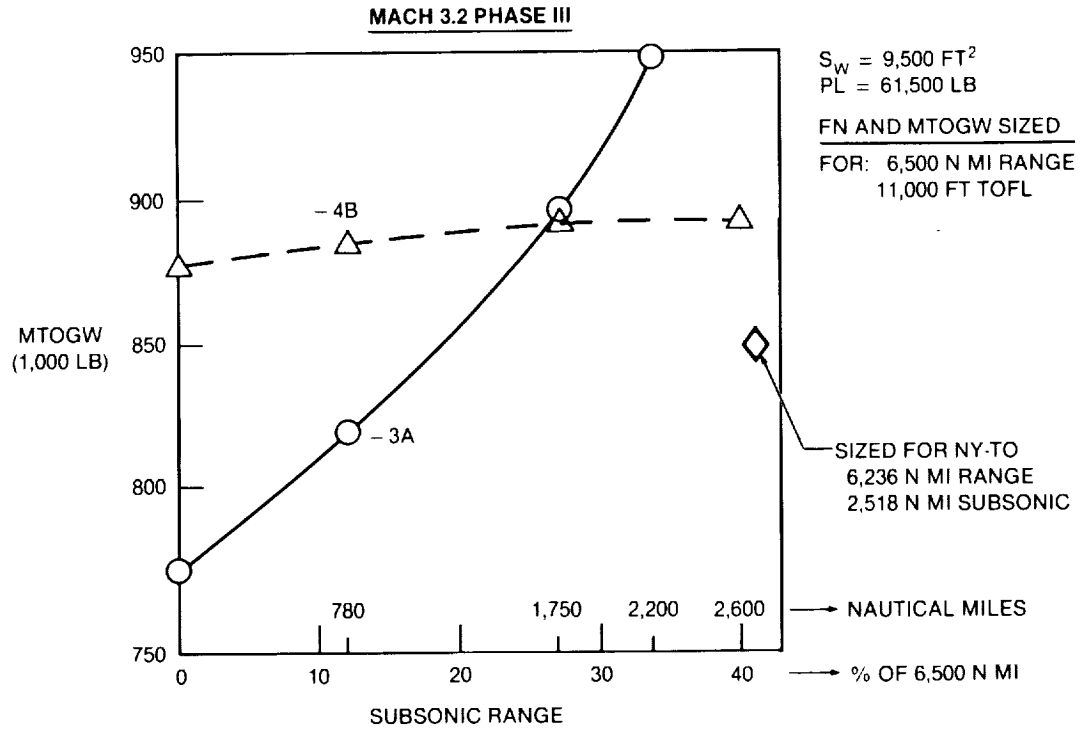

FIGURE 3-7. SIZINGS FOR PARTIALLY SUBSONIC RANGE

With this limited range capability, an economic comparison with other vehicles is not possible; therefore, technology improvements are required to produce a vehicle capable of a 6,500-nautical-mile range. Figure 3-8 compares the lift-to-drag ratio of different Mach 5.0 configurations versus the slenderness coefficient, τ = volume/(wing reference area)$^{3/2}$. The Phase II configuration, D5.0-5A without laminar flow control, shows a promising lift-to-drag ratio of 6.25. A refinement of the Phase III configuration D5.0-15 to D5.0-15A improved the lift-to-drag ratio from 5.1 to 5.4. Further configuration layout development (i.e., increased packing efficiency with improved volume use) and simultaneous computational fluid dynamics development of the external configuration lines to improve lift to drag is expected to lead to lift-to-drag levels of 6.75 as indicated in Figure 3-8. This corresponds to a 20-percent decrease in drag relative to the -15A. Further, considering that the Mach 5.0 engine efficiency is 13 percent below the potential level, a 10-percent decrease in fuel flow was applied (Figure 3-9). These technology advancements would have later technology readiness dates that those for the D5.0-15A. With these improvements in drag and fuel efficiency, the Mach 5.0 concept was sized using PC 50 (full augmentation) to determine minimum design takeoff gross weight for the 6,500-nautical-mile design mission (Figure 3-10). PC 40 required considerably larger engines and thus higher design takeoff gross weight. The PC 50 takeoff power results in a takeoff field length of 8,600 feet, and a maximum takeoff gross weight of 1,213,000 pounds.

Performance Summary. Figure 3-11 shows the maximum takeoff gross weight of the six sized airplanes and their design ranges. This figure shows the change in maximum takeoff gross weight in relation to design range. Table 3-1 shows the main characteristics of these concepts; Table 3-2 shows additional comparative information. Figure 3-12 presents the weights of the airplanes used for economic analyses in graphical form, and Figure 3-13 presents the block times of these airplanes versus range.

Figure 3-14 depicts the overall fuel efficiency of the airplanes in terms of pounds of fuel per available seat per nautical mile to enable comparison with other airplanes, such as the 108-seat, Mach 2.0 Concorde. The values given are for 3,500 nautical miles as a representative system average length of the all-supersonic range and of the split half-subsonic, half-supersonic flight. The Concorde data are for the 3,000-nautical-mile range. Values for the DC-10 (277 seats) and 747 (365 seats) are shown as 1970's subsonic data.

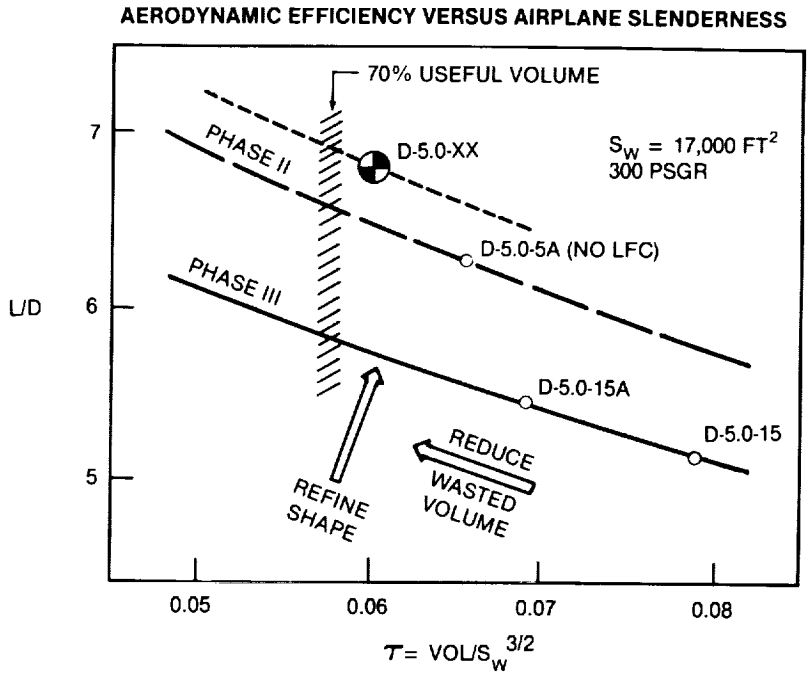

FIGURE 3-8. MACH 5.0 AERODYNAMIC DEVELOPMENT

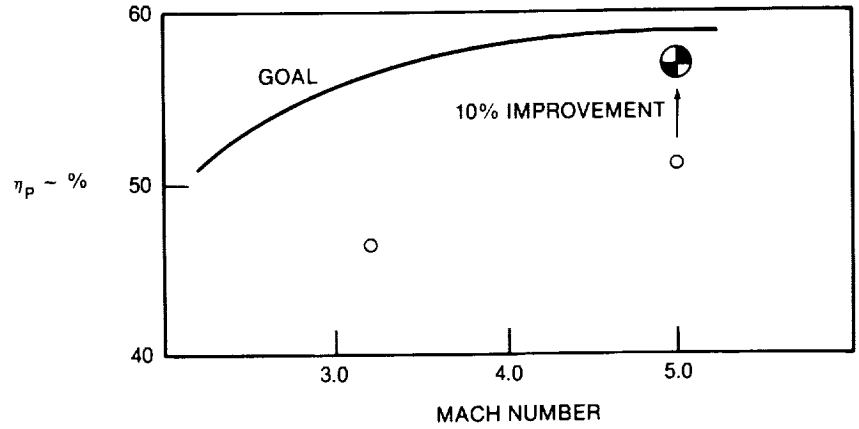

FIGURE 3-9. OVERALL PROPULSIVE EFFICIENCY IN CRUISE

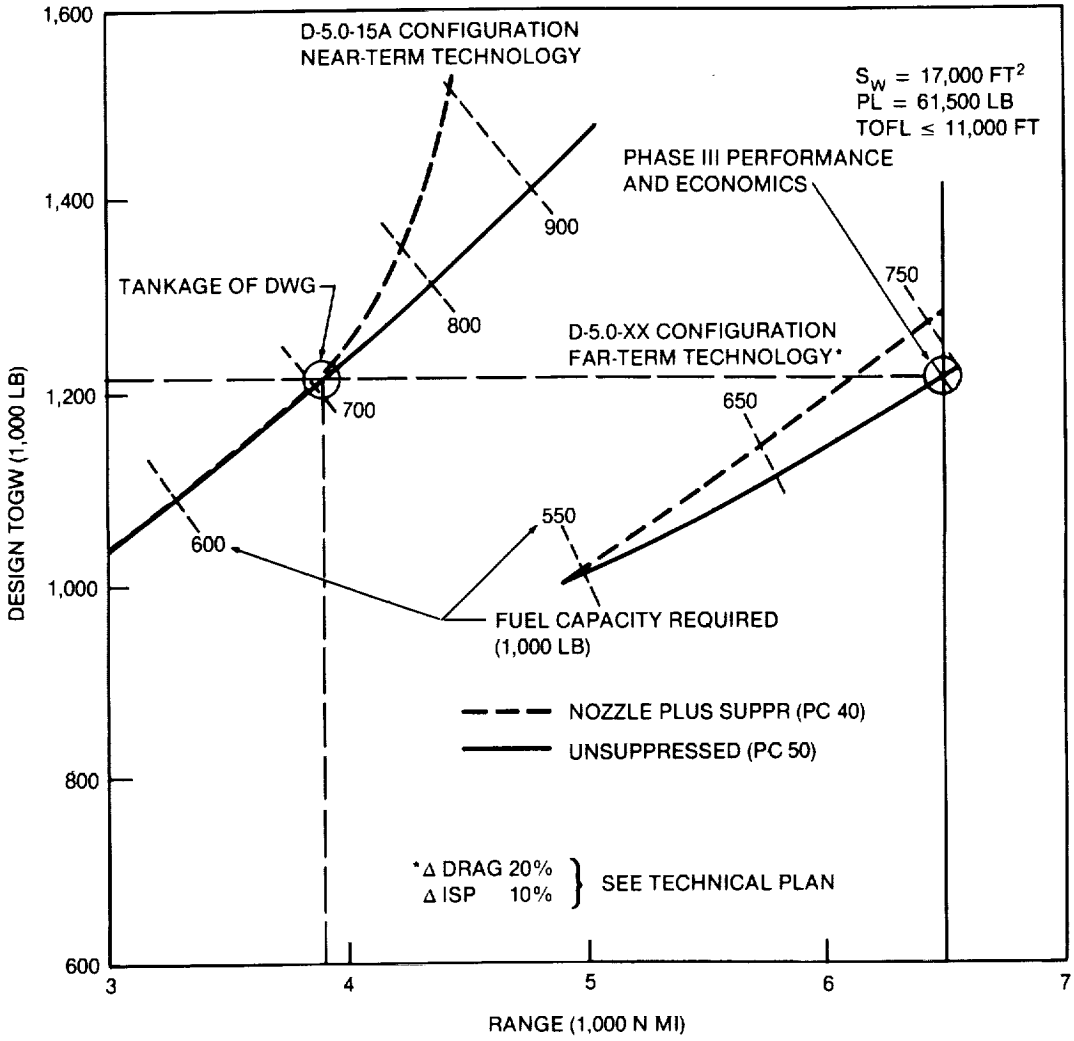

FIGURE 3-10. PHASE III MACH 5.0 SIZINGS VERSUS TECHNOLOGY AND POWER CODE

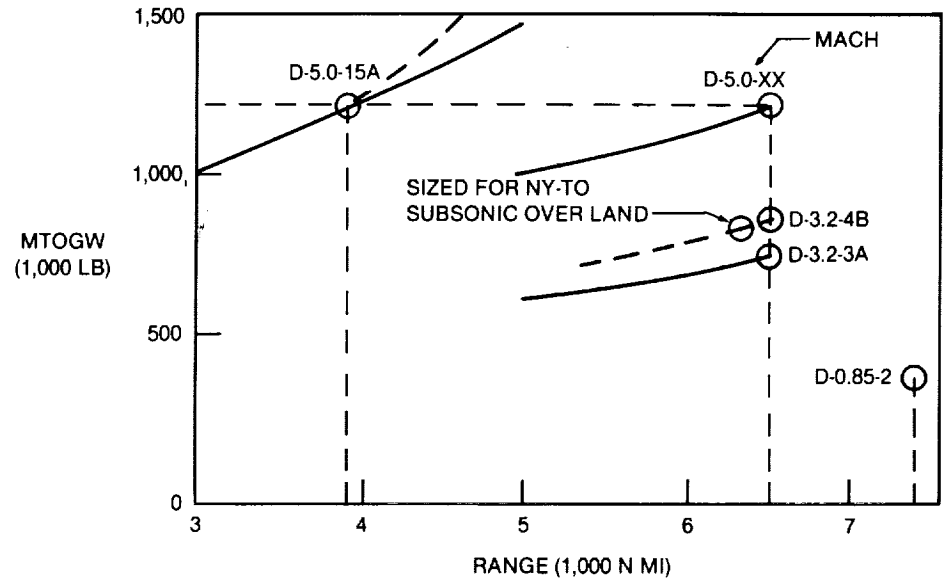

FIGURE 3-11. PHASE III SIZED HSCTs AND REFERENCE TRANSPORT

TABLE 3-1
HSCT SIZING SUMMARY

PAYLOAD = 300 PSGR = 61,500 LB

CONFIGURATION	D-	0.85-2	3.2-3A	3.2-4B		5.0-15A	5.0-XX
CRUISE MACH NO.	—	0.85	3.2	3.2	3.2	5.0	5.0
SUPERSONIC RANGE	N MI	0*	6,500	6,290**	6,500	3,903	6,500
WING REF AREA	FT^2	2,700	9,500	9,500	9,500	17,000	17,000
MTOGW	1,000 LB	397	769	847	880	1,213	1,213
OEW	1,000 LB	189	231	246	250	474	426
BLOCK FUEL	1,000 LB	129	424	486	511	628	678
THRUST/ENGINE	LB SLST	35,000	61,500	60,200	63,900	85,350	101,000
ENGINE/PC	—	DUCTED FAN	PW/DBTF/100	PW/DBTF/100		GE/VCHJ/40	GE/VCHJ/50
SIZED BY	—	CR ALT	TO	TO	TO	TO	MTOGW
TOFL	FT	7,000	11,000	11,000	11,000	11,000	8,600
APPROACH	KN	130	135	127	129	134	127

*EQUIVALENT STILL-AIR RANGE 7,400 N MI
**SIZED FOR NEW YORK-TOKYO, 40 PERCENT OVER LAND

TABLE 3-2
HSCT CHARACTERISTICS VALUES

CONFIGURATION	D-	085-2	3.2-3A	3.2-4B		5.0-15A	5.0-XX
WING LOADING	$MTOGW/S_W = W/S$	148	81	89	93	71	71
THRUST LOADING	$N_E \times F_N/MTOGW = T/W$	0.26	0.32	0.28	0.29	0.28	0.33
EMPTY WT RATIO	OEW/MTOGW	0.48	0.30	0.29	0.28	0.39	0.35
LIFT/DRAG	(L/D) CRUISE	21.6	8.8	14/7.9	8.0	5.7	7.1
SPECIFIC IMPULSE	(F_N/W_F) CRUISE (SECONDS)	6,830	2,120	3,740/2,080	2,110	1,680	1,850
CRUISE ALTITUDE	(1,000 FT)	35/39	66-76	30/69-75	62-75	83-94	84-92

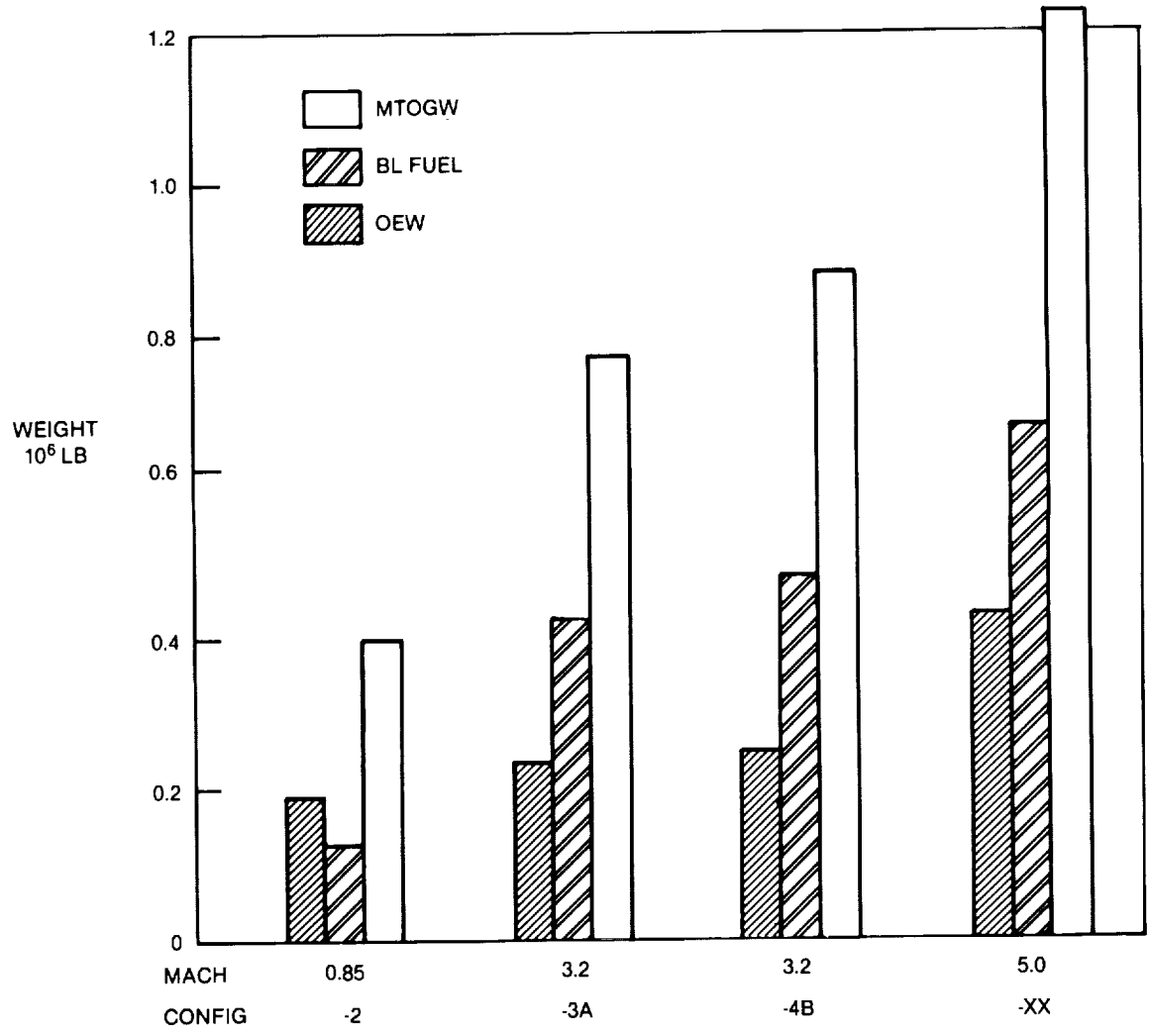

FIGURE 3-12. WEIGHT COMPARISON

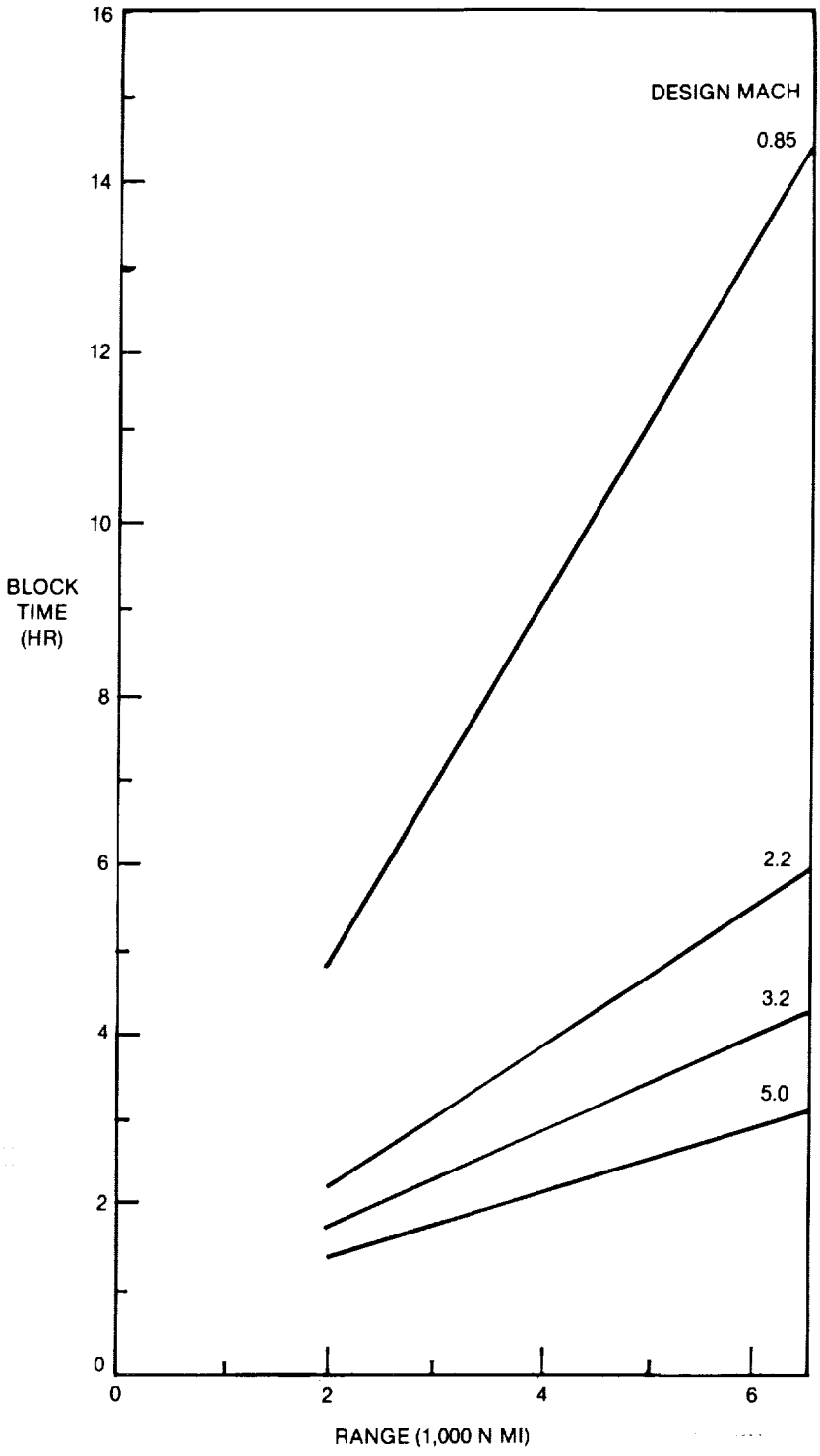

FIGURE 3-13. BLOCK TIME

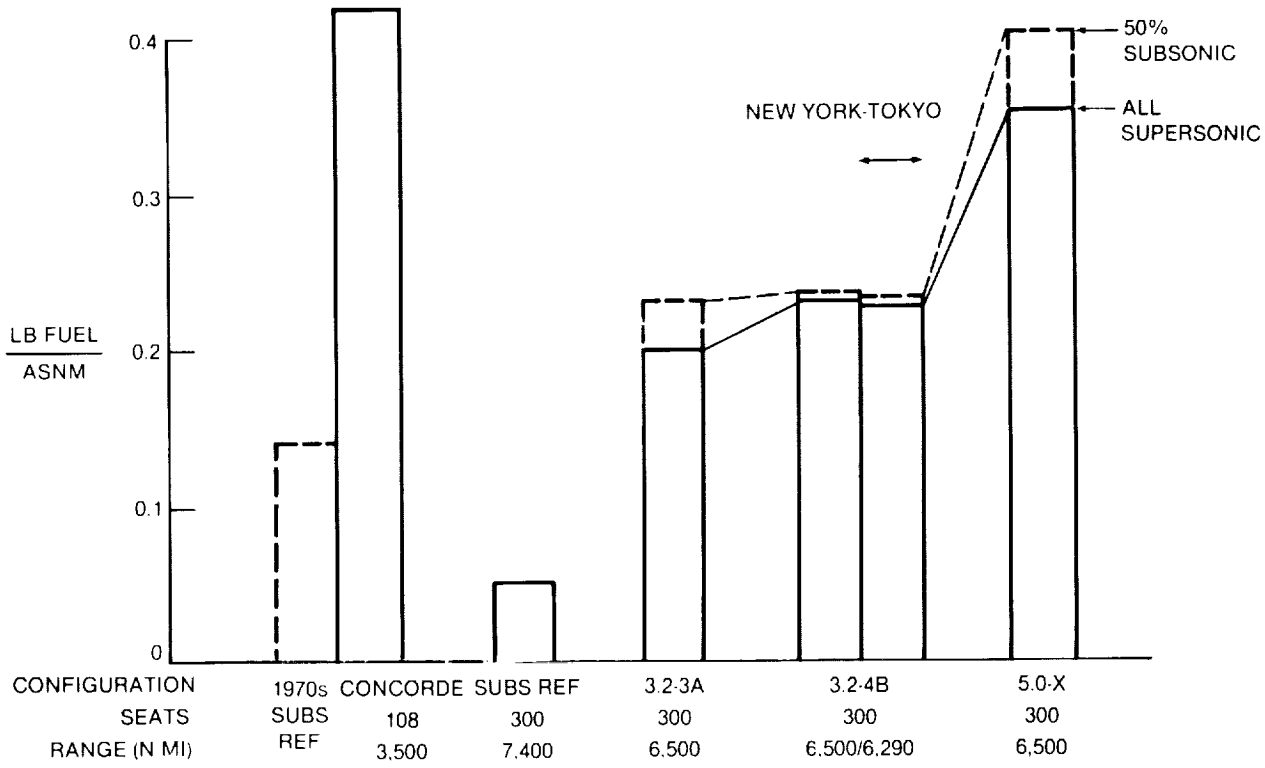

FIGURE 3-14. FUEL EFFICIENCY

Trade-Offs and Sensitivities. Table 3-3 shows the sensitivities of wing area, engine thrust, maximum takeoff gross weight, operating empty weight, and block fuel to changes in drag, fuel flow, or empty weight for the Mach 3.2 and 5.0 concepts. Maximum takeoff gross weight change due to either drag, fuel, or empty-weight is almost one-to-one for either concept. The sensitivity of block fuel is greater (1.35 to 1) to drag and fuel efficiency, but smaller (0.77 to 1) to weight. Changes in weight effect wing and engine size as well as block fuel, but have the greatest effect (1.6 to 1) on operating empty weight.

Figure 3-15 presents these sensitivities in graphical form. Maximum takeoff gross weight versus lift-to-drag ratio, specific impulse (I_{SP} = 3600/SFC) and operating empty weight, are nearly linear relationships, within ±10-percent excursions.

TABLE 3-3
SENSITIVITIES

DUE TO 1% CHANGE OF ↓		PERCENT CHANGE IN: S_W	F_N	MTOGW	OEW	BL FUEL
DRAG	M = 3.2	0.65	1.04	0.92	0.57	1.35
	M = 5.0	0.29	1.31	0.91	0.53	1.33
FUEL	M = 3.2	0.95	0.93	0.97	0.65	1.40
	M = 5.0	0.31	1.31	0.92	0.54	1.34
WEIGHT	M = 3.2	0.70	1.20	1.04	1.60	0.76
	M = 5.0	0.20	1.66	1.04	1.56	0.78

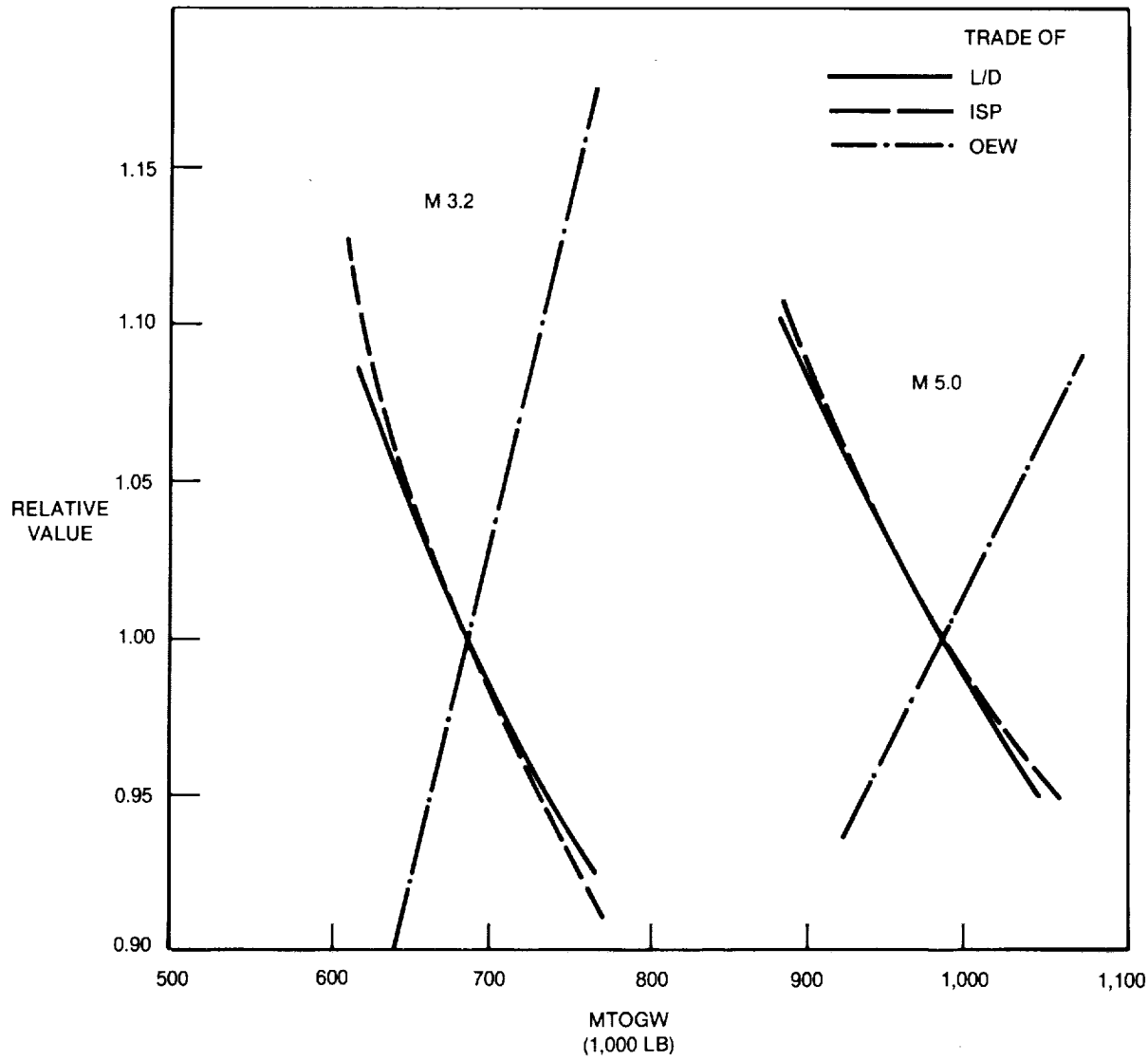

FIGURE 3-15. SENSITIVITY OF MAXIMUM TAKEOFF GROSS WEIGHT

Trade studies are made for:

- 250 passengers versus 300 passengers
- 5,500 nautical miles maximum range versus 6,500 nautical miles maximum range
- Reduced fuel reserves – elimination of descent and climb-to-cruise altitude to fly to alternate destinations without the additional half-hour hold
- Supersonic cruise at the cruise ceiling rather than at the altitude for maximum range
- Takeoff field length of 12,000 feet rather than 11,000 feet

The results are presented in Table 3-4 and show that a 15-percent decrease in range is much more effective in reducing weight parameter levels than a 50-passenger (17-percent) decrease in payload.

The fuel reserves are significantly reduced by assuming that the alternate airport destination is determined before descending through 30,000 feet and diverting directly to that point and by eliminating the half-hour hold. This results in reserves that are approximately half the total fuel required under the base case assumption (i.e., 6.9 percent instead of 13.7 percent for the Mach 3.2 concept, and 6.9 percent instead of 12.3 percent for the Mach 5.0 concept). This results in considerable savings in block fuel and weight.

TABLE 3-4
TRADE STUDIES

SUBJECT	BASELINE VALUE	TRADE VALUE	PERCENT CHANGE IN:				
			S_W	F_N	MTOGW	OEW	BL FUEL
PAYLOAD	300 PSGR	250 PSGR	M = 3.2 −4.0 M = 5.0 −0.7	M = 3.2 −4.0 M = 5.0 −4.2	M = 3.2 −4.1 M = 5.0 −2.8	M = 3.2 −3.8 M = 5.0 −1.6	M = 3.2 −3.2 M = 5.0 −2.1
RANGE	6,500 N MI	5,500 N MI	M = 3.2 −10.0 M = 5.0 −4.5	M = 3.2 −12.1 M = 5.0 −14.2	M = 3.2 −11.7 M = 5.0 −10.3	M = 3.2 −7.6 M = 5.0 −6.4	M = 3.2 −2.5 M = 5.0 −0.5
RESERVES	5% + 200 N MI 0.5 HR HOLD	5% + 200 N MI W/O CLIMB	M = 3.2 −10.9 M = 5.0 −1.5	M = 3.2 −8.3 M = 5.0 −12.1	M = 3.2 −9.7 M = 5.0 −8.0	M = 3.2 −6.8 M = 5.0 −4.3	M = 3.2 −10.8 M = 5.0 −8.9
CRUISE ALTITUDE	OPTIMUM	CEILING	M = 3.2 29.1 M = 5.0 2.5	M = 3.2 4.5 M = 5.0 2.1	M = 3.2 14.2 M = 5.0 2.1	M = 3.2 12.9 M = 5.0 1.8	M = 3.2 14.4 M = 5.0 2.3
TOFL	11,000 FT	12,000 FT	M = 3.2 −2.9 M = 5.0 −0.9	M = 3.2 −4.3 M = 5.0 −5.2	M = 3.2 −0.7 M = 5.0 −0.4	M = 3.2 −1.9 M = 5.0 −1.5	M = 3.2 −0.7 M = 5.0 ≈ 0

For vehicles sized by the takeoff field length, the operational ceiling altitude is higher than the altitude for best range. For the Mach 3.2 concept, the difference between these altitudes is more than 12,000 feet, compared to 3,500 feet for the Mach 5.0 concept. Resizing to cruise at the ceiling would be considerably more penalizing at Mach 3.2 than at Mach 5.0. In general, forcing cruise altitudes away from the optimum altitude bring considerable penalties in fuel and weights. For aircraft sized by the 11,000 feet takeoff field length, relaxing this requirement to 12,000 feet brings only slight improvement in weight and size.

3.2 Airframe and Engine Maintenance

Maintenance costs per flight-hour play a significant role in determining the life cycle cost to operate and maintain an aircraft and are an integral part of the overall economics analysis of the high-speed civil transport. Total labor-hour and material costs per flight-hour for both airframe and engine are expressed as:

Total Labor-hours per Flight-hour =
Labor-hours per Flight-hour + (Labor-hours per Flight/Flight-cycle Time)

Total Material Costs per Flight-hour =
Material Costs per Flight-hour + (Material Costs per Flight/Flight-cycle Time)

A breakdown of the total airframe labor-hour costs per flight-hour for eight large (A300B4-600, A310-300, DC-10-40, DC-8-73, L1011-500, 747-300, 757-200, and 767-200ER) operating transport aircraft indicates that 57 percent of the total is flight-hour related, and 43 percent is flight-cycle related. For total airframe material costs per flight-hour, 47 percent of the total is flight-hour related and 53 percent is flight-cycle related. Engine labor-hour and material costs per flight-hour are 85 percent flight-hour related and 15-percent flight-cycle related. Commercial and military aircraft have grossly different operating systems, sizes, characteristics, and roles. HSCT aircraft will have similar operating systems, sizes, characteristics, and to some extent roles of large commercial aircraft. Therefore, quantitative information used to forecast baseline maintenance costs for HSCT aircraft was based on commercial aircraft system maintenance costs only. Effects of supersonic flight on specific SR-71 and Concorde aircraft system maintenance requirements were used subjectively within the forecasting model.

Airframe Maintenance Cost. Airframe maintenance cost predictions utilized baseline airframe labor-hour and material cost data for eight large, commercial transport aircraft and the estimated effect of future high-speed civil transport technologies factored into the airframe maintenance labor-hour and material predictions. The main statistical techniques used were correlation analysis and nonlinear regression. The

correlation analysis compared baseline dependent variables (airframe labor-hours and material costs per flight-hour and per flight-cycle) derived from independent variable data (e.g., takeoff gross weight, operational empty weight, fuel capacity). The analysis indicated that takeoff gross weight (TOGW) is the independent variable that correlates best with airframe labor-hours and material cost baseline values. TOGW was the only variable used in the nonlinear regression predictions. The predictions are midpoint values within a 95-percent confidence interval range.

Baseline airframe maintenance labor-hour and material cost data were analyzed to determine the most maintenance intensive operating systems by ATA chapters. The percentage of total labor-hours and material costs for each aircraft's ATA chapters clearly indicates a high percentage of aircraft maintenance is attributed mainly to a few ATA chapters. Predicted airframe maintenance values were factored accordingly.

The following revised predicted airframe maintenance costs were used in the economic analysis:

D3.2-3A

- Labor-hour per Flight-hour = 5.1
- Material Costs per Flight-hour = $100
- Labor-hour per Flight-cycle = 13.2
- Material Costs per Flight-cycle = $257

D3.2-4B

- Labor-hour per Flight-hour = 6.4
- Material Costs per Flight-hour = $141
- Labor-hour per Flight-cycle = 21
- Material Costs per Flight-cycle = $400

D5.0-15A

- Labor-hour per Flight-hour = 9.8
- Material Costs per Flight-hour = $254
- Labor-hour per Flight-cycle = 46.2
- Material Costs per Flight-cycle = $826

Figures 3-16 and 3-17 compare airframe maintenance cost predictions to various large commercial transport aircraft as identified above.

A data set derived from Concorde maintenance information was considered in the correlation analysis, but because of its unique operating environment, the data were judged to be nonrepresentative and was excluded from the nonlinear regression prediction process. Concorde requires a total of 65 labor-hours per flight-hour including both airframe and engine. This value is considered abnormally high and is attributable to the operating conditions of the Concorde: small fleet size, early technology, limited support away from its home basing, high occurrence of unique operations (charters), limited number of spare parts available leading to cannibalization, and limited number of technical support personnel with necessary expertise.

Operating and configuration data from the X-15 and SR-71 were analyzed to determine peculiar support requirements of those aircraft operating systems.

Engine Maintenance Cost. Predicted engine maintenance costs were derived from data provided by P&W and GE. Total labor-hour and material costs per flight-hour were broken down through labor-hour, material costs, and flight-hour times provided by the manufacturers. Following review of engine manufacturers' estimated maintenance costs, a Douglas-derived estimate was developed for the high-speed civil transport economic analysis. The following predicted engine maintenance costs were used in the economics analysis:

D3.2-3A & -4B

- Labor-hour per Flight-hour = 0.95
- Material Costs per Flight-hour = $694
- Labor-hour per Flight-cycle = 0.61
- Material Costs per Flight-cycle = $453

D5.0-15A

- Labor-hour per Flight-hour = 1.43
- Material Costs per Flight-hour = $940
- Labor-hour per Flight-cycle = 0.75
- Material Costs per Flight-cycle = $486

Figures 3-18 and 3-19 compare engine maintenance cost predictions to engines operated on various large commercial transport aircraft.

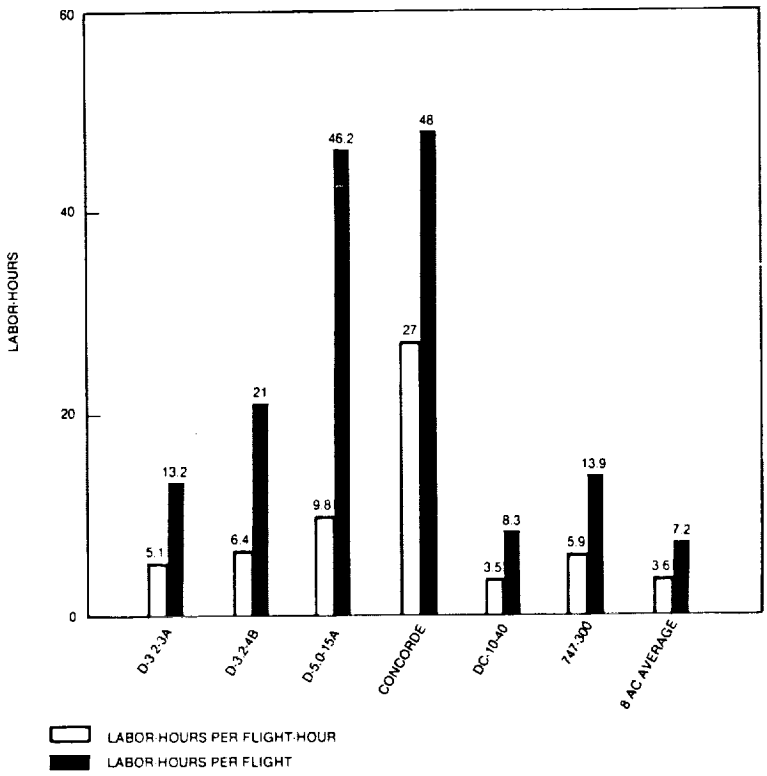

FIGURE 3-16. AIRFRAME MAINTENANCE LABOR-HOURS BASELINE VALUES

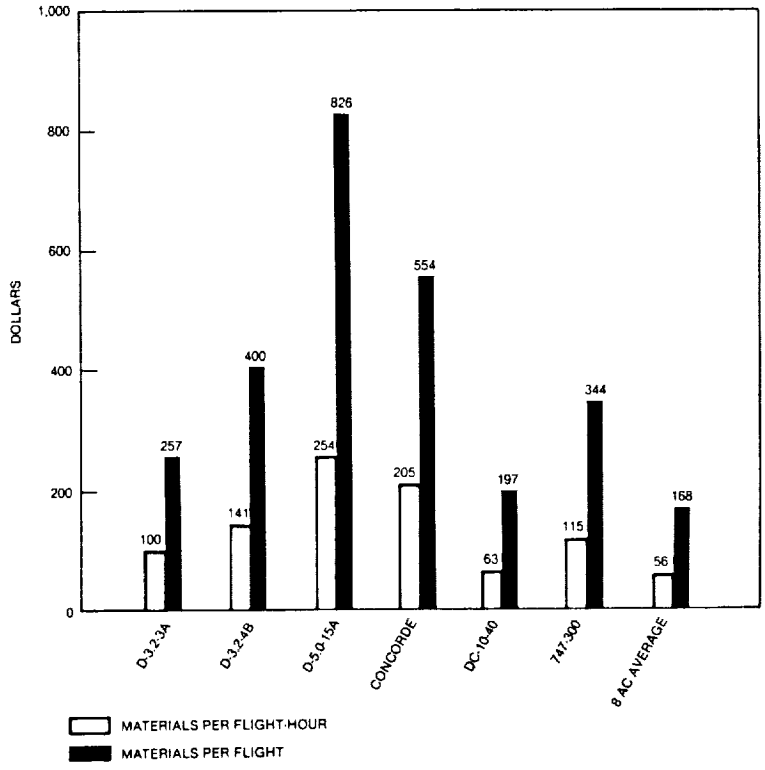

FIGURE 3-17. AIRFRAME MAINTENANCE MATERIAL COSTS BASELINE VALUES

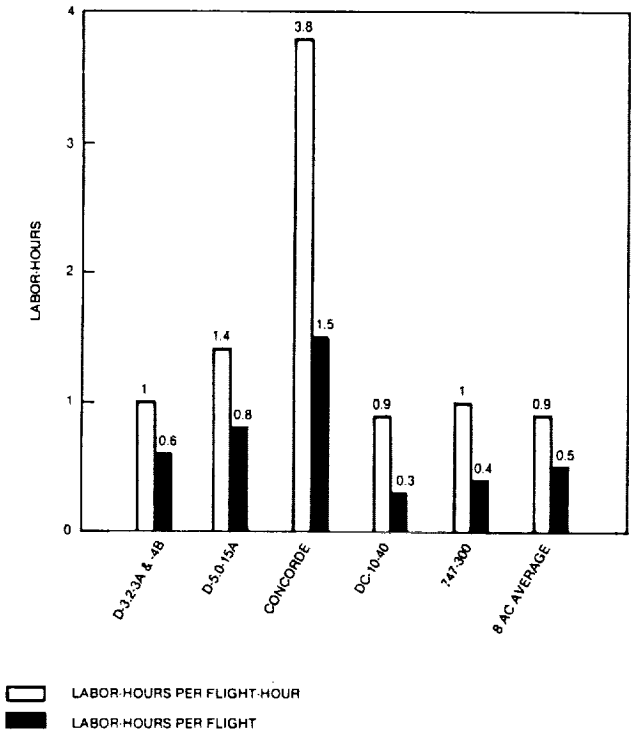

FIGURE 3-18. ENGINE MAINTENANCE LABOR-HOURS BASELINE VALUES

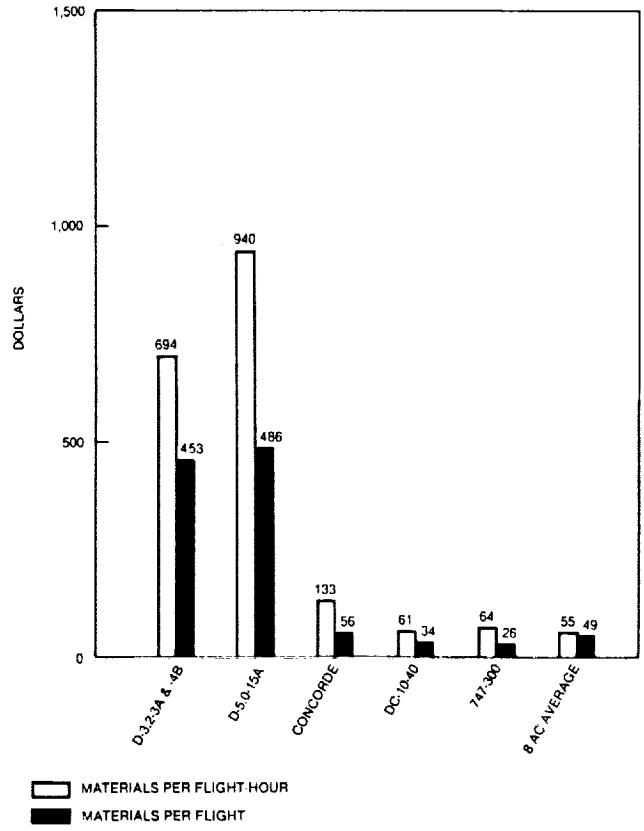

FIGURE 3-19. ENGINE MAINTENANCE MATERIAL COSTS BASELINE VALUES

3.3 Airport Infrastructure

The portions of the airport infrastructure that must accommodate the high-speed commercial transport consist of the airfield, terminal area, and fueling facilities. Most, if not all of the world's international airports that are likely candidates for future HSCT service already experience DC-10 and 747 aircraft. McDonnell Douglas and Boeing are working on larger versions of these high capacity aircraft.

Airports. Table 3-5 illustrates a comparison of the physical characteristics of wide-body jets and the Mach 0.85, Mach 3.2, and Mach 5.0 baseline concepts.

Douglas has established the objective that the HSCT must be able to operate from existing airports necessitating compatible approach speeds, touch down speeds, takeoff field lengths, and noise limitations. The overall length of both the Mach 3.2 and Mach 5.0 concepts will present problems with airfield maneuvering and operations and also in the terminal area. Both aircraft present servicing difficulties due to the wing shape. In addition, the Mach 3.2 concept presents a servicing challenge due to door sill heights of 25 feet to 27 feet, which are significantly greater than commercial transport aircraft. Both the Mach 3.2 and Mach 5.0 concepts will require new fuel facilities, although LNG facilities are more complex and site demanding.

Few new airports are expected to be developed in the future for three reasons. First, the very high cost associated with new facilities that must satisfy all concerns. For example, the new Osaka Airport is reported to cost in excess of $5 billion. The new Denver Airport, the only new major airport in the U.S. in the last 15 years, is estimated to cost more than $2.8 billion. Second, the lack of public acceptance of new airport proposals causes planned projects to be significantly delayed. During the long delays, construction costs rise

TABLE 3-5
AIRCRAFT CHARACTERISTICS COMPARISON BASELINE STUDY CONCEPTS

MODEL	MD-11	747-400	MACH 0.85	MACH 3.2-3A	MACH 5.0-15A
FUEL	JP	JP	JP	TSJF	METHANE
SPAN (FT)	169.5	211.0	195.0	121.2	136.7
LENGTH (FT)	200.9	231.8	189.6	315.0	297.7
HEIGHT (FT)	57.8	60.2	62.5	60.5	49.0
WHEELBASE (FT)	80.7	84.0	76.7	104.0	96.3
WHEEL TREAD (FT) (STRUT - CENTER TO CENTER)	35.0	36.1	39.8	38.7	42.5
CABIN DOORS SILL HEIGHT (FT)					
FWD	15.8	15.5 (24.8)*	16.0	22.5	12.2
AFT	15.2	15.0	18.0	25.3	12.7
CARGO DOOR SILL HEIGHT (FT)	9.2	8.8	9.5	17.0	11.7
TOGW (1,000 LB)	602.5	850.0	397.0	769.0	1,213.0

* UPPER DECK

with inflation resulting in even greater expense. The resistance to new airports has forced development in more remote locations that are, in general, less convenient for the traveler. Third, most cities have consumed the flatter terrain for development. If there are nearby undeveloped land areas, topographic problems inappropriate for airport development generally exist. For the above reasons, new airports are not good solutions for HSCT operations.

The best location for an HSCT to operate is an existing airport facility, located as close as possible to the centroid of demand. This way, the traveler will be facilitated by fast transportation from portal to portal rather than compromise for time spent traveling to distant airports. Therefore, it is assumed that HSCT aircraft must be designed to be compatible with existing airports.

Airfield. The HSCT will affect three airfield characteristics: ground maneuvering space, clearance areas, and pavement strength. The overall length will present difficulties in maneuvering on existing taxiway-to-taxiway and runway-to-taxiway intersections. Current large-capacity aircraft have caused airports to increase their pavement fillet sizing as the main gear track is large. Figure 3-20 illustrates a typical intersection fillet design.

Pilots maneuver their aircraft by maintaining the cockpit over the centerline at most International Civil Aviation Organization (ICAO) airports. In the U.S. this technique is rarely used, as pilots maneuver by judgmentally positioning the cockpit beyond the centerline, attempting to maintain the main gear track as small as possible to avoid running off the pavement. This technique requires less fillet pavement. However, if the nose gear is located significantly aft of the cockpit, pilots may prefer to use the cockpit-over-the-centerline technique. This is because the pilot's visual ques – the pavement that he wants to turn onto – is no longer in view because the cockpit is well forward of the nose gear.

Since the cockpit-to-the-main gear distance is significantly greater for the Mach 3.2 concept versus current airplanes, the main gear requires greater fillet pavement area than that available at airfields. Use of an on-board closed circuit television (CCTV) system to provide a view of the nosegear tracking may solve the guidance visibility problems. By maneuvering the Mach 3.2 concept with the nose gear over the centerline, the fillet requirements may be no more extensive than is required for stretched versions of the MD-11 trijet.

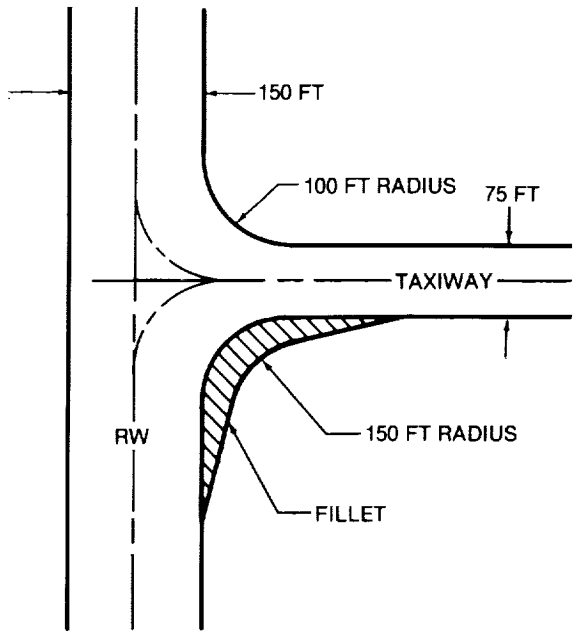

FIGURE 3-20. FILLET REQUIREMENTS

Worldwide category IIIC airport capability, together with guidance to gates through a nonvisual form of centerline identification, could result in nose gear-over-the-centerline maneuvering during zero-zero visibility conditions.

The only clearance problem that may exist on the airfield will occur under current operating procedures on an airport, such as Los Angeles, with close parallel runways (700 feet center-to-center). In this case a 315-foot-long Mach 3.2 aircraft will not be able to hold on a connecting perpendicular taxiway between the two runways without restricting operations on one of the runways, Figure 3-21. Under ICAO rules, the taxi holding line for large airports with large aircraft is 274.3 feet from the runway centerline. The consequence is operational delay on the runway.

The previously stated objective that HSCT pavement loads will not exceed those of current aircraft results in specification of the number of tires and their spacing. Further, the Mach 5.0 airplane will be restricted from operating on current bridges and overhangs that have not been designed for aircraft weighing more than one million pounds.

Fuel Facilities. Thermally stable jet fuel (TSJF) used to fuel the Mach 3.2 aircraft is assumed to involve special handling to control contamination based on engineering specifications regarding JP-7 fuel facilities. Therefore, new storage, distribution, and dispensing facilities will be required for the exclusive use of TSJF. Routine aircraft fueling and emergency activities to take care of spills and leaks is similar to handling JP fuels such as Jet A fuel. LNG, which will be used in the Mach 5.0 aircraft, will also require new storage, distribution, and dispensing facilities.

In an effort to determine the cost impact of LNG as an aircraft fuel, a study was conducted to identify the airport facility requirements associated with an LNG system. Both capital and operating costs of the system were developed. Since fixed costs are affected by demand volumes, three levels were studied representing high, medium and low volume systems. The high volume system is one capable of supplying fuel to a 19-gate system with 70 daily flights. The medium system is one with four gates supplying fuel for 22 daily flights, and the low volume system has one gate supplying LNG to five daily flights. Fluor Engineers and Air Products performed this study comparing the costs of LNG with costs associated with TSJF, as both systems will require new facilities. A summary of the capital and operating costs for the three volume levels for each fuel type is illustrated in Table 3-6.

The use of LNG fuel includes a provision for an on-airport liquefaction facility that has two requirements. First, the plant will require a dedicated ground area. A facility sized to the fueling demands of an airport such as San Francisco, considered a medium-sized airport in terms of HSCT fuel requirements, will require 43 acres.

The second requirement is the size of some of the plant equipment. The referenced Flour Daniels study depicts a preliminary liquefaction facility concept with a heat exchange tower height of 250 feet. Concept sizing is based on preliminary considerations including production volume. This height exceeds

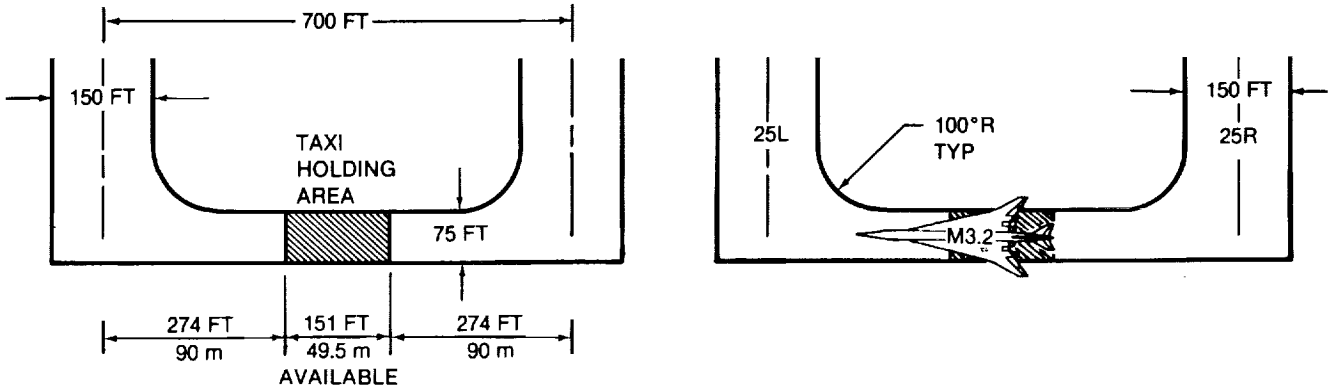

FIGURE 3-21. AIRFIELD CONSTRAINTS

TABLE 3-6
SUMMARY OF COSTS AND SCHEDULE
($ MILLIONS)

	FUEL					
	LIQUID METHANE FUEL			TSJF FUEL		
FUEL VOLUME	LOW	MEDIUM	HIGH	LOW	MEDIUM	HIGH
FACILITY ENGINEERING, MATERIALS AND CONSTRUCTION COSTS	254.5	435.5	652.4	26.2	38.4	71.5
INTEREST DURING CONSTRUCTION	61.0	105.0	158.0	4.5	6.5	12.0
START-UP COST	10.0	25.0	38.0	0.6	0.8	1.4
WORKING CAPITAL	4.1	13.3	22.7	2.3	11.0	35.0
TOTAL CAPITAL REQUIREMENT	329.6	578.8	871.1	33.6	56.7	119.9
CENTS/LB FUEL/ 20 YR LIFE	3.2	1.1	0.9	0.4	0.2	0.1
SCHEDULE, ENGINEERING AND CONSTRUCTION (IN MONTHS)	57	57	57	39	39	39
ANNUAL OPERATING COSTS	25	61	99	2.2	3.0	5.7
CENTS/LB FUEL	4.8	2.2	2.0	0.5	0.2	0.1
RECOMMENDED FACILITY OPERATING LIFE (IN YEARS)	20	20	20	20	20	20

current airport limits of 150 feet. Consideration would be given to reduced height, or, alternatively, the tower would be treated as an obstacle. Also, the plant could not be located below the approach/departure surfaces of the runways. In each airport case, facility design trade offs between tower height and ground area requirements would be made to minimize the facility impacts.

Routine LNG fueling will be similar to current procedures with only the addition of a boil-off return line connected to the aircraft. Grounding of the aircraft prior to fueling to prevent spark generation will be similar to subsonic aircraft. From a fueling operation standpoint, the Mach 3.2 aircraft will not differ from present aircraft types.

Ground crew who fuel the Mach 5.0 aircraft with LNG will be required to use gloves for protection against cold fuel equipment temperatures (LNG at −259°F). Special training with the use of new equipment and methods will be required to handle LNG leaks or spills. Likewise special training associated with TSJF is expected to be required for any deoxygenation or inerting process.

Terminals. Terminal gate facilities will undergo changes to accommodate the HSCT due to fuselage length and height. Most major terminal gate parking areas were developed to handle aircraft that are no longer than 231 feet in length with door sill heights up to 17.6 feet.

Consequently, the HSCT will have to be angle parked, as illustrated in Figure 3-22, at existing gate areas if the gates have been modified to allow for the very high door sill heights. Alternatively, or new gate areas will have to be developed in other available locations to accommodate a 315-foot fuselage length with a door sill height of 26.1 feet. As is shown in Figure 3-22, angle-parking does not require additional terminal frontage beyond that required for the 747-400 because the wing span is relatively small. All aircraft servicing

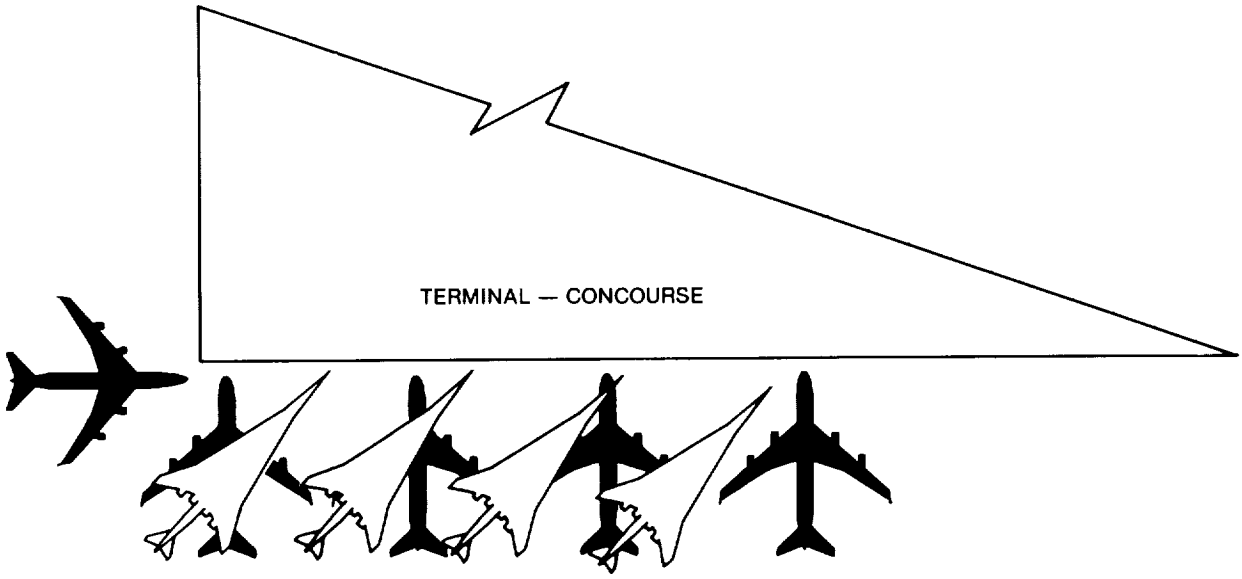

FIGURE 3-22. GATE PARKING

will require special terminal building and service equipment modification due to the high elevation of all doors and access panels. The L1 (left first door aft of the nose) sill height is 22 feet 6 inches for the Mach 3.2 aircraft. This compares to 17.6 feet for the 747-400. Current loading bridges cannot be raised to the door sill heights of the Mach 3.2 aircraft because the bridge ramp would exceed the recommended maximum 8-percent slope. HSCT passenger loading will probably take place from a third level that must be added to the terminal/concourse building.

The delta or arrow wing planform makes it difficult to gain access to mid-fuselage doors and discourages use of mid-fuselage doors for servicing because their use would require long, cantilevered, over-the-wing ramps to be added to the service vehicles. The L1 door will be used for all passenger entry/exit; forward galley servicing will be through the R1 (right first door aft of the nose). The aft right and left doors would be used for aft galley servicing, cabin cleaning, and crew access. A special, very tall galley servicing truck will be required because of (1) close proximity of the engine nozzles to the galley truck maneuvering space and (2) the height of the fuselage. The truck will not be able to approach at right angles to the fuselage as a safety measure to avoid collision with the engine nozzle. Consequently, a special angled platform will be required between the fuselage and the galley truck, allowing the truck to park on an angle to the fuselage.

Aircraft servicing will almost exclusively be turn-around activities as opposed to quicker through-stop activities. Today's international flight turn-around scheduled time for high capacity aircraft is two hours. Economic analysis indicate added benefit of shortened turn around times for the HSCT. A goal of one hour has been established. An analysis of turn-around activities is seen in Figure 3-23 where the total time is projected at 75 minutes. This time analysis takes into account a highly automated systems self-test sequence. Loading of passengers is part of the critical path in Figure 3-23. If the passengers can be onboard during the systems self-testing, then the total turn-around time can be reduced by as much as 10 minutes toward the one hour goal. Although there is no safety problem involved, the passengers may create motion that may disturb the self-testing. Further studies must be undertaken to determine the reasonability of this goal. Discussions, with the airlines have highlighted the desirability of achieving this goal.

Air Traffic Control. Scheduled NAS Plan increases in automation of ATC navigation and communication equipment and procedures should provide efficient safe routing of all commercial aircraft including the HSCT. It is assumed that the HSCT will not have any special approach or departure priorities and as such will experience ground and approach delays equally with all other subsonic aircraft.

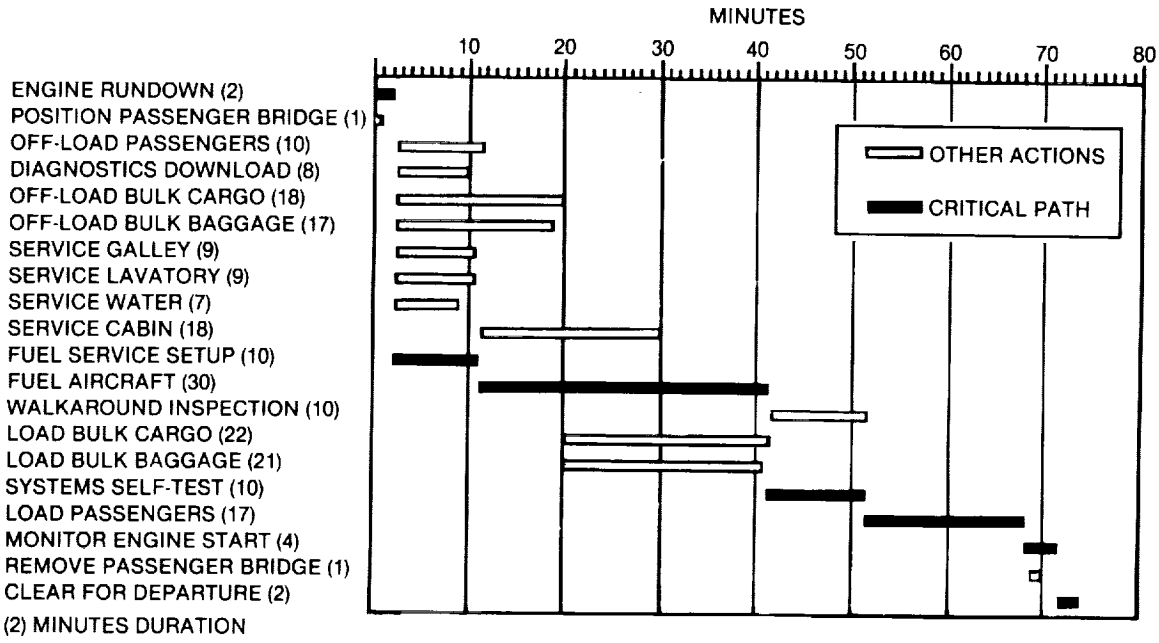

FIGURE 3-23. PROJECTED HSCT TURNAROUND TIME LINE

The following supplemental systems will enhance the ability of the HSCT to integrate with the future ATC environment, as well as reducing flight crew workload and improve economic viability and profitability:

- Automatic separation assurance, threat-alert, and collision-avoidance to the flight crew with conflict alert and resolution advisories without controller intervention
- Fuel Advisory Departures (FAD) that consider departure and arrival airport on-ground and airborne holding delays to minimize engine running time, fuel consumption, and destination terminal area airspace congestion
- Integration of en route and terminal area traffic flow metering and spacing that considers wake vortex avoidance, airport traffic capabilities, and aircraft flight management capabilities to minimize airborne holding delays and flight times. Because of the reduced wing span for similar weight, the HSCT may produce stronger vorticies and possibly require increased separations with trailing aircraft
- Fuel efficient flight trajectories and clearances will be planned and automatically generated through the proposed Automatic En Route ATC (AERA). Datalinks will be used to deliver clearances to the flight crew
- Automated Dependent Surveillance (ADS) to frequently communicate aircraft derived position reports to alleviate the necessity of flight crew reporting

Additionally, the HSCT must achieve international acceptability in all aspects -- operational, regulatory, and political – to be able to operate effectively in the future ATC system. Current navigational aids will not completely satisfy the needs of Mach 3.2 or Mach 5.0 aircraft. The HSCT could use the Global Positioning System (GPS) effectively as an en route navigational service where current navigational aids over water are inadequate. High altitude routing of the HSCT, and use of GPS, must be considered in view of global military operations. It should be noted that high altitude cruise of the HSCT will alleviate the subsonic en route space, although the approach and departure space must accommodate the HSCT with all other aircraft.

International agreements involving global acceptance of an HSCT crossing international borders and flying within international airspace must be obtained. Regulations regarding flights above the current level of positive-controlled airspace (above 60,000 feet) must be developed.

Expanded high altitude global weather information (i.e., winds, temperatures, turbulence, and the like) reporting and trend forecasting will be required to ensure safe and comfortable climb and decent tracks. Since long distance routes will be completed in a fraction of the time that subsonic aircraft use, weather predictions will be more reliable, thus minimizing flight delays and rerouting, and should have a favorable effect on fuel reserve planning.

3.4 Economics and Market Study

This section summarizes the methods and results of the Phase III economic analysis and market research efforts. The overall evaluation process, specially designed economic and operational models, and supporting data were the products of Phases I and II of this study.

Assessment of commercial value of the HSCT requires a comparison between its economic worth and cost-based price. This includes the following:

- Projection of future traffic levels
- Share of the market considering time savings, passenger values of time, and fare premiums
- Generation of realistic productivity estimates from scheduling studies including the effects of curfews and speed restrictions over land
- Calculation of fleet sizes from the market share and airplane productivity estimates
- Determination of annual revenue from various fare levels
- Estimation of the annual cash operating cost using Air Transport Association (ATA) cost relationships and fleet operating statistics
- Calculation of economic worth based on the annual cash flow, target return on investment for the operator, current tax law, and useful life
- Estimation of a cost-based price dependent on the quantity produced, development cost, recurring production cost, and manufacturers' target return on investment
- Projection of the economic benefits to the U.S. economy

Frequent consultation with airlines, including Northwest, Federal Express, American, Delta, United, Pan Am, Japan Air Lines, Alitalia, and British Airways, provided invaluable exchanges regarding traffic projections, schedules, economic parameters, and related matters. Expert consultation on such issues as aircraft scheduling, utilization, and productivity as well as passenger value of time was received from Massachusetts Institute of Technology, Purdue University, and Quinnipiac College.

Figure 3-24 presents a flow chart of the commercial value assessment procedure. The Phase I and II procedures to carry out this work were modified during Phase III in order to account for four additional assumptions: (1) supersonic flight over land is disallowed, (2) passenger market is segmented into four fare classes, (3) interior seating is configured based on the on-board passenger mix, and (4) fuel price is station-specific and function of the annual fuel volume at each station. All costs are expressed in 1987 dollars.

Traffic Demand. Douglas-developed econometric methods were used to forecast traffic through the year 2000. For the period of 2000 through 2025, three economic scenarios provided three traffic projections. Scenario 1 assumes uninhibited growth throughout the period 2000-2025 at the rates applicable in the final years of the 1986-2000 time period. Scenario 2 is considered most likely and results in the preferred traffic figures. It assumes continued rapid growth in the Pacific Rim countries with rates moderating in the latter half of the 25-year period. The trans-Pacific and intra-Asian markets are the fastest growing. Scenario 3 results in much lower traffic. Growth rates in the commercial aviation industry are assumed to decrease to the levels of the projected rates in the general economies of the regions. The best estimate of traffic (provided by the second scenario) is used in the HSCT base case.

The traffic estimates for the 18 international IATA regions were the source for HSCT passenger traffic. Further considerations of range, traffic, and mileage over land reduced the base to 10 regions. These 10 regions were used as the arena of competition between the HSCT and the advanced subsonic reference vehicle. These regions are primarily intercontinental, over water, and long range. Table 3-7 presents poten-

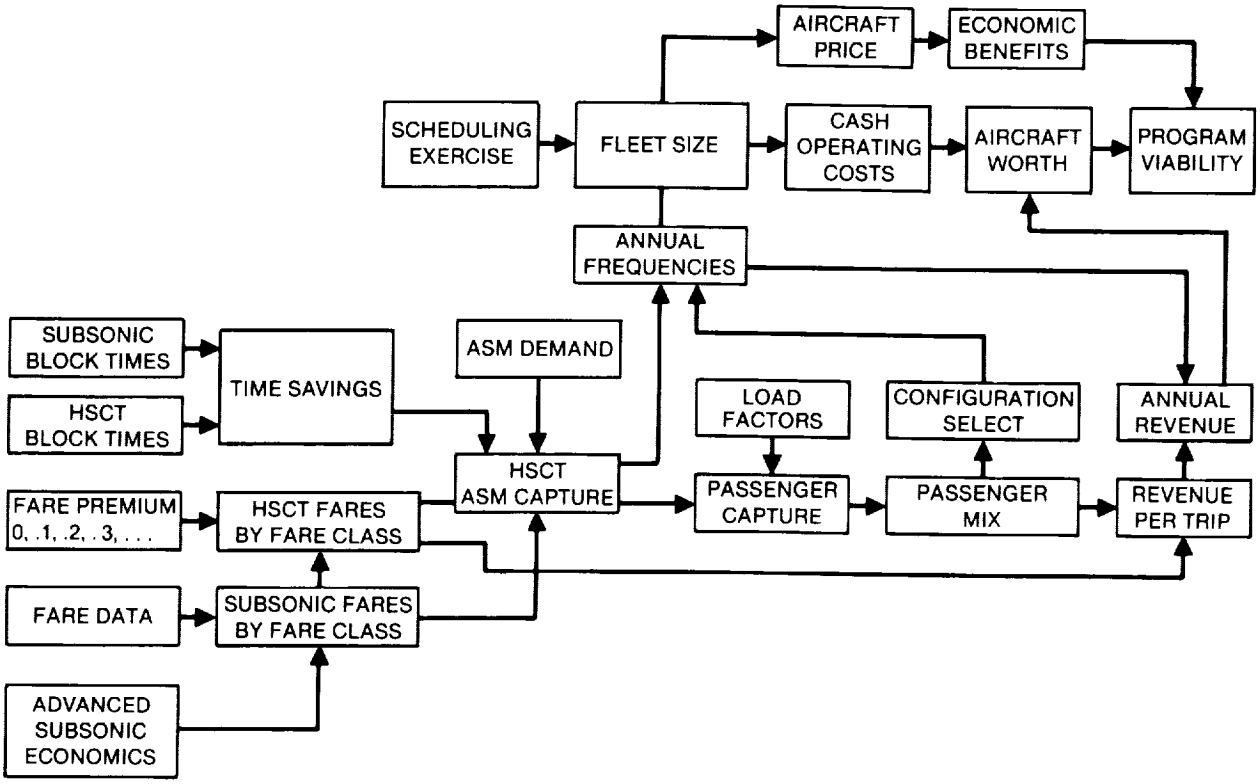

FIGURE 3-24. ECONOMIC AND MARKET STUDY APPROACH

TABLE 3-7
PASSENGER TRAFFIC FOR TEN SELECTED REGIONS (PHASE II DATA)

	ANNUAL SEAT-MILES GREATER THAN 2,000 STATUTE MILES (BILLIONS)				
REGION	ACTUAL 1986	FORECAST 2000	SCENARIO 1 2025	SCENARIO 2 2025	SCENARIO 3 2025
NORTH-SOUTH AMERICA	5.3	11.9	51.2	64.8	32.6
NORTH ATLANTIC	61.7	120.7	450.0	346.0	307.0
MID-ATLANTIC	4.2	8.7	33.3	26.2	25.6
SOUTH ATLANTIC	6.3	13.0	49.5	41.9	40.9
EUROPE-AFRICA	11.3	28.9	174.0	103.0	80.8
EUROPE-FAR EAST	13.2	39.7	272.0	183.0	179.0
NORTH AND MID-PACIFIC	32.2	135.9	1,470.0	975.0	672.0
SOUTH PACIFIC	6.6	15.3	65.7	54.4	54.9
INTRA NORTH AMERICA	1.1	2.3	9.7	5.3	5.1
INTRA FAR EAST/PACIFIC	17.6	69.7	946.0	587.0	455.0
	159.5	446.1	3,521.4	2,386.6	1,852.9

tial high-speed travel without sonic boom restrictions. These are input data and do not include increases in traffic due to high-speed travel opportunities.

The traffic model under the speed restriction over land consists of eight regions - a subset of the unrestricted model. Europe-to-Africa and Europe-to-the-Far-East were eliminated because all routes involved long subsonic distances. Each city pair in the eight-region model was studied to estimate the length of subsonic and supersonic cruise legs and to devise a better route that minimizes travel over land. In some cases city pairs were eliminated because of the reduced range capability under subsonic cruise conditions.

Assumptions. Phase III assumptions differ from those of the earlier Phase I and II due to (1) the nature of the Phase III focus and (2) update through supporting analysis. Major differences include no supersonic cruise over land allowed (base case), fuel costs including airport fuel facility costs related to fuel volume, aircraft maintenance costs, and turn around time. Results from Phases I and II are presented for comparison purposes. Generally, these data are not sensitive to the base case assumptions because they are either more fundamental in nature or concern issues independent of the assumptions.

The base case traffic model consists of eight international IATA regions with Scenario 2 traffic levels, no flights under 2,000 statute miles, and no supersonic travel over land permitted. Ten percent traffic stimulation is assumed, which means that ten percent of the dollar value of the passenger's time savings, excluding fare premium, is used to purchase additional trips. The advanced subsonic airplane is used for calibration purposes and as competition with the HSCT in the market capture calculations. Tables 3-8 through 3-12 contain additional information describing the base case.

TABLE 3-8
BASELINE AIRCRAFT

	CRUISE MACH	
	MACH 3.2	MACH 5.0
DESIGN RANGE (N MI)	6,500	6,500
MTOGW (LB)	769,000	1,213,000
TURNAROUND TIME (HR)	2	2
ECONOMIC LIFE (YR)	10	10
FUEL TYPE	TSJF	LNG
*SEATS — HIGH DENSITY	392	392
— LOW DENSITY	243	243
— 3-CLASS	300	300

*CONFIGURATION SELECTED CONSISTENT WITH PASSENGER MIX.

TABLE 3-9
PASSENGER MARKET

			COACH	
	FIRST	BUSINESS	FULL-FARE	DISCOUNT
MEAN VALUE OF TIME ($/HR)	90	30	23	5
DEMAND (% OF TOTAL)	10	30	20	40
FARE FACTOR (× FULL FARE)	1.2	0.7	0.6	0.3

TABLE 3-10
LOAD FACTOR

REGION	LOAD FACTOR
NORTH-SOUTH AMERICA	0.63
NORTH ATLANTIC	0.69
MID ATLANTIC	0.70
SOUTH ATLANTIC	0.70
NORTH AND MID PACIFIC	0.73
SOUTH PACIFIC	0.73
INTRA NORTH AMERICA	0.68
INTRA FAR EAST AND PACIFIC	0.72

TABLE 3-11
FUEL COST

	FEEDSTOCK PRICE ($/LB)	FUEL FACILITY COST* FUNCTION OF FACILITY SIZE ($/LB)
JET-A	0.0906	NONE
TSJF	0.1132	0.004 TO 0.019
LNG	0.0568	0.05 TO 0.154

*FROM FLUOR-DANIEL STUDY.

TABLE 3-12
MAINTENANCE COSTS

	D-3.2-3A		D-5.0-15A	
	AIRFRAME	ENGINE	AIRFRAME	ENGINE
LABOR-HOURS/FLIGHT-HOUR	5.10	0.95	9.8	1.43
LABOR-HOURS/CYCLE	13.20	0.61	46.2	0.75
MATERIAL DOLLARS/FLIGHT-HOUR	100.0	694.0	254.0	940.0
MATERIAL DOLLARS/CYCLE	257.0	453.0	826.0	486.0
DOLLARS/LABOR-HOUR	18.0	18.0	18.0	18.0
LABOR BURDEN ($/LABOR-HOUR)	63.0	63.0	63.0	63.0

Emissions Data. Ozone studies were based on engine emissions data integrated on a worldwide fleet basis using the appropriate market scenerios. One representative city pair was selected from each of the ten regions in the traffic model; and altitude, cumulative fuel burn, and latitude were calculated as a function of horizontal distance from the point of origin. From these data, an annual fuel burn matrix was generated for each region. Each element in the matrix is the amount of fuel burned within a corresponding altitude and latitude band. It is assumed that all the fuel is burned during flights between the cities defining the representative city pair for the region. The regional fuel burn matrices are then added to produce a matrix of system fuel burns. Finally, numerical engine exhaust parameters provided by the engine companies are applied to convert the fuel burns into amounts of the various products of combustion. Figure 3-25 and 3-26. present fuel burned in various altitude levels and latitude bands for Mach 3.2 and Mach 5.0, respectively. These data serve as inputs to atmospheric chemistry models executed by agencies under direct contract to NASA. The results of these analyses will provide guidance and direction for follow-on engine technology development.

Market Demand. Passenger values of time, fare premiums, and blocktime differences between the HSCT and the competing subsonic airplane interact with market share. The resulting output shows the fraction of the forecast traffic that is expected to be captured by the HSCT. The complementary traffic is carried by the subsonic fleet. The assumption underlying market share calculations is that a traveler will be an HSCT passenger if the monetary value of the time savings exceed the fare premium. This assumption is applied to all city pairs in the traffic model with the fare premiums varying from zero to fifty percent or more for sensitivity analysis. The passenger market is segmented into four different fare classes ranging from first class travelers with a relatively high value of time to a highly price-sensitive aft cabin or discount coach market.

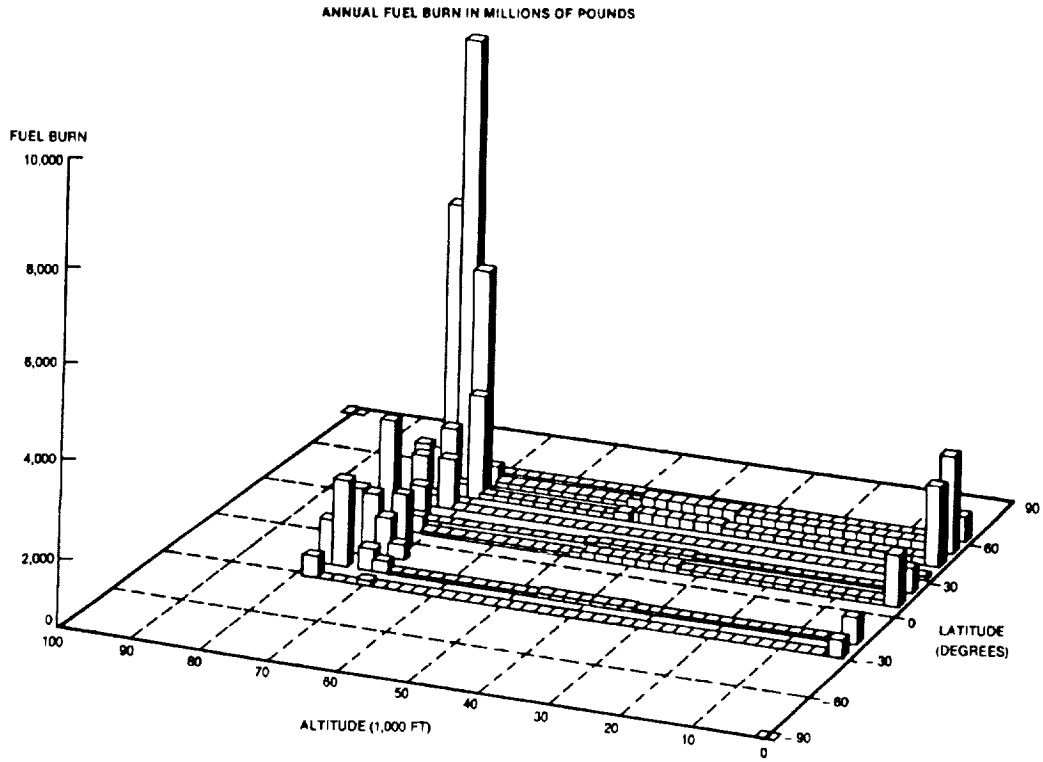

FIGURE 3-25. FUEL BURN BY ALTITUDE AND LATITUDE (MACH 3.2)

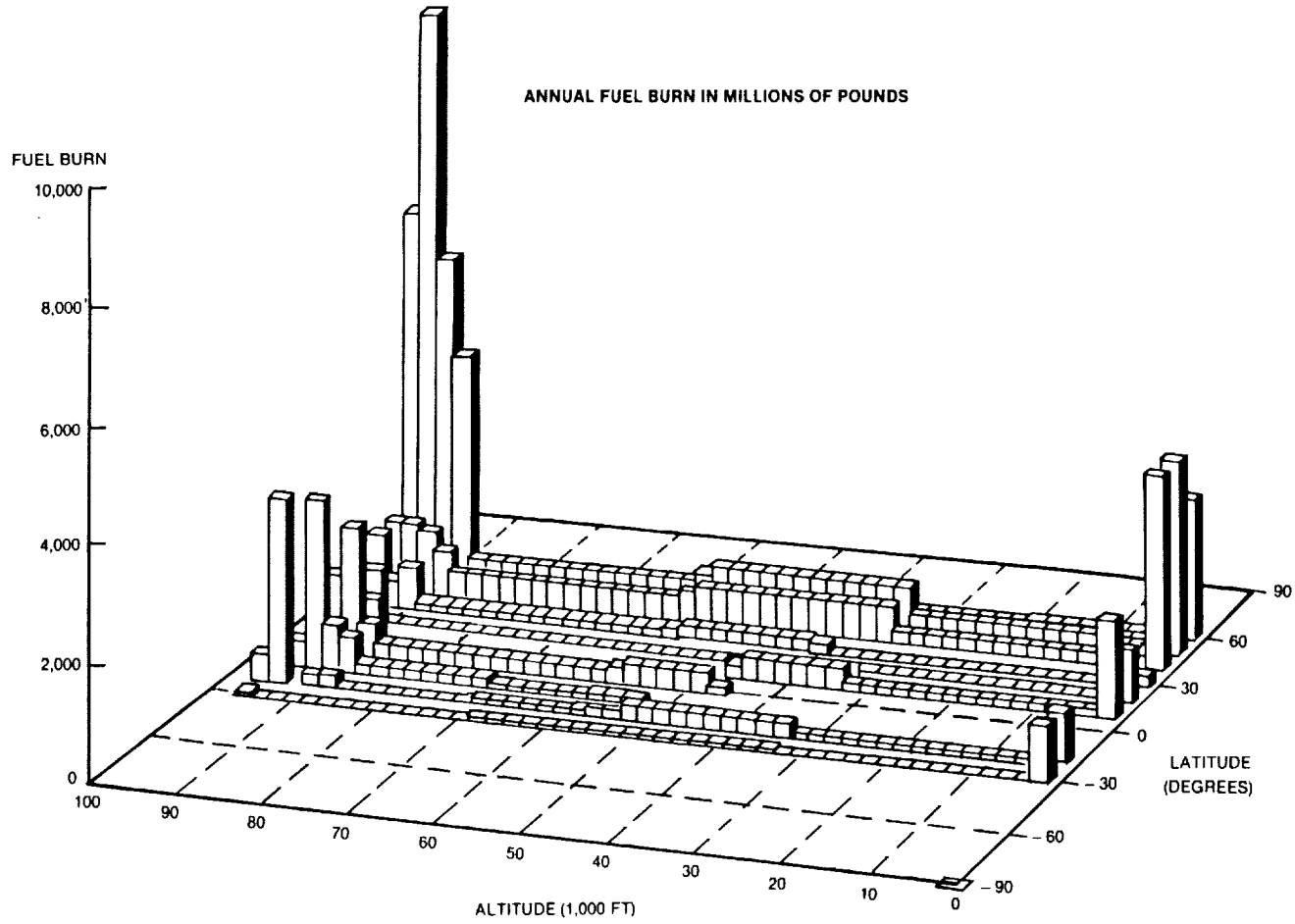

FIGURE 3-26. FUEL BURN BY ALTITUDE AND LATITUDE (MACH 5.0)

Figures 3-27 and 3-28 show potential traffic under the speed restriction over land and the effect of fare premium on market capture. The data are dependent on the HSCT including effects of subsonic cruise range performance. Traffic stimulation is slightly more for the Mach 5.0 concept due to high-speed travel opportunities.

Utilization and Productivity. Aircraft schedules were prepared with consideration given to curfews and time of day in order to obtain realistic estimates of airplane utilization (blockhours per day) and productivity (seat-miles per year). These scheduling activities were performed manually for all ten regions and for several individual airlines with and without the high-speed restriction. Computer generated schedules were produced with and without the high-speed restriction and curfews. Results are generally in agreement when the same assumptions concerning curfews and sonic boom restrictions are applied. Geographical differences among groups of city pairs and range and orientation appear to be more important factors than network topology.

The speed restriction reduces productivity between 10 percent and 15 percent, which reflects two significant factors. First, city pairs with long distances over land may not be flown in the restricted case because they exceed the range capability (reduced because of the subsonic cruise requirement). These city pairs are precisely the ones for which the potential penalty is greatest. Secondly, the restriction causes rerouting to avoid land masses. Although the diverted flight path is longer, it is flown at high speed and the flight time is favorable compared to that of the great circle, subsonic flight paths. Finally, whether aircraft cruise over land at subsonic speed or fly a longer path to avoid land or a combination of the two, blocktime is certain to increase.

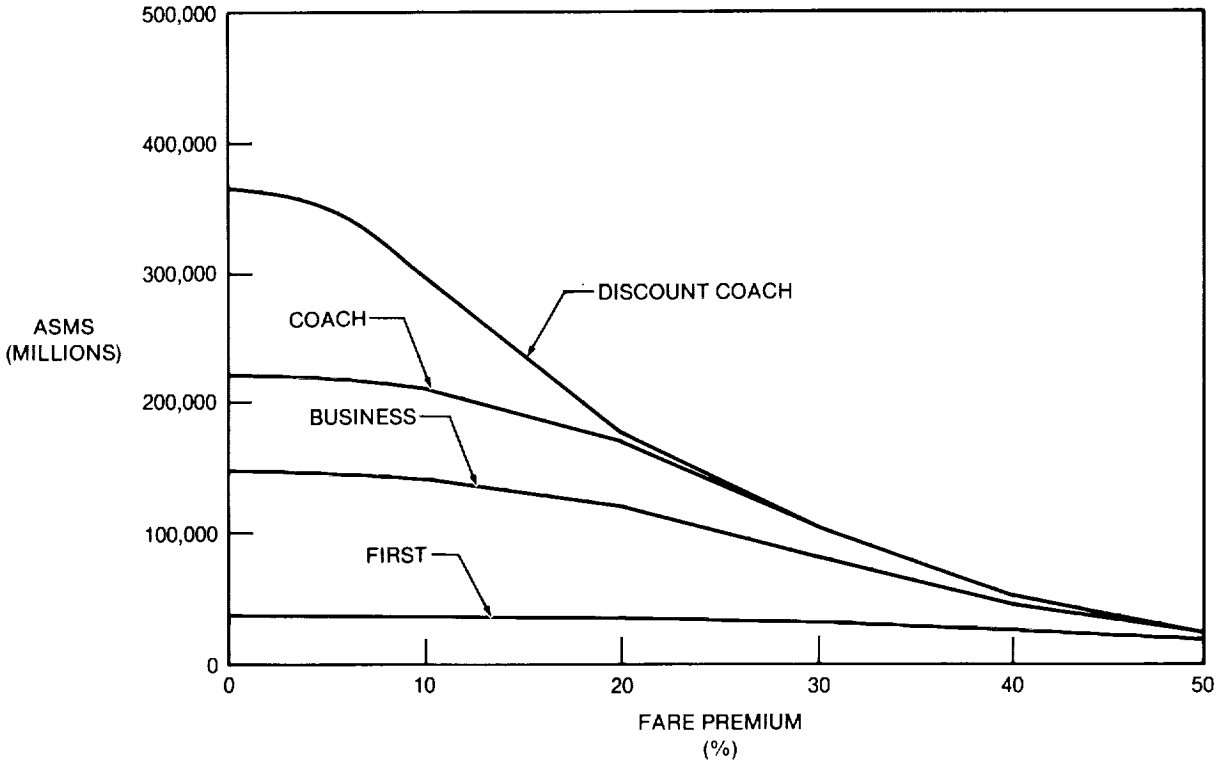

FIGURE 3-27. MARKET CAPTURE — MACH 3.2 — BASE CASE, YEAR 2000

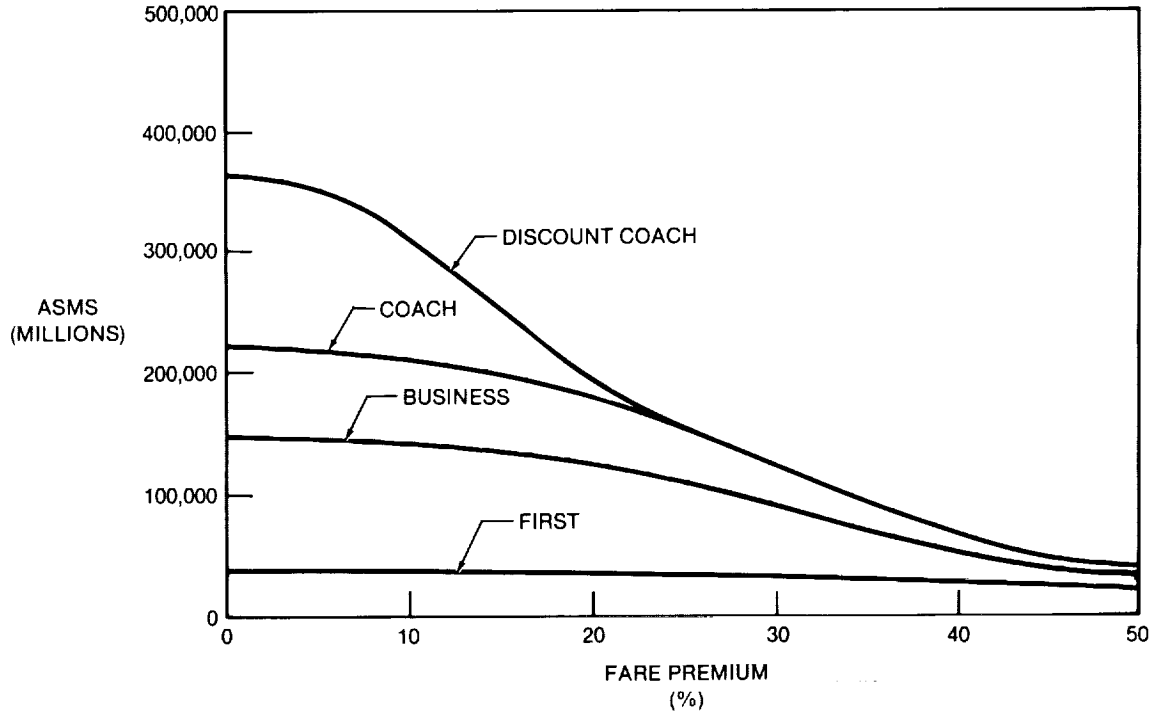

FIGURE 3-28. MARKET CAPTURE — MACH 5.0 — BASE CASE, YEAR 2000

Figure 3-29 displays data from manual scheduling analysis performed during Phase I for ten selected IATA traffic regions. These data account for curfews and a two-hour turnaround time. It is assumed that great circle routes are flown with no speed restriction. These data can be used to estimate productivity under subsonic restrictions provided that the curves are entered at an effective cruise Mach number. This Mach number is based on the great circle distance and the actual blocktime over whatever path was flown.

Manual scheduling was used to study effects of the subsonic requirement over land. Analysis of a Tokyo-based airline indicates a 10- to 15-percent productivity loss. Similar analysis of a Paris-based system showed 7- to 28-percent losses. There is no clear evidence from this work that favors any design range or Mach number over another. These results are corroborated by independent computer-generated schedules produced by MIT and based on the eight IATA region model. The MIT work indicates an 8- to 20-percent loss in productivity. Productivities from the Douglas computer model show a 10- to 15-percent loss compared to the potential supersonic flight over land. These data are shown in Table 3-13.

Fleet Requirements. The data of Table 3-14 show the fleet requirements for the HSCT. The aircraft needs in the year 2000 and the year 2025 for the eight region system is the base case. Note that at high fare premiums more Mach 5.0 aircraft are needed than are Mach 3.2 aircraft. This is because the added speed of the Mach 5.0 concept allows it to capture more traffic. The result is not intended to serve as an estimate of the potential market although such estimates can be derived from these ratios. For example, the year 2000

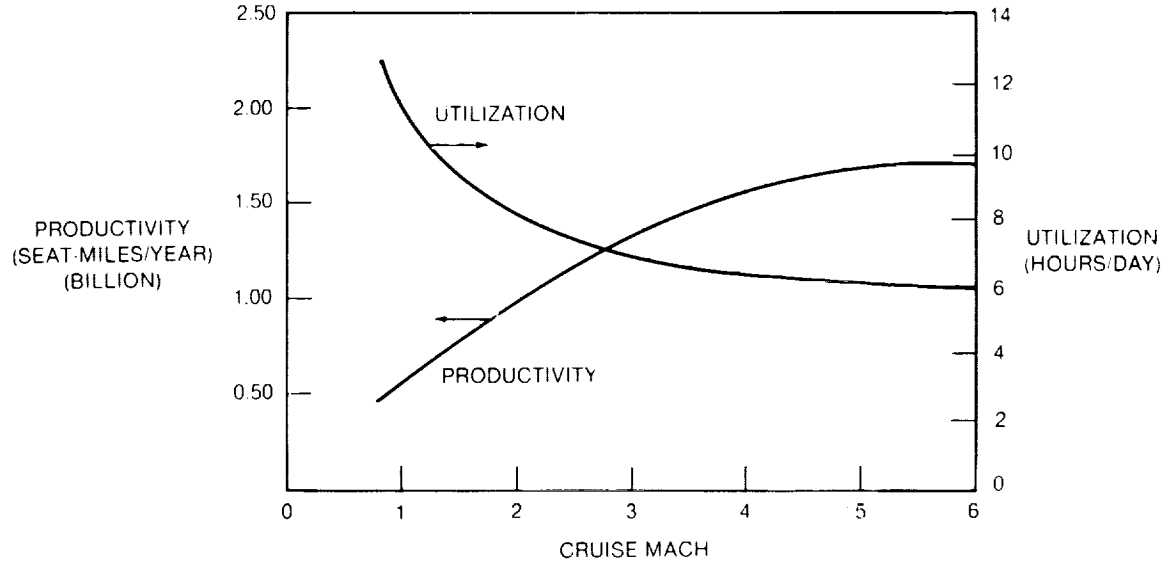

FIGURE 3-29. AIRCRAFT PRODUCTIVITY AND UTILIZATION (PHASE I DATA)

TABLE 3-13
AIRCRAFT PRODUCTIVITY (BASE CASE)

	ANNUAL SEAT-MILES (MILLIONS)	
	NO SPEED RESTRICTION	SPEED RESTRICTED OVER LAND
MACH 3.2	1,260	1,132
MACH 5.0	1,522	1,289

TABLE 3-14
AIRCRAFT NEEDED (BASE CASE)

FARE PREMIUM % OF SUBSONIC	MACH 3.2/SUBSONIC MIX						MACH 5.0/SUBSONIC MIX					
	MACH 3.2		SUBSONIC		TOTAL		MACH 5.0		SUBSONIC		TOTAL	
	2000	2025	2000	2025	2000	2025	2000	2025	2000	2025	2000	2025
0	310	1660	149	713	459	2373	284	1508	151	713	435	2221
10	256	1400	265	1271	521	2671	245	1315	241	1136	486	2451
20	164	901	473	2376	637	2466	162	879	443	2201	605	3080
30	100	569	599	3029	699	3598	107	598	563	2826	670	3424
40	50	295	690	3529	740	3824	59	343	659	3342	718	3685
50	25	147	735	3797	760	3944	31	182	716	3676	747	3858

is prior to the introduction date; therefore, there would be no HSCT aircraft in the fleet in year 2000. Also, subsonic aircraft that will remain in the fleet for several years will satisfy the need in 2000. If production rates are no greater than the rate of growth of the market, then production quantities can be absorbed without premature retirement of the subsonic fleet. The share of the long-range market depends on fare premium and, ultimately, on the operating costs.

World passenger jet aircraft requirements (excluding the USSR) are expected to total about 10,000 aircraft in 2000 with about 1,800 aircraft in the long-range (greater than 3,500-nautical-mile range) class. Approximately one-half of this long-range market is represented by the ten-region HSCT arena. Therefore, the HSCT with no fare premium may replace a maximum of 900 aircraft. Because the HSCT is some 2.5- to 3-times as productive as a subsonic aircraft of the same size, 300 to 450 HSCT could do the work of 900 subsonic aircraft. If high-speed cruise over land is prohibited, then requirements will be reduced further by as much as 20 percent. If premium fares are required, then the fleet sizes are further reduced. The foregoing remarks apply to 2000. For 2025 the numbers are larger (see Table 3-14).

Revenue. Passenger revenue is based on published International Civil Aviation Organization (ICAO) fare data, fare premium assumptions, and corresponding HSCT market share statistics. As noted previously, the fare premium is varied from zero (same as the subsonic fare) up to fifty percent or more. As fare premium increases, the HSCT market share is reduced. Yield (cents per passenger-mile) is improved because fares increase and the on-board passenger mix changes to favor the higher yield business and first class passengers.

The passenger market is assumed to consist of equal numbers of business and personal travelers. Both the business and personal components are further segmented by fare classes. Each fare class has its own average value of time and fare level (related to ICAO full fares).

Effective yields are significantly different from what might be predicted from load factors and published fare data. Frequent flyers, upgrades to first class because of a sold-out aft cabin, nonrevenue passengers, and special low fares from interline agreements cause the effective yield to be diluted and significantly lower than that predicted from load factors and ICAO fares. This has been treated by calibrating the revenue model to a known aircraft. The revenue based on ICAO fares is adjusted by a factor such that an advanced MD-11 would have an investment value (aircraft worth) equal to its selling price. The calibrating factor is then held constant throughout the HSCT evaluation. This ensures that the HSCT revenues are based on real-world yields and that HSCT aircraft worth estimates are consistent with the market price of a known airplane. Table 3-15 presents HSCT yield and revenue-per-mile data. Note that yield increases more rapidly than revenue per mile with larger fare premiums. This is because low-density seating configurations are

TABLE 3-15
YIELD AND REVENUE PER MILE (BASE CASE)

FARE PREMIUM (% OF SUBSONIC)	MACH 3.2		MACH 5.0	
	($/ST MI)	($/RPM)	($/ST MI)	($/RPM)
0	21.67	0.102	21.68	0.102
10	24.79	0.121	24.46	0.118
20	30.42	0.160	29.93	0.156
30	33.98	0.187	33.43	0.183
40	39.61	0.225	38.16	0.214
50	46.89	0.273	44.66	0.257

required for the all business- and first-class loads that result from high fare premium. Table 3-16 summarizes the differences in revenue generating capabilities of the Mach 3.2 and Mach 5.0 concepts.

Operating Cost. The components of operating cost follow CAB Form 41 format for direct and indirect cash costs. These are (1) flying operations, (2) maintenance, (3) passenger service, (4) aircraft and traffic servicing, (5) promotion and sales, and (6) general and administrative. Cost estimates are computed by Douglas operating cost formulas. Input data included (1) operational statistics (blocktime, departures, fleet size) from the HSCT operational analysis, (2) information generated during the study such as fuel costs and fuel infrastructure costs, and (3) results of analysis of HSCT concepts including blocktimes, fuel burn, maintenance cost, and turnaround time. Table 3-17 shows a percentage breakdown of cash operating cost with the predominant DOC element (fuel) increasing from about 1/4 of the cash operating cost for a current subsonic transport to nearly half for the Mach 3.2 aircraft to two-thirds for the Mach 5.0 aircraft. Ownership related expenses are not included because the stream of cash flows over the life of the HSCT is used to compute its value as an investment. Table 3-18 shows these costs for the Mach 3.2 and Mach 5.0 aircraft and for a subsonic aircraft of the same size for reference. The Mach 3.2 aircraft cash operating costs are estimated to be nearly 30 percent higher than for a current subsonic transport. The Mach 5.0 aircraft is estimated to have a cash operating cost 140 percent higher than a current subsonic transport.

TABLE 3-16
ANNUAL REVENUE PER AIRCRAFT (BASE CASE)

FARE PREMIUM % OF SUBSONIC	MACH 3.2 (MILLION $)	MACH 5.0 (MILLION $)
0	85.1	92.8
10	99.6	106.0
20	122.0	132.0
30	139.0	151.0
40	164.0	178.0
50	195.0	211.0

TABLE 3-17
OPERATING COST BREAKDOWN — NO OWNERSHIP-RELATED COSTS (BASE CASE)

	CURRENT SUBSONIC (% OF TOTAL)	MACH 3.2 (% OF TOTAL)	MACH 5.0 (% OF TOTAL)
FLYING OPERATIONS	26.2	47.7	68.1
MAINTENANCE	10.5	7.8	7.6
PASSENGER SERVICE	17.7	7.5	3.3
AIRCRAFT/TRAFFIC SERVICING	12.0	10.4	6.7
PROMOTION AND SALES	26.9	21.2	11.4
GENERAL ADMINISTRATION	6.8	5.4	2.9
TOTAL	100.0	100.0	100.0

TABLE 3-18
OPERATING COSTS — NO OWNERSHIP-RELATED COSTS (BASE CASE)

	CURRENT SUBSONIC	MACH 3.2	MACH 5.0
DOLLARS PER BLOCK HOUR	7,394	22,191	50,162
DOLLARS PER STATUTE MILE	13.66	17.36	32.30
DOLLARS PER SEAT-STATUTE MILE	0.045	0.058	0.107
AVERAGE RANGE (ST MI)	4,221	4,140	4,132

Aircraft Worth. Aircraft worth is the investment value of an airplane to the airline operator. The worth of an HSCT is estimated by an iterative process that determines the price to the operator so that a target rate of return on investment is achieved by the operator. This process includes 1987 tax law and depreciation schedules, life of the asset, and, most importantly, the annual operating cash flow. All of the airplane characteristics such as size, weight, speed, lift to drag ratio, propulsion efficiency, and other parameters are embodied in the cash flow estimates. Also involved in the cash flow (and hence, aircraft worth) are operational parameters such as utilization, turnaround time, passenger mix, load factor, fare differences in various regions of the world, and fare premium. Results are shown in Tables 3-19 and 3-20 for various values of fare premium and operator's return on investment, highlighting the significant advantage estimated for the Mach 3.2 aircraft compared to the Mach 5.0 aircraft.

Aircraft Price. Cost/prices were developed using the total McDonnell Douglas base of experience and knowledge in the field of high-speed technology and support efforts (e.g., materials, processes, and the like) to the maximum extent. This base provided the bench marks from which to continue the estimating process following the identification and assessment steps referred to above. Labor and material resources were estimated on a discrete evaluation basis coupled to the analogous technique. Resources were estimated by

TABLE 3-19
ANNUAL CASH FLOW PER AIRCRAFT (BASE CASE)

FARE PREMIUM % OF SUBSONIC	MACH 3.2 (MILLION $)	MACH 5.0 (MILLION $)
0	19.0	– 14.2
10	31.0	– 4.6
20	49.9	11.9
30	63.8	22.1
40	84.9	35.9
50	110.3	56.2

TABLE 3-20
AIRCRAFT WORTH (BASE CASE)

FARE PREMIUM (% OF SUBSONIC)	OPERATOR'S RATE OF RETURN (%)	MACH 3.2 (MILLION $)	MACH 5.0 (MILLION $)
0	5	151	– 113
	10	114	– 85
	15	89	– 67
10	5	247	– 37
	10	186	– 28
	15	146	– 22
20	5	397	95
	10	299	71
	15	235	56
30	5	509	176
	10	384	133
	15	301	104
40	5	677	286
	10	510	216
	15	400	169
50	5	880	448
	10	663	338
	15	519	265

major aircraft system/component and by functional category. Development costs included all of the necessary resources and tasks required to design, develop, produce and demonstrate an aircraft that can be FAA certified.

Labor hours were translated into constant 1987 dollars using the aerospace fully-burdened labor rates for the different categories of labor (e.g., Engineering, Tooling, Quality Assurance, and so on). Material and equipment were estimated separately except that propulsion system costs were furnished by the subcontractors.

The end product of the estimating process is a flyaway cost (price) in which the development cost is amortized over each assumed production program with a manufacturer's targeted rate of return. Flyaway prices are shown in Figure 3-30 as a function of quantity for both baseline configurations.

Economic Viability. Necessary conditions for economic viability include: (1) airplane revenues covering operating costs plus an attractive rate of return to the operator and (2) fares low enough to provide HSCT service, and (3) a market large enough to permit a selling price lower than the investment value of the airplane. The evaluation procedure places the HSCT in competition against the advanced subsonic airplane on a city pair basis. This ensures that the HSCT is applied to those markets in which it performs best. Repetition of this procedure for various fare levels will determine whether conditions (1), (2), and (3) above can be simultaneously satisfied. Results are shown in Figure 3-31.

The parametric data for aircraft price are based on unit production costs from $250 million to $700 million and development costs ranging from $6 billion to $18 billion. The curves labeled Mach 3.2 and Mach 5.0 are from the aircraft worth data of Table 3-20 for an operator's rate of return of 10 percent.

The Mach 3.2 (D3.2-3A) concept is potentially viable with a fare premium of 20 percent if recurring unit production costs are $250 million. A fare premium of 40 percent is required if recurring production costs are about $375 million. These data show that the Mach 5.0 (D5.0-XX) concept is not economically viable at any fare premium.

Additional assessments of aircraft worth have been made for various values of fuel price, turnaround time, maintenance cost, and with and without the subsonic restriction. Results are shown in Figure 3-32 and Figure 3-33 with changes from base case data noted.

Economic Benefits. The HSCT promises economic benefits including higher levels of U.S. gross national product (GNP), a better balance of trade, and increased employment. The size of these benefits depend upon the size and timing of the effort from research through production and delivery. They also

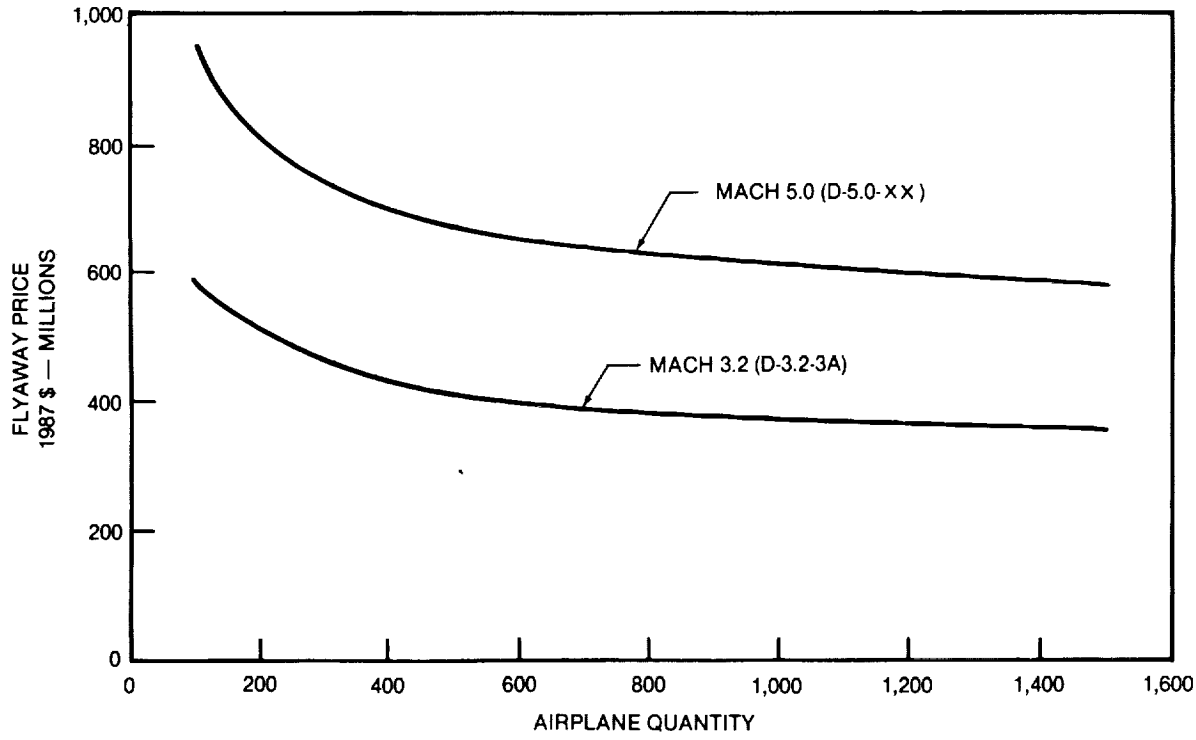

FIGURE 3-30. CUMULATIVE AVERAGE PRICE VERSUS QUANTITY PRODUCED — MACH 3.2 AND MACH 5.0

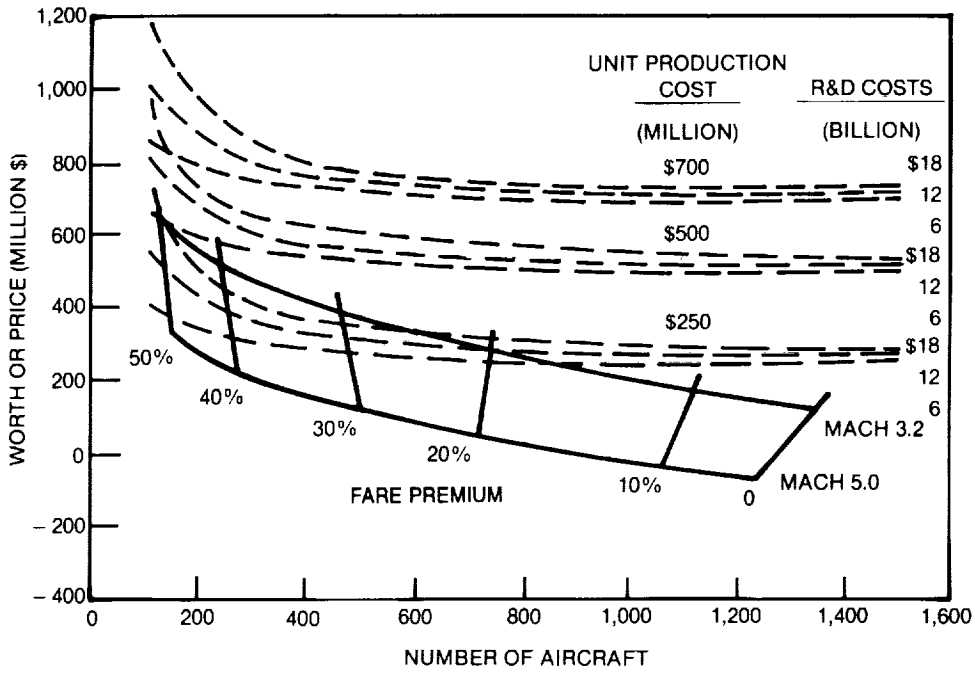

FIGURE 3-31. AIRCRAFT WORTH AND PRICE

depend upon the ability of the economy to absorb the increased spending. Generation of great magnitudes of spending over too short a period of time will lead to displacement of other business investment (crowding out), higher interest rates, and increased inflation. A moderately sized program, however, will generate favorable changes in the economy. Historically, for every dollar of direct expenditures in the U.S. aerospace industry, approximately $1.20 of indirect gross national production occurs. This results in a total effect of $2.20 on GNP for every $1.00 spent on aerospace. The multiplier of 2.2 incorporates a normal amount of crowding out. For every new aerospace job created by the HSCT, there will be other indirect jobs created. It is estimated that each direct aerospace job will lead to about 1.5 indirect jobs. This results in an employment multiplier of 2.5. There can be a crowding out effect in employment; if the unemployment rate becomes too low, then wages will be bid up and inflation and unfilled jobs may result. None of the scenarios considered here, however, seem likely to present significant dangers of employment crowding out given a baseline prediction of 5-percent unemployment in 2013.

Several of the key parameters of the economic benefits analysis have been identified. In order to bound the problem numerically, a range of values is assumed for some of the key parameter: (1) total production is 500 and 1,000 aircraft; (2) unit production cost is $322 million and $301 million; (3) development cost is $14.4 billion; (4) domestic content is 50 percent, 70 percent, and 85 percent of production cost. Also it is assumed, from a sales standpoint, that 73 percent of the aircraft sold are exported. This figure is based on past U.S. commercial aircraft programs. Table 3-21 presents results for each of the scenarios possible under the assumptions. Row 8 in the figure gives the sum of the increase in GNP from 2004 to 2025. Row 11 of the figure shows the largest percentage increase in GNP in one year. If this value is too large, then a large amount of crowding out may occur and prevent the predicted growth in GNP. The last row in the figure gives the sum of the improvement in the U.S. balance of trade from 2004 to 2025. The peak effect on GNP occurs in 2013 when production levels first reach their highest level. This date depends on the assumed profile of spending for R&D and production. The calculations were made assuming that R&D expenditures occur between 2004 and 2011 with 80 percent spent from 2006 to 2010. Production expense is spread over the 15-year period following 2010 with 85 percent spent between 2012 and 2022.

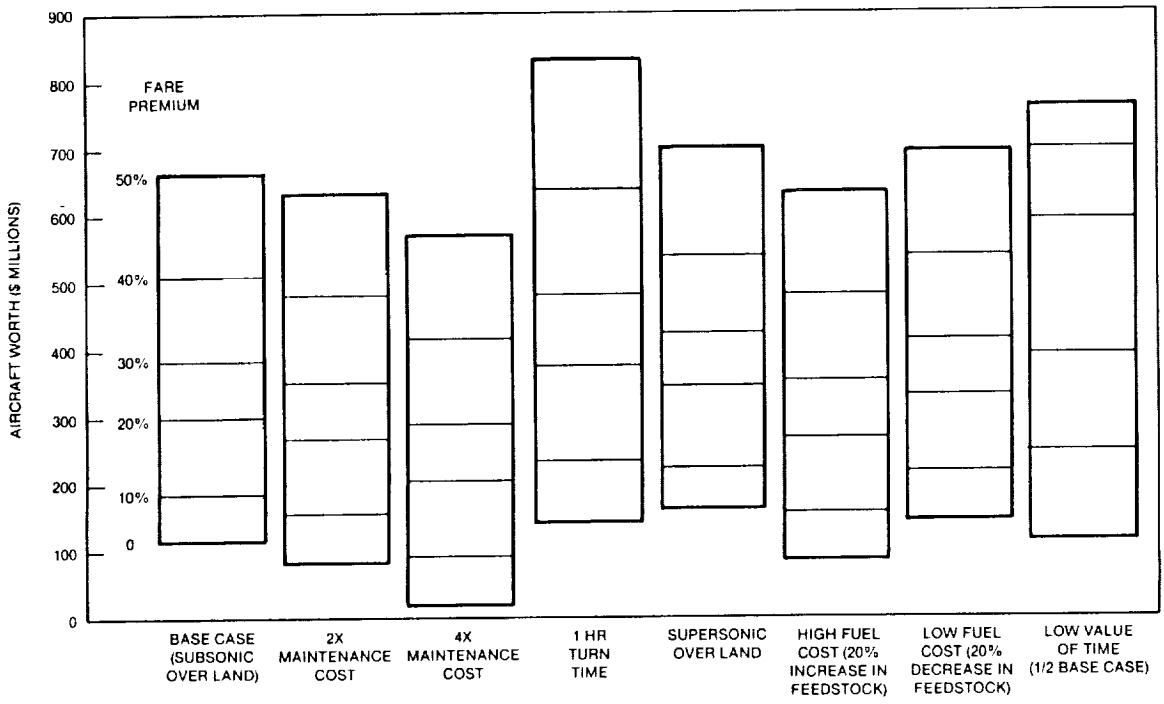

FIGURE 3-32. SENSITIVITY OF AIRCRAFT WORTH TO ASSUMPTIONS — D3.23A (FARE PREMIUMS OF 0 TO 50 PERCENT OVER SUBSONIC)

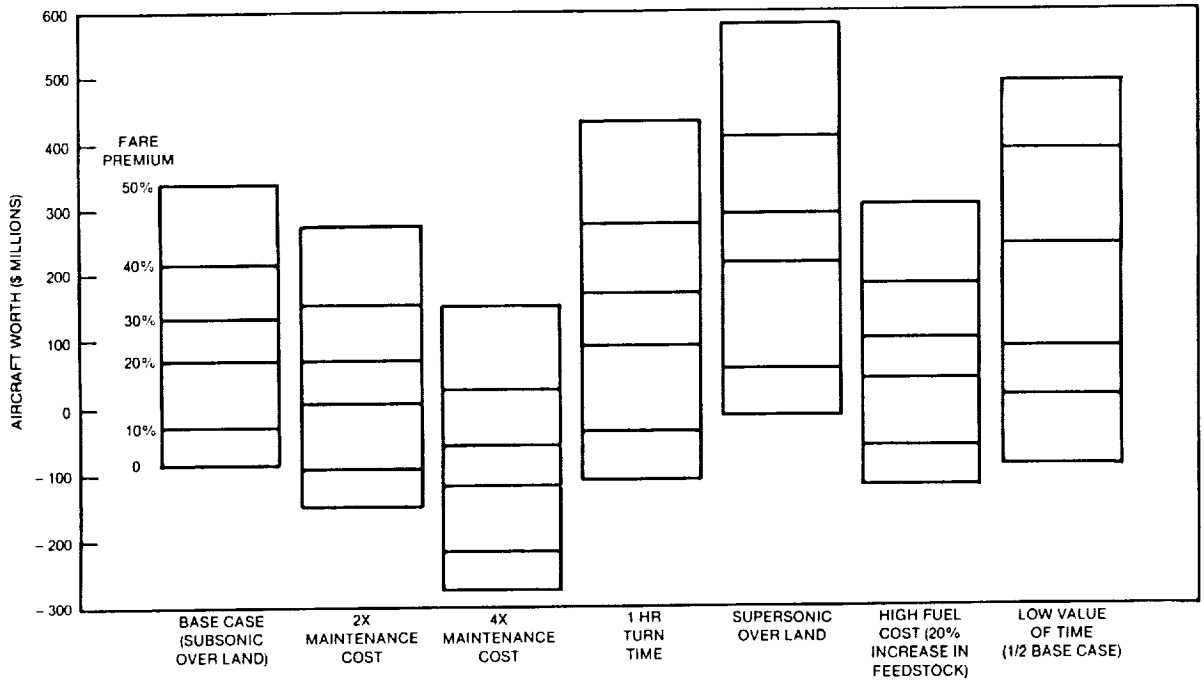

FIGURE 3-33. SENSITIVITY OF AIRCRAFT WORTH TO ASSUMPTIONS — D5.0-15A (FARE PREMIUMS OF 0 TO 50 PERCENT)

TABLE 3-21
ECONOMIC BENEFITS — MACH 3.2 (D3.2-3A)

	SCENARIO 1	SCENARIO 2	SCENARIO 3	SCENARIO 4	SCENARIO 5	SCENARIO 6
R&T EXPENDITURES ($ BILLION)	$14.4	$14.4	$14.4	$14.4	$14.4	$14.4
UNITS PRODUCED	500	500	500	1,000	1,000	1,000
PRODUCTION COST PER AIRPLANE ($ MILLION)	$322	$322	$322	$301	$301	$301
PERCENT U.S. PRODUCTION	50	70	85	50	70	85
AVG EMPLOYMENT GAIN	108,000	144,000	171,000	186,500	254,000	304,500
PEAK EMPLOYMENT GAIN	167,000	234,000	284,000	312,500	437,500	531,000
PEAK DECREASE IN UNEMPLOYMENT RATE (FROM BASE RATE OF 5 PERCENT)	0.11	0.16	0.19	0.21	0.29	0.35
TOTAL GNP GAINOVER PROGRAM LIFE ($ BILLION)	$209	$280	$333	$363	$495	$595
AVG GNP GAIN PER YEAR ($ BILLION)	$9.9	$13.3	$15.8	$17.3	$23.6	$28.3
PEAK GNP GAIN — YEAR 2013 ($ BILLION)	$14	$20	$24	$26	$37	$45
PERCENT INCREASE IN GNP — YEAR 2013	0.17	0.23	0.28	0.31	0.44	0.53
TOTAL IMPROVEMENT IN BALANCE OF TRADE OVER PROGRAM LIFE ($ BILLION)	$37	$69	$92	$69	$129	$175

Very large programs with effects in excess of 0.5 percent of GNP may dampen the growth through crowding out and result in multipliers considerably less than 2.2. Scenarios 5 and 6 fall into this category. All of the scenarios show an improvement in balance of trade. In perspective, so long as 30 percent or more of the production of the HSCT is performed in the U.S., the project will improve the balance of trade. This follows from the assumption that 73 percent of total HSCT production will be exported. The analysis of the balance of trade effects treats only direct effects of importing and exporting.

3.5 Human Factors

High-speed commercial transport flights will have a number of effects upon the crews who operate the aircraft and the passengers. This section will address jet lag, ozone, decompression, and radiation which vary considerably from experience with subsonic transport aircraft.

Jet Lag. Jet lag is defined as the signs and symptoms experienced by travelers crossing a number of time zones within a relatively short period. It encompasses the feelings of irritability, mental and physical lethargy, disorientation, fatigue, and other symptoms, as well as a number of measurable physical signs related to the normal daily biorhythm, or circadian cycle. Some of the parameters are sleep dependent — that is, they vary with the individual sleep cycles that adapt to time changes almost immediately. There are other parameters that seem to be dependent on an internal physiological clock that takes time to reset.

When the biorhythm cycles are out of phase with one another, there is a correlation with the symptoms the passenger calls jet lag. Figures 3-34 to 3-36 show the various waveforms of different body and mental parameters – variations of two hormones (ACTH and cortisol), body temperature, and mental capabilities, respectively.

Some symptoms change in real time and the others with a lag. It is not surprising, therefore, that adjustment for the jet lag occurs in about the time that it takes for the sleep-dependent and physical

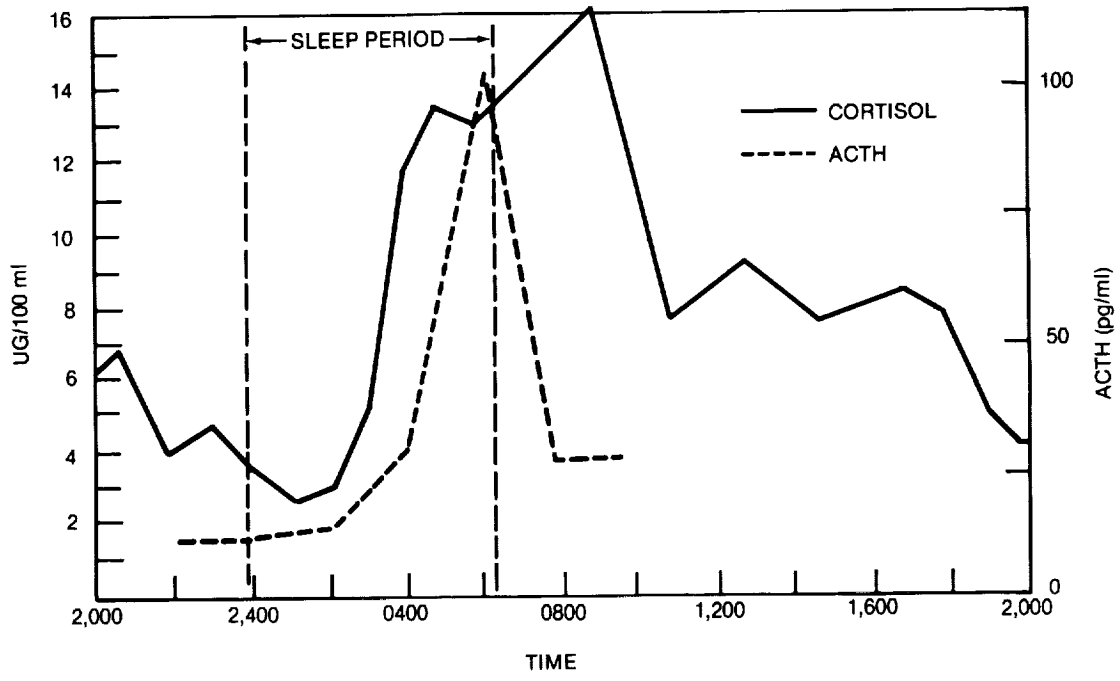

FIGURE 3-34. DIURNAL ACTH AND CORTISOL SERUM CONCENTRATION

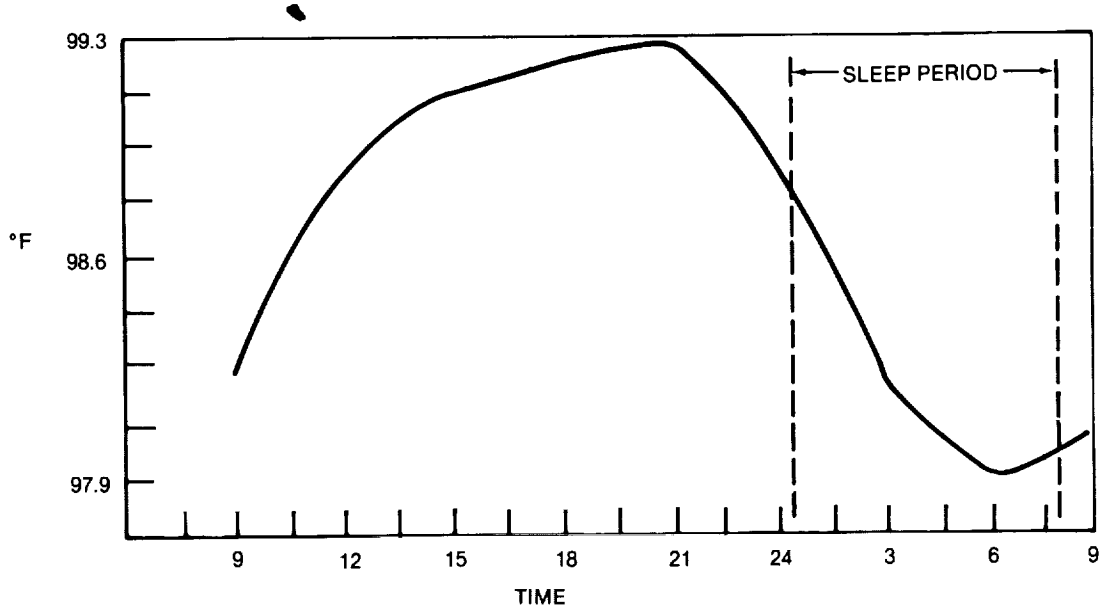

FIGURE 3-35. CIRCADIAN BODY TEMPERATURE

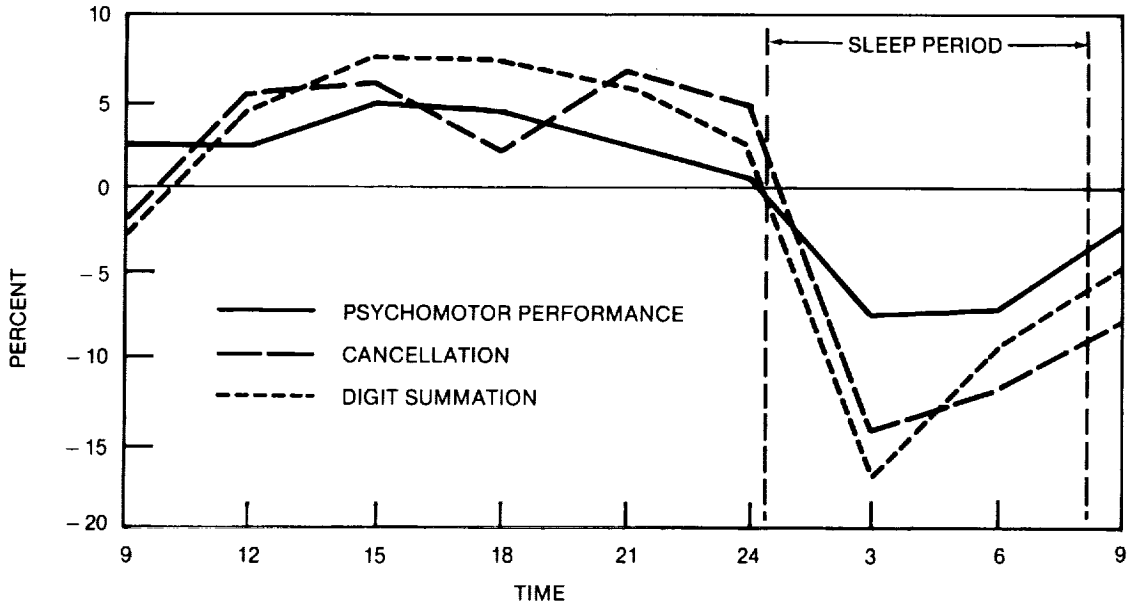

FIGURE 3-36. CIRCADIAN RHYTHM

parameters to fall back into phase. Figure 3-37 shows composite decay rates of the phase differences for time changes of 12, 9, and 6 hours, respectively. The following conclusions have been reached:

- Jet lag is real and does degrade passengers' performance and enjoyment at the destination
- The sooner a passenger arrives in the new time zone, the sooner the readjustment begins. Since phase lag has an exponential decay, a matter of hours is significant
- Round-trip in one day should not create jet lag problems for the crew, or for those business travelers who take advantage of the short travel times and return home the same day

It is appropriate to mention that other medical problems, which are aggravated by long flights, and readjustment of time schedules will be ameliorated by shorter flights. Some of the medical problems that

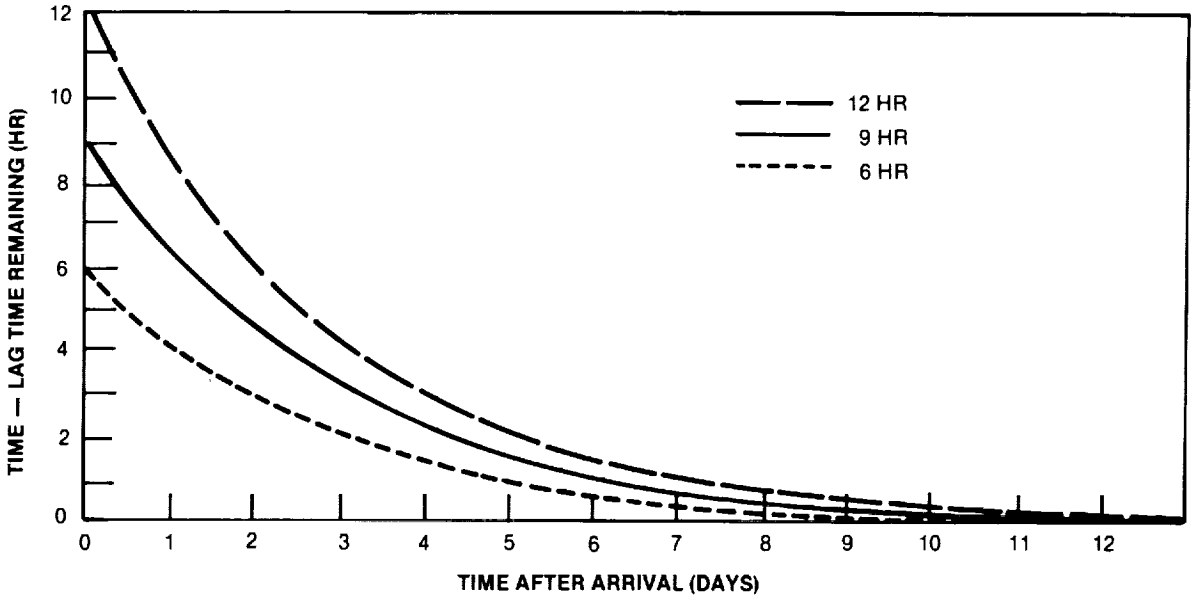

FIGURE 3-37. JET LAG RECOVERY

will benefit from shorter duration flights are prostatitis, edema, thromboembolic disease, constipation, arthritis, and insulin dependent diabetes.

Ozone. High-speed civil transports are expected to travel at altitudes of 60,000 feet and above. This may subject passengers and crew to unacceptable levels of ozone exposure. The FAA has set guidelines for ozone levels in aircraft cabins during flight to be 0.25 parts per million by volume (ppm) at any time above a flight level of 32,000 feet, and 0.1 ppm time-weighted average during any 3 hour interval above 27,000 feet. The EPA standards that ozone concentration must not exceed 0.12 ppm during the peak hour has been criticized as too high (Reference 3-1).

Ozone cabin levels will not be the same as outside, but it has been determined that flight in the 34,000- to 40,000-foot altitude range have cabin levels of 0 to 0.12 ppm with outside cabin measurements of 0 to 1.5 ppm. Levels as high as 0.57 ppm have been reported in aircraft at 34,000 feet on polar routes. The implications of the significantly greater ozone concentrations at 60,000 to 100,000 feet is evident, necessitating "ozone control" that is currently achievable.

Decompression. Decompression incidents pose serious medical problems – hypoxia and barotrauma. Hypoxia, generally speaking, may be corrected up to an altitude of about 40,000 feet by breathing 100-percent oxygen. This results in about 84-percent saturation of the hemoglobin in the blood, which is a good functional level of saturation. At altitudes of 60,000 to 80,000 feet, lower atmospheric pressure precludes oxygenating the blood with 100-percent oxygen – this poses a new problem.

Another important consideration of decompression is the time of useful function. Breathing air at 40,000 feet, the time of useful function is 15 to 20 seconds. At 35,000 feet, it is 30 to 60 second. Partial oxygenation of air breathing at these altitudes provides sufficient time to perform the useful function of transferring to breathing 100-percent oxygen, thus the solution to the decompressions hypoxia problem at these altitudes. On the other hand, above 43,000 feet the time of useful function has fallen to 9 to 12 seconds. This is probably insufficient time to transfer to positive face mask pressure breathing of 100-percent oxygen; therefore, additional measures need to be considered.

Barotrauma may either be concentrated or diffuse. In the first case, trapped volumes of air in body cavities (such as the lungs) try to expand more rapidly than the body can accommodate. This could result in mechanical trauma such as rupture of a lung. Explosive ($<$ 3 seconds) and rapid decompressions (3 seconds to 3 minutes) can cause this kind of barotrauma. Slow decompressions ($>$ 3 seconds) as well as the explosive and rapid decompressions may result in diffuse barotrauma – the decompressions sickness syndrome popularly referred to as the bends. In this instance, slowly forming bubbles diffusely spread throughout the body causing trauma to tissues by blocking capillary perfusion.

The solution to the decompressions problem is multifactorial, impacting basic HSCT design (e.g., structural safeguards, rapid means of plugging small holes, quick activation of cabin repressurization equipment), as well as necessitating new procedures such as rapid descent maneuvers and positive pressure breathing masks.

Radiation. At high altitudes, radiation levels are higher due to less atmospheric protection or the presence of post-nuclear explosion debris. Radiation may be considered as ionizing or non-ionizing radiation depending on levels relative to 40 nanometers on the electromagnetic spectrum. All particle radiation of practical interest is considered as ionizing radiation.

The allowable doses of ionizing radiation are 0.5 rem and 5 rem per year for non-occupationally exposed and occupationally exposed persons, respectively. It is concluded that the maximum dose is about 8 rems during a solar cosmic ray event. The risk of a solar cosmic ray event is small, and warning devices and the existing solar flare warning network could be used to prevent these levels of doses. For the galactic cosmic ray background, the doses for the crews are expected to range above 0.5 rem per year but remain below 5 rem per year. Rather than shortening crew hours, it might be better to have crewmen reclassified at radiation workers standards (i.e., occupationally at risk).

In the case of the resumption of nuclear atmospheric tests or a Chernobyl-type disaster, the clouds are estimated to produce doses from 0.02 rem for a 25 kiloton explosion to 0.8 rem for a 1 megaton

explosion. If passengers are contaminated, the doses will be higher and exposure more persistent if there is internalization of materials such as strontium-90.

Non-ionizing radiation is ultraviolet radiation that principally will affect the cockpit inhabitants. There are many factors to consider before concluding that there is a harmful effect. Exposure will be greater the higher the aircraft flies, and thus implications for the high-speed civil transport are that there will be more exposure. The amounts and effects of the exposures are still to be determined.

3.6 Benefits

The prime benefit of high-speed commercial transport is the reduction in travel time afforded to the customer. Savings corresponding to a two-thirds or greater reduction in travel time or block time (Figure 3-38) offers considerable market attraction (e.g., less fatigue and jet lag, more time for business or vacation

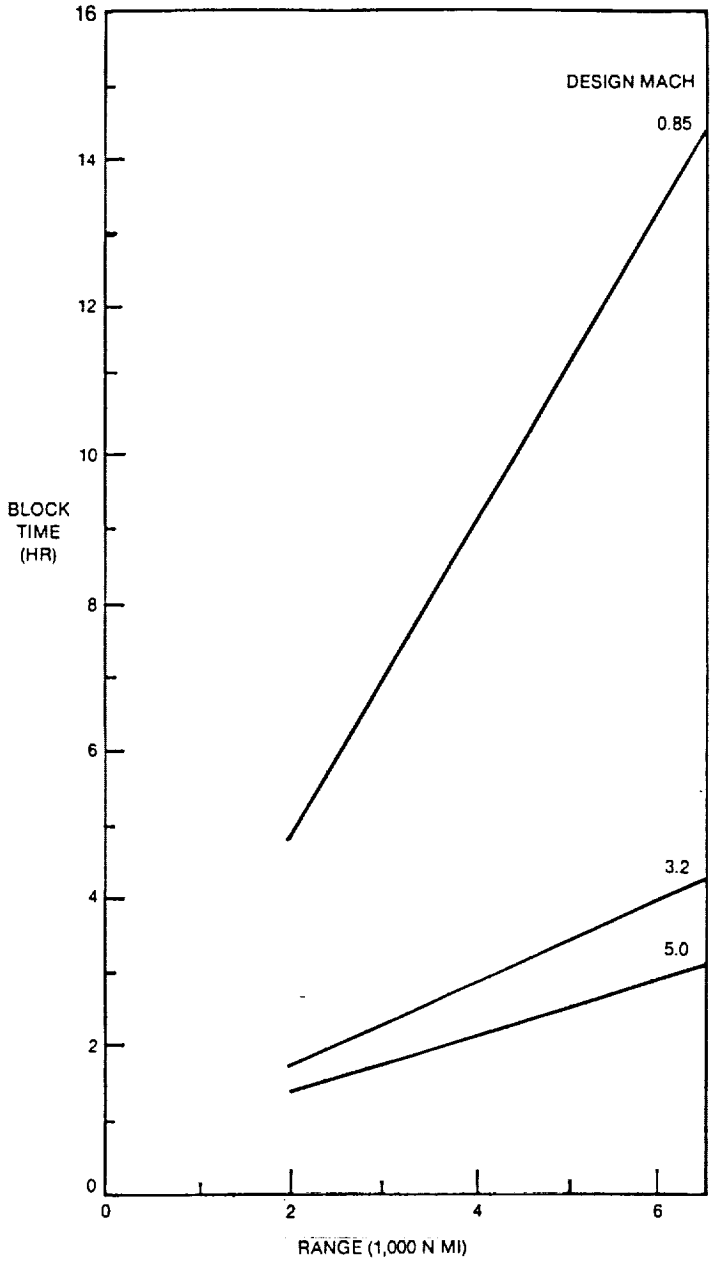

FIGURE 3-38. BLOCK TIME

activities, more nights at home for the business traveler, and extended horizons in terms of distant destinations). As a result, HSCTs will offer many advantages compared with current, "subsonic" air transportation (Table 3-22). Quantification of market stimulation (passenger and cargo) was beyond the scope of these studies. However, all airlines contacted during this phase of the study expressed the opinion that significant travel time savings would, without question, noticeably stimulate market growth, as well as create new markets – particularly at the longer distances.

Realization of worldwide commercial HSCT service will only come about if the HSCT can be operated profitably and is environmentally compatible. Increased speed results in reduction of certain time-related aircraft operating costs on a trip basis. Increased speed contribute to greater productivity – seat-miles generated per year, and productivity is the major offset to aircraft investment. HSCTs in the Mach 3.2 to Mach 5.0 range offer 200 percent or greater increases in productivity compared with subsonic transport of the same passenger capacity (Figure 3-39). Beyond the Mach 5 to Mach 6 range, productivity increases only slightly with increased Mach number. Aircraft revenue is a direct function of productivity and, providing competitive aircraft-related operating costs can be achieved, HSCT profitability will result.

TABLE 3-22
HIGH-SPEED, COMMERCIAL TRANSPORT ADVANTAGES

FOR PASSENGERS, REDUCED TRAVEL TIME RESULTS IN
- REDUCED JET LAG
- LESS PHYSICAL HARDSHIPS, ENHANCED COMFORT

FOR BUSINESS TRAVELERS
- "SAME DAY" BUSINESS
- REDUCED "EN ROUTE" COSTS

FOR BUSINESS
- EXPRESS WORLDWIDE MAIL/PACKAGE SERVICE
- SHORTENED INVENTORY PIPELINES

FOR AIRLINES
- MARKET STIMULATION
- INCREASED PRODUCTIVITY/REVENUE AND PROFIT
- REDUCED TIME-RELATED COSTS

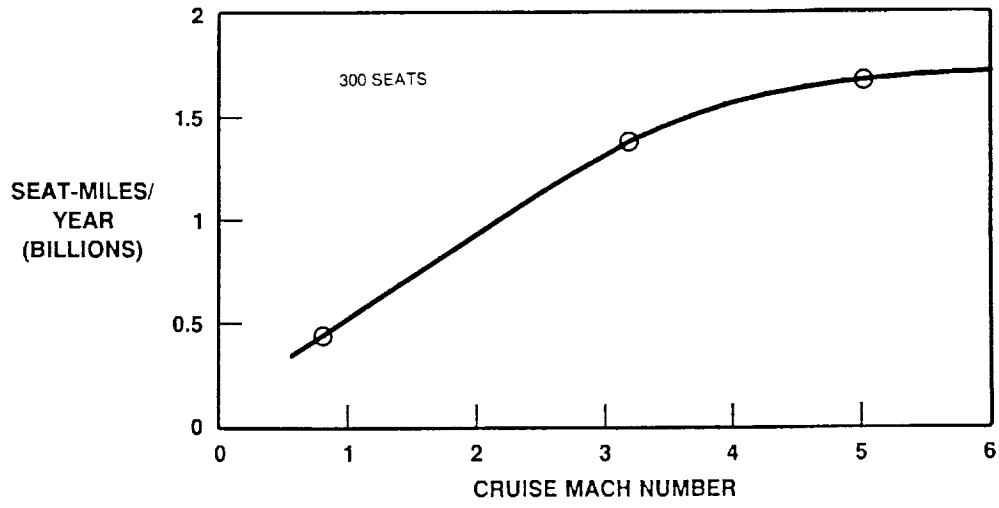

FIGURE 3-39. AIRCRAFT UNIT PRODUCTIVITY

With economic viability and environmental compatibility, the HSCT will provide still further benefits beyond those discussed earlier. These benefits will be accorded in terms of significant contributions to the U.S. gross national product, trade balance, and helping to maintain U.S. technological and aerospace leadership on a worldwide basis (Table 3-23). Technology spinoffs and contributions to other industries/products would be expected; the U.S. space program provided new technologies in the form of advanced materials, high-speed computing ability, and medical advances possibly not otherwise available in the same time frame.

TABLE 3-23
NATIONAL BENEFITS

- GNP CONTRIBUTION
- EXPORT/FAVORABLE TRADE
- OTHER INDUSTRIES/PRODUCTS
- U.S. LEADERSHIP

4.0 ENVIRONMENT

4.1 Engine Emissions

One of the key goals of the propulsion system studies was to determine the requirements for achieving low levels of NOx emissions consistent with providing the appropriate level of thrust and efficiency. Current technology engines do not offer the prospects for environmentally acceptable HSCTs from the emissions standpoint. Additional technology must be developed to reduce the magnitude of harmful combustion products.

As part of the Phase III environmental focus, both GE and P&W, under subcontracts, conducted studies of the impact of advanced technology combustors on engine emissions and engine performance. For the Mach 3.2 concept, projections were made of the impact of the use of advanced technology combustion systems for the purpose of reducing emissions of oxides of nitrogen from engines. Projections were made of the exhaust gas composition and incremental engine performance for engines incorporating progressively more advanced technology combustor systems relative to an engine with current or near term combustor technology levels.

The engine exhaust constituents – specifically the nitrogen oxides – were estimated at engine operating conditions corresponding to points along the flight profile. The supersonic cruise condition is of particular interest because oxides of nitrogen emissions are most critical at this high altitude flight condition. The combustor inlet temperatures are at their highest level at supersonic cruise. These emissions were then integrated with fleet modeling results to obtain total emissions estimates at prescribed altitude-latitude positions. The fleet modeling accounted for global operations of an equivalent fleet based on IATA traffic data.

Reference Engine. The reference engine for Phase III is the P&W VSCE designed for operation at a supersonic cruise Mach number of 3.2. Because of the elevated temperature encountered at this flight Mach number and the heat sink demands on the fuel system, the engine operates on TSJF.

Many of the exhaust gas constituents are dependent only on the composition of the fuel. These include oxides of sulphur, trace metals, and, excluding an attempt to operate in a regime of low combustion efficiency, water vapor and carbon dioxide. Table 4-1 presents a summary of the concentrations of configuration independent fuel constituents in the engine exhaust. Emissions of carbon monoxide, unburned

TABLE 4-1
EXHAUST GAS COMPOSITION CONFIGURATION-INDEPENDENT CONSTITUENTS

ALL CONCENTRATIONS IN LB/1,000 LB FUEL
P&W VSCE/JP-7 FUEL

FLIGHT CONDITION	CRUISE	CRUISE	CLIMB	CLIMB
MACH NUMBER	0.95	3.2	0.95	0.95
ALTITUDE (1,000 FT)	30	65	30	30
AUGMENTATION	NO	YES	NO	YES
CONSTITUENT				
OXYGEN (O_2)	18,450	10,300	4,100	890
WATER (H_2O)	1,350	1,350	1,350	1,350
SULFUR TRIOXIDE (SO_3)	0.0	0.0	0.0	0.0
SULFUR DIOXIDE (SO_2)	1.0	1.0	1.0	1.0
CARBON DIOXIDE (CO_2)	3,120	3,120	3,120	3,120
TRACE METALS	$< 10^{-9}$	$< 10^{-9}$	$< 10^{-9}$	$< 10^{-9}$

hydrocarbons, oxides of nitrogen and smoke were estimated from measurements from existing combustors, test rigs, and laboratory scale combustion devices. Because the main burner of the VSCE operates at a high temperature rise, the emissions characteristics were based on those of an experimental high temperature rise combustor tested by NASA (Reference 4-1)

Table 4-2 presents a summary of the projected emissions characteristics of the P&W VSCE with these near term technology combustor systems. The resulting NOx Emissions Index level – 39.5 – is significantly above estimates for the 1971 SST just prior to program cancellation. The engine manufacturers were commissioned to devise possible solutions that would reduce the NOx to acceptable levels.

Advanced Combustors. The next level of combustion technology addressed was the Rich Burn-Quick Quench concept in the main burner. All of the fuel is initially consumed in a combustion zone having a very rich mixture. Lack of sufficient oxygen for complete combustion means the temperature in this zone is moderate, and the formation rate of oxides of nitrogen is low. The combustion products pass through a second reaction zone in which the mixture strength is lean and temperatures are sufficiently high while avoiding the higher levels at which formation of oxides of nitrogen can be accelerated. The rich-to-lean mixture transition must be accomplished in the quick quench section of the combustor located axially between these zones. Emissions characteristics of the rich burn-quick quench combustor were estimated from data obtained in parametric rig tests of small scale combustors. The projections indicate substantially lower NOx emissions – 12.1 – than the current technology main burner. Table 4-3 presents a summary of the emissions characteristics of the VSCE engine with this main burner and the near term technology duct burner. At supersonic cruise condition, emissions of oxides of nitrogen are less than a third those of the reference engine of Table 4-2, based on JP-7 fuel assumed to represent TSJF for the Mach 3.2 concept. Complexity factors include length requirements, variable geometry features, fuel preparation and the need for novel material and/or cooling concepts for the liner in the rich zone.

TABLE 4-2
CURRENT TECHNOLOGY MAIN BURNER CONFIGURATION-SENSITIVE CONSTITUENTS

ALL CONCENTRATIONS IN LB/1,000 LB FUEL
P&W VSCE/JP-7 FUEL

	CRUISE	CRUISE	CLIMB	CLIMB
FLIGHT CONDITION				
MACH NUMBER	0.95	3.2	0.95	0.95
ALTITUDE (1,000 FT)	30	65	30	30
AUGMENTATION	NO	YES	NO	YES
CONSTITUENT				
CARBON MONOXIDE (CO)	4.0	2.4	23.0	88.5
UNBURNED HYDROCARBONS (THC)	0.4	0.2	1.5	3.7
OXIDES OF NITROGEN (NO_X)	9.0	39.5	18.3	8.1
NIGROGEN MONOXIDE (NO)	7.7	33.6	15.6	6.9
NITROGEN DIOXIDE (NO_2)	1.3	5.9	2.7	1.2
CONDENSATION NUCLEI ($\times 10^8$)	0.8	2.3	1.8	1.0
PERFORMANCE				
MAIN BURNER COMBUSTION EFFICIENCY (%)	99.83	99.87	99.50	99.50
Δ TSFC	BASE	BASE	BASE	BASE

TABLE 4-3
RICH BURN-QUICK QUENCH MAIN BURNER CONFIGURATION-SENSITIVE CONSTITUENTS

ALL CONCENTRATIONS IN LB/1,000 LB FUEL
P&W VSCE/JP-7 FUEL

	CRUISE	CRUISE	CLIMB	CLIMB
FLIGHT CONDITION				
MACH NUMBER	0.95	3.2	0.95	0.95
ALTITUDE (1,000 FT)	30	65	30	30
AUGMENTATION	NO	YES	NO	YES
CONSTITUENT				
CARBON MONOXIDE (CO)	1.0	1.2	23.0	89.2
UNBURNED HYDROCARBONS (THC)	0.1	0.2	1.5	3.9
OXIDES OF NITROGEN (NO^x)	2.7	12.1	17.2	8.1
NIGROGEN MONOXIDE (NO)	2.3	10.2	14.5	6.8
NITROGEN DIOXIDE (NO_2)	0.4	1.9	2.7	1.3
CONDENSATION NUCLEI ($\times 10^8$)	0.8	2.3	1.8	1.0
PERFORMANCE				
MAIN BURNER COMBUSTION EFFICIENCY (%)	99.96	99.95	99.50	99.50
Δ TSFC	−0.13	−0.05	0.0	0.0

The lean, pre-mixed, pre-vaporized combustion system is the most aggressive technology considered applicable to aircraft engines. This combustor achieves very low NOx by not only burning at lean overall mixture strengths, but also by avoiding any locally rich regions or burning around fuel droplets. This is accomplished by pre-vaporizing the fuel and injecting it into the air in a pre-mixing passage to deliver a homogeneous droplet-free mixture to the combustion zone. The mixture strength is set as lean as possible, but above stability or inefficiency thresholds. The pre-mixed, pre-vaporized combustor is theoretically capable of producing very low NOx emissions. Operation of the combustion zone over a very narrow range of mixture strengths requires variable geometry of air passages to produce the necessary shifts in airflow with overall fuel/air ratio. A practical combustor using pre-vaporized liquid fuel has never been demonstrated. Use of the lean, pre-mixed, pre-vaporized combustor requires that the fuel be externally heated to about 800°F before entering the combustor.

Table 4-4 presents the estimated emissions characteristics of the engine with this main burner and, for comparison purposes, with both the near term and the pre-mixed, pre-vaporized duct burner pilot stage at the augmented flight conditions. The total oxides of nitrogen emissions at supersonic cruise are less than one fourth that of the engine with the current technology main burner. (Emissions index of 8.65 versus 39.5) Substituting the lean, pre-mixed, pre-vaporized duct burner pilot stage for its near term counterpart reduces the supersonic cruise NOx emissions by another 30 percent to 6.10.

A combustor concept projected to produce the lowest NOx emissions is considered to be a very high risk approach. Substantial additional development is required to produce viable pre-vaporizing and pre-mixing systems for use with liquid fuels and the variable geometry airflow systems required for stochiometry. There are also fundamental risk elements such as pre-ignition and flashback in the pre-mixing passages.

Differences in engine performance with the three main burner concepts are projected to be extremely small. Combustion efficiency should be above 99.0 percent. Some variants in main burner combustion efficiency are noted at the subsonic and supersonic cruise conditions and the corresponding increments in TSFC are listed in Tables 4-3 and 4-4. There is no projected difference in duct burner performance parameters with the use of the lean, pre-mixed, pre-vaporized as opposed to the current technology pilot stage.

TABLE 4-4
LEAN PREMIXED PREVAPORIZED MAIN BURNER CONFIGURATION-SENSITIVE CONSTITUENTS

ALL CONCENTRATIONS IN LB/1,000 LB FUEL
P&W VSCE/JP-7 FUEL

	CRUISE	CRUISE	CRUISE	CLIMB	CLIMB	CLIMB
FLIGHT CONDITION						
MACH NUMBER	0.95	3.2	3.2	0.95	0.95	0.95
ALTITUDE (1,000 FT)	30	65	65	30	30	30
AUGMENTATION	NO	YES	YES	NO	YES	YES
DUCT BURNER PILOT STAGE	N/A	CURRENT	PREMIXED	N/A	CURRENT	PREMIXED
CONSTITUENT						
CARBON MONOXIDE (CO)	8.20	2.47	2.47	11.50	84.80	84.80
UNBURNED HYDROCARBONS (THC)	0.80	0.22	0.22	0.35	3.30	3.30
OXIDES OF NITROGEN (NOx)*	0.60	8.65	6.10	5.65	3.45	3.15
NITROGEN MONOXIDE (NO)*	0.51	7.30	5.20	4.80	2.92	2.67
NITROGEN DIOXIDE (NO_2)*	0.09	1.35	0.90	0.85	0.53	0.48
CONDENSATION NUCLEI ($\times 10^8$)	0.60	1.97	1.60	1.05	0.68	0.68
PERFORMANCE						
MAIN BURNER COMBUSTION EFFICIENCY (%)	99.65	99.87	99.87	99.84	99.84	99.84
Δ TSFC (%)	+0.18	0.00	0.00	−0.34	−0.12	−0.12

*OXIDES OF NITROGEN ESTIMATES ARE GOALS BASED ON DATA FROM IDEAL LABORATORY EXPERIMENTS

4.2 Sonic Boom

Sonic boom analyses conducted in Phase I and II were primarily limited to the estimation of sonic boom overpressures on the ground. During these phases, DAC developed new technologies and conducted independent research in the area of advanced prediciton methods to allow for more accurate, in-depth sonic boom analyses. The main thrust of the Phase III sonic boom activity was to generate accurate sonic boom estiamtes for the baseline Mach 3.2 (D3.2-3A) concept, and to investigate means to minimize these booms through both operational and planform shape modifications.

Criteria. Sonic booms caused by supersonic aircraft flyovers exhibits vastly different acoustic characteristics than subsonic aircraft flyover noise. The different nature of these two types of sound is shown in Figure 4-1, which provides a comparison of acoustic time histories for a representative sonic boom and subsonic aircraft flyover. A sonic boom is a high energy, impulsive sound that generates a large subaudible, low-frequency component. This is in contrast to subsonic flyover noise that is primarily in the audible range. Although the exact role of low frequency energy from sonic booms and human response has not been quantified, it is not acceptable to assess human response using metrics that excessively attenuate low-frequency noise, such as dBA and EPNdB.

Sonic boom levels are typically measured by peak overpressure, which is reflected in the fact that maximum overpressure is the most commonly cited boom metric. However, human response to sonic booms is a function of the entire waveshape, not just the peak overpressure (References 4-2 and 4-3). A wide variety of laboratory and field testing has been conducted in the attempt to determine metrics that best quantify the subjective human response to sonic booms and corresponding acceptable levels. A comprehensive survey of this data was conducted with the goal of arriving at a single metric to quantify subjective response. The sonic boom response tests conducted to date can be broken down into two different sets –

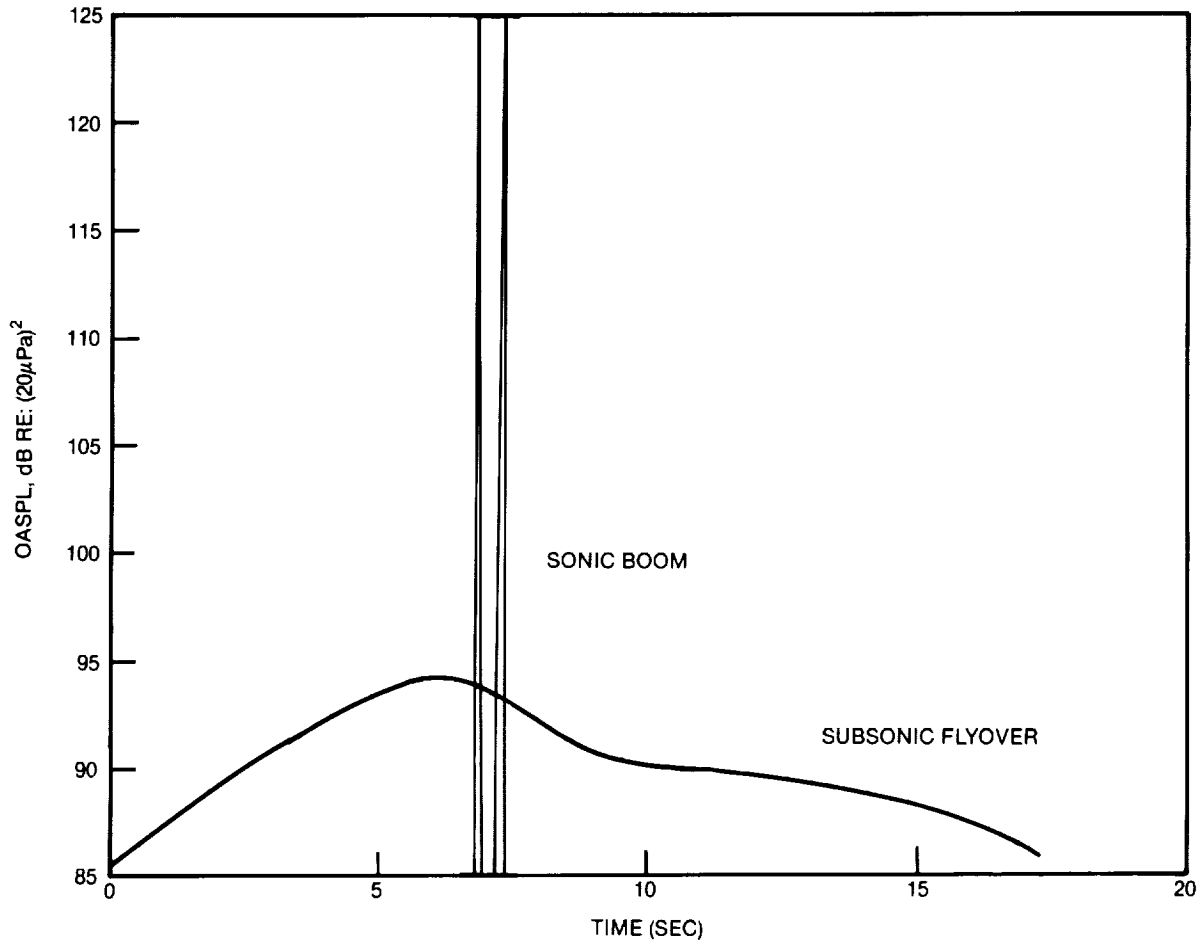

FIGURE 4-1. COMPARISON OF SONIC BOOM AND SUBSONIC FLYOVER TIME HISTORIES

studies of relative acceptance of individual sonic boom events and studies on community response to multiple daily events from simulated operation of a supersonic transportation system. The relative acceptance of individual sonic boom events is best measured with a loudness descriptor. The best metric of this type would appear to be Stevens (Mark VII) model for Perceived Level in PLdB (Reference 4-4) because of the solid foundation upon which it was developed and its sensitivity to fine changes in waveform shape.

A large community, consisting of listeners in a variety of conditions and locations, both indoors and outdoors, is not sensitive to the fine changes in waveform shape to which a loudness descriptor is sensitive. Community response to multiple daily sonic boom events seems to be best measured with a Day-Night Average C-Weighted Sound Exposure Level (LCdn) (Reference 4-5). This metric has been derived from the extensive attitude surveys conducted during the Oklahoma City test and has been verified with testing done by the Army Construction Engineering Research Laboratory (Reference 4-6). The details concerning L_{Cdn} and its application to environmental impact studies can be found in the report of Working Group 84 of the National Research Council (Reference 4-7).

A summary is presented in Table 4-5 which is a compilation of three of the more notable tests in which sonic boom acceptability was studied. The weighted average values were calculated by weighting the Edwards test by a factor of three to reflect the improved accuracy of a field test with actual booms as opposed to a laboratory test with simulated booms. This type of summary has led to the development of tentative sonic boom design criteria at Douglas, a Perceived Level of 90 PLdB and a C-Weighted Sound Exposure Level of 102 dB. Further response testing is needed before one specific metric can be selected and precise criteria set.

TABLE 4-5
SUMMARY OF VARIOUS CRITERIA FOR ACCEPTABLE LEVELS, MEASURED OUTDOORS AT THE GROUND SURFACE FOR A SINGLE SONIC BOOM EVENT HEARD INDOORS

TEST	% NOT AFFECTED OR % ACCEPTING	PERCEIVED LEVEL, PLdB	L_{CE}, dB
HIGGINS AND SAN LORENZO (10)	95 80	84 92	98 105
MABRY AND ONCLEY (11)	95 80	94* 96*	106* 108*
EDWARDS AFB (12)	95 80	88 91	100 103
WEIGHTED AVERAGE	95 80	88 92	101 104

*ESTIMATED OUTDOOR LEVELS

Analysis. Sonic boom waveforms for HSCT configurations were predicted using two different methods; one for the Mach 3.2 concept (supersonic), and one for the Mach 5.0 concept (hypersonic). The sonic boom for the Mach 3.2 concept was calculated using MDBOOM, a modified version of FOBOOM written by Kenneth Plotkin of Wyle Laboratories. A schematic of MDBOOM operation is shown in Figure 4-2. Volume and lift distributions are generated along the Mach cutting plane and are used to calculate the corresponding F-function for each discrete azimuthal angle. Atmospheric propagation is performed via Thomas' waveform parameter method (Reference 4-8) to yield sonic boom waveforms on the ground at each point along the boom footprint. Rise times are calculated for each shock using Taylor's shock solution. MDBOOM accepts a user-defined arbitrary flight path input and performs boom calculations, including the effects of focusing. MDBOOM has been validated, and a comparison of an MDBOOM prediction with flight test data from an SR-71 is shown in Figure 4-3.

The limitation of MDBOOM is that the propagation routine and F-function calculation are based on quasilinear theory, which breaks down for highly nonlinear hypersonic pressure fields. In order to overcome this and generate accurate estimates for the Mach 5.0 concept, which would be expected to generate strong shocks, a nonlinear numerical code was used to calculate the flow field out to a radius where linear theory is viable. Currently, the calculation is limited to the under track azimuth with scaling for the off-track component.

The sonic boom waveforms and their corresponding response metrics are shown for each configuration at the beginning and end of cruise in Figure 4-4. Except for focus conditions, the most critical sonic boom occurs at the beginning of cruise directly under the flight track. As the aircraft decreases in weight and increases in altitude over the course of a mission (for a constant C_L cruise) the sonic boom levels drop significantly. At Mach 3.2, the beginning to end-of-cruise level drops from 1.9 psf to 1.2 psf, and at Mach 5.0, the level drops from 2.0 psf to 1.6 psf. These results imply that an aircraft which cannot meet boom design goals and fly supersonically over land at the beginning of cruise may be able to do so at some point along its flight path.

The sonic boom carpets at the beginning of cruise for the Mach 3.2 and Mach 5.0 concepts are shown in Figures 4-5 and 4-6, respectively. These figures show that the off-track boom overpressures decrease significantly from under-track levels. More than one-half of the boom carpet for the Mach 3.2 concept at the beginning of cruise experiences an overpressure of less than 1.0 psf, even though the centerline overpressure

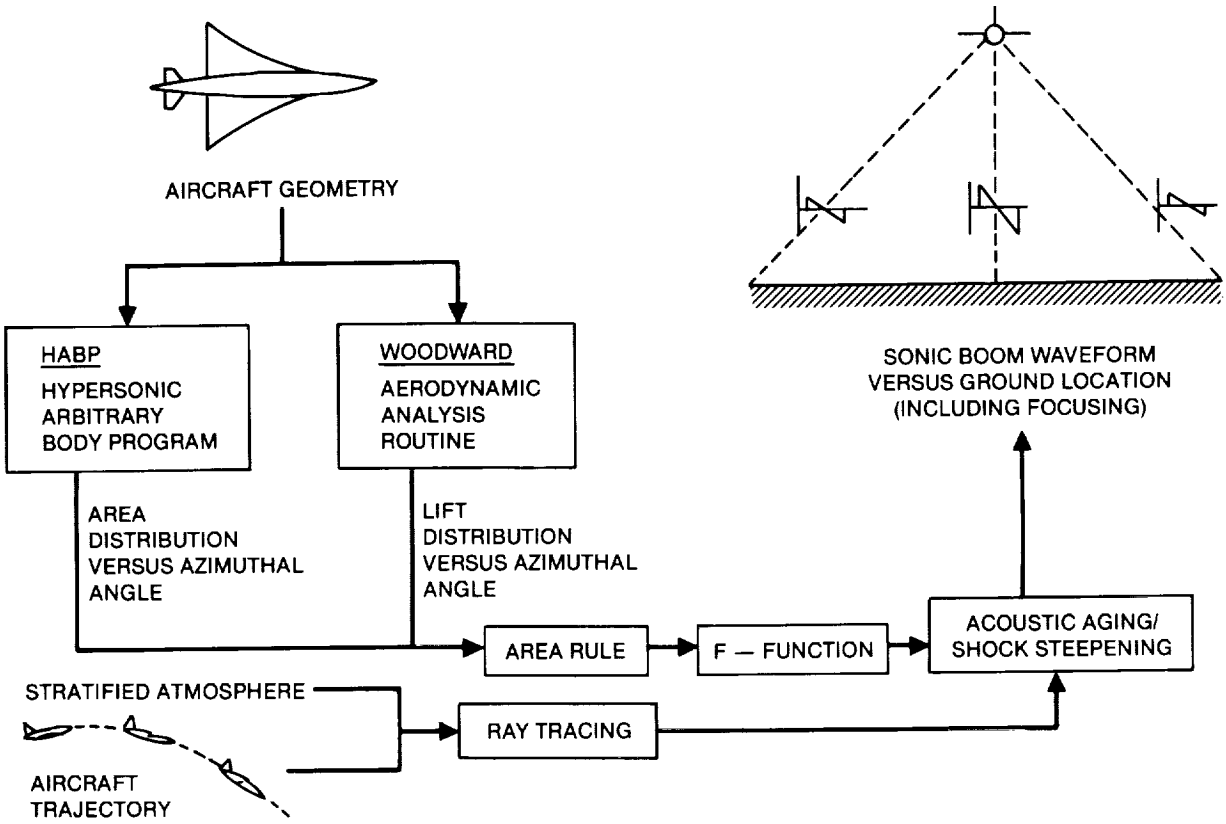

FIGURE 4-2. SUPERSONIC BOOM PREDICTION METHODOLOGY VIA MDBOOM

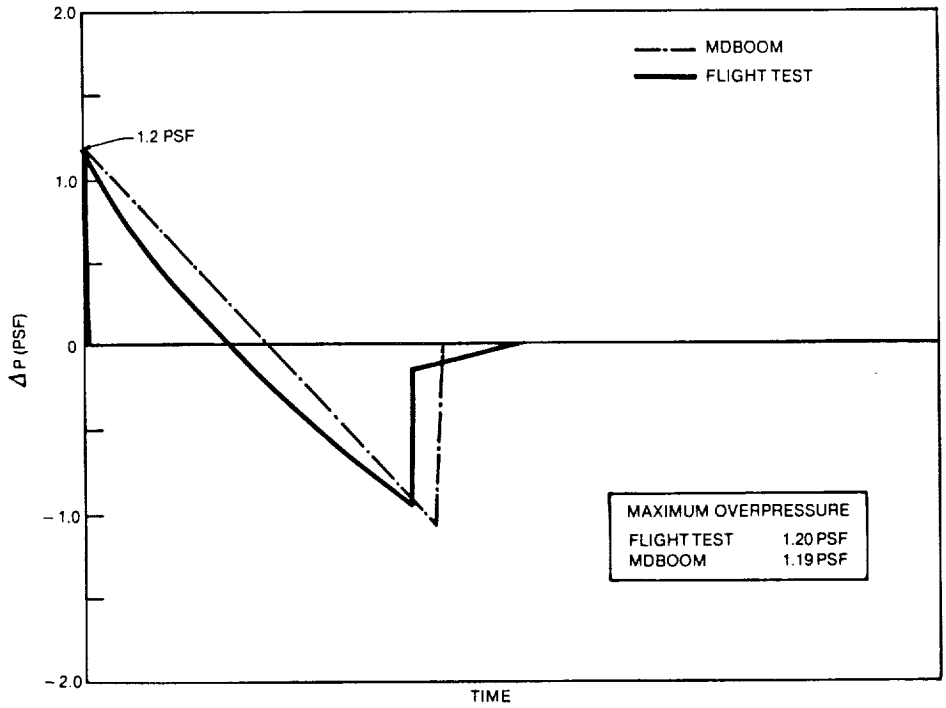

FIGURE 4-3. FLIGHT TEST DATA OF SR-71 SONIC BOOM VERSUS PREDICTION FROM MDBOOM

HUMAN RESPONSE METRICS

	3.2	5.0
P, PLdB	102.1	100.7
L_{CE}, dB	107.4	106.1
ΔP MAX, PSF	1.9	2.0

HUMAN RESPONSE METRICS

	3.2	5.0
P, PLdB	95.9	97.2
L_{CE}, dB	103.0	103.8
ΔP MAX, PSF	1.2	1.6

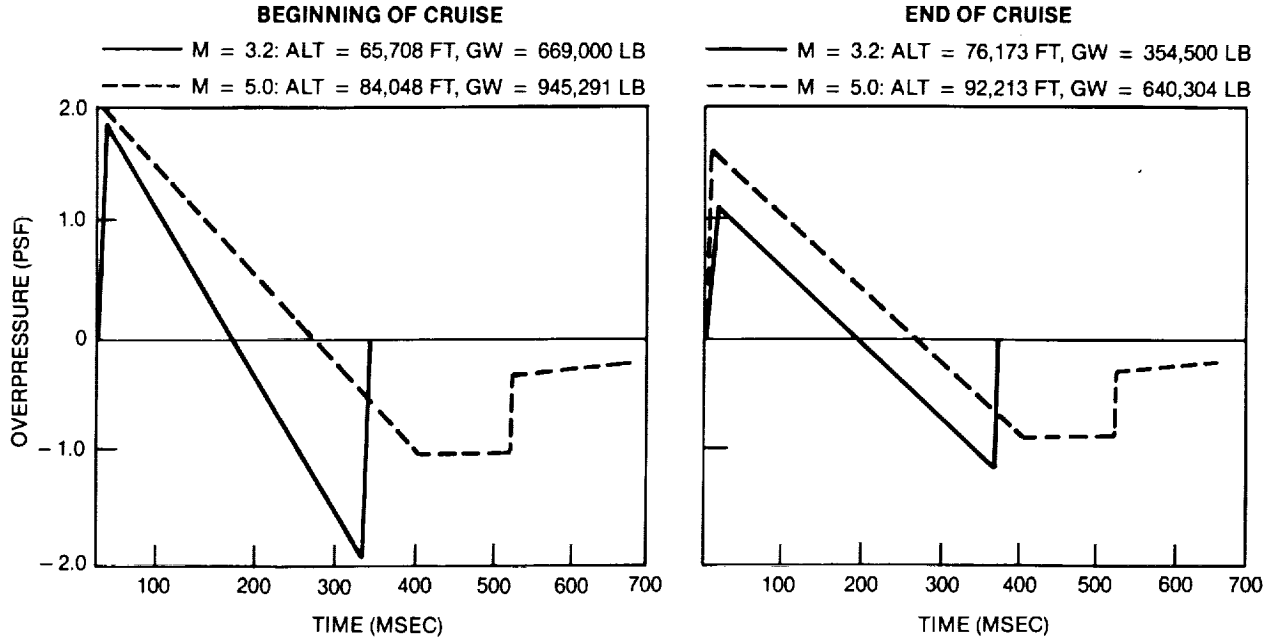

FIGURE 4-4. SONIC BOOM WAVEFORMS

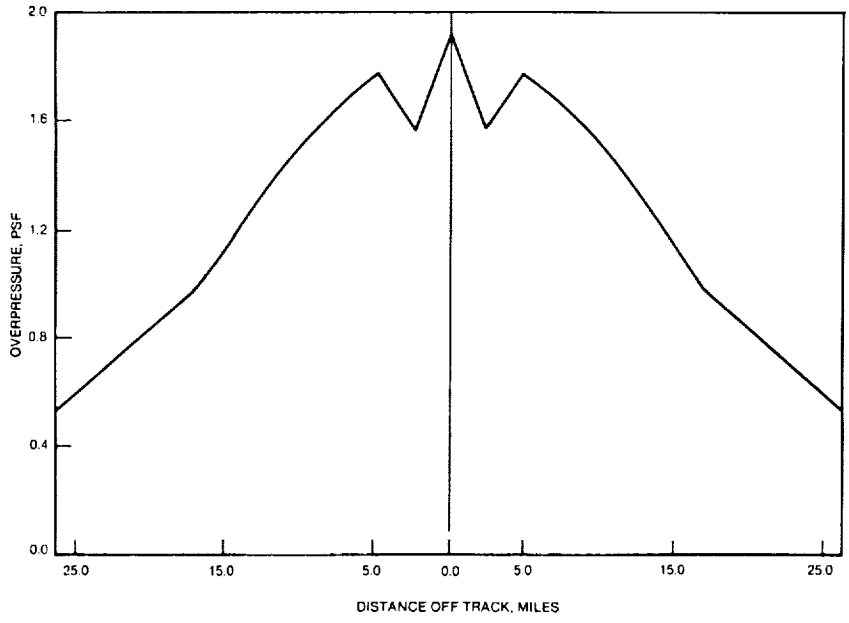

FIGURE 4-5. SONIC BOOM OVERPRESSURES ON THE GROUND FOR MACH 3.2 CONCEPT

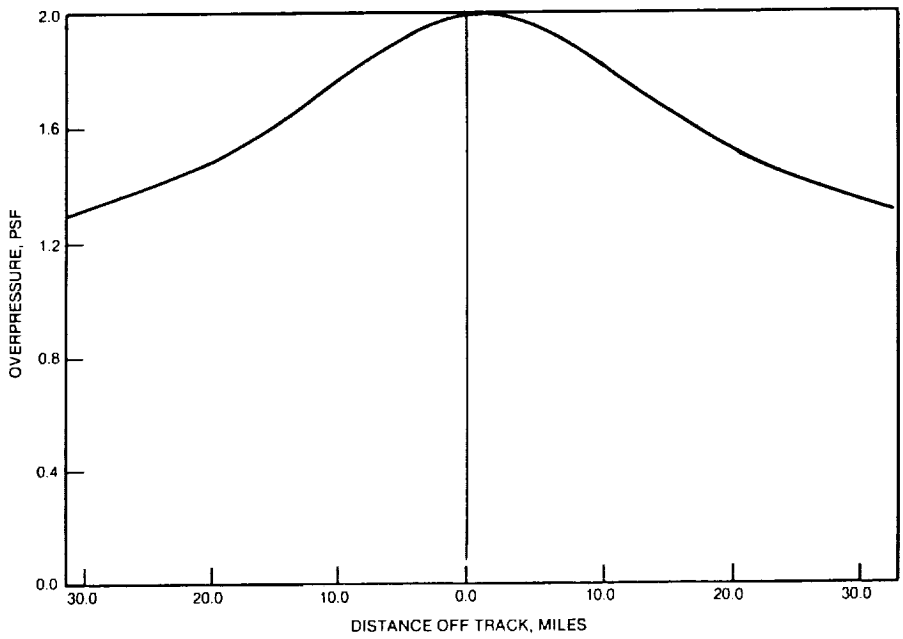

FIGURE 4-6. SONIC BOOM OVERPRESSURES ON THE GROUND FOR MACH 5.0 CONCEPT

is 1.9 psf. However, in the case of the Mach 5.0 concept, the off-track boom overpressures decay at a slower rate. The large width of the boom corridor (52 miles at Mach 3.2, 65 miles at Mach 5.0) indicates that the off-track boom levels are important and need to be considered for environmental impact. A method that integrates boom level and affected area may be necessary.

Sonic Boom Minimization. Sonic boom minimization can be approached from two different perspectives. The most direct approach is to design and operate the aircraft in such a way that the shock strength, and hence peak overpressure at the ground, is minimized. Aerodynamically slender, long vehicles are typically the end product of this type of approach. The second approach is that of sonic boom shaping. This approach involves creating sonic boom waveshapes with minimum shock strengths, thereby reducing the amount of high frequency energy contained in the boom. This method is considerably more difficult from a design standpoint and will require aircraft configurations that depart considerably from aerodynamically optimized designs. It may be necessary to cruise at lower altitudes to avoid the formation of a far field N-wave. Both of these approaches were considered in an attempt to minimize the boom from the Mach 3.2 concept.

Various modifications were made to the baseline Mach 3.2 concept to try to reduce the N-wave overpressures. These configurations were evaluated assuming a uniform lift distribution and a common fuselage with the baseline. The most promising configuration involved a modification and extension of the wing, which allowed for a 20-percent reduction in overpressure. A comparison of this configuration with the baseline is shown in Figure 4-7. Further sonic boom minimization potential exists in increased altitude cruise. A trade study of cruise altitude and gross weight versus boom overpressure, shown in Figure 4-8, revealed that a 20-percent reduction in overpressure can be obtained by increasing the cruise altitude from 65,000 to 85,000 feet. A further 20-percent reduction in overpressure is available through a 30-percent weight reduction. These results indicate that a combination of careful aircraft shaping, weight reduction, and high altitude cruise can lead to far field N-waves of 1.0 psf or less.

The attempt to shape the boom into a flat-top waveform was unsuccessful, although promising results were obtained. The closest achievement at creating a flat-top waveform was an aircraft with front canards extending back to the wing. The F-function for this planform is shown in Figure 4-9, along with the theoretical goal. The flat-top waveform will have to be a primary design constraint from the start if it is to be realized.

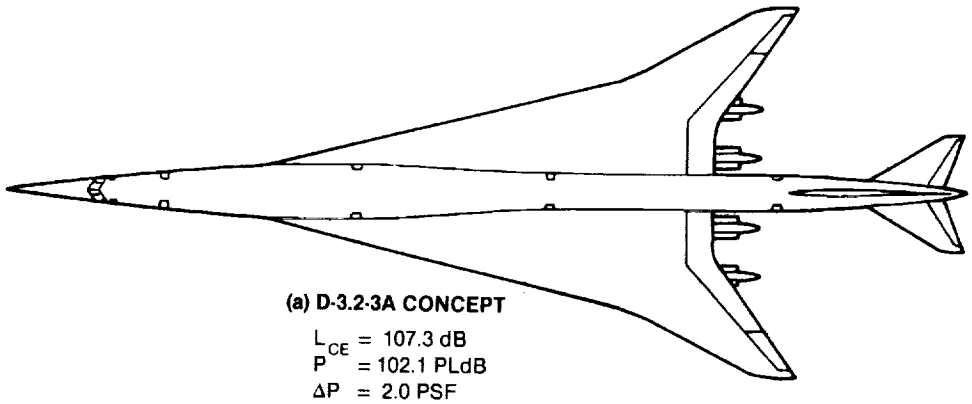

(a) D-3.2-3A CONCEPT

L_{CE} = 107.3 dB
P = 102.1 PLdB
ΔP = 2.0 PSF

TENTATIVE CRITERIA
L_{CE} ~ 102 dB
P ~ 90PLdB
ΔP ~ 1 PSF

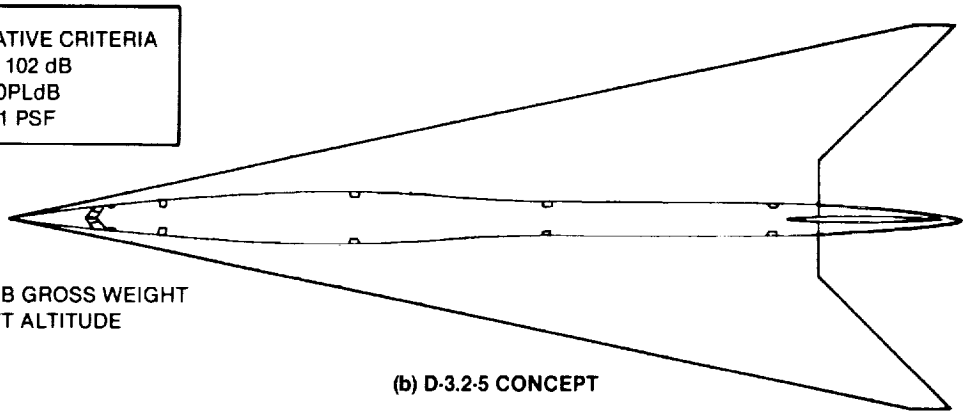

618,000-LB GROSS WEIGHT
65,000-FT ALTITUDE

(b) D-3.2-5 CONCEPT

L_{CE} = 105.6 dB
P = 99.7 PLdB
ΔP = 1.6 PSF

FIGURE 4-7. MACH 3.2 SONIC BOOM MINIMIZATION

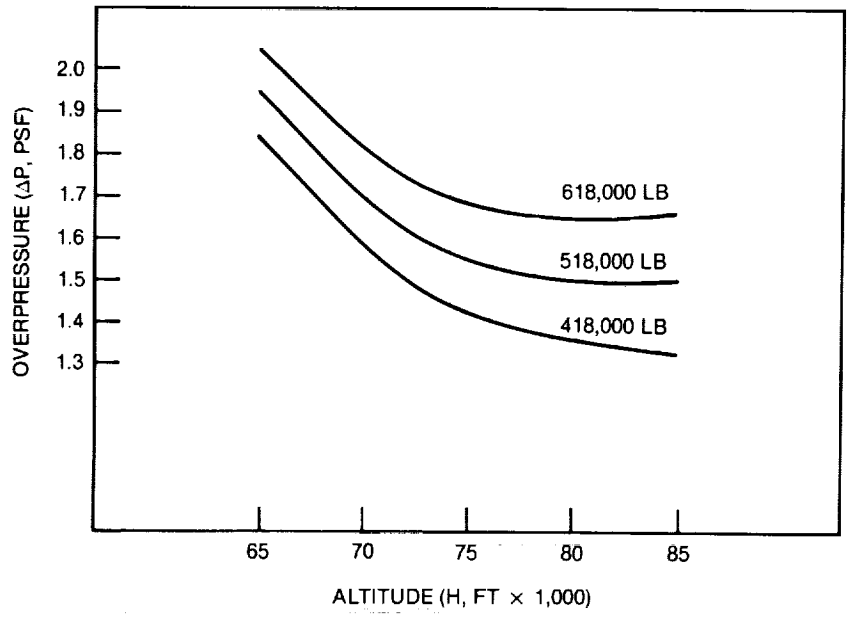

FIGURE 4-8. SONIC BOOM TRADE STUDY FOR D3.2-3A CONCEPT

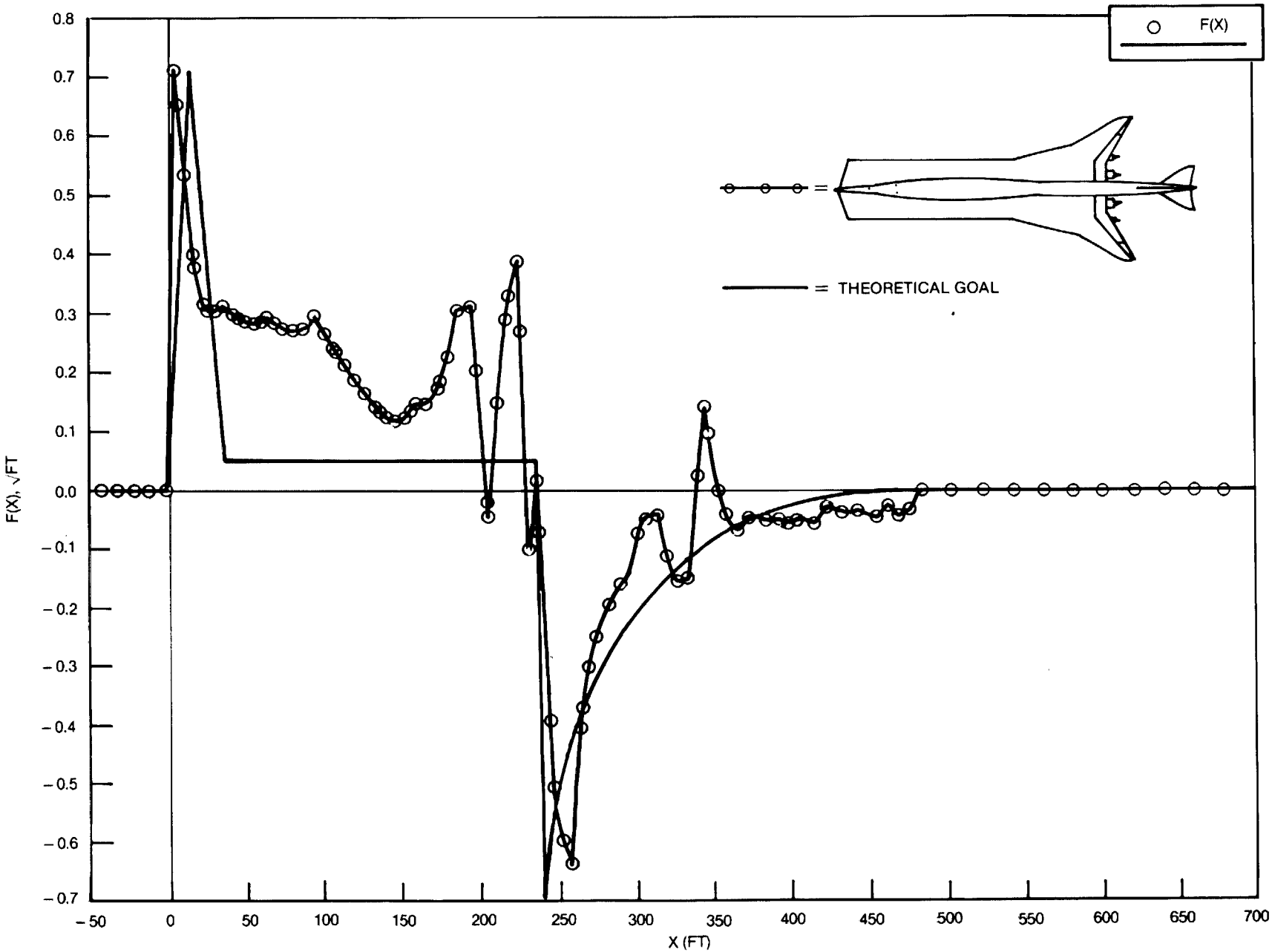

FIGURE 4-9. FUNCTION COMPARISON

4.3 Community Noise

The large majority of the subsonic fleet will be Stage 3 at the time the HSCT enters service. Hence, it was assumed that the HSCT fleet also must meet FAR Part 36 Stage 3 noise requirements. The airlines generally agree that Stage 3 is an appropriate HSCT design goal. The airlines also believe that HSCT development will require international cooperation (e.g., within ICAO) to achieve an acceptable HSCT community noise standard. The public and regulatory agencies have more than 20 years experience with Effective Perceived Noise Level (EPNL). Other noise metrics, such as dB(A), have been considered and would result in lower numerical values (100 EPNdB $\simeq$ 87 dB(A)). However, the airplane would not be any quieter. Introduction of a new noise metric could be interpreted as misleading; therefore, EPNL will be used.

Various noise reduction concepts considered by Douglas that may be used to control jet noise are listed in Table 4-6, together with the expected range of noise attenuations. The individual noise attenuations are not additive. Combinations of these concepts could provide 10 to 20 dB noise attenuation. Some of these noise reduction concepts have been tested and verified under past research and technology development programs. However, the tests were not conducted at the higher jet temperatures and velocities expected for the HSCT engine cycles. Therefore, more tests are required to extend existing data bases.

Douglas Noise Estimates. Noise levels were estimated at the FAR Part 36 reference locations for the Phase III Mach 3.2 (D3.2-3A) and Mach 5.0 (D5.0-15A) concepts and are listed in Table 4-7. The noise levels in the table include the noise reduction effects of the inverted velocity profile (IVP) and a jet noise suppressor, and a treated ejector for the VSCE concept only. The ejector may not be compatible with the VCE concept single expansion ramp nozzle (SERN).

The Part 36 sideline noise estimates have assumed 12-dB and 5-dB suppression for the VSCE and VCE concepts, respectively. The sideline noise levels for the Mach 3.2 concept exceed the Stage 3 require-

TABLE 4-6
JET NOISE REDUCTION CONCEPTS

CONCEPT	REDUCTION (EPNdB)* (RE: CONICAL NOZZLE)
INVERTED VELOCITY PROFILE	4-6
SUPPRESSOR	6-8
SUPPRESSOR AND EJECTOR	7-15
THERMAL SHIELD	2-4
POROUS CENTERBODY	2-5

*NOISE REDUCTIONS ARE NOT ADDITIVE

TABLE 4-7
ESTIMATED FAR PART 36 NOISE LEVELS (EPNdB)

CONCEPT	ENGINE	TOGW (LB)	SIDELINE	TAKEOFF (CUTBACK)	APPROACH
D-3.2-3A	P&W VSCE	769,000	112 (– 12)	110 (– 8)	106 (– 6)
STAGE 3 REQUIREMENTS			102.5	105.4	105
D-5.0-15A	GE VCE	1,213,000	116 (– 5)	N/A	N/A
STAGE 3 REQUIREMENTS			103	106	105
CONCORDE	OLYMPUS 593	385,000	112.0	119.5	117.0

NOTE: ABOVE NOISE ESTIMATES DO NOT INCLUDE SHOCK CELL, DUCT BURNER, OR TURBOMACHINERY NOISE

( ) SUPPRESSION ASSUMED EXCLUDING IVP

INCLUDES INVERTED VELOCITY PROFILE PLUS SUPPRESSION DEVICES

ments by 9.5 dB. The Mach 5.0 concept sideline noise is 13 dB above the requirement. An additional 2- to 3-dB reduction in sideline noise could be achieved with an operational procedure where engine thrust is reduced early in the flight path. However, the takeoff cutback noise levels would increase slightly due to a lower airplane height over the takeoff monitor.

A parametric study at Phase II takeoff weights was conducted to determine the effect of oversizing the engine on Part 36 noise levels. Details of engine parameters for the various engine sizes is given in Table 4-8. The noise results for the Mach 3.2 and Mach 5.0 concepts are given in Tables 4-9 and 4-10, respectively. Increasing the Mach 3.2 engine size by 110 percent reduced the sideline noise by up to 19 dB, but resulted in an aircraft range loss of 1,400 nautical miles. A lift/drag improvement of 20 percent reduced takeoff and approach noise levels, but did not affect sideline noise. In order to achieve the design range of 6,500 nautical miles for a maximum takeoff gross weight equal to 684,000 pounds, an engine thrust of 60,000 pounds at power code 100 is necessary for D3.2-3A. For the Mach 5 configuration at a maximum takeoff gross weight equal to 984,000 pounds on engine thrust, 66,000 pounds at power code 40 is required. Oversizing the engine by 164 percent decreases the sideline noise by 9 dB.

P&W Noise Estimates. P&W predicted FAR 36 sideline noise over a range of available engine thrust for a 600 pounds per second airflow VSCE. Noise estimates were generated for both a baseline, unsuppressed VSCE and for a VSCE with stowable outer stream jet noise suppressor. The suppressor features 12 chutes with 24 tubes at the outer rim, having a base area to jet area ratio of 2.6. A treated ejector with I/II ratio of 1.6 is included with 1.5 inch deep acoustic treatment, similar to and scaled from that used in the VCE Testbed program.

Use of independently variable fan and core jet areas is a key feature of the VSCE. This allows optimization of the takeoff part power airflow lapse rate of the VSCE enabling "high flowing" of the engine over a range of takeoff power conditions. The engine thereby maintains maximum airflow and achieves thrust variation primarily through changes in jet velocity.

The VSCE with a suppressor nozzle would normally have a fixed duct stream (suppressor) jet area when deployed over the sideline and community noise monitors. For purposes of this sideline noise study, however, a variable area suppressor was assumed. This will allow optimization of jet noise at the sideline condition. Once the amount of engine scaling/oversizing for sideline noise has been determined (along with

TABLE 4-8
ENGINE SIZING PARAMETERS (SEA LEVEL STATIC CONDITIONS)

CONCEPT	ENGINE SCALE FACTOR	ENGINE THRUST FN (× 1,000 LB)	CORE STREAM FLOW			DUCT STREAM FLOW		
			V_J (FPS)	T_J (R)	A_J (SQ IN.)	V_J (FPS)	T_J (R)	A_J (SQ IN.)
D-3.2-3A P&W VSCE								
PC50FN60	2.1	60	1,180	1,410	2,245	1,700	805	910
PC50FN60 (+ 20% L/D)	2.1	60	1,180	1,410	2,245	1,700	805	910
PC50FN80	2.8	80	1,180	1,410	2,245	1,700	805	910
PC70FN60	1.4	60	1,570	1,545	1,275	2,670	2,080	1,100
PC70FN80	1.9	80	1,570	1,545	1,275	2,670	2,080	1,100
PC100FN60	1.0	60	2,090	1,805	735	3,555	3,970	1,280
PC100FN120	2.0	120	2,090	1,805	735	3,555	3,970	1,280
D-5.0-15A GE VCE								
PC40FN66	1.0	66	1,490	855	435	1,070	1,755	1,645
PC50FN66	1.6	66	3,310	2,125	1,215	N/A	N/A	N/A
PC32FN66	0.6	66	1,070	760	165	1,900	1,455	1,505

TABLE 4-9
ESTIMATED FAR PART 36 NOISE LEVELS (EPNdB)
INCLUDES INVERTED VELOCITY PROFILE ONLY
TOGW = 684,000 LB P&W VSCE (D-3.2-3A CONCEPT)

	ENGINE SCALE FACTOR	SIDELINE	TAKEOFF (CUTBACK)	APPROACH	RANGE (N MI)
STAGE 3 REQUIREMENT		102.1	104.8	105.0	
CONFIGURATION*					
PC50FN60	2.1	105.0	103.0	102.0	– 1,400
PC50FN60 (20% L/D)	2.1	105.0	98.0	98.0	– 1,400
PC50FN80	2.8	106.0	89.0	99.0	– 2,400
PC70FN60	1.4	122.0	111.0	107.0	– 200
PC70FN80	1.9	123.0	96.0	103.0	– 1,100
PC100FN60	1.0	124.0	118.0	112.0	REF DESIGN RANGE (6,500)
PC100FN120	2.0	126.0	94.0	103.0	– 1,800
CONCORDE	—	112.0	119.5	117.0	3,200

NOTES: — NO SHOCK CELL OR DUCT BURNER NOISE INCLUDED IN ESTIMATES
— APPROACH NOISE ESTIMATES EXCLUDE TURBOMACHINERY NOISE
*SEE TABLE 4-8 FOR POWER CODE INFORMATION

TABLE 4-10
ESTIMATED MACH 5.0 FAR PART 36 NOISE LEVELS (EPNdB)
INCLUDES INVERTED VELOCITY PROFILE PLUS EJECTOR*
TOGW = 984,000 GE VCE (D-5.0 -15A CONCEPT)

	ENGINE SCALE FACTOR	SIDELINE	TAKEOFF (CUTBACK)	APPROACH	RANGE (N MI)
STAGE 3 REQUIREMENT		103.0	106.0	105.0	
CONFIGURATION**					
PC40FN66	1.0	116.0	N/A	N/A	REF DESIGN RANGE (6,500)
PC32FN66	1.6	107.0	N/A	N/A	– 3,000
PC50FN66	0.6	132.0	N/A	N/A	+ 1,905
CONCORDE	—	112.0	119.5	117.0	3,200

*NOTE: — THIS NOISE REDUCTION CONCEPT US NOT COMPATIBLE WITH THE SERN NOZZLE

**SEE TABLE 4-8 FOR POWER CODE INFORMATION

the associated suppressor jet area), that suppressor jet area would then be held fixed at that design duct jet area for future studies such as cutback noise. Full two-stream nozzle variability is still available at all other flight conditions with the suppressor in the stowed position.

Total and individual component noise levels for the engine performance points used by P&W are given for the unsuppressed and suppressed VSCE in Tables 4-11 and 4-12, respectively. The major noise sources are the jet mixing noise (high and low frequency components) and the duct burner combustion noise. Jet shock noise is not found to be a significant contributor, except at the lowest powers. A noise benefit on the order of 4 dB was estimated by P&W to be available from a 180 degree circumferential Thermal Acoustic Shield. This benefit should apply to both the jet and duct burner sources at the nozzle.

P&W assumed a four-engine HSCT aircraft with a takeoff gross weight of 769,000 pounds (D3.2-3A) and a sea level static takeoff thrust of 61,500 pounds (57,700 pounds at 1,000 feet altitude sideline condition), and 0.3 Mach number for the oversizing study. The four variants of the VSCE candidate engine of the study, with 600 pounds per second design airflow size, are jet noise dominated at this takeoff thrust and are projected to exceed the Stage 3 sideline noise limit.

TABLE 4-11
P&W VSCE NOISE ESTIMATES — UNSUPPRESSED

IVP/DUCT BURNER UNSUPPRESSED WITH TREATED EJECTOR								
FNT (LBF)	WEIGHT (LBM/SEC)	EFFECT. JET VEL. (FPS)	EPNL TOTAL	JET TOTAL	HIGH FREQUENCY JET	LOW FREQUENCY JET	SHOCK EPNL	EPL D/B*
49,111	608.36	2,937.80	118.7	117.3	112.5	115.3	96.9	112.5
48,607	607.80	2,913.50	118.4	117.1	112.3	115.1	96.2	112.2
45,008	604.29	2,736.70	116.7	115.4	110.7	113.4	90.6	110.1
40,734	600.73	2,521.80	114.2	113.0	108.3	110.9	89.9	107.7
35,308	591.16	2,261.60	110.5	109.2	104.4	107.0	93.4	103.8
25,636	527.08	1,908.20	103.7	103.0	96.3	99.9	96.4	94.3
20,231	488.70	1,671.40	100.6	100.5	89.9	93.2	98.4	82.6

TABLE 4-12
P&W VSCE NOISE ESTIMATES — SUPPRESSED

IVP/DUCT BURNER SUPPRESSED WITH TREATED EJECTOR								
FNT (LBF)	WEIGHT (LBM/SEC)	EFFECT. JET VEL. (FPS)	EPNL TOTAL	JET TOTAL	HIGH FREQUENCY JET	LOW FREQUENCY JET	SHOCK EPNL	EPL D/B*
43,174	604.25	2,639.1	114.9	112.8	108.7	110.2	88.1	110.1
39,053	600.27	2,433.3	111.9	109.5	103.6	107.6	85.5	107.7
33,865	590.71	2,184.4	108.0	105.5	98.5	103.9	89.7	103.8
24,701	526.74	1,848.4	101.3	100.0	91.6	96.8	94.0	94.3
19,477	488.86	1,621.3	98.5	98.3	86.6	89.9	96.7	83.6

*D/B = DUCT BURNER

For engines dominated by jet noise at takeoff powers, one means of reducing sideline noise at a given fixed thrust is to oversize the engines (increased airflow, diameter, and thrust) and operate them at a lower relative power (and exhaust velocity) takeoff condition. The noise penalty associated with increased size – engine noise ~10 log (airflow size) – is more than offset by operation at a lower percent of full power with attendant reduced jet velocity – jet noise of order ~60 log (velocity). The larger engines, however, are heavier and do not operate at optimal power in the cruise regime, thus having increased fuel burn and either an aircraft takeoff gross weight (at constant range) or range penalty (at constant gross weight).

The basic noise predictions for this study were made for an engine having a 600 pounds per second design inlet airflow (reference) size. The engine can be easily resized using the relationship that noise scales as:

Δ SPL = 10 log (design airflow/600 pps) ~dB

Similarly, thrust of the 600 pounds per second engine would scale directly as:

Thrust = Ref. Thrust × (design airflow/600 pps) ~dB

Figure 4-10 shows the oversizing relative to the reference 600 pounds per second required for the suppressed VSCE to meet the FAR 36 Stage 3 sideline noise requirement. Relative size is shown both with and without addition of the Thermal Acoustic Shield. Dependent on use of jet suppression and use of thermal acoustic shield, the engine oversizing required to meet the FAR 36 Stage 3 sideline noise limit is 90 percent to 150 percent relative to the 600 pounds per second reference design size or 1140 to 1500 pounds per second airflow size. The engine weight penalty would be directly proportional to this airflow size. This result is similar to that found by Douglas.

GE Noise Estimates. The objective of the GE noise study was to make sideline noise estimates for the Mach 5 (D5.0-15A) concept with a 2D-CD wedge SERN nozzle (Single Expansion Ramp Nozzle). Development of the GE noise estimate for Mach 5 VCE is shown in Table 4-13, which identifies the various correction factors involved. The sideline noise estimate of 109.7 dB is based on the unscaled (748 pounds per second) engine. The scale factor based upon a takeoff gross weight of 1,213,000 pounds is 1.842 which, using the equation outlined earlier, results in a sideline EPNdB of 109.7 + 2.7, or 112.4 dB, or ~9 dB over the Stage 3 limit of 103.0 dB.

Community Noise. A study was conducted to determine what impact the Mach 3.2 concept might have on noise levels in the vicinity of airports. This consisted of generating 100 EPNdB (approximately 87 dB(A)) noise contours using the Part 36 takeoff procedure and comparing the contours to those for a typical long-haul subsonic turbofan airplane (747-200) flying the same procedure (Figure 4-11). The comparison shows the HSCT, with the IVP and suppression devices to be considerably noisier than the B747-200. Contour areas are 2.2 square miles for the 747-200, compared to 8.7 square miles for the HSCT. In order

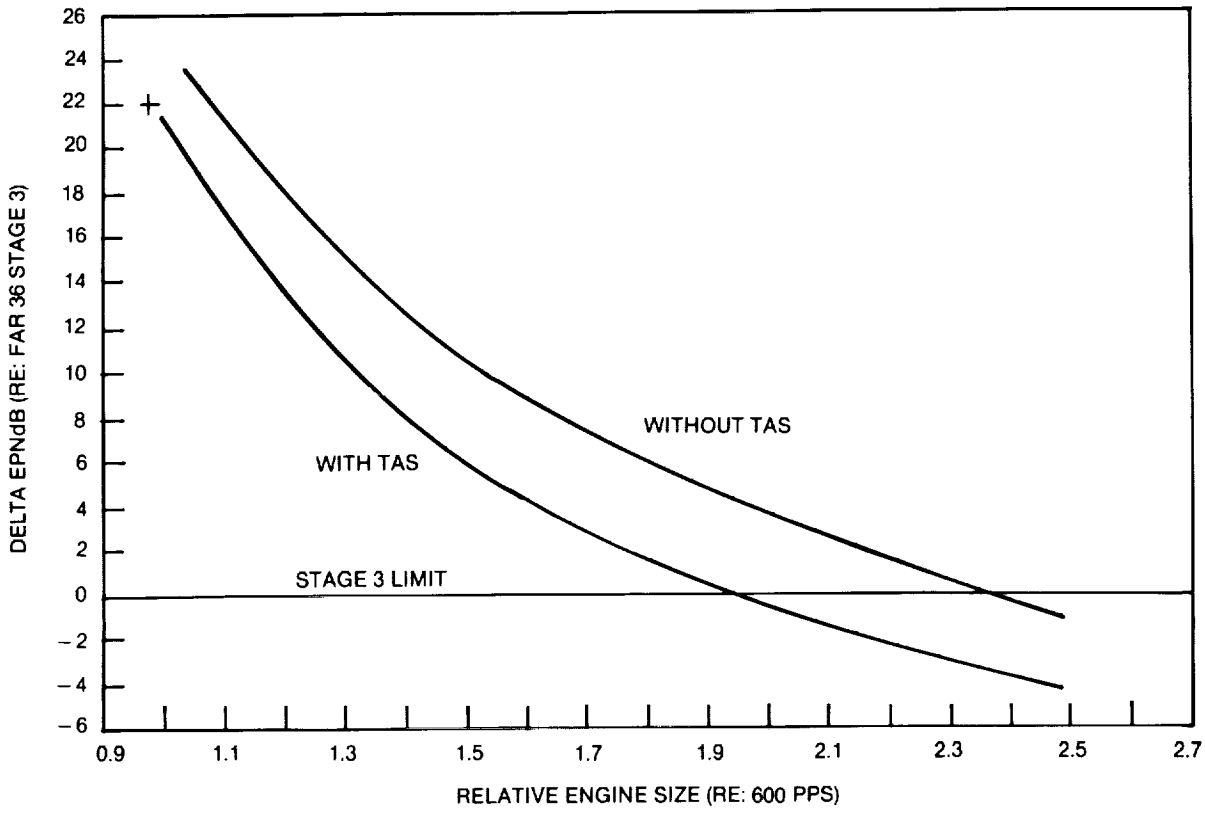

FIGURE 4-10. P&W MACH 3.2 VSCE DATA — SIDELINES NOISE VERSUS ENGINE SIZE — SUPPRESSED CYCLE PER FNT = 57,000 LB

TABLE 4-13
GE VCE NOISE ESTIMATES

	EPNL
EQUIVALENT CONIC NOZZLE NOISE dB (FROM M/S PROGRAM)	113.1
ADJUSTMENTS FOR GEOMETRY	
SUPPRESSION DUE TO 20-CHUTE SUPPRESSOR, dB (V_j^{mix} ~ 2,250 FPS)	-7.5
BENEFIT DUE TO 2D NOZZLE dB (V_j^{mix} ~ 2,250 FPS)	-2.0
ESTIMATED NOISE AMPLICATION DUE TO SERN, dB	+1.5
1 ENGINE FREEFIELD NOISE LEVEL WITH 2D-CD SUPPRESSOR SERN, dB	105.1
SYSTEM NOISE CORRECTIONS	
4 ENGINE AIRCRAFT, dB	+6.0
SOFT GROUND REFLECTION, dB	+1.5
ENGINE TO ENGINE SHIELDING AND EGA, dB	-2.9
NET SYSTEM NOISE LEVEL, dB*	109.7

*NO MARGIN CORRECTION INCLUDED

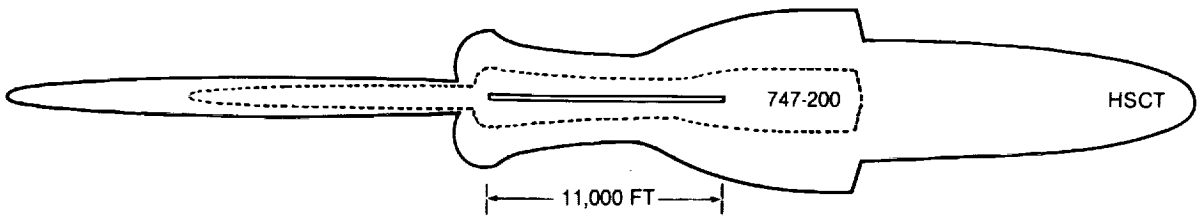

FIGURE 4-11. 100 EPNdB NOISE CONTOURS — D3.2-3A CONCEPT

for the Mach 3.2 concept to be comparable, a further noise reduction of 8 dB and 7 dB at sideline and takeoff, respectively, is required.

The effects of oversizing the unsuppressed reference engine on airport noise contour areas were determined. An HSCT engine, with 2.1 oversizing, reduces the 100 EPNdB contour area to 3.5 square miles. Oversizing the engine produces smaller contour areas, but results in an unacceptable reduction in aircraft range of more than 1,000 miles. The addition of a noise suppression device would reduce the contour areas by approximately 50 percent. The total HSCT contour area could be reduced in size by optimizing the takeoff procedure for minimum area rather than flying the Part 36 cutback procedure.

5.0 CONCLUSIONS AND RECOMMENDATIONS

5.1 Research and Technology Needs

The HSCT study was primarily an assessment of technology in terms of potential commercial value with a continuing emphasis on narrowing the range of Mach number design options. The purpose of the study is to assist NASA to plan follow-on research and technology activities. Early in Phase I it was concluded that current technology was insufficient to support a production development program. Throughout the study, technology needs were monitored as part of the HSCT concept definition process.

A compilation of insights which focuses on the Mach range suited to a kerosene fueled HSCT is presented. The range of interest extended to Mach 3.2 using a kerosene-based fuel, which has higher thermal stability characteristics than the currently available kerosene-based jet fuel (Jet A).

Airframe technology needs are grouped in three categories: environmental, key performance technologies, and integration and supporting technologies (Figure 5-1). These are based on relative priorities, significance, and program logic. The time period is predicated on a year 2000 to 2010 HSCT certification (kerosene-based fuel) with configuration development commencing in 1996-97. It should be emphasized that the following is a first order statement of technology needs without considerations of NASA's resources: personnel, laboratory facilities, and budgets.

Technology needs include the following disciplines: aerodynamics, acoustics, propulsion, thermal, fuels, engine emissions, airframe materials, structures, systems, human factors, safety, reliability, maintainability, product support, and costing.

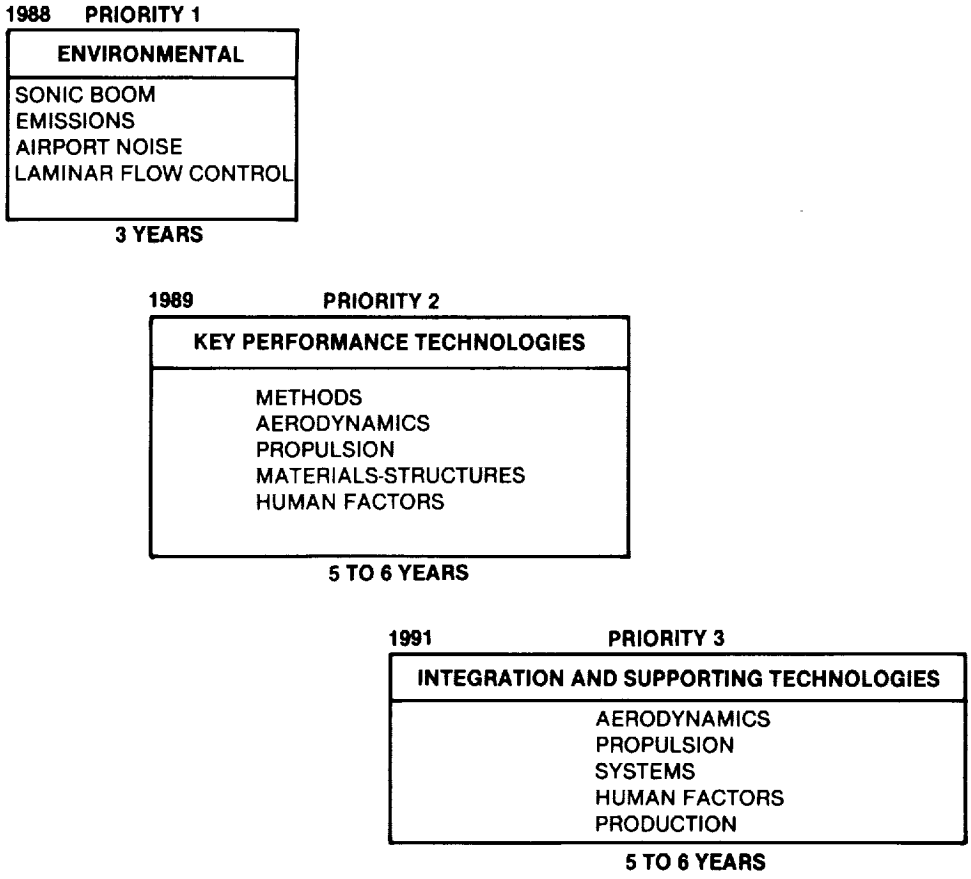

FIGURE 5-1. TECHNOLOGY PLAN

5.2 Conclusions and Recommendations

Market

1. Market projections for the 2000 to 2025 time period indicate sufficient passenger traffic for ranges beyond 2,000 nautical miles to support a fleet of economically viable and environmentally compatible high-speed commercial transports. Fleet needs could total 1,500 or more 300-seat aircraft by 2025.
2. The Pacific Rim area will become the major traffic region after the year 2000, leading to the establishment of design range objectives of 6,500 nautical miles.
3. Ticket prices above competitive subsonic commercial service provide considerable leverage for economic viability. Market elasticity is much greater for coach passengers compared to first class for high-speed transports. Market capture of coach passengers erodes sharply with ticket prices as small as 10 percent to 20 percent above subsonic fare level.
4. Economic viability places emphasis on environmentally acceptable supersonic flight over land. The constraint of no supersonic flight over land reduces potential aircraft productivity (i.e., seat miles per year) by 10 to 20 percent for the Mach 3.2 concept.

Cruise Speed

1. Aircraft productivity increases with cruise speed up to about Mach 5 to Mach 6 for market applications ranging from 2,000 to 6,500 nautical miles. Above this point, the relative significance of cruise speed diminishes and productivity is virtually constant.
2. Design mission gross weights increase with cruise Mach number and correspondingly, advanced technology requirements and costs are greater.
3. Cruise speeds of Mach 5 and Mach 6 using cryogenic fuels (LNG) do not result in competitive opportunities before the 2010 time frame. Liquid methane's energy content falls short of Mach 5 requirements, and liquid hydrogen aircraft (Mach 6) are not competitive due to the high fuel cost.
4. Economic studies of the Mach 3.2 concept suggest viability could be achieved through modest fare premiums and successful research in providing significant gross weight reductions and propulsive efficiency improvements.

Technology Needs

1. Current technology is not adequate to produce an economically viable high-speed transport nor warrant go-ahead on full-scale HSCT design and development.
2. Technology needs can be defined to allow development of an economically attractive Mach 3.2, next generation after Concorde, high-speed transport.

Environmental Considerations

1. Advanced engine technology has been identified that offers the potential for reductions in nitrous oxides to very low levels. The determination of specific engine emission requirements must await the results of studies involving models of the earth's atmosphere and engine emission projections for worldwide HSCT fleet applications.
2. FAR 36 Stage 3 airport noise requirements for a design range of 6,500 nautical miles cannot be met with technology projections of this study. Oversizing engines to reduce the noise is not economically attractive; further innovative suppressor research is required.

3. Concepts considered in this study are estimated to be capable of significant performance objectives – 300 passenger/6,500 nautical miles – with slightly lower sonic boom characteristics than Concorde – 100 passengers/3,200 nautical miles. Sonic boom acceptability criteria plus further refinement of HSCT concepts through configuration shaping and operational constraints is necessary to determine conditions of environmental compliance.

Economy

1. From the standpoint of the U.S. economy, a 1,000-unit HSCT program would create an estimated 200,000 jobs over the life of the program. This translates into a projected $500 billion GNP increase and represents improvement in the balance of trade of approximately $100 billion.

Recommendations

1. Research must focus on resolving environmental issues; criteria acceptability must be achieved on a international basis in concert with the research before production development begins.
2. Research and technology development should focus on concepts using a kerosene-type fuel targeting on initial aircraft deliveries in the 2000 to 2010 time frame.
3. NASP technology and learning will have measurable value; however, a commercially oriented high-speed technologies development program is vital to any ongoing efforts by the U.S. industry to maintain aviation technology leadership.

This Page
Intentionally Left Blank

6.0 REFERENCES

2-1. Yip, L.P. and Parlett, L.P., NASA Report No. TM80152, Low-Speed Wind-Tunnel Tests of a 1/10-Scale Model of an Advanced Arrow-Wing Supersonic Cruise Configuration Designed for Cruise at Mach 2.2, August 1979.

2-2. Woodward, F.A.; Tinoco, E.N.; and Larsen, J.W.; Analysis and Design of Supersonic Wing-Body Combinations, Including Flow Properties in the Near Field, Part I – Theory and Application. NASA CR-73106, 1967.

2-3. Gentry, A.E.; Smyth, D.N.; and Oliver, W.R.; Report No. AFFDL-TR-73-159, U.S. Air Force, The Mark IV Supersonic-Hypersonic Arbitrary-Body Program, November 1973.

2-4. Morris, R.E. and Brewer, G.D., NASA Report No. CR158926, Hypersonic Cruise Aircraft Propulsion Integration Study, Volumes I and II, September 1979.

2-5. Cubbage, J.M. and Kirkham, F.S., NASA Report No. TN D-6060, Investigation of Engine-Exhaust-Airframe Interference on a Cruise Vehicle at Mach 6, January 1971.

2-6. Darden, C.M., NASA Report No. TP1348, Sonic-Boom Minimization with Nose-Bluntness Relaxation, January 1979.

2-7. Corning, G., Supersonic and Subsonic, CTOL and VTOL, Airplane Design, College Park, Maryland, 1976.

2-8. Oates G.C., Aerothermodynamics of Gas Turbine and Rocket Propulsion, AIAA Education Series, 1984.

2-9. Küchemann, D. and Weber, J., An Analysis of Some Performance Aspects of Various Types of Aircraft Designed to Fly Over Different Ranges at Different Speeds, Progress in Aeronautical Sciences, Volume 9, D. Küchemann, ed., Pergamon Press, Inc., C. 1968, pp. 329-456.

2-10. Builder, C.H., On the Thermodynamic Spectrum of Airbreathing Propulsion, AIAA Paper 64-243, June 1964.

2-11. Pearce, W.E.; McNay, D.E.; and Thelander, J.A.; Laminar Flow Control Leading Edge Glove Flight Test Article Development, NASA CR-172137, November 1984.

3-1. Medical Tribune, August 25, 1988, pp 3-18.

4-1. Diehl, L.A. and Biaglow, J.A., Swirl-Can Combustor Performance to Near-Stochiometric Fuel/Air Ratios, NASA TMX-71794, March 1976.

4-2. Zepler, E.E. and Harvel, J.R.P., The Loudness of Sonic Booms and Other Impulsive Sounds, J. Sound Vib., 2(3), pp. 249-256, 1965.

4-3. Johnson, D.R. and Robinson, D.W., The Subjective Evaluation of Sonic Bangs, Acoustica, 18(5), 1967.

4-4. Stevens, S.S., Perceived Level of Noise by Mark VII and Decibels (E), Journal of the Acoustical Society of America 51 (2) (Part 2), pp. 575-601, 1972.

4-5. Borsky, P.N., Community Reactions to Sonic Booms in the Oklahoma City Area, National Opinion Research Center, AMRL-TR-65-37, U.S. Air Force, 1965.

4-6. Schomer, P.D. and Neathammer, R.D., Community Reaction to Impulsive Noise: A Final 10-Year Research Summary: Revised. CERL-TR-N-167-REV, June 1985.

4-7. National Research Council, Assessment of Community Response to High-Energy Impulsive Sounds, Committee on Hearing, Bioacoustics, and Biomechanics, 1981. (No document number.)

4-8. Thomas, C.L., Extrapolation of Sonic Boom Pressure Signatures by the Waveform Parameter Method, NASA TN D-6832, June 1972.

NASA
National Aeronautics and Space Administration

Report Documentation Page

1. Report No.	2. Government Accession No.	3. Recipient's Catalog No.
NASA CR-4235		

4. Title and Subtitle
Study of High-Speed Civil Transports

5. Report Date
December 1989

6. Performing Organization Code

7. Author(s)
Douglas Aircraft Company
New Commercial Programs

8. Performing Organization Report No.

10. Work Unit No.
505-69-01-01

9. Performing Organization Name and Address
Douglas Aircraft Company
3855 Lakewood Blvd.
Long Beach, CA 90846

11. Contract or Grant No.
NAS1-18378

13. Type of Report and Period Covered
Contractor Report

12. Sponsoring Agency Name and Address
National Aeronautics and Space Administration
Langley Research Center
Hampton, VA 23665-5225

14. Sponsoring Agency Code

15. Supplementary Notes
NASA Program Manager: Charles E. K. Morris, Jr.
Douglas Program Manager: Donald A. Graf
Douglas Contract Manager: George W. Lawrence
Final Report

16. Abstract

A systems study to identify the economic potential for a high-speed commercial transport has considered technology, market characteristics, airport infrastructure, and environmental issues. Market forecasts indicate a need for HSCT service in the 2000/2010 time frame conditioned on economic viability and environmental acceptability. Design requirements focused on a 300 passenger, 3 class service, and 6500 nautical mile range based on the accelerated growth of the Pacific region. Compatibility with existing airports was an assumed requirement. Mach numbers between 2 and 25 were examined in conjunction with the appropriate propulsion systems, fuels, structural materials, and thermal management systems. Aircraft productivity was a key parameter with aircraft worth, in comparison to aircraft price, being the airline-oriented figure of merit. Aircraft screening led to determination that Mach 3.2 (TSJF) would have superior characteristics to Mach 5.0 (LNG) and the recommendation that the next generation high-speed commercial transport aircraft use a kerosene fuel. The sensitivity of aircraft performance and economics to environmental constraints (e.g., sonic boom, engine emissions, and airport/community noise) was identified together with key technologies. In all, current technology is not adequate to produce viable HSCTs for the world marketplace. Technology advancements must be accomplished to meet environmental requirements (these requirements are as yet undetermined for sonic boom and engine emissions). High priority is assigned to aircraft gross weight reduction which benefits both economics and environmental aspects. Specific technology requirements have been identified which was the prime objective of this study. National economic benefits are projected.

17. Key Words (Suggested by Author(s))	18. Distribution Statement
High-Speed Civil Transport Market Environment Aircraft Concept Airport Infrastructure Economics	Unclassified - Unlimited Subject Category 05

19. Security Classification (of this report)	20. Security Classification (of this page)	21. No. of pages	22. Price
Unclassified	Unclassified	188	A09